Cellular responses to ischaemic brain damage in adult and aged mice

A thesis submitted to the University of Manchester for the degree of Doctor of Philosophy in the Faculty of Medicine, Dentistry and Nursing

July 2000

Lee Anne Rothwell

Biological Sciences
(Division of Neuroscience)

Contents

Contents

Abstract

Cerebral ischaemia results in a complex series of events that ultimately lead to irreversible neuronal and glial cell death. Despite the importance of age in the prevalence of stroke in man the vast majority of *in vivo* studies have used young adult animals. There are several changes in the aged brain that may influence its response to injury. This study examined the effect of age on underlying changes in neurones and glial cells, and on infarct volume and permeability of the blood-brain barrier (BBB) to horseradish peroxidase after permanent focal cerebral ischaemia. Changes in the number of reactive (glial fibrillary acidic protein; GFAP positive) astrocytes, activated microglia/macrophages (*Griffonia simplicifolia* isolectin B4 (GSA) positive), intercellular adhesion molecule-1 (ICAM-1) positive vessels, interleukin-1β (IL-1β) positive glial cells and neutrophils were also examined. In addition the effect of the recombinant IL-1 receptor antagonist (rIL-1ra) on infarct volume was assessed.

Adult (4-6 month) and aged (26-30 month) C57/Icrfa^t mice underwent middle cerebral artery occlusion (MCAo) and brain tissue removed 24 hours later. Infarct and swelling volumes were measured on 500μm coronal brain slices stained with tetrazolium chloride (TTC). Brain slices were then resin embedded and the number of neurones and glial cells, and pyknotic profiles per mm^3 of layer V of the frontal cortex were determined using the disector method. Immunocytochemistry and lectin cytochemistry performed on 10μm cryostat brain sections was used to investigate the numbers of reactive astrocytes, activated microglia/macrophages, ICAM-1 vessels, neutrophils and IL-1β positive glial cells per unit area in adult and aged animals at 0, 12 and 24 hour after MCAo. BBB permeability to HRP was assessed at 1/2, 1, 2, 4 and 24 hour after MCAo. The effects of central (2.5μg, 30 minutes before and 10 minutes after MCAo; i.c.v.) and peripheral (100mg/kg, at 0, 4, 8, 12 and 18 hour post MCAo; s.c.) administration of rIL-1ra were measured 24 hour after MCAo in adult animals.

There was a significant increase in infarct volume after MCAo in aged animals, but no significant difference in swelling volume. Ageing was not associated with changes in the number of neurones/mm^3 or changes in neuronal area or maximal neuronal nuclear diameter. There was a significant increase (35%) in glial cell density and a significant reduction (27%) in the neurone:glial cell ratio with age. This was related to an increase in the number of reactive astrocytes and activated microglia/macrophages with age. The number of reactive astrocytes and activated microglia significantly increased with time after MCAo in adult and aged animals. There was no significant difference in this astroglial response with age, however there was a significant age-related increase in the microglial/macrophage response to ischaemia. The permeability of the BBB to the tracer HRP increased with time after MCAo, but there was no significant difference in BBB permeability with age. Ischaemia induced an increase in the expression of ICAM-1 on vessels and the invasion of neutrophils into the brain with time in both adult and aged animals. However there were no significant differences in these responses with age. There was an increase in the expression of IL-1β by astrocytes and microglia/macrophages after MCAo. The increases in the numbers of IL-1β positive astrocytes and microglia with time were similar in adult and aged animals. The only exception to this was in the corpus callosum of aged animals where there was an increased expression of IL-1β with time by astrocytes. rIL-1ra significantly reduced infarct volume in adult animals when administered centrally (46%) and peripherally (40%).

The reasons for the age-associated increase in infarct size are not known but it does not appear to be due to alterations in glial activation, leukocyte invasion or adhesion molecule expression. The altered microglial response and IL-1β expression after MCAo may be of fundamental importance to the progression of ischaemic brain damage (IBD) and warrants further investigation.

Declaration

No portion of the work referred to in this thesis has been submitted in support of an application for another degree or qualification of this or any other university or other institute of learning.

Copyright

Acknowledgements

I wish to express my gratitude to Dr Ioan Davies, my principal supervisor, and Professor Nancy Rothwell for their assistance and guidance during the course of this study. Many thanks are also due to Andy Fotheringham for his invaluable technical assistance and friendship. A general thanks to fellow students and post docs in the lab.

I would also like to thank Research into Ageing whose funding made this research possible. A special thank you must go to my spinal surgeon Mr. Raymond Ross whose skill and dedication returned me to full health and gave me the opportunity to complete my studies.

Final thanks must go to Ian Griffiths whose encouragement and financial support were greatly appreciated throughout the preparation of this thesis.

The Author

The Author graduated from the University of Manchester, School of Biological Sciences, in 1992 with a first class honours degree in Anatomical Sciences. She then worked in industry as a pharmacologist at the Neuroscience Research Centre for Merck, Sharpe and Dohme.

In 1994, the author began studies at the University of Manchester, in the Division of Neuroscience, for the degree of doctor of philosophy. After two years of study she sustained a back injury that required surgical intervention. The diagnosis, treatment and recovery from this injury resulted in a two and a half year absence. The author then returned to the University to complete research activities and prepare this thesis. This had implications for the experimental data discussed in chapter seven, which is more limited in scope than originally intended.

Chapter 1

Introduction

1.0 Introduction

The incidence of stroke (cerebrovascular ischaemia) is 250-400 cases per 100,000 people, and has a mortality rate of about 30% making it the third most common cause of death after cancer and heart disease in the developed world (Dirnagl, 1999). Although it afflicts individuals of all ages, the incidence doubles with each decade over the age of 45 (Mulley, 1992). This increase is probably related to the age-associated increase in the incidence of all types of cardiovascular pathology including atheroma and hypertension.

Stroke is a heterogeneous condition that includes a diverse range of cerebrovascular accidents that reduce blood supply to the brain, causing a cascade of biochemical and cellular events that ultimately lead to irreversible neuronal and glial cell death. Recent studies have shown that not all cells die immediately, but the factors that contribute to this delayed progression of injury are unclear (Obrenovitch, 1995; Walz, 1997). One of the processes that could be involved is post-ischaemic inflammation, including glial activation and the involvement of cytokines.

1.0.1 Categories of stroke

Stroke refers to a number of pathological conditions classified according to both the initial cause, and the extent of interruption to the blood supply. Ischaemic injury to the brain is of two types; global ischaemia, produced by systemic alterations in blood pressure or by conditions that simultaneously affect the perfusion pressure of the entire cerebrum; and focal or regional ischaemia, produced by a permanent or transient reduction in blood supply to a particular brain area, generically called ischaemic strokes. The majority (over 80%) of strokes are ischaemic in nature, most of which are the result of occlusion to the middle cerebral artery or one of its penetrating branches (Garcia, 1984).

The major causes of stroke are classified as either haemorrhagic or ischaemic. Intracerebral haemorrhage represents the rupture of a weakened blood vessel and causes blood to leak into the brain tissue itself. Subarachnoid haemorrhage causes blood to leak onto the surface of the brain and usually occurs from the rupture of a small aneurysmal (sac-like) dilatation in an artery. Ischaemic strokes occur when an artery becomes blocked and starves the brain of oxygen and other nutrients. Blockage may result from atherosclerosis forming a plaque within the blood vessel. Alternatively, a particle of clotted blood could be carried through the arteries to a place where it is too large to pass, and consequently blocks the vessel (a process known as embolism).

1.0.2 Therapy

The development of drugs that could protect brain tissue against ischaemic damage would be of benefit because of the seriousness of the disorder and its prevalence. The events that follow the onset of cerebral ischaemia are extremely complex and dependent on the exact nature and duration of the ischaemic insult. Given the multiplicity of conditions which may lead to cerebral ischaemia, it is most unlikely that a single agent will be developed that is effective in treating all types of ischaemia.

Traditionally viewed as an incurable neurological disorder, clinical therapy was aimed at eliminating risk factors (e.g. hypertension and smoking) and decreasing platelet aggregation (aspirin) and clot formation (anticoagulants). Indeed the incidence of stroke has been markedly reduced by these preventative measures (Wolf *et al.*, 1992; Silver *et al.*, 1996). Recently attitudes towards acute stroke treatment were challenged by the success of the thrombolytic agent alteplase (a tissue plasminogen activator). However administration is restricted to the first three hours after onset (Barone and Feuerstein, 1999),

of which very few patients (about 5%) qualify for treatment. Other potential drug treatments to reduce mortality and improve neurological outcome following stroke have focussed on ways of halting the chemical events leading to ischaemic brain damage (IBD; see del Zoppo *et al.*, 1997; DeGrabba, 1998; Barone and Feuerstein, 1999). The clinical therapeutic aims are three-fold: a) rapid restoration of cerebral blood flow and O_2 delivery; b) inhibition of the inflammatory response of IBD, and c) maintenance of neurone integrity and function to effect rescue of tissues within the ischaemic territory. There are many potential drugs currently in clinical trials and a promising target for therapeutic intervention is post-ischaemic inflammation (DeGrabba, 1998; Barone and Feuerstein, 1999).

1.1 Experimental studies on cerebral ischaemia

Fundamental understanding of the physiological changes associated with clinical stroke is essential before apparent therapeutic strategies for treating cerebral ischaemia can be developed. However the difficulty of obtaining patients immediately after the onset of stroke, coupled with problems in studying cerebral function, have restricted experimental investigations in humans. Due to these limitations experimental investigation into IBD requires suitable animal models that can provide information pertaining to the clinical situation.

1.1.1 Animal models of ischaemic brain damage

There are substantial research efforts being made to develop drugs that are "neuroprotective", that is drugs that can be given to minimise the neuronal damage that follows a stroke. A key factor in this process is the development of an animal model(s) that mimics the neuropathological consequences of stroke. Since there are many causes of

stroke in humans a single model of "stroke" cannot mimic all clinical pathologies.

Current animal models of cerebral ischaemia employ many different species and techniques (see Hunter *et al.*, 1995; Green and Cross, 1997). Generally, animal models are grouped into those producing either global or focal ischaemia. Global ischaemia is produced by transiently occluding blood vessels supplying the brain, thereby resulting in a wide spread hypoxic ischaemic episode, usually in the forebrain. Focal ischaemia is generally produced by occlusion (transient or permanent) of specific and selective cerebral vessels, thus producing damage to more defined regions of the brain. It is generally assumed that global models are more relevant to cardiac arrest, while focal models are of greater relevance to acute ischaemic stroke (Green and Cross, 1997). The pathomechanisms that induce neuronal and glial cell death vary slightly depending on the technique used.

The majority of focal ischaemia models involve occlusion of the middle cerebral artery (MCA), as this is widely regarded as the most relevant to 'stroke' in humans (Mohr *et al.*, 1986, Hunter *et al.*, 1998). Unilateral occlusion of the MCA produces a single localised infarction of the territory supplied by the MCA. Permanent occlusion of the MCA in the rat by microsurgical coagulation (Tamura *et al.*, 1981) and its modifications (Bederson *et al.*, 1986) have gained wide acceptance over the last decade and are commonly used to induce reproducible and quantifiable focal lesions. Although the majority of studies have been performed on rats there is increasing interest in characterising the murine model of focal ischaemia due to the availability of transgenic mice (e.g. Chan *et al.*, 1995; Kondo *et al.*, 1995; Mikawa *et al.*, 1995; Schielke *et al.*, 1998). The use of transgenic mice has enabled our knowledge of the pathomechanisms of IBD to be further elucidated. For example the use of superoxide dismutase knockout mice has provided

evidence that free radicals are involved in the pathophysiology of IBD (Kondo *et al.*, 1995; Mikawa *et al.*, 1995; see Section 1.3.3).

Some authors stress that measurement of physiological variables, such as blood pressure, haematocrit, blood glucose and blood gases is necessary to ensure that these variables in individual animals are maintained within acceptable limits during the surgical procedures. Severe variation from normal values may indicate the effect of a treatment on factors other than neuroprotection, eg. by lowering blood pressure. However, unlike larger animals that can sustain frequent blood samplings and volume depletion, systemic hypotension develops in the mouse after withdrawing only a few hundred microlitres of blood, which is not 'typical' of clinical ischaemia (Dalkara *et al.*, 1995). One way forward has been the study of sub-sets of animals under identical conditions, which provide that information (e.g. Dalkara *et al.*, 1995; Hara *et al.*, 1996; Yang *et al.*, 1997). Experimental MCAo leads to the occurrence of brain swelling and oedema (Green and Cross, 1997), which results in enlargement of the infarcted hemisphere, leading to an overestimation of the infarct volume (Brint *et al.*, 1988; Swanson *et al.*, 1990; Lin *et al.*, 1993). Therefore, it is important that measurements of infarct volume following MCAo are corrected for the effects of oedema, eg. by subtracting the volume of swelling from the infarct volume (see Swanson *et al.*, 1990; see Section 2.5.3). Another important consideration, particularly when using aged animals in animal models of ischaemia is their health status. Animals should be bred and maintained under specific pathogen free barrier (SPF) conditions to ensure that they are free from infection and potential pathology due to illness (Miller and Nadon, 2000).

1.2 Physiological responses to cerebral ischaemia

The brain is one of the most metabolically active organs of the body, and is well supplied with oxygen and nutrients by the blood vessels of the cerebrovascular system. When cerebral blood flow (CBF) falls below a certain critical flow rate a cascade of events occur leading to ischaemic brain damage (IBD). The classic concept of the viability thresholds of ischaemia differentiates between two critical blood flow rates (Symon *et al.*, 1977); the upper critical threshold (electrical failure; UCT) and the lower critical threshold (membrane failure; LCT) below which there is irreversible IBD. More recent investigations of functional and metabolic disturbances suggest a more complex pattern of thresholds (Hossmann, 1994). At declining flow rates, protein synthesis is first inhibited at a threshold of about 0.55ml/g/min, followed by a stimulation of anaerobic glycolysis at 0.35ml/g/min. The release of neurotransmitters, and the beginning of the disturbance of energy metabolism, occurs at about 0.20ml/g/min, and finally anoxic depolarisations occur at flow rates less than 0.15ml/g/min.

As seen from the threshold data above occlusion of a cerebral artery does not cause all cells to die immediately. The affected region consists of a *core* of infarcted tissue, where blood flow has fallen below the LCT and neurones undergo irreversible cell death. Surrounding the ischaemic core is a heterogeneous *penumbral* region of reduced blood supply. Due to collateral blood flow in this region CBF does not fall below the LCT and therefore the neurones are functionally inactive but still viable (Astrup *et al.*, 1981; Hossmann, 1994). The concept of an ischaemic *penumbra* has triggered much interest because it offers a window of therapeutic intervention in acute stroke. The penumbra is a time-limited condition, with a tendency to evolve towards infarction and propagate to adjacent viable tissue unless "rescued" by pharmacological intervention. The rapid

progression from penumbral to core tissue is the result of a complex cascade of events, including the occurrence of "spreading depression" (or peri-infarct depolarisations), cellular acidosis, generation of cytotoxic substances (e.g. excitatory amino acids (EAAs), calcium) and post-ischaemic inflammation (Obrenovitch, 1995; Walz, 1997; Dirnagl *et al.*, 1999).

Animal studies show that the therapeutic window for pharmacological intervention in ischaemic stroke is narrow (3-4h after onset (Ginsberg and Pulsinelli, 1994; Ginsberg, 1996)). Although there is plenty of evidence to support the existence of the penumbra in human stroke patients (see, for example, Saunders *et al.*, 1995; Furlan *et al.*, 1996; Read *et al.*, 1998), the extent and temporal dynamics of this area are less well defined. The penumbra might be smaller and exist for a shorter time period in humans (Kaufmann, 1999).

1.2.1 Energy failure and ionic disturbance

A critical reduction in CBF results in anaerobic metabolism of glucose in the ischaemic brain tissue. This triggers several important biochemical events. Firstly, intra- and extracellular pH decreases (to about pH 6.8) due to activation of glycolysis, with the production of lactate and H^+ leading to cellular acidosis which precedes changes in membrane potential (Martin *et al.*, 1994). Secondly, energy stores in the form of adenosine triphosphate (ATP) and phosphocreatinine are depleted resulting in the disruption of intracellular ion homeostasis by inhibition of ATP-dependent active transport mechanisms (see Martin *et al.*, 1994; Katsura *et al.*, 1994) in cell membranes.

Due to the rapid depletion of intracellular ATP, there is insufficient energy available to drive the sodium,potassium ATPase (Na, K- ATPase) pump in cell membranes, responsible for maintaining the resting membrane potential at around -60mV. Without

ATP, the control over resting membrane potential is lost and the membrane potential drifts towards zero. This loss of control is thought to be the origin of the neurodegenerative cascade that leads to neuronal death. Failure of the Na, K- ATPase pump results in a rapid loss of potassium from the cell to the extracellular fluid (ECF), leading to depolarisation of neurones and glial cells and a rise in intracellular sodium due to decreased exclusion (Martin *et al.*, 1994; Katsura *et al.*, 1994). Sodium also enters the cells via voltage-dependent sodium channels, which open in response to depolarisation. Consequently, voltage-dependent Ca^{2+} channels become activated and excitatory amino acids (EAAs, i.e. glutamate) are released into the extracellular space (Choi, 1994; Choi, 1998). Concurrently, energy dependent processes, such as presynaptic re-uptake of EAAs, are impaired, which further increase the accumulation of glutamate in the extracellular space. Activation of EAA receptors (see section 1.3.1) contributes to the elevated level of intracellular Ca^{2+} concentration ($[Ca^{2+}]_i$) that has deleterious consequences on cell survival (Obrenovitch and Richards, 1995; Choi *et al*, 1998; see section 1.2.2).

To maintain ionic equilibrium, the entry of sodium ions is followed by the passive entry of chloride ions, along with water following the osmotic gradient. The ensuing oedema can adversely affect the perfusion of regions surrounding the core and lead to vascular compression and increased intracranial pressure (Dirnagl *et al.*, 1999). The increase in cell volume leads to a disruption of organelles and cell lysis, releasing cellular contents into the extracellular fluid.

1.2.2 Calcium

Cells can tolerate large increases in $[Ca^{2+}]_i$ under physiological conditions by extruding (via the ATP-dependent Ca^{2+}/Na^{+} exchanger) or sequestering excess Ca^{2+} (by

mitochondria and the endoplasmic reticulum). For example, during spreading depression, neurones become heavily loaded with Ca^{2+} without damaging consequences (Nedergaard and Hansen, 1988). However, under compromised energy conditions, such as cerebral ischaemia, pumps and sequestration mechanisms fail and the large sustained increase in $[Ca^{2+}]_i$ initiates a cascade of destructive metabolic processes that ultimately lead to neuronal cell death (see Morley *et al.*, 1994; Kristián and Siesjö, 1998).

The increase in $[Ca^{2+}]_i$ initiates a series of cytoplasmic and nuclear events that influences the development of IBD, such as activation of Ca^{2+} dependent proteolytic enzymes (such as proteases, lipases and endonucleases) that degrade cytoskeletal, extracellular matrix and cellular membrane proteins (Morley *et al.*, 1994; Furukawa *et al.*, 1997; Chen and Strickland, 1997). In addition, activation of phospholipase A_2 and cyclooxygenase generates free-radical species that overwhelm endogenous scavenging mechanisms, producing lipid peroxidation and membrane damage (Morley *et al.*, 1994; Kristián and Siesjö, 1996; Choi *et al.*, 1998; Dirnagl *et al.*, 1999). The Ca^{2+}-related activation of intracellular second messenger systems and the increase in oxygen free radicals trigger the expression of a number of proinflammatory genes e.g. nuclear factor-kB (O'Neill and Kaltschmidt, 1997) and STAT3 (Planas *et al.*, 1996). Consequently mediators of inflammation such as tumor necrosis factor-α (TNF-α) and interleukin-1β (IL-1β) are produced by injured brain cells (Rothwell and Hopkins, 1995; Rothwell, 1998). Sustained activation of these Ca^{2+}-dependent processes can result in immediate or delayed cell death. Ca^{2+} appears to have a pivotal role in both necrotic and apoptotic cell death (Lee *et al.*, 1999).

Evidence that high $[Ca^{2+}]_i$ has a critical role in the pathophysiology of IBD has been shown by a reduction in neuronal damage using a variety of compounds that reduce $[Ca^{2+}]_i$.

Removing extracellular Ca^{2+}, chelating intracellular Ca^{2+} or applying voltage-operated calcium channel or ligand-gated ion channel antagonists can protect neurones from ischaemic injury (see Morley *et al.*, 1994). The neuroprotection obtained is proportional to the ability of the intervention to restore normal Ca^{2+} homeostasis. Recent evidence indicates that Ca^{2+} may not be the only divalent cation whose toxic influx contributes to IBD. There is growing evidence that zinc (Zn^{2+}) also has a pathophysiological role in IBD (see Choi and Koh, 1998).

1.3 Mediators of ischaemic brain damage

1.3.1 Excitatory amino acids

The neurotoxic effects of EAAs were first demonstrated by Olney (*et al.*, 1971) giving rise to the term "excitotoxicity" to describe the neuronal injury induced by the neuroexcitatory action of glutamate and its analogues. It is now well established that EAAs and their analogues cause neurodegeneration both under *in vitro* and *in vivo* experimental conditions (see Choi, 1995; Choi, 1998). EAAs (particularly glutamate and aspartate) are rapidly released into the extracellular fluid after cerebral ischaemia (see Choi, 1998). Elevations in the extracellular concentrations of glutamate lead to excessive activation of N-methyl-D-aspartate (NMDA) and α-amino-3-hydroxy-5-methyl-4-isoxazole propionic acid (AMPA)-type glutamate receptors, with subsequent influx of Na^+ and Ca^{2+} ions through the channels gated by these receptors (Choi *et al.*, 1998). Excessive Ca^{2+} influx is mediated directly and predominantly by NMDA receptors, but is also triggered secondly by Na^+ influx through AMPA-, kainate- and NMDA-receptor gated channels through activation of voltage-gated Ca^{2+} channels and reverse operation of the Na^+/Ca^{2+} exchanger (Obrenovitch and Richards, 1995; Choi *et al*, 1998). These events lead to elevated

intracellular Ca^{2+} concentrations and initiates a cascade of deleterious events (see section 1.2.2) ultimately leading to cell death. Comparatively little is known about the role of metabotropic glutamate receptors in cerebral ischaemia, these do not gate ion channels but act via G proteins (Choi *et al.*, 1998). There is growing evidence, however, that activation of group-II and group-III metabotropic glutamate receptors is neuroprotective (Bond *et al.*, 1998). Evidence that EAA receptors are, at least in part, responsible for neuronal damage during ischaemia has been shown by a reduction in neuronal damage and improved functional outcome, in a variety of animal stroke models, using an assortment of NMDA and AMPA receptor antagonists. (see Buchan *et al.*, 1993; McCulloch, 1994; Doble, 1995, Choi *et al.*, 1998).

In vitro studies have shown that there are two main types of injury induced by exposure of neurones to glutamate (Choi, 1993, 1994, Choi *et al.*, 1998) depending on the class of receptor activated. "Rapidly-triggered excitotoxicity" is the term given to neuronal death observed after a brief exposure (2-3 minutes) to glutamate and is associated with over activation of the NMDA receptors. NMDA receptor over activation results in cell swelling induced by Na^+ influx followed by passive Cl^- and water influx. "Slowly-triggered excitotoxicity" describes neuronal death observed after longer exposure (hours) to glutamate (such as in the penumbra), and is dependent on the prolonged activation of AMPA receptors. Over activation of the AMPA receptors causes membrane depolarisation via the influx of Na^+, and subsequent Ca^{2+} entry via activation of voltage-operated calcium channels (Choi *et al.*, 1998).

The exact mechanisms of neuronal injury induced by EAAs are not known, but depolarisation, neuronal swelling, Ca^{2+} influx and activation of other second messenger systems may all contribute to neuronal damage (Rothman and Olney, 1986; Choi *et al.*,

1998). In addition NMDA-receptor activation is a prerequisite for the initiation of spreading depression (Obrenovitch and Richards, 1995). The intracellular signalling pathways activated during excitotoxicity trigger the expression of genes that initiate post-ischaemic inflammation (Dirnagl *et al.*, 1999), both of which may be deleterious to the outcome of focal ischaemia.

1.3.2 Free fatty acids

The increased $[Ca^{2+}]_i$ activates the enzymes phospholipase A_2 and C (PLA_2 and PLC), resulting in activation of the "arachidonic acid cascade" and an increased turnover of membrane phospholipids, that have long been implicated in the pathogenesis of IBD (Farooqui and Horrocks, 1992; Siesjo, 1992; Bazan, 1993). Activation of PLC results in transient accumulation of second messengers such as diacylglycerol (DAG) and inositoltriphosphate (IP_3). DAG activates protein kinase C (PKC) and IP_3 stimulates mobilisation of calcium from the endoplasmic reticulum which further increases $[Ca^{2+}]_i$. PKC regulates the release of neurotransmitters, activates the proton-sodium exchanger and regulates the opening of calcium channels (Kaczmarek, 1987; Kikkawa and Nishizuka, 1986). Activation of PLA_2, results in the release of free fatty acids, including arachidonic acid (AA), which exerts a variety of actions on membrane structures, membrane-bound enzymes, and neurotransmitter uptake systems (Chan *et al.*, 1983; Yu *et al.*, 1986) that may contribute to neurodegeneration. Furthermore, PLA_2 also leads to the synthesis of platelet-activating factor (PAF), a potent mediator of inflammatory and immune processes (Braquet *et al.*, 1987). The arachidonic acid cascade also potentiates the formation of free radicals and lipid hydroperoxides (Farooqui and Horrocks, 1991). The depletion of unsaturated lipids may be associated with alterations in membrane fluidity and permeability, and

changes in activities of membrane-bound enzymes and receptors (see Farooqui and Horrocks, 1992). In addition, released FFAs can cause membrane damage directly by acting as detergents and ionophores. Thus, increased turnover of phospholipids has many potentially damaging effects with respect to neuronal survival.

1.3.3 Free radicals and oxidative damage

Oxygen free radicals (e.g. superoxide anions, hydroxyl radicals) are highly reactive by-products of many metabolic pathways that avidly bind and damage DNA, lipids, carbohydrates and proteins and have been implicated in IBD (Braughler and Hall, 1989; Chan, 1996). Under normal physiological conditions oxygen radicals can act as cell signalling messengers and excess radicals are removed by antioxidants (such as vitamins E and C) and free radical scavenging enzymes (such as superoxide dismutase; SOD) (Kinuta *et al.*, 1989; Chan, 1996). However, during ischaemia/reperfusion, and in the *penumbral* region (following permanent MCAo), conditions are such that free radical generation may exceed the capacity of these protective mechanisms (Schmidley, 1990; Hall, 1993; Choi, 1996).

Evidence that free radicals are involved in the pathophysiology of IBD has come mainly from the use of transgenic animals. Transgenic mice overexpressing the radical scavenging enzyme SOD-1 showed reduced infarct volumes following MCAo compared with non-transgenic mice (Chan *et al.*, 1995; Yang *et al.*, 1994). In fact, ischaemic infarct volume is significantly increased in mice that lack the *sod-1* (homozygous and heterozygous) and *sod-2* (heterozygous) gene compared with wild type mice (Kondo *et al.*, 1995; Mikawa *et al.*, 1995). The use of free radical scavengers, particularly in ischaemia with reperfusion offers significant neuroprotection, for example administration of alpha-

phenyl-n-tert-butyl-nitrone (PBN; Zhao *et al.*, 1994).

Free radicals produce localised cell membrane lipid peroxidation (and may alter the morphology and also the function of membranes, receptors, ion channels and enzymes), amplify the increased $[Ca^{2+}]_i$, and enhance the release of EAAs (Braughler and Hall, 1989; Hall *et al.*, 1993; Chan, 1996) all of which have neurotoxic effects. Free radicals have also been implicated in injury-induced microvascular permeability and oedema formation (Hall *et al.*, 1993) and induce the formation of inflammatory mediators (Dirnagl; 1999).

1.3.4 Nitric oxide

There is increasing evidence that nitric oxide (NO), a free radical that can act both as a signalling molecule and a neurotoxin, is involved in the pathophysiology of cerebral ischaemia (Iadecola, 1997; Strijbos, 1998). NO is probably not stored or released in a vesicular manner but is generated *de novo* from L-arginine by a complex family of NO-synthesising enzymes (NOS, Marletta, 1994). Three distinct types of NOS have been identified (Dawson, 1994): type-I (located predominantly within neurones, nNOS), type-II (located predominantly within macrophages, neutrophils and glia, iNOS), and type-III (located predominantly within endothelium, eNOS). After focal cerebral ischaemia there is an immediate transient increase in NO levels, derived from the constitutive forms (nNOS and eNOS), that can be inhibited by glutamate receptor antagonists, indicating that the increased NO production is initiated by glutamate (Lin *et al.*, 1996). A secondary delayed increase in NO (starting 6-12h after MCAo) is derived from the inducible form (iNOS) initiated by specific stimuli such as endotoxins and cytokines. This leads to a more prolonged release of NO than by constitutive NOS (Dawson, 1994, Iadecola, 1997).

The precise role(s) that NO plays in the mechanisms of IBD have been the source

of much debate (Dawson, 1994; Dalkara and Moskowitz, 1994; Strijbos, 1998). On the one hand, NO, a potent vasodilator and an inhibitor of platelet aggregation and leukocyte adhesion (see Dawson, 1994; Dalkara and Moscowitz, 1994) might improve post-ischaemic blood flow by enhancing collateral circulation and preventing microvascular plugging. NO also scavenges reactive oxygen species (Wink *et al.,* 1993) and may inhibit Ca^{2+} influx through the NMDA receptor, and limit glutamate neurotoxicity (Lipton *et al.*, 1993, Fagni *et al.*, 1995).

On the other hand, there are several potential mechanisms of NO-mediated neurotoxicity including its ability to form highly toxic free radicals (e.g. nNOS reacts with a superoxide anion to form peroxynitrite), that cause peroxidative damage to cell membranes and induce DNA damage within the nucleus. NO also causes direct inhibition of aerobic respiration, by inactivation of mitochondrial enzymes; and activation of poly (ADP-ribose) synthase to repair DNA damage that results in further depletion of the cells energy stores (see Dawson, 1994; Iadecola, 1997; Strijbos, 1998). Furthermore, NO might exacerbate damage by enhancing the post-ischaemic release of excitatory neurotransmitters (Montague *et al.*, 1994).

NO can be protective or destructive depending on the stage of evolution of the ischaemic process and on the cellular source of NO. Increases, decreases, and no changes in IBD have been reported after administration of non-selective NOS-inhibitors to ischaemic rodents (Dalkara and Moscowitz, 1994). However, more consistent results have been obtained with relatively selective NOS inhibitors, and the use of knockout mice lacking specific NOS isoforms. These studies have shown that both nNOS and iNOS activity are detrimental to the outcome of ischaemia, while eNOS activity might be neuroprotective by maintaining regional cerebral blood flow (see Iadecola, 1997, Samdani

et al., 1997).

1.4 Characterisation of cellular events following cerebral ischaemia

Traditionally cell death following cerebral ischaemia has been attributed to the process of ischaemic necrosis. Ischaemic necrosis is characterised by cellular swelling, dissolution of intracellular organelles, fracture of external membranes, the appearance of 'red neurones' (having a very acidophilic cytoplasm) and a local inflammatory reaction to components of the extruded cytoplasmic contents (Chalmers-Redman *et al.*, 1997). Its mechanism is based on failure of the ionic pumps of the plasma membrane and the resultant Ca^{2+} overload (see sections 1.2.1 and 1.2.2).

Animal studies have provided increasing evidence to suggest that ischaemic neurones also undergo the process of apoptosis (Linnik *et al.*, 1995; Lawrence *et al.*, 1996; Chalmers-Redman *et al.*, 1997; Rosenblum, 1997; Lee *et al.*, 1999). Apoptosis is an active, genetically regulated process of "programmed cell death" resembling that occurring during normal embryonic development and in the course of immune-mediated cell killing. In mammals the genes involved in apoptosis include *bcl*-2 (a suppressor gene) and the caspases, a family of cysteine proteases that are critical in the later stages of apoptosis (see Akins *et al.*, 1996; Webb *et al.*, 1997; Nicholson and Thornberry, 1997). Apoptosis is characterised morphologically by cell shrinking, early blebbing of the plasma membrane and margination of nuclear chromatin (leading to "apoptotic bodies"), and biochemically by DNA fragmentation (Webb *et al.*, 1997). These features can be found in both neurones and glial cells after ischaemia, but in many cases these cell additionally exhibit morphological features of necrosis (Li *et al.*, 1995; Dalkara and Moskowitz, 1999).

The extent to which apoptosis is important in IBD has yet to be definitively

established. If necrosis and apoptosis are both triggered in parallel in the ischaemic brain, the duration and severity of focal cerebral ischaemia may determine which process predominates (Du *et al.*, 1996; Dirnagl *et al.*, 1999; Lee *et al.*, 1999). Dense ischaemia (such as in the core) causes rapid cell death, predominantly through ischaemic necrosis. Whereas mild to moderate ischaemia (such as very brief periods of ischaemia, or in the penumbra) may activate genes that regulate apoptotic cell death.

1.4.1 Oedema

Brain oedema is a common complication following various types of injury to the brain, including cerebral ischaemia. It is defined as an abnormal accumulation of fluid within the brain parenchyma producing a volumetric enlargement of the brain tissue (Klatzo, 1994). Based on experimental evidence, two major types of brain oedema can be recognised, vasogenic and cytotoxic/cellular (see Klatzo, 1994; Kimelberg, 1995). In vasogenic oedema the essential event is injury to the cerebral vessel (causing disruption of the blood-brain barrier; BBB) leading to increased vascular permeability and escape of serum constituents, including proteins and water into the extracellular compartment. In cytotoxic/cellular oedema, the essential event is a direct toxic action on various cellular elements leading to the intracellular accumulation of fluid by the injured brain cells. This leads to swelling of the involved elements, whereas BBB permeability itself may remain undisturbed.

Both types of oedema are present following permanent cerebral ischaemia. The initial phase involves cytotoxic oedema and the main cell types found to be swollen are astrocytes and necrotic neurones, which occurs in response to elevations in extracellular K^+ concentration (Kimelberg, 1995). Cytotoxic oedema progresses and leads to severe tissue

disruption, at which time there is usually breakdown of the BBB to serum proteins, introducing the vasogenic component of ischaemia (Klatzo, 1994).

1.5 Inflammatory responses in the CNS

Until recently the CNS was regarded as an immunologically privileged organ due to the presence of the BBB, a specialisation of capillary endothelial cells. On the abluminal surface the endothelial cells are ensheathed by a basement membrane, which splits in places to enclose a pericyte (Abbott and Revest, 1991). Beyond this basement membrane in parenchymal vessels is a close investment of neuroglial cell processes, predominantly astrocytes. The BBB functions as a selective barrier and restricts the entry of substances for example proteins and peripheral immune cells. However, recent observations suggest that the immunological privilege is not total and that during disease and or injury/insult, immune activation and inflammatory responses can occur within the brain (Fabry *et al.*, 1994; Lotan and Schwartz, 1994; Rothwell, 1997)

It is well recognised that astrocytes and microglia actively participate in the inflammatory response occurring within the brain, and if inflammatory responses are left unchecked, they have the ability to produce a variety of neurotoxic substances and contribute to neurodegeneration (see Chao *et al.*, 1996). During cerebral ischaemia inflammatory cells are locally activated to initiate the inflammatory response via the release of two key cytokines, interleukin-1β (IL-1β) and tumour necrosis factor-α (TNF-α), followed by a secondary response including interleukin-6 (IL-6) and interleukin-8 (IL-8). These cytokines work in co-operation with other inflammatory metabolites, such as prostaglandins and oxygen free radicals, to induce the expression of adhesion molecules on cerebral endothelial cells (DeGraba, 1998) that facilitate the entrance of peripheral

immune cells into the brain.

Increasing evidence that the inflammatory response contributes to IBD has come from a variety of studies showing that IBD is reduced by: preventing the infiltration of neutrophils by induction of systemic neutropenia (see section 1.5.2.2); blocking adhesion molecules or their receptors (see section 1.5.2.1); or, blocking the action of crucial inflammatory mediators, such as IL-1 (see section 1.6.2.1).

1.5.1 Activation of resident brain inflammatory cells following focal cerebral ischaemia

Glial cells were first recognised for their supportive functions within the CNS where they out number neurones by about eight to one. Astroglial cells are the most predominant cell type, comprising approximately 85% of the glial cell population, microglia about 10% and oligodendrocytes about 5% (Chao *et al.*, 1996). In recent years these cells have been receiving increased attention as reactive gliosis (hypertrophy of astrocytes and increased numbers of activated microglia) is a hall mark of normal ageing (see Section 1.7.3.1), and a variety of neurodegenerative diseases, such Alzheimer's disease (AD), Parkinson's disease (PD) and multiple sclerosis (MS; see Norenberg, 1994; Zielasek and Hartung, 1996; Wood, 1998). In addition, activated glial cells have the potential to release a variety of neurotoxic mediators, although the precise mechanism(s) underlying glial mediated neurotoxicity remains to be established. The roles of astrocytes and microglia following cerebral ischaemia will now be discussed.

1.5.1.1 Microglia

Microglia are derived from the mononuclear-phagocyte lineage and are resident

brain macrophages that serve specific functions in the defence of the CNS against invasions by infectious agents and tumors, and the removal of tissue debris in neurodegenerative diseases (Gehrmann *et al.*, 1995). Under "normal" conditions microglia are found in a *resting* or *ramified* form with long thin processes and act not only as immune surveillance cells, but are also involved in extracellular ion homeostasis and neurotransmitter inactivation (Glenn *et al.*, 1991; Perry *et al.*, 1993; Davis *et al.*, 1994). Microglia are randomly distributed through the brain parenchyma and some are incorporated in the perivascular glia limitans (Gehrmann *et al.*, 1995). When cell death or tissue trauma occurs, including cerebral ischaemia, microglial cells become rapidly activated with associated changes in morphology, immunophenotype, migration and proliferation (Zielasek and Hartung, 1996; Wood, 1998). Following cerebral ischaemia microglial activation occurs in two stages (Wood, 1998):

1) Initially morphological changes include shortening of their cytoplasmic processes and an enlarged rounded cell body. Although they undergo proliferation and express a limited number of immunomolecules (such as major histocompatibility complex (MHC) class I antigen) they are not phagocytic. The early changes of microglial activation can be detected by an increase in lectin and complement receptor type 3 (CR3 - also expressed on resting microglia) staining and are termed activated microglia (Davis *et al.*, 1994; Kato, 1998);

2) Eventually they transform into phagocytic microglia termed reactive microglia, which are fully developed brain macrophages, with an *amoeboid* morphology and express a number of immunomolecules (e.g. MHC class II and ED1) that are shared with cells of the mononuclear phagocyte system (Davis *et al.*, 1994; Kato, 1998).

The potential stimuli underlying the transformation of *resting* microglia into activated microglia and finally *amoeboid* microglia following cerebral ischaemia are

numerous, including changes in ion concentration (particularly K^+) and acid base balances (Zielasek and Hartung, 1996). Receptors on microglia have also been demonstrated for a number of known mediators of chemotaxis in inflammatory responses, including receptors for platelet activating factor (PAF), IL-8 and C5a (Wood 1998).

The role of activated microglia during IBD is not fully understood. It was originally thought they were merely scavengers removing neuronal and axonal debris, and that microglial activation was secondary to neuronal damage. However, studies showing that microglial cells invade the peri-infarct zone within 20 minutes to 2 hours after the initial ischaemic insult, lead to suggestions that they may contribute to the delayed cell death of neurones in the penumbra (Gehrmann *et al.*, 1992; Lees, 1993; Davies *et al.*, 1998). Vascular associated microglia are also activated following cerebral ischaemia (Gehrmann *et al.*, 1995). In certain clinical and experimental conditions, microglia can remain in an activated state for extended periods, and neurones in the local vicinity are prone to lytic attack, presumably via the complement cascade, by what has been termed "bystander lysis" (Wood, 1998). *In vitro* studies have shown that activated microglia are also capable of releasing a variety of cytotoxic substances such as oxygen free radicals, glutamate, hydrogen peroxide, nitric oxide, proteinases and inflammatory cytokines such as IL-1, IL-6 and TNF-α (Gehrmann *et al.*, 1995; Zielasek and Hartung, 1996; Wood, 1998).

On the other hand, following cerebral ischaemia *in vivo* activated microglial cells can be seen next to neurones that do not die and therefore microglial activation *per se* is not always pathogenic (Kato, 1998). Activated microglia are seen in the hippocampus of experimental animals that have acquired tolerance to ischaemia by preconditioning with sub-lethal ischaemia (Kato *et al.*, 1995) supporting the conflicting view that microglial activation may also have a beneficial role. Cultured microglial cells can secrete several

factors that promote neuronal and glial cell survival, such as plasminogen, transforming growth factor-β1 (TGFβ-1), basic fibroblast growth factor (bFGF), nerve growth factor (NGF) and thrombospondin (Nagata *et al.*, 1993; Gehrmann *et al.*, 1995; Wood, 1998). TGF-β1 promotes repair by controlling inflammation and immune responses in glia, by inducing and regulating astrogliosis, increasing the synthesis of neurotrophic factors in astrocytes and is a chemoattractant for microglia (Gehrmann *et al.*, 1995; Nicholls, 1999). Therefore following cerebral ischaemia, microglial activation may have a beneficial effect of debris removal and promotion of neuronal and glial survival, or cause further tissue destruction. There may be a fine balance between activation of microglia to promote protective mechanisms and over-activation producing detrimental effects.

1.5.1.2 Astrocytes

Astrocytes are a heterogeneous population of cells that are involved in many activities that are critical to brain function, such as maintenance of the BBB, uptake and inactivation of EAAs (such as glutamate and aspartate), regulation of extracellular water and ion concentrations (in particular H^+, K^+) and pH regulation (see Norenberg, 1994). Following various types of injury to the brain astrocytes undergo several cellular responses as many of the physiological functions of astrocytes are activated (Landis, 1994; Norenberg, 1997), for example in cerebral ischaemia where K^+ and glutamate levels rise (see sections 1.2.1 and 1.3.1). Astrocytic swelling occurs within minutes following CNS injury and astrocytes become activated and undergo reactive gliosis. The histological features of the reactive astrocyte are characterised by cytoplasmic hypertrophy, enlarged nuclei containing increased amounts of chromatin and increased expression of glial fibrillary acid protein (GFAP; Norenberg, 1997; Ridet *et al.*, 1997). GFAP is an

intermediate filament cytoskeletal protein located in astrocytes and is a reliable marker for the transformation of normal astrocytes into reactive astrocytes (Eddlestone and Mucke, 1993).

Following cerebral ischaemia astrocytes rapidly respond, with intensely stained GFAP immunoreactive astrocytes showing fragmented processes, observed as early as 30 minutes, even before necrotic neurones are identifiable (Garcia *et al.*, 1993; Davies *et al.*, 1998). These early reactive GFAP astrocytes in the core of the lesion disintegrate within the first few hours but there is an increase in the number and intensity of GFAP immunoreactive astrocytes in the expanding ischaemic zone from one hour onwards (Davies *et al.*, 1998). Subsequent analysis revealed that most of these astrocytes in the developing lesion would die by 24 - 48 hours. Others have reported increased GFAP immunoreactive astrocytes in the periphery of the infarct within 1-2 days (Clark *et al.*, 1993; Garcia *et al.*, 1993). The functional significance of the astrocytic response surrounding focal cerebral infarcts is unclear at present. For a long time it was thought that the glial barrier around the lesion was a major impediment to axonal regrowth. This view has been challenged in recent years as astrocytes can also secrete neurotrophins that provide a permissive substratum to support axonal regrowth (see Ridet *et al.*, 1997). It is also likely that these cells may be involved in the restoration of the extracellular *milieu* that has been disturbed as a result of injury.

Activation of astrocytes is accompanied by induction and upregulation of many proteins that promote neuronal and glial cell survival, such as TGFβ-1, bFGF and NGF (Norenberg, 1994; Ridet *et al.*, 1997). In addition specific enzyme systems enable astrocytes to metabolise ammonia, glutamate and free radicals, thus protecting the brain from the toxicity of these agents (Norenberg, 1994). These responses are mainly beneficial.

However, the unusual demands of injury may overwhelm the capacity of astrocytes to restore homeostasis and can trigger astrocytic changes that exacerbate the original injury (Ridet *et al.*, 1997). Astrocytes seem to be heavily involved in the propagation of spreading depression (Largo *et al.*, 1996; Walz, 1997) and in some instances the reactive astrocyte may secrete molecules that contribute to neurotoxicity (e.g. NO). As astrocytes swell they lose their normal homeostatic mechanisms, and as a result CO_2 may accumulate producing an acidic environment (Kraig *et al.*, 1995). Glial swelling may also result in an increased brain volume which if great enough will increase intracranial pressure, reduce vascular perfusion and may be associated with the release of excessive amounts of glutamate and lactate (Kimelberg and Norenberg, 1994). These responses would have detrimental effects on cell survival. Reactive astrocytes produce various immune mediators such as IL-1, IL-6, MHC class I and II antigens, and monocyte chemoattractant protein-1 (MCP-1) and may amplify or regulate the inflammatory response (Gourmala *et al.*, 1997; Ridet *et al.*, 1997).

1.5.2 Invasion of peripheral immune cells

1.5.2.1 Role of adhesion molecules

In addition to the intrinsic inflammatory response after CNS injury, peripheral immune cells can migrate across the cerebral microvasculature and infiltrate ischaemic tissue (see section 1.5.2.2). The recruitment of circulating leukocytes into inflammatory lesions initially requires the interaction of microvascular endothelial cells with these inflammatory cells. Three families of specific adhesion molecules are involved in this interaction, the selectin-, integrin- and immunoglobulin-family (Meerschaert and Furie 1995; DeGraba, 1998; see Table 1.1). Under normal physiological conditions leukocyte binding to CNS endothelium appears limited compared with that from endothelia from

other organs (Male *et al.*, 1990). However, adhesion molecule expression can be induced on CNS endothelial cells during inflammatory diseases or cerebral ischaemia (Couraud, 1994; Bell and Perry, 1995; Wang and Feuerstein, 1995), and by several cytokines, such as IL-1β, TNF-α, interferon-γ (IFN-γ; Kim, 1996; Meager, 1999, see Table 1.2).

The process of leukocyte extravasation from the circulation can be divided into three areas of adhesion molecule activity. In the initial phase, there is a transient adhesion characterised by a rolling action of leukocytes along the venular wall. This is mediated by members of the selectin family; endothelial-leukocyte adhesion molecule-1 (ELAM-1, E-selectin) found on activated endothelial cells; platelet activation dependent granule external membrane (P-selectin, PADGEM) found in platelets and on endothelial cells, and leukocyte adhesion molecule-1 (LAM-1, L-selectin) constitutively expressed on leukocytes. The lectin-like domain recognises and binds to specific carbohydrate ligands (e.g., sialyl-Lewis^x) and/or glycoproteins present on the cell surface of many cell types including activated neutrophils (see Harlan *et al.*, 1992; Beekhuizen and Furth 1993; Couraud, 1994; see Table 1.1). Although L-selectin may additionally bind to certain endothelial glycoproteins, it is only when endothelial cells are activated to release/express first P-selectin, then E-selectin that adhesion forces are sufficiently strong to permit "rolling" and a reduction in velocity (Meager, 1999). The second stage involves a stationary and firm adhesion known as leukocyte arrest. This occurs between members of the immunoglobulin family; such as intercellular adhesion molecule-1 (ICAM-1), ICAM-2, and vascular cell adhesion molecule-1 (VCAM-1) found on endothelial cells, and members belonging to the β_1-integrin (e.g. VLA-4) or β-integrin (CD11/CD18 (e.g. LFA-1, Mac-1, and p150, 95)) subfamilies found on leukocytes (Harlan *et al*, 1992; Beekhuizen and Furth 1993; Couraud, 1994, Meager, 1999; see Table 1.1). In the mediation of cell adhesion, lymphocytes chiefly

Adhesion Molecule	Ligand	Target	Cells expressing AM
Integrin family			
CD11a/CD18 (LFA-1)	ICAM-1, ICAM-2, ICAM-3	Endothelial cells (ECs)	All leukocytes
CD11b/CD18 (Mac-1; CR3)	ICAM-1, ICAM-2, iC3b, fibronectin, factorX	ECs	monocytes and PMNLs
CD11c/CD18 (p150,95; CR4)	iC3b, fibronectin, ICAM-1	ECs	monocytes and PMNLs
CD49d/CD29 (VLA-4)	VCAM-1, fibronectin	ECs	monocytes, lymphocytes, basophils and eosinophils
Immunoglobulin family			
ICAM-1 (CD54)	CD11a/CD18, CD11b/CD18 CD11c/CD18	ECs, monocytes and PMNLs	many cell types including endothelial cells
ICAM-2	CD11a/CD18	monocytes and PMNLs	many cell types including high constitutive expression on endothelial cells
PECAM-1 (CD31)	CD31-CD31	ECs, leukocytes and platelets	endothelial cell junctions, platelets and most leukocytes.
VCAM-1 (INCAM-110, CD106)	CD49d/CD29	Monocytes, lymphocytes	activated endothelium and macrophages
Selectin family (glycoproteins)			
E-selectin (ELAM-1, CD62E)	sLe^x, sLe^a and related structures	Leukocytes	activated endothelial cells
L-selectin (LAM-1, CD62L)	sLe^x, sLe^a and related structures	ECs	lymphocytes, monocytes and neutrophils
P-selectin (PADGEM, CD62P GMP-140),	sLe^x, sLe^a and related structures	PMNLs, ECs, monocytes, lymphocytes	platelets, endothelial cells and megakaryocytes

Table 1.1: Adhesion molecules involved in leukocyte-endothelial interactions

(sLe^x = sialyl Lewis X blood antigen, and sLe^a=sialyl Lewis A blood antigen (carbohydrate ligands found on activated neutrophils), iC3b = serum inactivated C3 fragment on membranes, PMNLs = polymorphonuclear lymphocytes.

Cytokine	Effect on adhesion molecule expression
TNF-α, TNF-β, IL-1α, IL-1β and LPS	Induce E-selectin, P-selectin, L-selectin, ICAM-1, and VCAM-1 expression.
IL-10	Potential inhibitor of TNF-α induced ICAM-1 expression.
IL-4, IL-13	Decrease late expression of IL-1- or TNF-α-induced E-selectin. Selective upregulation of VCAM-1 (synergises with TNF-α).
IFN-γ	Weakly induces ICAM-1, but strong synergy with TNF or IL-1. Maintains ELAM-1 expression.
TGF-β1	Inhibits E-selectin. Upregulates PECAM-1.

Table 1.2: Summary of the effects of cytokines on adhesion molecules expression (Pober *et al.*, 1986; Feuerstein *et al.*, 1994, Kim, 1996).

use LFA-1 and VLA-4 to attach to ICAM-1 and VCAM-1 respectively, whereas neutrophils appear to use both LFA-1 and Mac-1 to tether ICAM-1 expressing cells (Meager, 1999). The final stage is the migration of circulating leukocytes from the vascular compartment through the endothelial junctions and perivascular structures into the surrounding brain parenchyma. This requires the expression of integrins, platelet endothelial cell adhesion molecule-1 (PECAM-1; or CD31) and CD47 an integrin-associated protein (modulates integrin avidity), expressed on endothelial cells and is particularly important for neutrophil transmigration and chemokines (Newman, 1997; Andrew, 1998).

Within the brain parenchyma adhesion molecules have also been localised to glial cells (Rössler *et al.*, 1992; Cotman *et al.*, 1998). Cytokines (such as TNF-α, IL-1 and IFN-γ) induce upregulation of specific adhesion molecules e.g. VCAM-1, ICAM-1, ELAM-1 and LFA-1 on glial cells (astrocytes, microglia and oligodendrocytes (Feuerstein *et al.*,

1994; Kim, 1996)). The adhesion molecules on these cells may guide inflammatory cells through the brain in the course of inflammation.

Following focal cerebral ischaemia (in both permanent and transient MCAo models) there is a sequential upregulation of leukocyte-endothelial adhesion molecules E-selectin, P-selectin and ICAM-1 on cerebral vessels (Wang *et al.*, 1994a; Wang and Feuerstein, 1995; Zhang *et al.*, 1998). P-selectin immunoreactivity was observed 15 minutes after MCAo, increasing to peak levels at 6 hours followed by a gradual decline up to 96 hours (Zhang *et al.*, 1998). E-selectin immunoreactivity was seen 2 hours after MCAo (Zhang *et al.*, 1998), increasing to peak expression at 12 hours (Wang *et al.*, 1995; Wang and Feuerstein, 1995) and remaining elevated up to 48 hours. Increased expression of ICAM-1 mRNA was seen at 3 hours post MCAo with peak expression at 6-12 hours and levels remaining elevated for up to 5 days (Wang *et al.*, 1994a; Wang and Feuerstein, 1995). The adhesion molecules CD11a and CD18 (found on leukocytes) and endothelial ICAM-1 have also been shown to be upregulated in patients with ischaemic stroke (Kim *et al.*, 1995, Lindsberg *et al.*, 1996).

In order to determine if adhesion molecules play a significant role in the pathophysiology of IBD a number of studies have been conducted using agents that block either endothelial adhesion molecules or adhesion molecule ligands present on the surface of the leukocytes. Although adhesion molecules are upregulated following both permanent and transient ischaemia, the effects mediated by their increased expression have, until very recently (Zhang *et al.*, 1999) only been shown to be deleterious in transient ischaemia. In rats treated with monoclonal antibodies to ICAM-1 (Zhang *et al.*, 1994; Zhang *et al.*, 1995a), or a synthetic oligopeptide corresponding to the lectin domain of E-selectin (Morikawa *et al.*, 1996), a significant reduction in IBD was produced in transient but not

permanent cerebral ischaemia. In addition administration of CY-1503 (an analogue of sialyl Lewis X (sLe^x) antigen) significantly reduced infarct volume and myeloperoxidase activity after transient MCAo in the rat (Morikawa *et al* 1996). The most likely explanation for this discrepancy between transient and permanent ischaemia is leukocyte-mediated clogging of the microvasculature, which interferes with the reperfusion phase. The adhering cells mechanically reduce blood flow in reperfused cerebral vessels ("no reflow" phenomenon) and thereby prolong hypoxia with ensuing extension of the infarcted area, a process only relevant to transient MCAo. However, anti-adhesion therapy has shown beneficial effects in permanent ischaemia when used in combination with tissue plasminogen activator (Zhang *et al.*, 1999). The most convincing evidence for a role of cell adhesion molecules in stroke development has been obtained from experiments using ICAM-1 knock out mice that showed a five-fold decrease infarct volume and reduced neutrophil accumulation following transient focal ischaemia (Connolly *et al.*, 1996; Soriano *et al.* 1996) compared to wild type mice. Taken together these results suggest that adhesion molecules facilitate neutrophil adhesion and subsequent transmigration into the CNS and contribute to IBD.

1.5.2.2 Leukocyte invasion

The presence of leukocytes has been assessed by direct histological inspection, biochemical analysis of myeloperoxidase activity (a marker for neutrophils and monocytes), and by "radiolabelled tagging" of circulating neutrophils. Reports vary with respect to the timing of leukocyte invasion in the various animal models (see Feuerstein *et al.*, 1994). Intravascular polymorphonuclear leukocytes (PMNLs), particularly neutrophils, are detected in cerebral vessels in the ischaemic territory as early as 30 minutes after permanent MCAo in the rat, several hours before necrotic neurones were observed (Garcia, 1994).

Marked infiltration of neutrophils occurs 12 hours after ischaemia, reaching a peak at 1-3 days, and disappearing by 7 days after permanent MCAo (Barone *et al.*, 1991; Garcia *et al.*, 1994; Zhang *et al.*, 1994; Kato, 1998). Neutrophil accumulation after transient ischaemia is reported to occur earlier (Zhang *et al.*, 1994). Monocytes invade extensively as the second wave after 2-3 days and cover the entire lesion by 7 days (Kochaneck and Hallenbeck, 1992; Garcia *et al.*, 1994; Schroeter *et al.*, 1994). Chemokines such as interleukin-8 (IL-8; attracts neutrophils), cytokine-induced neutrophil chemoattractant (CINC; attracts neutrophils) and monocyte chemotactic protein-1 (MCP-1; attracts monocytes and macrophages) guide the migration of blood-borne inflammatory cells to the sites of injury/inflammation and are all upregulated following IBD (see Kim, 1996; Ransohoff and Tani, 1998).

The appearance of leukocytes has been classically considered to be secondary to brain damage and thought to be involved in the cleanup operation that prepares the wound for healing. However, evidence that leukocytes are involved in the progression of IBD derives from the use of anti-leukocyte interventions. Ischaemic damage is reduced by experimental depletion of circulating neutrophils by induction of neutropenia (Feuerstein *et al.*, 1994); or inhibition of leukocyte function/adhesion by administration of antibodies to surface glycoproteins on leukocytes (Mori *et al.*, 1992; Chen *et al.*, 1994; Chopp *et al.*, 1994; Jiang *et al.*, 1995; Lindsberg 1995). These studies have shown an associated decrease in myeloperoxidase activity indicating a reduction of neutrophil infiltration into the ischaemic tissue. In addition, inhibition of leukocyte adhesion to the endothelium using a variety of blocking molecules to endothelial adhesion molecules (see section 1.5.2.1) results in a reduction of IBD. Although mice treated with rabbit anti-rat PMNL sera showed a 40% reduction in lesion volume 24 hours after permanent MCAo (Lopez and Lanthorn,

1993), neutropenia was not induced in these animals. The authors speculate that a separate unknown effect (i.e. non-neutrophil) of the anti-serum likely underlies the protection observed. Another study failed to obtain protection when neutropenia was successfully induced in rats subjected to focal ischaemia (Hayward *et al.*, 1996). Despite these reports the majority of observations support the view that the invasion of leukocytes, particularly neutrophils, into ischaemic tissue may have detrimental affects on the outcome of stroke.

Many mechanisms have been proposed for the leukocyte-mediated cerebral injury that occurs as a result of the post-ischaemic inflammatory process. These include the physical obstruction of capillaries by vessel plugging (mediated by adhesion molecules) leading to a reduced CBF, increased vascular permeability and the release of chemical mediators from leukocytes that could contribute to the amplification of tissue damage (Korthuis and Granger, 1994; Degraba, 1998). These mediators include cytotoxic enzymes, hydrogen peroxide, the production of inducible NOS, oxygen free radicals leading to lipid peroxidation, and increased cytokine release such as IL-1 and IL-8 (Korthuis and Granger, 1994; Degraba, 1998; Forster *et al.*, 1999). Release of these mediators may ultimately be responsible for the alterations in the BBB, enhancing cerebral oedema. In addition, the inflammatory response may be linked to apoptosis because antibodies against adhesion molecules reduced apoptotic cell death in the ischaemic rat brain (Chopp *et al.*, 1996).

While the existence of the ischaemic inflammatory reaction and its contribution to brain injury is well established, the mechanisms responsible for initiation and propagation of the inflammatory reaction are poorly understood. Recent studies have indicated a potential role of brain cytokines in this process, particularly TNF-α and IL-1 (see section 1.6).

1.6 Cytokines

Cytokines are a diverse group of soluble polypeptides including interleukins (ILs), interferons (IFNs), chemokines, growth factors (GFs), neurotrophins and tumour necrosis factors (TNFs). Cytokines have diverse actions including the control of the growth, differentiation and function of most cell types and play a particular role as mediators of tissue damage and inflammation (see Hopkins and Rothwell, 1995; Rothwell and Hopkins, 1995). They are synthesised predominantly by peripheral immune cells, such as macrophages and lymphocytes and exert their biological effects by interacting with specific high affinity receptors on the cell surface. They can act on a variety of cell types sometimes displaying opposite effects (i.e. promoting or inhibiting cell proliferation) depending on the target cell.

1.6.1 Cytokines in the CNS

Several cytokines have been identified in the brain, where they have diverse actions. These include effects on specific cell types including neurones, glia and brain endothelial cells, and actions on complex physiological systems such as fever responses, behaviour, neuroendocrine and immune function (Rothwell and Relton, 1993; Rothwell and Hopkins, 1995; Rothwell, 1996).

Constitutive expression of cytokines in the brain, as in other tissues is low, but the synthesis of certain cytokines (e.g. IL-1, IL-2, IL-6, IL-8, MCP-1,TNF-α) are increased following injury, infection or inflammation, and have been implicated in the pathophysiology of a wide range of neurological diseases (see Rothwell, 1996). Such observations may, of course, reflect cytokine synthesis secondary to brain damage, rather than a causal event. However, the precise role of cytokines in the response to neuronal

injury is unclear, but several reports suggest that these molecules are directly/indirectly involved in neuronal damage and repair (Relton and Rothwell, 1992; Rothwell and Relton, 1993; Rothwell *et al.*, 1995; Rothwell and Strijbos, 1995, Rothwell, 1996, Rothwell, 1998). Of all the cytokines, IL-1 has been the most extensively studied and there is a growing body of evidence that proposes IL-1 as a mediator of neurodegeneration (Relton and Rothwell, 1992; Rothwell and Strijbos, 1995; Touzani *et al.*, 1999).

1.6.2 Interleukin-1

The IL-1 gene family comprises of at least three members, the two agonists IL-1α and IL-1β, and the endogenous IL-1 receptor antagonist (IL-1ra; see Dinarello, 1996). A potential fourth member, IL-1γ (also referred to as IFN-γ-inducing factor or IL-18) has been identified recently (Bazan *et al.*, 1996), though its actions are not identical to those of IL-1 (Kohno and Kurimoto, 1998). IL-1α and IL-1β bind to receptors and induce intracellular signal, however, IL-1ra binds to the same receptors as IL-1α and IL-1β but does not induce any intracellular signal (Dinarello, 1996; Martin and Falk, 1997). IL-1β is the major secreted molecule and the predominant form in brain tissue, whereas IL-1α is produced in a membrane-associated form (Dinarello, 1996). IL-1β mRNA has been localised to nerve cell bodies of the hypothalamus in humans (Breder *et al.*, 1988) and in neurones of the hypothalamus, hippocampus, cerebellum and cortex in the mouse and rat (Lechan *et al.*, 1990; Ban *et al.*, 1992; Schöbitz *et al.*, 1994). Other reported cellular sources of IL-1β in the brain are astrocytes, microglia and brain endothelial cells (Giulian *et al.*, 1986; Ban *et al.*, 1991, 1992; Breder *et al.*, 1988; Lechan, 1990; Schöbitz *et al.*, 1994). Both IL-1β and IL-18 are formed as inactive precursors (pro-IL-1β and proIL-18) that require cleavage by the interleukin-1β converting enzyme (ICE; Thornberry *et al.*, 1992; Touzani *et al.*, 1999).

ICE has been renamed Caspase-1 due to its involvement in apoptosis (Nicholson and Thornberry, 1997). ICE is present in various peripheral tissues and is constitutively expressed at low levels in the brain (Keane *et al.*, 1995).

IL-1ra is a naturally occurring competitive receptor antagonist expressed both in the periphery (e.g. peripheral immune cells such as macrophages (Eisenberg *et al.*, 1990)) and within the rat and mouse CNS (Licinio *et al.*, 1991; Gabellec *et al.*, 1995). IL-1ra has been shown to inhibit many actions of IL-1 (α and β) both *in vivo* and *in vitro* (Dinarello, 1991; Dinarello and Thompson, 1991; Dinarello, 1993; Dinarello, 1996). *In vitro* and *in vivo* studies show that very large excesses of IL-1ra over IL-1β are required to block IL-1 bioactivity (100-fold, *in vitro*; 1000-fold, *in vivo*; Lennard, 1995). This is consistent with a large excess of IL-1 receptors on cells compared with low occupancy required for biological responses to IL-1 (Dinarello and Thompson, 1991). The availability of recombinant IL-1ra has provided a useful experimental tool with which to investigate the role of IL-1 and IL-1ra in physiological responses.

1.6.2.1 IL-1 receptors

To date two types of IL-1 receptors have been identified, the type I (IL-1RI) and type II (IL-1RII) receptors. The IL-1RI is thought to be the primary signal transducing receptor mediating the actions of IL-1 (Dinarello, 1996). The IL-1RII has been postulated to function primarily as a "decoy" receptor that prevents IL-1 binding to the IL-1RI (Sims *et al.*, 1993; Colotta *et al.*, 1993). Additional members of the IL-1 receptor family have been cloned, such as IL-1 Receptor accessory protein (IL-1RacP) and IL-1Rrp (IL-1 Receptor related proteins; see Martin and Falk, 1997). The precise functional roles of these additional members remain largely unknown, although IL-1RAcP associates with IL-1RI

and facilitates high affinity binding of IL-1 to IL-1RI (Greenfeder *et al.*, 1995).

IL-1 receptors in the periphery have been well characterised, though much controversy exists over the location, type and functional importance of specific IL-1 receptors in the brain (Liu *et al.*, 1996; French *et al.*, 1999; Touzani *et al.*, 1999). mRNA for IL-1R1 has been detected in various regions in the rat and mouse CNS (particularly the hippocampus, the choroid plexus and the cerebellum), but little or no message for IL-1R1 has been reported at major sites of action of IL-1, such as striatum or hypothalamus (Rothwell, 1998). French *et al.* (1999) have shown that IL-1RII is expressed in the same regions as IL-1RI. It has been proposed that novel, as yet unidentified, receptor subtypes for IL-1 in the brain may exist, which are coupled to different effector mechanisms (Haour *et al.*, 1992; Rothwell and Luheshi, 1994; Marquette *et al.*, 1995, Rothwell, 1998; French *et al.*, 1999). The signal transduction pathways for IL-1 have not been fully elucidated for any cell type, and numerous mechanisms have been implicated including nuclear factor-κB and G-proteins (see O'Neill, 1995; Martin and Falk, 1997).

1.6.2.2 IL-1 and neurodegeneration

In the uninjured brain the constitutive expression of IL-1 is low, but, marked increases in the expression of IL-1 (predominantly IL-1β) have been reported in the rodent brain in response to various neurodegenerative conditions including cerebral ischaemia (Liu *et al.*, 1993; Wang *et al.*, 1994; Buttini *et al.*, 1994; Loddick, 1996; Rothwell, 1996; Rothwell *et al.*, 1997; Hill *et al.*, 1999; Touzani *et al.*, 1999). These studies have shown that over-expression of IL-1β in the brain occurs during the very early period (within 1 hour) of the insult and persists during the development of the infarct. The exact cellular source of IL-1β after cerebral ischaemia is still controversial. The major sources are

considered to be endothelial cells, microglia and invading immune cells (Buttini *et al.*, 1994; Zhang *et al.*, 1998; Davies *et al.*, 1999). However, other investigations report that neurones and astrocytes express IL-1β after the induction of brain ischaemia (Ban *et al.*, 1991, 1992; Sairanen *et al.*, 1997; Davies *et al.*, 1999).

The expression of other members of the IL-1 family (i.e. IL-1α and IL-1ra) following cerebral ischaemia has not been extensively studied. A couple of studies have detected increases in IL-1-α and IL-1ra in the ischaemic hemisphere (Hill *et al.*, 1999; Wang *et al.*, 1997 respectively). The temporal induction profile of IL-1ra mRNA after MCAo virtually parallels that of IL-1β, except that IL-1ra mRNA exhibited a more prolonged elevation up to 5 days after MCAo (Lui *et al.*, 1993; Wang *et al.*, 1997; Touzani *et al.*, 1999). The cellular sources of IL-1α and IL-1ra following cerebral ischaemia have not yet been identified.

Direct evidence for an involvement of IL-1 in neurodegeneration was first produced by Relton and Rothwell (1992), who showed that inhibition of the actions of endogenous IL-1 by central administration (i.c.v.) of IL-1 receptor antagonist (IL-1ra; 10μg) into rats, 30 minutes before and 10 minutes after MCAo, caused a dramatic reduction in the volume of neuronal death. Peripheral injection of higher doses of IL-1ra (50-100mg/kg) also reduced infarct volume in the rat even when administered after the induction of MCAo (Relton *et al.*, 1995). Corresponding studies have reported that injection of IL-1β (intracerebroventricular; icv) in animals subjected to MCAo significantly increases infarct volume in rats (Yamasaki *et al.*, 1995b; Loddick and Rothwell, 1996; Stroemer and Rothwell, 1998).

Additional support for the proposal that IL-1 is involved in the pathogenesis of IBD has come from the use of inhibitors of ICE. These supposedly reduce IL-1β production (by

preventing the cleavage of proIL-1β to its mature active form), and have been shown to decrease infarct volume following MCAo in rats and mice (Loddick *et al.*, 1996; Hara *et al.*, 1997b). Similarly transgenic mice expressing a mutant ICE protein, or having the ICE gene knocked out, also have reduced infarct volumes following MCAo (Hara *et al.*, 1997a; Schielke *et al.*, 1998; Yang *et al.*, 1999). In view of the involvement of ICE-like proteases in apoptosis, it remains to be determined if these data reflect inhibition of IL-1β production, apoptosis or both.

1.6.2.3 Mechanisms and mediators of IL-1 action in neurodegeneration

The findings reported above implicate IL-1 in neuronal death following cerebral ischaemia. However, IL-1 is not neurotoxic in the normal rodent brain and fails to cause neuronal death in primary neuronal cultures (Rothwell and Strijbos, 1995). In the latter, IL-1 actually *protects* against excitotoxic damage, while IL-1ra is without effect. Some seemingly beneficial effects of IL-1 have been obtained including, for example, inhibition of calcium entry and glutamate release, enhanced γ-aminobutyric acid (GABA) activity and induction of neurotrophins and other cytokines, such as IL-1ra (see Hopkins and Rothwell, 1995; Rothwell, 1996).

In contrast, in mixed neuronal-glial cultures, IL-1 is neurotoxic at low concentrations and this effect is blocked by IL-1ra (Martin *et al.*, 1997). Although IL-1 administered into the brain *in vivo* does not cause overt damage, injection of nanomolar quantities of IL-1 (i.c.v.) markedly enhance the damage induced by focal cerebral ischaemia, excitotoxins, or traumatic injury in rats (Relton and Rothwell, 1992; Loddick and Rothwell, 1996).

Reported actions of IL-1 in the brain that could explain the role of this cytokine in

the development of IBD include: increased $[Ca^{2+}]_i$ in neurones, the stimulation of arachidonic acid release and corticotropin releasing factor, the induction of β-amyloid and complement and the stimulation of free radical production (see Rothwell, 1996; Rothwell *et al.*, 1996, Rothwell *et al.*, 1997; Touzani *et al.*, 1999). All of these factors have been shown to damage neurones directly or exacerbate other insults (Lee *et al.*, 1999; see Sections 1.2.2 and 1.3). IL-1 could influence neurodegeneration through its effects on the cerebrovasculature, where it has been reported to decrease the integrity of the BBB, enhance oedema, and induce the expression of adhesion molecules leading to neutrophil, lymphocyte or macrophage invasion (de Vries *et al.*, 1995; Yamasaki *et al.*, 1995; Meager, 1999; Rothwell, 1996). IL-1 can also influence the inflammatory cascade by the induction of chemotactic cytokines, such as TNF-α, IL-6, IL-8, colony-stimulating factors (CSFs), and itself (Rothwell, 1997, DeGraba, 1998).

Thus, there are several potential actions of IL-1 that may lead to or inhibit neuronal damage, but the precise mechanisms of action of IL-1 in neurodegeneration are not known and may vary depending on the nature of the insult. It is probable that low levels of IL-1 may be neurotrophic/neuroprotective and are necessary for maintaining natural host defences. Abnormally high levels of IL-1, such as those seen after cerebral ischaemia, may have a neurotoxic effect. The presence of IL-1ra in the normal brain and the upregulation of IL-1ra mRNA after IBD (Loddick *et al.*, 1997; Wang *et al.*, 1997) suggests IL-1ra may function as a defence system to attenuate the IL-1 mediated brain injury. Thus the balance between the levels of IL-1β and IL-1ra expressed after ischaemia may be more critical to the degree of brain injury than IL-1 levels per se.

1.6.3 TNF-α

TNF-α is another pro-inflammatory cytokine that is rapidly released following several types of brain injury including focal cerebral ischaemia. TNF-α displays a pattern of activation very similar to that of IL-1β, mRNA expression for TNF-α is detected early (within the first hour) after ischaemia, increasing to peak levels at 12 hours and then rapidly decreasing (Liu *et al.,* 1994; Wang *et al.,* 1994; Buttini *et al.*, 1996). The exact cellular source of TNF-α after cerebral ischaemia is not fully understood. In the study by Liu *et al.* (1994) TNF-α immunoreactivity was confined to neurones in the evolving infarct. Botchkina *et al.* (1997) located TNF-α in neurones, astrocytes, microglia and infiltrating PMNLs.

Administration of TNF-α antagonists results in neuronal protection in focal cerebral ischaemia (Barone *et al.*, 1997; Dawson *et al.*, 1996) in the rat. Barone *et al.* (1997) also demonstrated that icv injection of TNF-α before permanent and transient MCAo, in spontaneously hypertensive rats, resulted in a worsening of both neurological deficit and infarct size. Blocking endogenous TNF-α with either anti-TNF-α monoclonal antibody or soluble TNF receptor results in a reduction of infarct size and the number of ICAM-1 positive vessels in the lesioned hemisphere (Barone *et al.*, 1997; Yang *et al.*, 1998). These data implicate TNF-α in the pathogenesis of cerebral ischaemia.

The detrimental effects of TNF-α during ischaemia include the stimulation of acute phase protein production, enhanced permeability of the BBB, induction of endothelial adhesion molecules expression, and other inflammatory mediators in macrophages, endothelial cells and glial cells (Briscoe *et al.*, 1992; Feuerstein *et al.*, 1994). In addition, TNF-α induces other cell types to produce cytokines (such as IL-1β, IL-6, CSFs, and TNF-α) and can influence the immune response by upregulating the expression of MHC class

I and II molecules on a number of different cell types (DeGraba, 1998). Overall these effects result in the emigration of immune cells to the site of the ischaemic injury leading to an exacerbation of IBD.

In contrast, *in vitro* evidence indicates that TNF may also protect neurones against metabolic and excitotoxic insults (Cheng *et al.*, 1994). In support of a neuroprotective role of TNF in cerebral ischaemia, mice lacking both TNF receptors (TNF receptor-knockout mice (TNFR-KO)) exhibit increased neuronal cell damage following focal cerebral ischaemia and suppressed injury induced microglial cell activation (Bruce *et al.*, 1996). TNF has been shown to induce the expression of the antioxidant enzyme manganese superoxide dismutase (Mn-SOD) in several cell types (Wong, 1995) and can protect neurones against oxidative (amyloid β-peptide) insults (Barger *et al.*, 1995). Therefore the neuroprotective effects of TNF may be related to the activation of antioxidant pathways.

1.6.4 IL-6

IL-6 is a pleiotropic cytokine with both pro-inflammatory and anti-inflammatory effects and is produced by neurones, glia and immune cells (DeGraba, 1998). Increases in the expression of IL-6 mRNA have been reported as early as 2 hours after permanent MCAo in the rat (Loddick *et al.*, 1998). Injection of recombinant IL-6 (icv) significantly reduced IBD after permanent MCAo in the rat (Loddick *et al.*, 1998). The exact mechanism of its neuroprotection is not known. IL-6 is important to the survival of cultured CNS neurones (Hama *et al.*, 1991), and can inhibit IL-1 synthesis (Schindler *et al.*, 1990) and protect against excitotoxicity *in vitro* (Yamada and Hatanaka, 1994). These properties may contribute to its neuroprotective effects. Recent studies using IL-6 knockout mice have shown that endogenous IL-6 has a significant anti-inflammatory role by

controlling the levels of proinflammatory cytokines (Xing *et al.*, 1998). Endotoxin-induced circulating levels of TNF-α, CSF, and IFN-γ were greatly elevated in the IL-6 knockout mice, and administration of endogenous IL-6 abolished these differences.

In contrast plasma and cerebrospinal fluid levels of IL-6 have been directly correlated with infarct volume and severity of patient outcome (Fassbender *et al.*, 1994; Tarkowski *et al.*, 1995). Transgenic mice overexpressing IL-6 in the brain develop severe neurological disease (Campbell *et al.*, 1993) suggesting that IL-6 may also have neurotoxic effects. These transgenic mice also have increased brain IL-1, TNF-α and ICAM-1 levels (Chiang *et al.*, 1994), all of which have been implicated in IBD (see Sections 1.5.2.1, 1.6.2.2 and 1.6.3) and may account for the neurotoxic effects of IL-6. Therefore it could be that low levels of IL-6 are protective, while overexpression of IL-6 is detrimental to neuronal survival.

1.7 Age-related changes in the brain

Although stroke is primarily a problem of middle or later life, paradoxically, most experimental animals used are invariably young rather than aged. Millikan (1992), Rosenblum (1995) and Koehler (1996) have highlighted the importance of using aged animals in experimental research on cerebral ischaemia. There are several age-related factors in the aged brains of humans and rodents that may influence its response to injury.

During normal ageing (i.e. in the absence of clinical disease) the brain decreases in weight and volume (Terry *et al.*, 1987; Albert and Moss, 1996) and the neurone to glial cell ratio is reported to decrease (Miquel *et al.*, 1983; Terry *et al.*, 1987). It was originally thought these changes were due to continuing neuronal loss with age, however more recent reports indicate that neuronal loss is either not significant or not as extensive as previously

reported (see Flood and Coleman, 1988; Finch, 1993; Goldman *et al.*, 1994; Johnson and Finch, 1996; Wickelgren, 1996). Studies in humans suggest that the decrease in brain tissue observed is primarily the result of decreases in white matter with age, supporting the view that substantial loss of neurones in the cortex does not occur with age (Albert and Moss, 1996). However, there are regions of particular vulnerability to neuronal loss, such as in selected subcortical regions responsible for the production of neurotransmitters important for memory function, such as the basal forebrain and locus coeruleus (Albert and Moss, 1996; Johnson and Finch, 1996).

Instead of neuronal loss, neurone atrophy (a decrease in the size of the perikaryon, nucleus or nucleolus) is a common change during ageing in laboratory rodents and humans that may explain the earlier view of substantial cell loss (see Finch, 1993). Such issues still cause controversy and may depend on the investigator's ability to discriminate small neurones from glia (Johnson and Finch, 1996). Cell atrophy is not necessarily detrimental to cell function as atrophied cells can remain metabolically active, though the nuclear shrinkage implies a decreased production of ribosomes and RNA (Finch, 1993). Although global qualitative changes in the number of different proteins and mRNAs are not found in neural tissues at advanced ages (at least for the rat), the synthesis and turnover of RNA and protein may be slowed (Finch and Morgan, 1990; Johnson and Finch, 1996). Following injury to the brain many genes become activated, therefore any changes in the production of proteins with age could effect brain responses to injury. The dendritic arbour of neurones shows atrophy during normal ageing in many brain regions (Finch, 1993), though the injured brain is still capable of reactive synaptogenesis (Cotman and Neeper, 1996). Surviving neurones increase their dendritic branching to fill in the area vacated by the dead neurone. There are also prominent changes in glial cells and vascular endothelial

cells during normal ageing (see Sections 1.7.2 and 1.7.3.1).

Lipid peroxidation increases with age in most tissues including the brain as evidenced by the accumulation of lipofuscin in neurones (Yu, 1993; Finch, 1993). The cerebral vessels of aged rats have also been reported to accumulate lipid peroxidation by-products (Mooradian and Smith, 1992). Many lipid peroxidation products, such as aldehydes are highly reactive and can interact with DNA causing damage, although there is no evidence that lipofuscin is toxic (Finch, 1993). Age-related increases in oxidative damage (caused by free radicals) to DNA have been reported in the human and rodent brain (Mecocci *et al.*, 1993; Venugopal and Rao, 1991; Johnson and Finch, 1996), together with diminished antioxidant defence mechanisms (Bondy and LeBel, 1993). Damage to DNA was found to increase in both astrocytes and neurones in the ageing rat brain (Bhaskar and Rao, 1994). These changes could potentially predispose the aged brain to increased cellular damage after ischaemia.

β-amyloid protein has also been shown to accumulate in the brains of aged monkeys and humans and is localised to neurones and activated astrocytes and microglial cells (Martin *et al.*, 1991; Martin *et al.*, 1994). The presence of β-amyloid is one of the hallmarks used in the diagnosis of Alzheimer's disease. *In vitro* studies have shown that β-amyloid is neurotoxic (Yankner *et al.*, 1989; Pike *et al.*, 1991) and therefore the increased deposition of β-amyloid during ageing may render aged neurones more susceptible to injury. Although this may be of relevance to stroke in humans there is little evidence of β-amyloid deposition in the ageing rodent brain (Goldman *et al.*, 1994).

There are age-related changes in several neurotransmitter systems, including the cholinergic, serotonergic and glutamatergic systems (see Goldman *et al.*, 1994). Of particular interest to ischaemia, are the marked reductions in the density, sensitivity and

function of cortical NMDA receptors found in the brains of aged rats (Wenk *et al.*, 1991; Gonzales *et al.*, 1992). Since over-activation of these receptors by EAAs results in excitotoxic damage (see section 1.3.1), these findings may reduce the susceptibility of the aged brain to excitotoxic damage. On the other hand, ageing is associated with an increase in extracellular basal concentration of glutamate (Freeman and Gibson, 1987) which may render aged neurones more susceptible to excitotoxic damage. However, there are conflicting findings in the literature. Some authors have reported an increased vulnerability to EAA damage (systemic kainate injection) with age (Dawson and Wallace, 1992; Wozniak *et al.*, 1991), whilst others have reported a reduced vulnerability to EAA damage (intrahippocampal kainate injection) with age (Kesslak *et al.*, 1995). Differences in the availability of kainate in the brain due to altered drug metabolism or changes in the permeability of the BBB to kainate with age may account for the differences between studies. In experimental cerebral ischaemia, neuroprotection was obtained in aged rats, using the competitive NMDA receptor antagonist 3-[2-carboxypiperazin-4-yl]propyl-1-phosphonate (D-CPPene), although neuroprotection was less marked than in the adult age group (Davis *et al.*, 1995).

1.7.1 Age-related changes in brain calcium metabolism

There are several reported impairments in aged neurones of molecular cascades that regulate changes in intracellular calcium ion concentration $[Ca^{2+}]_i$. These include a decline in both the Na^+/Ca^{2+} and (Ca^{2+}/Mg^{2+})-ATPase extrusion mechanisms, a decreased Ca^{2+} uptake into mitochondria and a region-specific, decrease in neuronal Ca^{2+}-buffer capacity (by Ca^{2+}-binding proteins, such as calbindin-28 and calretinin; Michaelis *et al.*, 1984; Verkhratsky and Toescu, 1998). Since most of the reports have analysed one or more of

the Ca^{2+}-regulatory systems in isolation, it is not clear whether these translate into age-related abnormalities of either Ca^{2+} homeostasis, or stimulus-evoked Ca^{2+} signalling and requires more thorough investigations (see Verkhratsky and Toescu, 1998). The most consistent findings of directly measured $[Ca^{2+}]_i$ levels from aged neurones demonstrate an increase in resting $[Ca^{2+}]_i$ and after stimulation a prolongation of $[Ca^{2+}]_i$ recovery towards the resting concentration (see Verkhratsky and Toescu, 1998). Since calcium plays such an important role in the pathophysiology of IBD (see Section 1.2.2) changes in calcium metabolism with age could potentially influence the ischaemic process.

1.7.2 Age-related changes in the cerebral vasculature and BBB

There are several well-documented structural changes in cerebral microvessels with age including the loss of capillary endothelial cells, elongation of the remaining endothelial cells, a decrease in endothelial cell thickness and capillary luminal diameter, and gliofibrillar proliferation (see Burns *et al.*, 1981; Mooradian, 1988). Histochemically, the cerebral vasculature of all mammals show increased periodic acid-Schiff reactions for hyalinisation (Sobin *et al.*, 1992), which may indicate the presence of glycated or oxidised proteins. Cerebral microvessels from ageing rats also show perivascular deposition of collagen fibrils and protein debris (de Jong *et al.*, 1990). The density of cerebral cortical arterioles and capillaries is reported to decrease by about 35% in old rats (Finch, 1993).

In addition to age-related structural changes in the BBB, there are age-related alterations in BBB function including a decrease in choline and glucose transport across the BBB (Mooradian, 1988; 1994). Haemodynamic changes in cerebral microcirculation may contribute to these age-related findings (Mooradian and McCuskey, 1992). These potential haemodynamic alterations include leukocyte-plugging, attachment of blood cells to

endothelial walls of vessels, arteriovenous shunting, and changes in vascular reactivity altering regional blood flow. These parameters were examined in aged Fischer 344 rats using intravital fluorescence microscopy and it was shown that the only significant change was an increase in arteriovenous shunting (Mooradian and McCuskey, 1992). This increase in itself would reduce the delivery of nutrients to the capillary bed and impair the metabolism of cerebral tissue, which may partly account for reports of reduced brain uptake of various nutrients with ageing.

Most animal studies have failed to show a significant age-related alteration of BBB permeability to water-soluble substances (eg. [^{14}C] sucrose) or blood-borne macromolecular tracers (such as horseradish peroxidase; HRP) in the absence of neurological disease (Edvinsson *et al.*, 1993; Mooradian, 1988, 1994; Wadhwani *et al.*, 1991). However, if stressed, eg. during amphetamine-induced hypertension, the senescent BBB becomes more permeable (Edvinsson *et al.*, 1993). Ueno *et al.* (1993) found an age-related increase in the leakage (by 31-51%) of intravenously injected isotope-labelled albumin to brain parenchyma in mice. However, Vorbrodt and Dobrogowska (1994) reported that the barrier to endogenous albumin appears to be functioning normally in the majority of aged mouse brain blood microvessels, but observed a limited "escape" of the plasma albumin across the BBB in about one-quarter of examined vessels. These observations suggest that during senescence, structural changes may occur in some segments of the brain microvascular network. Whether these changes are the cause or the result of focally increased BBB permeability remains unclear.

Most evidence concludes that barrier function is basically intact, while the carrier or transport function of the BBB is somewhat compromised during ageing. However, it is not known if the functional and structural changes in the BBB with age further compromise

BBB function following ischaemia.

1.7.3 Age-related changes in inflammatory responses

Ageing is associated with several altered inflammatory responses (see Miller, 1996) including alterations in the cytokine secretion profile of isolated peripheral immune cells, such as T-cells and peritoneal macrophages. These include a reduced IL-2 production (Gillis *et al.*, 1981; Weigle, 1993; Wakikawa *et al.*, 1999) and an increase in the production of IL-1, TNF-α, IFN-γ and IL-4 when stimulated with lipopolysaccharide (LPS) or anti-CD3 antibody (Miller, 1991; Hobbs *et al.*, 1993; Segal *et al.*, 1997; Wakikawa *et al.*, 1999).

Very few studies have examined the effects of age on cytokine levels within the brain. IL-1β expression has been shown to increase in hippocampal homogenates from old rats compared to young rats (Murray *et al.*, 1997). Following injection (icv) of LPS aged rats had significantly higher levels of TNF-α and PAF in the cerebrospinal fluid compared to young animals (Siren *et al.*, 1993). However, the production of cytokines following ischaemia in aged animals has not been investigated. Age-associated changes in cytokine production like IL-1β and TNF-α could have vast implications in the pathophysiology of stroke since it may alter the inflammatory responses occurring at the BBB and within the brain parenchyma.

The number of macrophages infiltrating the infarct following embolic stroke has been reported to be reduced in the aged rat measured on day four (Futrell *et al.*, 1991). The cause(s) of the reduction in macrophage infiltration is not known. The invasion of neutrophils into the infarct or the expression of adhesion molecules on cerebral endothelial cells after ischaemia have not been investigated in the aged brain. Changes in the expression of adhesion molecules with age could affect the infiltration of leukocytes into

the brain following injury.

There is evidence for age-related increases in the expression of some immune/inflammatory genes in the brain. Age-related increases in mRNAs for apolipoprotein E, antichymotrypsin (an acute phase protein) and complement component C1q (initiation complex for the complement cascade) have been reported (Johnson and Finch, 1996). These genes are found in astrocytes and microglial cells and are also upregulated in AD (Johnson and Finch, 1996). Although much additional evidence is needed, existing information suggests that there may be low-level inflammation in the aged brain.

1.7.3.1 Age-related changes in glial cells

The most often seen age-related change in glia is reactive gliosis, which consists of hypertrophy of astrocytes (astrogliosis) and an increased number of activated microglia (Nichols, 1999). It is well-known that astrocytes hypertrophy, with an increase in size and fibrous appearance during ageing, as studied using conventional histological procedures (see Johnson and Finch, 1996; Nichols, 1999). The morphological changes resemble those of reactive astrocytes found in the brain after injury (Nichols, 1999; see Section 1.5.1.2). Astrocyte hypertrophy during ageing is accompanied by an accumulation of intermediate filaments, which principally contain GFAP (Johnson and Finch, 1996). Increases in GFAP gene expression (mRNA) and immunoreactivity have been reported in the brains of aged humans and rodents (Goss *et al.*, 1991; Johnson and Finch, 1996; Nichols, 1999). Increases in S100β (an astroglial derived protein) have also been observed in the cortex and hippocampus of senescence acceleration-prone mice (SAMP; Griffin *et al.*, 1998) and in the brains of normal ageing humans (Sheng *et al.*, 1996). There are conflicting reports as

to whether the number of astrocytes increase or remain stable with age. Many studies have concluded that there are no significant differences in the number of astrocytes (using semi-thin or paraffin sections, or other markers for astrocytes eg. S100β) between adult and aged animals in the hippocampus and cerebral cortex (Gordon and Morgan, 1991; Berciano *et al.*, 1995; see Nichols, 1999). However, other studies have found an increase in the number of astrocytes with an activated morphology in specific brain regions during ageing (Hansen *et al.*, 1987; Topp *et al.*, 1989; Pilegaard and Ladefoged, 1996).

Although the functional significance of astrogliosis is not fully understood (Berciano, 1995; Johnson and Finch, 1996) these activated astrocytes could influence intercellular communication and the regulation of the brain's microenvironment. Astrocytes respond to many different physiological stimuli or homeostatic perturbations, therefore if reactive astrocytes are compromised in their ability to carry out normal functions additional burdens (eg. enhanced oedema) may be placed on the aged brain during injury. Activated astrocytes are also associated with several neurodegenerative diseases including AD, PD and MS (see Norenberg, 1994; Zielasek and Hartung, 1996; Wood, 1998). Following cerebral ischaemia astrocytes respond rapidly and become activated (see Section 1.5.1.2), however very few studies have examined astrocyte responses in aged animals. A qualitative study using an embolic stroke model in the rat found a decrease in astroglial hypertrophy with age (Futrell *et al.*, 1991). Another qualitative study found more abundant and intensely GFAP labelled astrocytes in aged animals following MCAo in mice (Fotheringham *et al.*, 2000).

Most studies report an increase in microglial cell number and activation with age (Peters *et al.*, 1991; Perry *et al.*, 1993; Ogura *et al.*, 1994; Sheffield and Berman, 1998; Nichols, 1999). The morphological changes resemble those of activated microglia found

in the brain after injury (Nichols, 1999; see Section 1.5.1.1). Microglial activation is characterised by increased expression of macrophage markers including CR3, and MHC class I and II antigens (Perry *et al.*, 1993; Sheffield and Berman, 1998; Nichols, 1999). The number of microglia staining for MHC class II and ED1 (macrophage marker of the lysosomal apparatus) were found to increase throughout the brain (with highest numbers in the white matter) in aged rats compared to young rats (Perry *et al.*, 1993; Ogura *et al.*, 1994). The upregulation of ED1 antigen indicates that microglia in the aged brain are capable of phagocytic activity (Thomas, 1992). Increases in the expression of MHC class II has also been detected in the white matter by middle age in nonhuman primates in the absence of disease (Sheffield and Berman, 1998). There is also an increase in the expression of TGF-β1 by microglia in the brains of aged mice (Nichols, 1999). *In vitro* studies suggest that TGF-β1 promotes repair and regeneration in the CNS by inducing astrogliosis, and increasing the synthesis of neurotrophic factors by astrocytes (Streit *et al.*, 1998). However, the effects of TGF-β1 are context dependent and chronic effects may be detrimental owing to overexpression of extracellular matrix molecules and maintenance of astrocytes in an activated state (Flanders *et al.*, 1998). Activated microglia are also found in association with neurodegenerative diseases such as AD, and following cerebral ischaemia (see Norenberg, 1994; Zielasek and Hartung, 1996; Wood, 1998; see Section 1.5.1.1). These age-related changes in microglia could potentially affect the immune/inflammatory responses that occur after injury to the brain. However, it is not known what effect ageing has on microglial cell activation following cerebral ischaemia. Since glial cells are capable of both beneficial and neurotoxic roles in ischaemia, any changes with age in glial responses could potentially effect outcome.

1.8 Summary and remaining questions

In summary, the data presented above describe the complex pathology that leads to neuronal death after cerebral ischaemia. Most of the data has been obtained from experimental studies in young animals. However, there are several age-related changes in the brain, such as vascular pathology, neuronal atrophy, astrogliosis and microglial activation that could influence the pathophysiology of IBD. Neurones from the brains of aged subjects may be more susceptible to death due to the presence of subclinical injury. The age-related changes in glial cells may affect their ability to respond to injury or restore homeostasis after injury. Age-related changes in glial cells may also influence the permeability of the BBB in the aged brain after injury. If there are changes in brain cytokines with age due to subclinical pathology this could influence many of the post-ischaemic inflammatory responses. However, many of the cellular responses to ischaemia have not been investigated in aged animals and it is not known if there are alterations with age in these responses.

1.9 Aims of this thesis

The overall aim of this thesis was to examine if the previously reported changes in neurones and glial cells lead to altered changes in the response of the aged brain to injury. Specific objectives were:

1) To determine the loss of neurones and glial cells after IBD in young adult and aged mice induced by MCAo (Chapter 4).

2) To investigate the activation of glial cells, ICAM-1 expression, IL-1β expression and neutrophil invasion after MCA occlusion and evaluate if there are any changes with age in these responses (Chapter 5).

3) To examine the effect of age (if any) on the permeability of the BBB to the tracer HRP following MCAo (Chapter 6).

4) To determine the role of the interleukin-1 receptor antagonist (IL-1ra) in IBD in adult animals (Chapter 7).

Chapter 2

Materials and Methods

2.0 Materials and methods

2.1 Animals

All experiments were carried out on male, adult (4-6 months) or aged (26-30 months) C57/Icrfa^{t} mice in accordance with the Animals Scientific Procedures Act 1986 (UK). These animals were sampled from a SPF barrier reared colony maintained under the current FELASA recommendations for health monitoring (Rehbinder *et al.*, 1995). Mice were housed in cages of up to 10, in a controlled environment, with a 12 hour light/dark cycle. Mice had free access to drinking water and a pelleted diet (Beekay International, UK) both before and after surgery. The animals were screened for macroscopic pathology prior to inclusion in the study.

2.2 Anaesthesia

For all surgical procedures mice were anaesthetised by Fluothane inhalation using a Blease Minor anaesthetic machine (Blease Medical Equipment Ltd., UK.). For induction of anaesthesia, animals were placed in an anaesthetic induction chamber and a mixture containing approximately 2.5 % Fluothane (Zeneca Pharmaceuticals, UK) in 50:50 oxygen:nitrous oxide was used at a flow rate of 3 litres per minute. To obtain a suitably low flow rate to the animal during surgery, a tee connector with a valve was fitted so that approximately 100ml per minute went via a Sho-rate flow meter (Brookes Inst. Div., UK.) to a nosepiece, and excess gases went to waste. During surgery anaesthesia was maintained using 1.5 - 2% Fluothane.

2.3 Surgical procedures

2.3.1 Implantation of lateral cerebroventricular guide cannulae

Guide cannulae, for the injection of solutions into the cerebral ventricles, were

implanted at least seven days prior to subsequent studies. Anaesthesia was induced and maintained by Fluothane (see Section 2.2). Mice were secured in a stereotaxic frame (Narishigue, Scientific Instrument Laboratory, Japan) by fixing the jaw in an incisor bar and positioning the ear bars in the external auditory meatae. The frame was adapted (in the Department of Geriatric Medicine, University of Manchester, from the design of Jones *et al.*, 1977) for the mouse by means of a small table, onto which the animal is placed. The holder was modified to allow ear bars to be used, and a rubber nosepiece was placed around the nose bar to allow Fluothane delivery to the mouse (see Figure 2.1).

Fur covering the ventral surface of the scalp was trimmed, and a 1cm-midline incision, extending caudally from just behind the eyes was made along the scalp, and the skin retracted using a metal clip. An alignment device (following the design of Jones *et al.*, 1977 (see Figure 2.2)) was brought into position to allow accurate orientation of the head, such that the posterior pin was located on the Bregma intersection. The head was adjusted in each plane so that all four pins touched the skull simultaneously. The alignment device was then removed and the frame tilted anterior end down, through 6° in order to bring the skull into a horizontal position. The guide cannula (constructed from a 23 gauge hypodermic needle, with the needle length approximately 1.5 - 2mm) was then secured to the stereotaxic manipulator in the vertical position and positioned at Bregma. Bregma was taken as the antero-posterior (AP) and lateral (L) zero co-ordinates. Co-ordinates for the lateral ventricle were determined by reference to the atlas of Sidman *et al.* (1971). The guide cannula was then moved R (+1.6), AP (- 0.4) and a small burr hole drilled at this location, using a Casalli dental drill (Wright Dental Sales, UK) with a fine burr (1 mm diameter). Two more burr holes were drilled either side of the guide cannula, to permit the positioning of two small retaining screws (1mm diameter). The dura mater was pierced with a sterile needle, and the guide cannula was then lowered into the first hole, so that the

tip of the cannula was positioned approximately 2 mm above the desired site of injection (the lateral ventricle contralateral to the future lesioned hemisphere). The guide cannula and retaining screws were secured to the skull by the application of methyl methacrylate dental cement (Simplex Rapid, Austen Dental Products Ltd., UK). The cement was allowed to harden for 10 minutes after which the manipulator was raised leaving the guide cannula in place and the skin around the guide cannula was sutured.

On completion of the procedure the animals were removed from the stereotaxic frame, placed in single cages on a heated pad under an infrared lamp and allowed to recover for 1 hour, before being returned to their controlled environment.

2.3.1.1 Injection into the lateral ventricle of mice

Injection cannulae were constructed from stainless steel tubing (31 gauge; Stainless Tube and Needle Co. Ltd., UK) cut and filed to a length of 6.5mm (optimal length for accurate delivery of solutions into the lateral cerebral ventricle) and connected to a 5µl Hamilton syringe via a length (approximately 3cm) of PE10 tubing.

Animals with previously implanted guide cannulae (left for 7 days) were anaesthetised by Fluothane (see Section 2.2) ready for middle cerebral artery occlusion. The animal was placed in the prone position and the injection cannula positioned into the guide cannula to permit administration of drug or the appropriate vehicle into the lateral ventricle. The injection of 1µl of solution was performed slowly over a period of about one minute.

2.3.1.2 Verification of the injection site

Prior to decapitation, toluidine blue was infused via the guide cannula into the lateral ventricle.

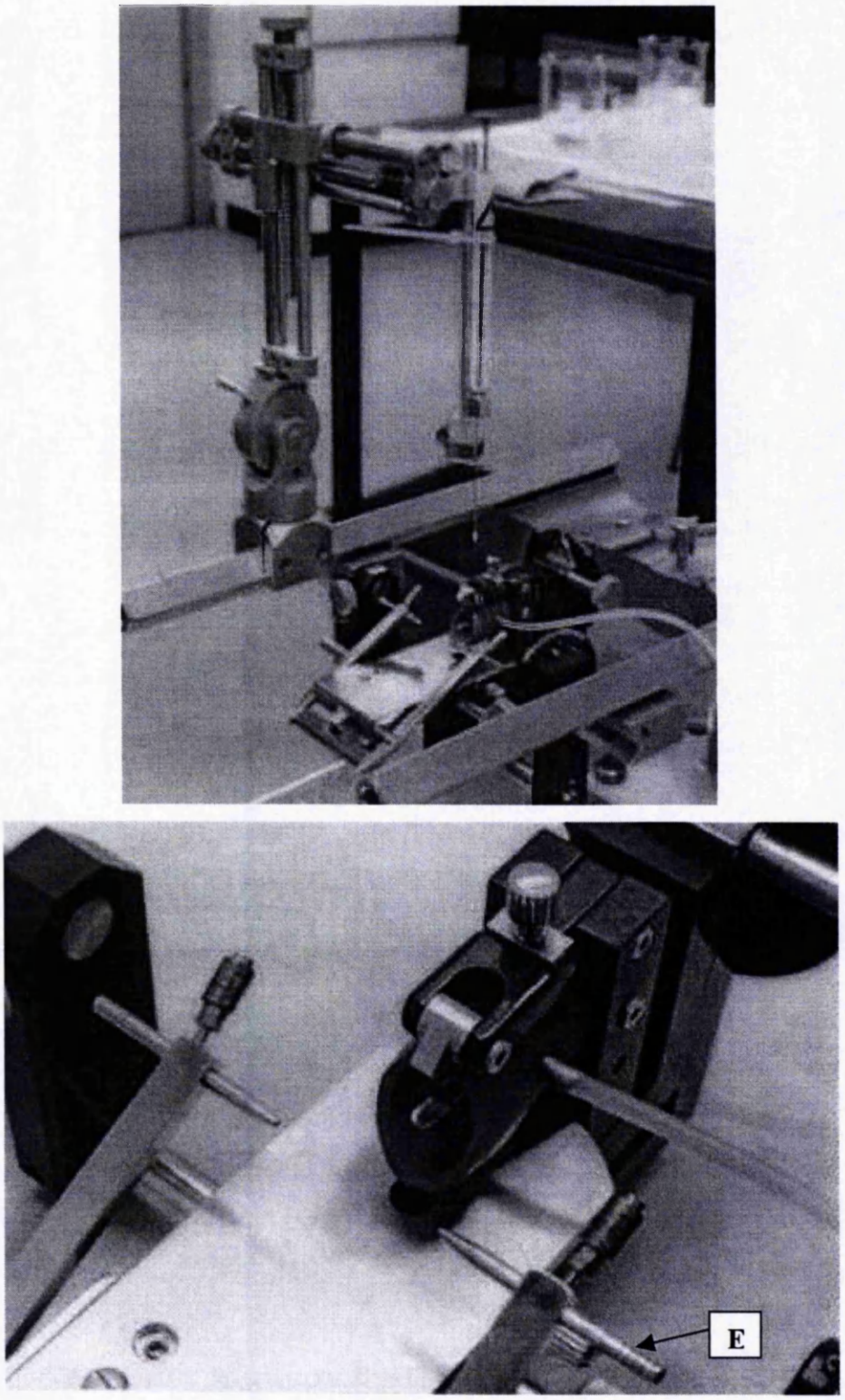

Figure 2.1: The stereotaxic frame adapted for the mouse (from Jones *et al.*, 1977)

The stereotaxic frame was adapted for the mouse by means of a small table onto which the animal is placed, and a rubber nose-piece around the nose bar which allows Fluothane delivery to the mouse. The holder was also modified to give adjustable ear bars (E).

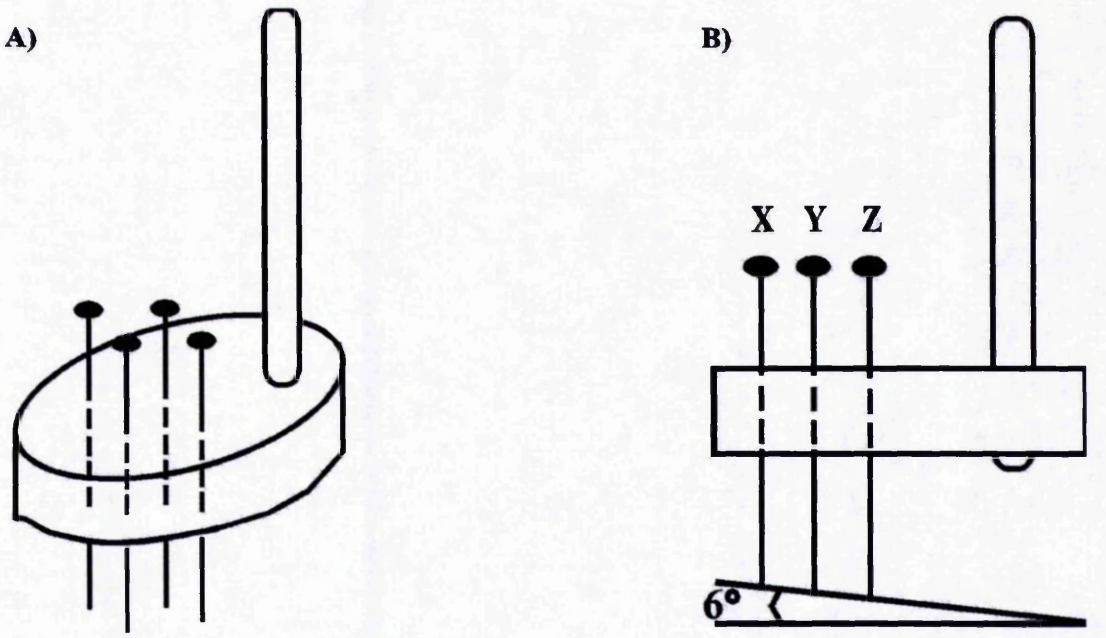

Figure 2.2: The alignment device

(a) Three-dimensional schematic diagram of the alignment device (Jones *et al.*, 1977) showing four pins set into a Perspex block.
(b) Section through the device shows the pins in a plane inclined at an angle of 6° to the true horizontal axis, the anterior pin X being uppermost. X and Z are 4mm apart. The two lateral pins, Y, are 3mm apart (superimposed in this diagram).

Subsequent sectioning of the fresh brain using a Vibratome revealed the distribution of toluidine blue, only data from animals that had clear blue staining of the lateral ventricles were included in the central IL-1ra experimental groups.

2.3.2 Middle cerebral artery occlusion and sham-operations

Focal cerebral ischaemia was induced using an adaptation of a method described previously (Welsh *et al.*, 1987). Anaesthesia was induced and maintained by Fluothane (see Section 2.2). Animals were positioned with their left side uppermost on a heated pad to maintain body temperature at approximately 37°C. The left temporoparietal region of the head was shaved and a 1-cm incision was made between the lateral margin of the left

orbit and the external auditory canal. Subsequent procedures were performed with the aid of an Olympus dissection microscope with zoom lens. Skin overlying the parotid gland and temporalis muscle was released from the connective tissue, and held back from the muscle using sutures. The parotid gland and surrounding soft tissue was partially freed, and held off the temporalis muscle, to expose the superficial temporal vein which was electrocoagulated using bipolar forceps (Eschmann Bros. & Walsh Ltd., UK). An incision was made superiorly on the upper margin of the temporal muscle and the midline of the temporal muscle, and the left lateral aspect of the skull was exposed by reflecting the temporal muscle forward. Under high power magnification, a small burr hole (1mm) was made, using a dental drill, through the outer surface of the semi-translucent skull just over the visibly identified middle cerebral artery. The inner layer of the skull was removed using fine forceps, and the dura was carefully opened. Care was taken to avoid damaging the MCA or other blood vessels. Occlusion of the middle cerebral artery was performed at two points by bipolar coagulation using fine angled bipolar forceps. The first occlusion was at a point just distal to the lenticulostriate artery, and the second occlusion was approximately 1mm above this. A fine ophthalmic knife was used to transect the artery between these two points, to ensure permanent disruption of the blood supply. Care was taken to avoid brain damage by lifting the artery off the surface of the brain prior to coagulation. Sham-operated animals underwent identical surgical preparation, but instead of occluding the artery, it was simply lifted from the surface of the brain. The temporalis muscle and parotid gland were replaced and the skin was sutured. On completion of surgery, Fluothane exposure was terminated, and the animals placed in single cages on a heated pad under an infrared lamp for one hour before being returned to their controlled environment.

2.3.3 Perfusion fixation

Where brain tissue was required for subsequent histological processing, horseradish peroxidase staining or immunocytochemistry, animals were killed by perfusion of fixative as follows. Mice were anaesthetised with 4% Fluothane (see Section 2.2) and placed in the supine position on absorbent tissue. The animal was dissected open to reveal the heart and lungs. A Portex intravenous cannula filled with normal (0.9%) saline (connected to a 3-way tap) was inserted into the left ventricle of the heart. An incision of the wall of the right atrium was made using fine scissors. A steady pressure was applied to the syringe containing the saline. When the effluent from the right atrium was free of blood (approximately 5ml of saline), the tap was switched to allow perfusion of fixative. Approximately 10-12 ml of fixative was infused over 10 min using an electric pump, after which the cannula was removed. The brain was then carefully dissected from the skull and stored in the appropriate fixative for subsequent histological processing.

The fixatives used were 4% phosphate buffered formaldehyde pH 7.4 for resin embedding, Karnovsky fixative for HRP staining, and 2% Periodate-lysine-paraformaldehyde (PLP) fixative for immunocytochemistry (see Appendix 1).

2.4 Experimental treatments

2.4.1 Interleukin 1- receptor antagonist (rIL-1ra)

Recombinant human IL-1 receptor antagonist (rIL-1ra) protein was generously donated from Dr R. Thompson (Synergen, USA.). rIL-1ra was dissolved in 10mM sodium citrate, 0.5mM EDTA and 140mM sodium chloride to give a stock solution of 250mg/ml at pH 6.5. The stock rIL-1ra was diluted to a concentration of 2.5 mg/ml using sterile, non-pyrogenic 0.9% saline, and administered, into the lateral cerebral ventricle (icv) at a dose of 2.5μg (in 1μl). The same volume of sterile, non-pyrogenic 0.9% saline was administered

icv as a control.

For peripheral administration, animals were injected subcutaneously with either 150µl vehicle (0.9% sterile saline) or an equivalent volume of 100mg/kg of rIL-1ra at 0h, 4h, 8h, 12h and 18h after MCAo.

All injections and infarct volume measurements for these experiments were done in a blinded fashion.

2.5 Histological assessment of brain damage on fresh tissue

2.5.1 Dissection of the brain

Where fresh brain tissue was required (TTC staining- see below) animals were sacrificed 24 hours after MCAo by an overdose of Fluothane anaesthesia, followed by decapitation. The skin and muscle overlying the skull was removed, and the skull cut down the midline and carefully pulled back laterally to expose the brain. The brain was removed from the surrounding bone using a spatula, cutting the optic nerves with fine scissors.

2.5.2 Tetrazolium chloride staining on fresh brain tissue

The extent of neuronal damage was assessed 24 hours after MCAo. The brain was removed from the animal as described in Section 2.5.1. The hindbrain was removed, using a sharp blade, and discarded and the cut surface of the brain was fixed to a Teflon block using cyanoacrylate glue. The tissue was immersed in phosphate buffered saline (PBS; see Appendix 7), and 500µm coronal sections (approximately 9-12 sections) were cut using a 753M tissue vibroslice (Campden Instruments Ltd., UK). The slices were placed immediately in a 2,3,5-triphenyl tetrazolium chloride medium (TTC; see Appendix 2), which stains for activity of the mitochondrial enzyme NADPH-diaphorase, and therefore indicates tissue viability (Lojda *et al.*, 1979). The slices were incubated for 30 min at 37°C

on a water bath after which the infarcted area was visible as an unstained region of the slice. The tetrazolium medium was then removed and replaced with 4% phosphate buffered formaldehyde pH7.4 (see Appendix 1). The sections were fixed for a minimum of 24 hours at 0-4°C. Before analysing the sections they were rinsed in 0.9% saline and carefully mounted on gelatin subbed microscope slides (see Appendix 3).

2.5.3 Determination of infarct volume

An indirect method, similar to that proposed by Swanson *et al* (1990) was used to determine infarct volume on TTC stained brain slices using a semi-automated image analysis system (Imagan 2, Leitz / Kompira, UK) or a Seescan image analysis system (Seescan, UK; see Appendix 5). Three measurements were made on each slice to calculate the size of the infarct and correct it for the effects of brain swelling (oedema):

a = area of the infarct (mm^2), **b** = area of the left (infarcted) total hemisphere (mm^2), **c** = area of the right (non-infarcted) total hemisphere (mm^2), **d** = brain swelling (mm^2) = (b-c) and t = slice thickness.

The volume of the infarct (mm^3) corrected for swelling = Σ **(a.t)** - Σ **(d.t)**

2.6 Histological assessment on resin embedded brain tissue

Perfusion fixed brain tissue required for detailed histological assessment or cell counting methods was cut using a 735M tissue vibroslice into 500μm coronal sections prior to resin embedding. The 500μm sections were dehydrated in an ascending series of alcohols and embedded in JB-4 resin (Polysciences, Inc., USA; see Appendix 4). 3μm sections were cut on a LKB Historange microtome using an 8mm glass knife, and mounted on gelatin subbed slides. The sections were stained with 0.1 % toluidine blue and mounted in DePeX mounting medium (DPX; BDH Chemicals, UK).

2.7 Cell counting methods on resin sections

2.7.1 Serial-section reconstruction

Thick coronal slices (1mm) of perfusion fixed brain tissue were prepared as described above (Section 2.6). One coronal slice (taken near +0.86mm with respect to Bregma), in the mid-infarct region was selected per animal. A fine punch hole was made in the slice as a reference point prior to dehydration and embedding in JB-4 resin (Polysciences, Inc., USA). The resin blocks were serially sectioned on a Historange microtome (LKB) at 3μm using a glass knife. Twenty sections were collected from each tissue slice and stained with 0.1% toluidine blue.

All counts were carried out at a magnification of x40, using a square eyepiece graticule (Graticules Ltd., UK). The area of the eyepiece graticule was measured using a stage micrometer. Using specified co-ordinates with respect to a reference point (see Fig.2.3) ensured the exact matching of fields of view for examination. At x10 magnification, the eyepiece graticule was aligned parallel to the cortical surface, so that the centre point of the eyepiece graticule fell in layer V of the cortex of the first section. The co-ordinates at which the reference hole was located were noted, and these co-ordinates were used on subsequent sections from the same brain so that exactly the same field of view in all sections could be located. The cells intercepted by the right vertical and top grid bars were included in the counts; those intercepted by the left vertical and bottom bars were not. Only neurones that had clearly visible nucleoli were included in the counts. Glial counts included astrocytes, oligodendrocytes and microglia, and the inclusion criteria was a well-outlined nucleus. Other non-neuronal cells such as pericytes and endothelial vascular cells were not counted.

The total number of cells (for example neurones) per mm^3 of layer V of the frontal cortex in the sample of tissue described above was determined by serial reconstruction.

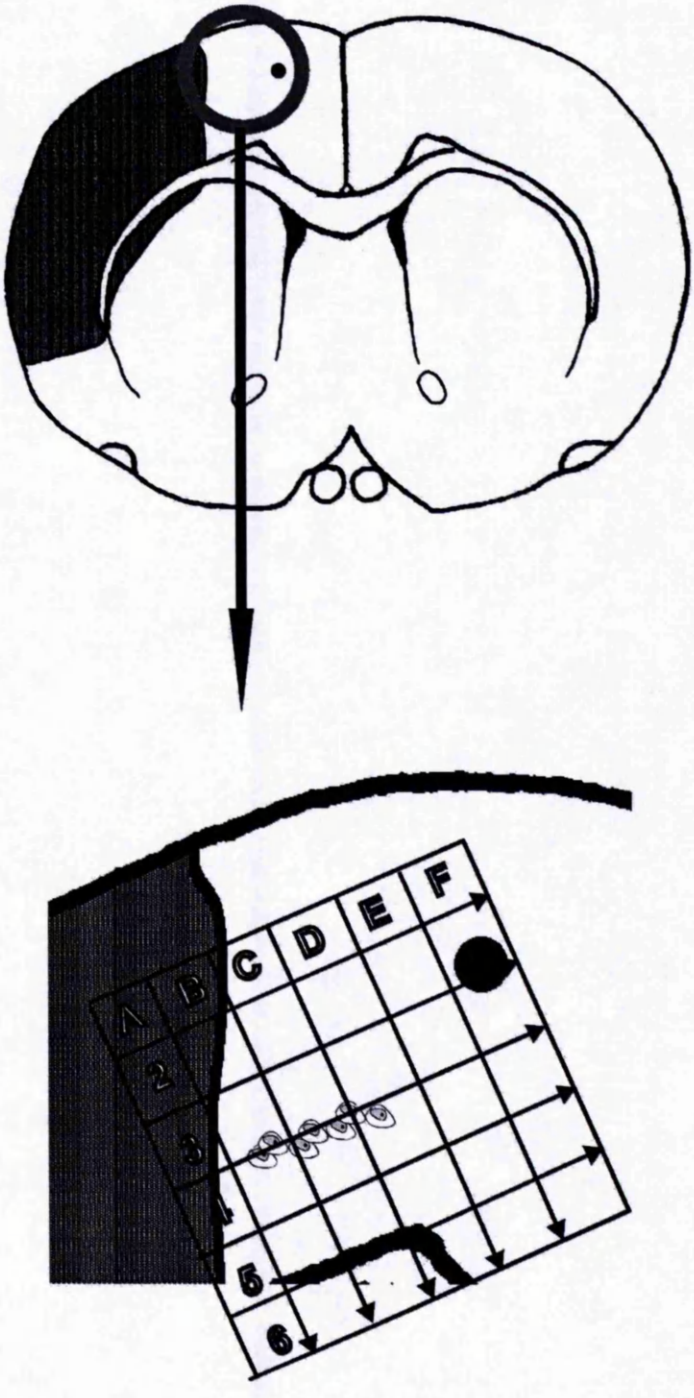

Figure 2.3: Schematic diagram of the determination of the co-ordinates to be applied to brain sections allowing exact matching of fields of view

At x10 magnification, the eyepiece graticule was aligned parallel to the cortical surface, so that the centre point of the eyepiece graticule fell in layer V of the cortex. The co-ordinates at which the reference hole was located were noted, and these co-ordinates were used on every section from the same brain so that exactly the same field of view in all sections could be located.

The formula for determining the total number of neurones in the sample (Konigsmark, 1970) was as follows:

$$N_t = N_s \times P$$

(Where N_t = total neurone population, N_s = neurone population of sample (sum of the counts from each section), P = sampling period (in this case 1 as every section was used)).

The volume of cortex in which cells were counted was calculated as follows (Konigsmark, 1970):

$$V = t_{mm} \times P \times A_s$$

(where t_{mm} = section thickness, P = sampling period, A_s = sum of the areas (of the eye-piece graticule) of sections counted.)

The mean neuronal count/mm^3 (N_v) was obtained by dividing the population estimate N_t by the volume V, and the results expressed in numbers / mm^3. This procedure was repeated for glial cells in layer V of the non-infarcted cortex and pyknotic profiles in layer V of the infarct.

2.7.2 The disector method

The disector method (Sterio, 1984; Gunderson *et al.*, 1988; Coggeshall, 1992) produces an unbiased estimate of the number of cell profiles per unit volume of tissue (N_v). Tissue was processed as for serial-section reconstruction (see Section 2.7.1). Briefly, one coronal slice from the mid-infarct region was selected per animal and embedded in JB-4 resin (Polysciences, Inc., USA). 3μm coronal brain sections were stained with 0.1% toluidine blue. The exact matching of fields of view was ensured by using specified co-ordinates with respect to the reference point (see Figure 2.3). Tissue sections were photographed at a magnification of x40. The disector method was then applied to these photomicrographs (for a full description on the workings of the disector method see

Chapter 3). The disector method was used to estimate the number of neurones and glial cells in layer V of the frontal cortex, and the number of pyknotic profiles in the lesion.

2.8 Horseradish peroxidase (HRP) tracer techniques to study the permeability of the blood-brain barrier

Mice aged either 4-6 months, or 28-30 months, underwent MCAo and were injected with 100mg/kg of type VI Horseradish Peroxidase (HRP; Sigma, UK) in 50µl of 0.1M PBS. Control animals underwent sham operations but the MCA was not occluded. HRP was administered intravenously (iv) via the tail vein, 30 minutes prior to sacrifice at various times following MCAo, or sham operation (30 minutes, 1, 2, 4 and 24 hours, n = 4 at each time point following MCAo, n = 3 at each time point for sham-operation).

The method used for the visualisation of HRP was that described by Broadwell and Brightman (1983). Briefly, animals were fixed by vascular perfusion through the left cardiac ventricle (see Section 2.3.3), using Karnovsky fixative (see Appendix 1) in 0.1M PBS (pH 7.2-7.4). The fixed brain was removed from the skull, rinsed in PBS and 50-60µm coronal sections cut on a vibratome. The sections were rinsed in PBS to wash out any glutaraldehyde to prevent the formation of non-specific reaction products. Peroxidase activity was visualised by incubating the sections, for 20 minutes at room temperature in filtered Fahimi medium (10mg of diaminobenzidine, 10ml of 0.1 M phosphate buffered saline, and 0.2ml of 1% H_2O_2 with a final pH of 7.1-7.4). The incubated sections were rinsed in PBS, mounted on gelatin-coated slides and left to dry overnight. The slides were immersed in xylene for 5 minutes and mounted with a coverslip using DPX.

HRP extravasation was assessed by measuring the area of HRP staining in the brain and expressing it as a % of the left-infarcted hemisphere. All measurements were made using a semi-automated image analysis system (Imagan 2; Leitz, UK).

2.9 Evaluation of glial cell activation, ICAM-1 and IL-1β expression and neutrophil invasion

For evaluation of the time-course for glial cell activation, neutrophil invasion and the expression of ICAM-1 and IL-1β, frozen brain sections were processed using standard immunocytochemical techniques to identify astrocytes, neutrophils or cells expressing ICAM-1 or IL-1β. Lectin histochemistry was used to identify microglia/macrophages.

2.9.1 Tissue preparation

Animals were fixed by vascular perfusion through the left cardiac ventricle (see Section 2.3.3), using 2% paraformaldehyde, lysine and periodate (PLP; McLean and Nakane, 1974; see Appendix 1) containing 0.05% glutaraldehyde 12 and 24 hours after MCAo or immediately following sham surgery (see Section 2.3.2). The brains were removed from the skull and postfixed for a further 6 hours in 2% PLP on a rotator at 4°C. For cryoprotection the brains were left overnight in a tube containing 25% sucrose solution on a rotator at 4°C (until the brain sank to the bottom of the tube). Each brain was then embedded in OCT on a cork block and snap frozen in isopentane, cooled by liquid nitrogen and stored at -80°C until required. 10μm coronal sections were cut using a cryostat (Brightman, UK) at -20 to -24°C and the sections collected onto 3-aminopropylmethoxysilane (APES; Sigma, UK) coated slides (see Appendix 3) and left to air dry overnight prior to immunocytochemical or histochemical staining. Sections from three different levels of the brain were collected corresponding to A: +1.5mm; B: +1.0 mm and C: +0.5 mm relative to Bregma (Sidman *et al.*, 1971).

2.9.2 Immunocytochemical and histochemical staining on frozen sections

All staining was carried out using the avidin-biotin peroxidase method (see

Appendix 6). All primary and secondary antibodies (see Section 2.9.3) were diluted with 0.05M TRIS-buffered saline (TBS; pH 7.6), containing 0.1% bovine serum albumin (TBS/BSA). Briefly, endogenous peroxidase activity was quenched by incubation in 0.3% hydrogen peroxide in 0.05M TBS (15 minutes; room temperature) followed by washes in 0.05M TBS. Sections were incubated serially in 10% normal animal serum (rabbit, donkey or goat as appropriate; 45 minutes; room temperature); primary antibody (120 minutes; room temperature); biotinylated secondary antibody (60 minutes; room temperature), and finally in Vector ABC kit (30 minutes; room temperature; Vector, UK). Sections were washed for 5 minutes in three changes of 0.05M TBS between each incubation, except after the animal sera when there are no washes before application of the primary antibody. 3,3'-diaminobenzidine tetrahydrochloride dihydrate (DAB; 0.025%; Sigma, UK; see Appendix 6) containing 0.5mg of glucose oxidase was used as the substrate to reveal antibody binding in the tissue. Control sections were processed at the same time and in the same way but instead of incubation in the primary antibody the sections were incubated with TBS/BSA. All sections were counterstained with 1% methyl green, dehydrated through alcohols and mounted with coverslips in DPX.

Lectins are multivalent proteins or glycoproteins that are useful probes for glycoproteins or lipids associated with the surfaces of cells. Lectin from *Griffonia simplicifolia* isotype B4 (GSA) was used to identify microglia/macrophages in tissue sections. After quenching endogenous peroxidase activity, sections were incubated in trypsin (Type II; Sigma, UK; 0.25μg/ml trypsin in 0.05M TBS containing 1mM $CaCl_2$ (pH 7.6)) for 5 minutes at 37°C, followed by washes in TBS. Sections were incubated in biotinylated GSA (L-2140; Sigma, UK; 20μg/ml in 0.05M TBS/$CaCl_2$; 120 minutes; room temperature), then processed through Vector ABC kit and DAB as above. GSA was omitted from control sections.

For all stains adult and aged animals from the same time point were stained in the same run, under the same conditions and the same length of time in the chromogen.

2.9.3 Antibodies used

Optimisation of primary and secondary antibody concentrations and incubation times used in staining protocols were determination by checkerboard titrations. The optimal combination of dilutions was represented by the slide with the most intense specific staining and the least amount of background staining. This was done for all antibodies tested. Concentrations of antibodies, animal sera and incubation times are given in Table 2.1.

Localisation of:	Primary antisera	Secondary antisera	Animal serum
Astrocytes	Rabbit anti-GFAP (G-9269; Sigma, UK) at 1:4000	Biotinylated goat anti-rabbit IgG (Vector Laboratories, UK) at 1:200.	Normal goat serum (Sigma, UK).
IL-1β*	Sheep anti-rat IL-1β (S328/B4b/Ap; Steve Poole, NIBSC, UK) at 1:500.	Biotinylated donkey anti-sheep (mouse adsorbed) at 1/500 (Chemicon, UK).	Normal donkey serum (Sigma, UK).
ICAM-1	Rat anti-mouse ICAM-1 (Serotec, UK) at 1:150.	Biotinylated rabbit anti-rat (mouse-adsorbed) at 1/200 (Dako, UK).	Normal rabbit serum (Sigma, UK).
Neutrophils	Rat anti-mouse neutrophil (Serotec, UK) at 1:150.	Biotinylated rabbit anti-rat (mouse-adsorbed) at 1/200 (Dako, UK).	Normal rabbit serum (Sigma).

Table 2.1: Antibody concentrations used for immunocytochemistry
(* This antibody has been shown to cross react with mouse IL-1β in Western blot (Helen Ashdown, personal communication)

2.9.4 Double staining

To determine which glial cell type(s) expressed ICAM-1 or IL-1β, sections were

stained for either GSA, or GFAP (as described above) using nickel DAB as the chromogen. Subsequently all antibodies and DAB used in the first immunostaining were eluted from the brain sections by a 1 hour wash in 0.2M glycine-HCL buffer (pH 2.2; see Appendix 6). The second step was the immunostaining of sections for IL-1β or ICAM-1 (as above but primary antibody incubation was overnight at 4°C), using VIP Vector kit (Vector, UK) as the chromogen, which produces a purple end product.

2.9.5 Cell counts on immunocytochemical and histochemically stained frozen brain sections

To assess possible ageing effects on astrocyte and microglial activation following IBD, cells were counted in the peri-infarct zone and equivalent contralateral region (see Figure 2.4) of 4 month and 26/27 month old mice, 12 and 24 hours post-MCAo and in equivalent regions in sham-operated animals (n = 3 /time point /age). The peri-infarct zone is the transitional zone between the area of total cell death and the area adjacent to the infarct where there is no apparent cell death. The peri-infarct zone (of the frontal cortex) of each section was located by staining the adjacent section with cresyl-violet (see Appendix 2). This region was usually in the frontal cortex. The author conducted counts on immuno-stained sections "blind" and codes were revealed only when all counts had been done. Counts were performed on 3 immuno-stained sections from each of the 3 levels A,B and C, 500μm apart. For cortical counts ten non-overlapping fields of a square eyepiece graticule (Graticules Ltd., UK; area of field of view = 0.0529mm^2) at x40 from the pial surface to the corpus callosum were counted (representing two cortical strips) from each section. Astrocyte counts were also performed in the white matter, which represented two fields of view of the eye-piece graticule (at x40) in the corpus callosum that were in line with the two cortical strips (see Figure 2.4).

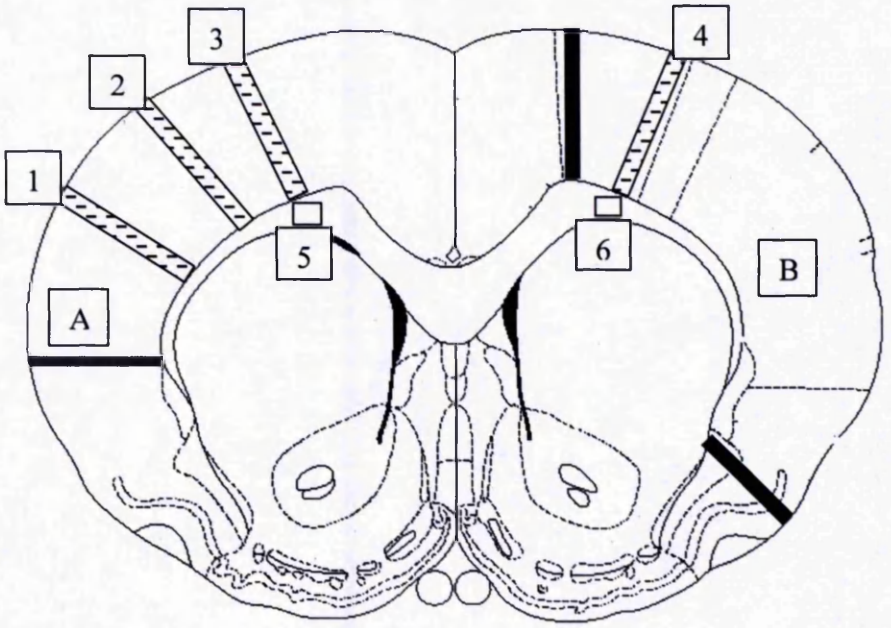

Figure 2.4: Illustration of the areas of brain section where cell counts were performed in order to assess changes in cellular variables following MCAo.

1) central zone of lesion, 2) outer zone of lesion A = region of infarct.
3) peri-infarct zone in frontal cortex and 4) the corresponding area in the contralateral cortex. 10 fields of view per section, representing two cortical strips at x40 (from the pial surface to the corpus callosum) were counted in regions 1-4.
5) peri-infarct zone of white matter (corpus callosum) and 6) the corresponding area in the contralateral cortex. 2 fields of view per section (at x40) were counted in regions 5 and 6. Counts were performed in regions: 1-4 for ICAM-1 vessels, 3 + 4 for microglia, 3 - 6 for astrocytes. Neutrophils counts were done from all cortical regions in B, and the corresponding region in the ipsilateral hemisphere.

The values from the three sections in the same area of each brain were averaged, and the three averages from regions A, B and C summed to give one cell count per animal from 30 fields of view at x40 (total area investigated = 1.59mm^2), or white matter astrocytes from 6 fields of view at x 40 per animal (total area investigated = 0.317mm^2). Only microglia and astrocytes with a clearly identifiable cell body and immuno-positive cytoplasm and cell processes were counted (for microglia at least one cell process). The cells intercepted by the right vertical and top horizontal limits of the eyepiece graticule were included in the counts, those intercepted by the left vertical and bottom limits were not.

This process was repeated to assess possible ageing effects on ICAM-1 positive

vessels and IL-1β positive cells following IBD. In addition to ICAM-1 positive vessel counts in the peri-infarct zone and corresponding area of the ipsilateral cortex, ICAM-1 positive vessels in the central and outer zone of the infarct were counted as above (see Figure 2.4). When one or more vessels were in contact with each other (i.e. smaller vessels branching from a larger vessel) the structure was only counted as one. Using an eye piece micrometer, vessels were separated into those less than 10μm in diameter and those over 10μm. Neutrophil invasion was assessed by counting the number of vascular and parenchymal neutrophils in the ipsilateral and contralateral cortex of each of the three 10μm thick sections from each region (see Figure 2.4). The average values from each of the three regions were summed to give a neutrophil count per 3 sections per animal (total area investigated = 9.787mm^2).

2.10 Data presentation and statistical analysis

All data are presented as the mean (standard deviation; SD) of a number of observations. Statistical advice was given by Dr. Hillier (Medical Statistician, Manchester) and data were analysed using either the Students *t*-test for unpaired data (two-tailed), or two-way analysis of variance (2-way ANOVA), as indicated in the result sections. A probability of less than 0.05 was assumed for statistical significance. Statistical testing was carried out using the package SPSS for Windows (Version 9.0; SPSS Inc., USA). Photomicrographs of brain slices or sections were taken using either Tungsten Ektachrome colour film (100 ASA) or Ilford Delta (100 ASA) black and white film. Colour images were captured with an SV Micro-digital scanning camera (SV Micro, USA) mounted on a MEIJI microscope and processed through Adobe Photoshop (Version 5; Adobe Sytems Inc., USA).

2.11 Summary of animals used in each experiment

Chapter /section	Experiment	Time point	Age of animal	Number
4.1.1 *	Effects of age on infarct volume and swelling volume	24 hours	4-6 month	10
			26-30 month	10
4.1.3	Effects of age on cellular variables	24 hours	4-6 month	7
			26-30 month	7
Ch 5 *	Effects of age on glial activation, ICAM-1 and IL-1β expression and neutrophil invasion	Sham	4-6 month	3
			26-30 month	3
		12 hours	4-6 month	3
			26-30 month	3
		24 hours	4-6 month	3
			26-30 month	3
Ch 6	Effects of age on BBB permeability	1/2 hour	4-6 month	3
			26-30 month	3
		1 hour	4-6 month	3
			26-30 month	3
		2 hours	4-6 month	3
			26-30 month	3
		4 hours	4-6 month	3
			26-30 month	3
		24 hours	4-6 month	4
			26-30 month	4
7.1	Reproducibility of MCAo	24 hours	4-6 month	20
7.2	Effects of central administration of rIL-1ra on infarct volume	24 hours	4-6 month (vehicle)	14
			4-6 month (rIL-1ra)	14
7.3	Effects of central administration of rIL-1ra on cellular variables	24 hours	4-6 month (vehicle)	7
			4-6 month (rIL-1ra)	7
7.4	Effects of peripheral administration of rIL-1ra on infarct volume	24 hours	4-6 month (vehicle)	13
			4-6 month (rIL-1ra)	13

(* MCAo surgery performed by A. Fotheringham; all other surgery performed by author)

Chapter 3

Methodological Considerations

3.0 Introduction

The complex mechanisms involved in the development of IBD and the numerous methods for inducing cerebral ischaemia were discussed in Chapter 1. The overall aim of this thesis was to investigate the cellular responses in IBD and determine if there are any changes with age in these processes. The methods used for the quantification of the resultant brain damage, induced by permanent occlusion of the MCA, throughout this thesis are standard techniques that do not require special attention. More detailed histological assessment and estimates of neuronal and glial cell numbers were performed on toluidine blue stained resin sections. The aim of the experiments described in this chapter was to assess the suitability of the stereological disector method for determining unbiased estimates of cell numbers/unit volume in the mouse brain.

Stereological methods are simple and efficient techniques for quantification of three-dimensional microscopic structures. They are specifically directed to provide reliable data from observations made on two-dimensional sections. For statistical information to be unbaised a few requirements must be fulfilled about the sections and the way they are made (Gunderson, 1988; Coggeshall, 1992). Particle counts (i.e. neurones) are derived from counts of profiles, a profile being a slice of a particle that appears in a histological section. When counting profiles from the field of view, such as from a photograph, artificial boundaries are imposed on the visible part of the section. If all profiles in the photograph were to be counted this would produce a baised estimate of cell number. Therefore profiles must be counted from fields of view using an unbaised counting frame (Gunderson, 1988). The profiles intercepted by the right vertical and top horizontal limits of the photomicrograph are included in the counts, those intercepted by the left vertical and bottom limits are not (see Figure 3.1). A second consideration is how the fields of view are sampled. Fields should be sampled

systematically (every section, every second, every third etc) and independent of their content - and of the observer (Gunderson, 1988). Enough fields of view from the region of interest should be sampled to eliminate any variation from field to field.

The best methods presently available to obtain unbiased estimates of cell numbers, are serial-section reconstruction and the disector method (Sterio, 1984; Coggeshall, 1992). Serial-section reconstruction is very accurate, as there are no assumptions and no sampling, a population is simply reconstructed and the number of particles is then automatically known. However, it is extremely laborious and time consuming as every profile is counted from every section (see Section 2.7.1). The disector method is a much more efficient method for obtaining estimates of cell number as fewer profiles are counted and fewer sections are needed. The disector method identifies profiles in a known volume of tissue by comparing pairs of sections called disectors (see Figure 3.1). These sections are referred to as the reference section and the look-up section, which are not necessarily adjacent serial sections. The look up section must be in exactly the same field of view, a certain depth below the reference section. This depth is determined by the sampling interval used and is the sum of the thickness of the intervening sections. The optimal sampling interval and the number of disectors required are best determined by comparison with serial-section reconstruction values (see Section 3.2). Profiles found in the reference section but not in the look up section are known as *tops* (Q^-) (see Figure 3.1). Only *tops* are counted as this prevents overestimation of cell number. A profile will be discarded from a reference count if its position overlies a profile in the look-up section. Once the *tops* count has been performed on the reference section the corresponding look-up becomes the reference, and a new section is considered, for the next disector pair (see Figure 3.1). From the number of *tops* counted a set of calculations can be applied to produce an estimate of the number of cells/unit volume (see Section 3.2).

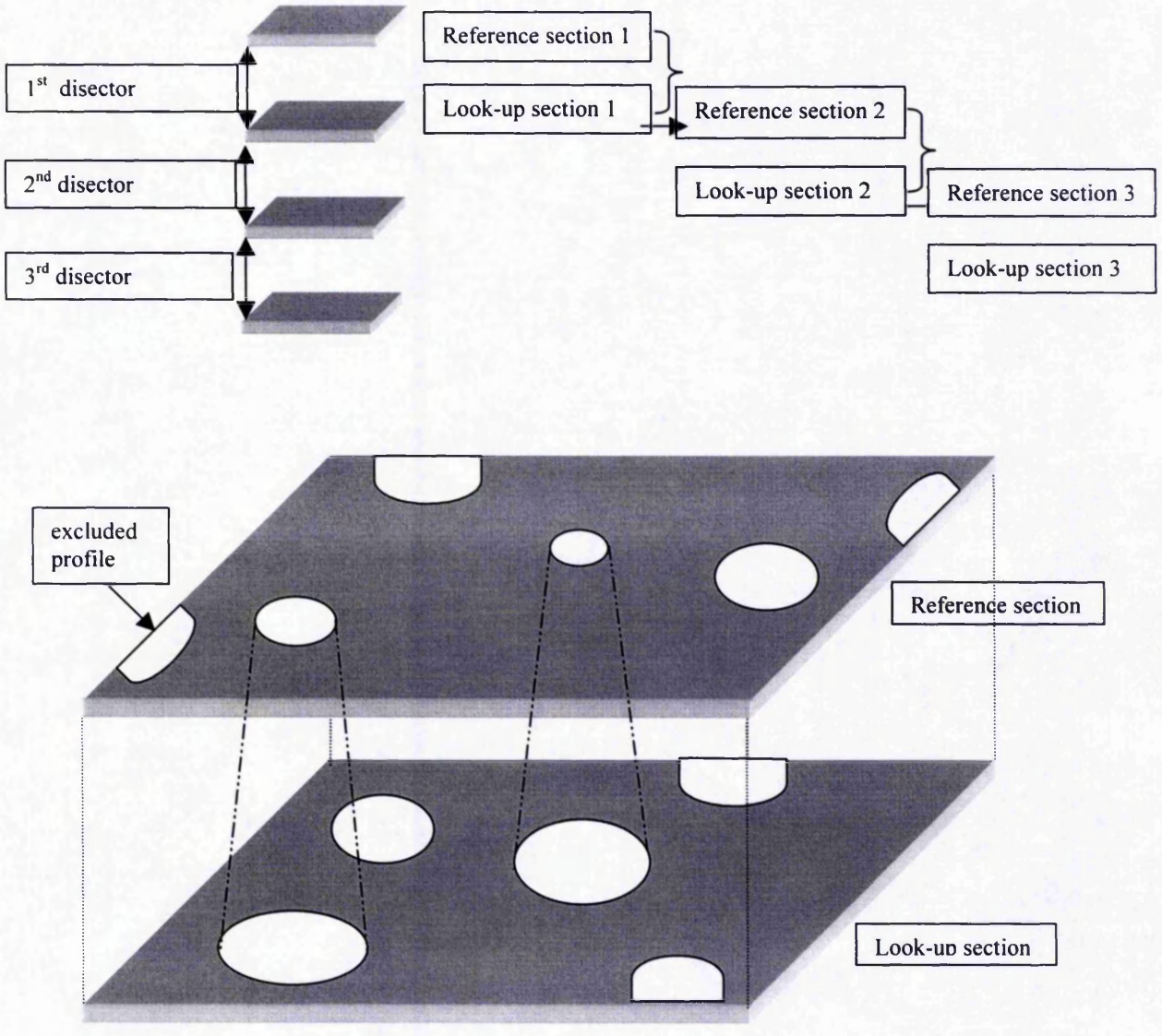

Figure 3.1: Illustration of the disector method showing the sampling sequence and identification of *tops*

The disector method identifies profiles in a known volume of tissue by comparing pairs of sections called disectors. A disector consists of a reference section and a look-up section, which are not necessarily adjacent serial sections. The look up section must be in exactly the same field of view, a certain depth below the reference section. Profiles found in the reference section but not in the look up section are known as *tops* (Q^-). If a profile in the reference section overlies a profile in the look-up it is not counted. Profiles that are intersected by the upper and right edges of the field of view are counted. Those intercepted by the lower and left edges are not counted. The number of *tops* in the reference section above = 3. Once the *tops* count has been performed on the reference section the corresponding look-up then becomes the reference section for the next disector pair.

The only way to verify the values obtained from the disector method are to compare them with those obtained from a serial-section reconstruction (Coggeshall, 1992). It is not necessary to reconstruct a whole population for use as a verification standard, a sample population can be constructed and the verification done on the sample.

Therefore the aims of this chapter were to establish cell number / unit volume using serial-section reconstruction and determine the optimal sampling interval and number of disectors required for subsequent application of the disector method. Finally the cell number estimate/unit volume obtained using the disector method was compared to the serial-section reconstruction to assess its suitability for use in this thesis.

3.1 Determination of neuronal and glial cell number/mm^3 using serial section reconstruction

Profiles of neurones and glial cells in layer V of the non-infarcted region of the ipsilateral frontal cortex were counted from serial sections stained with Toluidine Blue (see Section 2.7.1). Counts were performed on one field of view of an eyepiece graticule at x40 magnification from each section. Profiles intercepted by the right vertical and top horizontal limits of an eyepiece graticule were included in the counts; those intercepted by the left vertical and bottom limits were not. This was repeated for all the serial sections from the brain slice. The exact matching of the field of view in each section was done by using eyepiece co-ordinates with respect to the reference hole (see Figure 2.3). The dimensions of the eyepiece graticule were measured using a stage micrometer and the area of the eyepiece graticule calculated. This was multiplied by section thickness (3μm) and the number of serial sections (n = 22) to determine the total volume in which the cells were counted. The mean cell number/mm^3 was calculated by dividing the total profile count of the sample by the total volume in which the profiles

was counted (Konigsmark, 1970; see Section 2.7.1). From serial-section reconstruction the mean cell number/mm^3 (N_v) in layer V of the non-infarcted region of the ipsilateral frontal cortex was 48053/mm^3 for neurones, and 78870/mm^3 for glial cells.

3.2 Determination of parameters for use in the disector method

The objective of this section is to establish the optimal sampling interval and number of disectors required for application of the disector method. From the serial-section reconstruction, estimates of the total number of profiles in the sample were calculated using every second serial-section, every third serial-section and so on. The formula for determining the total number of profiles in the sample (Konigsmark, 1970; see Section 2.7.1) = profile population of the sample x sampling period (taking every second section =2, every third = 3 etc). Again this is divided by the total volume in which the profiles were counted (see above) to obtain cell number estimates/mm^3, these values are shown below (Table 3.1).

Serial-section reconstruction	**Nv for Neurones**	**Nv (neuro nes) +5%**	**Nv (neuro nes) - 5%**	**Nv for Glial cells**	**Nv (glial) +5%**	**Nv (glial) -5%**
every section	48053	50456	45650	78870	82814	74926
Section interval	**Estimate of Nv for neurones**	**Is estimate within 5% of serial-section Nv using every section**		**Estimate of Nv for Glial cells**	**Is estimate within 5% of serial-section Nv using every section**	
every 2nd	52928	No		80088	Yes	
every 3rd	44397	No		76258	Yes	
every 4th	50142	Yes		85660	No	
every 5th	50490	No		84441	No	

Table 3.1: Nv (mean cell number/mm^3) obtained from serial-section reconstruction using every nth section (where n = 1 to 5).

By comparing the estimates of Nv (using every nth sections, where n = 2 to 5) with the value obtained from the serial-section reconstruction the sampling interval

giving cell number estimates/mm^3 ± 5% of the serial section value can be found. This sampling interval was found to be every fourth section for neurones, and every second or third section for glial cells (see above, Table 3.1). The sampling interval used in this study was every fourth section for neurones and every second section for glial cells.

To determine how many disectors (pairs of sections) profiles need to be counted, the disector method was applied to the sections used in the serial-section reconstruction. Nv was calculated using one, two, three and so on disectors. For this photomicrographs of layer V of the non-infarcted region of the ipsilateral frontal cortex were taken from the serial sections. An acetate sheet was placed over the reference section photomicrograph and profiles of the cells of interest outlined onto it. This acetate sheet was then placed over the look up section photomicrograph. Profiles found in the reference section photomicrograph but not in the look up section photomicrograph were counted (these are known as tops Q^-). Profiles intercepted by the right vertical and top horizontal limits of the photomicrograph were included in the counts; those intercepted by the left vertical and bottom limits were not included. The total volume (V_{dis}) in which the profiles were counted was calculated by (Sterio, 1984):

$V_{dis} = h \times a_{dis}$ (area of photomicrograph);

(where h = thickness of the section if sections are adjacent, if there are intervening sections these must be added; a_{dis} = area of the photomicrograph.).

The mean cell number/mm^3 (Nv) was calculated by (Sterio, 1984):

$$Nv = \sum Q^- / \sum V_{dis}$$

The value for Nv was calculated using 1 to 6 disectors and are presented below (Table 3.2). By comparing the estimates of Nv using different numbers of 'disectors' with the

value obtained from the serial-section reconstruction the number of 'disectors' giving cell number estimates/mm^3 ± 5% of the serial section value can be found. From table 3.2 it can be seen that 4, 5 or 6 'disectors' are required to give neuronal and glial cell estimates within 5% of the value obtained from serial-section reconstruction. Since 5 'disectors' gave an estimate closest to the value obtained from serial-section reconstruction this was chosen for subsequent applications of the disector method. From the disector method, using 5 'disectors' the mean cell number/mm^3 (N_v) in layer V of the non-infarcted region of the ipsilateral frontal cortex was 47886/mm^3 for neurones, and 78159/ mm^3 for glial cells.

Serial-section reconstruction	**Nv for Neurones**	**Nv (neurones) +5%**	**Nv (neurones) -5%**	**Nv for Glial cells**	**Nv (glial) +5%**	**Nv (glial) -5%**
every section	48053	50456	45650	78870	82814	74926
No. of 'disectors'	**Estimate of Nv for neurones**	**Is estimate within 5% of serial-section Nv for neurones**		**Estimate of Nv for Glial cells**	**Is estimate within 5% of serial-section Nv for glial cells**	
1	41281	No		55042	No	
2	45409	No		68802	No	
3	43116	No		71554	No	
4	47473	Yes		77058	Yes	
5	47886	Yes		78159	Yes	
6	47703	Yes		76141	Yes	

Table 3.2: Nv obtained from the disector method using different numbers of 'disectors' (1 to 6) on sections from the serial-section reconstruction.

3.3 Discussion

Although serial-section reconstruction provides the most accurate particle count/mm^3, this study shows that the resulting counts obtained from the use of the disector method provided an accurate estimate (± 5%) of the 'true' cell number/mm^3. The disector method is later used in Chapters 4 and 7. The disector method has the advantage that it is much less laborious and considerably quicker than the serial section

reconstruction (Coggeshall, 1992). In this study 3μm was chosen as the section thickness, as section thickness for use in the disector must be less than the height of the particle in the direction perpendicular to the disector (only 1/3 the size of the particle). Another main requirement of the disector is that the *top* (profile of the particle of interest) must be unique and recognisable for it to remain in a fixed position independent of the direction of the section (see Sterio, 1984; Gunderson *et al.*, 1988). These conditions can be met in mononuclear cells (neurones and glial cells) and even more efficiently in cells with just one nucleolus (such as neurones).

In summary, the data presented in this chapter confirms the validity of the disector method for reliable estimates of neuronal and glial cell numbers in mouse brain tissue.

Chapter 4

Effects of ageing on cellular variables, and infarct volume following permanent MCAo

4.0 Introduction

Stroke is a disease associated with old age but most *in vivo* experimental studies of focal cerebral ischaemia, including the evaluation of neuroprotective agents, have involved the use of young adult animals. Several editorials have highlighted the need to focus on the correct age category of animal for use in experimental research on ischaemia (Millikan, 1992; Rosenblum, 1995; Koehler, 1996). The effects of age on infarct volume have produced differing results. Davis *et al.,* (1995) reported that infarct volumes were significantly higher in aged rats after permanent MCAo. Similarly, after transient forebrain ischaemia in spontaneously hypertensive rats (Yao *et al.*, 1993), and more recently in aged Wistar rats (Sutherland *et al.*, 1996) there was an age-related increase in infarct volume. Others have recorded no change in infarct volume with age after permanent ischaemia (Duverger and MacKenzie, 1988; Fotheringham *et al.*, 2000). An increase in the volume of brain water was observed by Fotheringham *et al.* (2000) in aged mice after ischaemia and this study is the only report to correct infarct volume for the effects of oedema. It is difficult to speculate what results would have been obtained by the earlier reports had they corrected for the effects of oedema. Although the effects of age on infarct volume have been examined, the underlying morphological changes in neurones and glial cells with age have not been investigated.

There are several age-related changes in the brain that could affect the ischaemic process and the outcome of stroke. These include age-related alterations in neuronal and glial cell structure, function and number, and changes in the cerebrovasculature and BBB (see Section 1.7; Mooradian, 1988; 1994; Finch, 1993) all of which may influence the brain's cellular response to injury. These changes are not universal and age-related changes in neuronal and glial cell number are often species and strain specific (Flood

and Coleman, 1988). Therefore detailed assessment of cellular changes occurring with ageing are necessary before cellular changes after injury can be compared in young adult and aged animals. Different layers of the cerebral cortex contain different cell densities, therefore it is important that comparisons of cell number are done from the same cortical layer (Terry *et al.*, 1987; Peinado *et al.*, 1997). Since layer V of the cerebral cortex contains large pyramidal cells and is easily identifiable from other regions this was the area chosen in this study. The aims of this chapter were to examine the effects of age on 1) infarct volume and swelling volume following permanent MCAo, 2) neuronal and glial cell number in layer V of the cerebral cortex.

4.1 Results

4.1.1 Effects of age on infarct volume and swelling volume 24 hours after MCAo

The objective of this study was to determine the effects of age on infarct volume and swelling volume following permanent MCAo. Brain sections used for the measurement of infarct and swelling volume in this section were obtained from a study in this laboratory comparing permanent MCAo induced by two different methods (intraluminal filament occlusion or via craniotomy with electrocoagulation) in young adult and aged animals (Fotheringham *et al.*, 2000). Only tissue from animals aged 4-6 months (adult) and 26-30 months (aged) from the MCAo (via craniotomy, see Section 2.3.2) part of the study were examined. Infarct volume was measured 24 hours after MCAo, on brain sections stained with TTC (Section 2.5.2), using a semi-automated image analysis system (Imagan 2; Leitz, UK). The data were analysed using the Students *t*-test for unpaired data (two-tailed) and are presented as the mean infarct

volume (mm^3) ± S.D, or mean swelling volume (mm^3) ± S.D. The adult mice showed no mortality over the 24 hours after surgery to induce IBD, however, one aged mouse did not recover from anaesthesia. Aged animals showing obvious signs of pathology (external or internal tumors found at postmortem) were excluded from the study.

There was no significant difference in the weights of the two groups of animals (mean weight adult = 30.53 ± 2.55, compared with 30.49 ± 3.83 in aged mice; t = 0.03, df = 18, p = 0.978). With age there was a significant increase in infarct volume. The mean infarct volume in adult mice was 13.18 mm^3 ± 6.84 (n = 10), compared with 20.04 mm^3 ± 7.33 (n = 10) in aged mice (t = 2.17, df = 18, p = 0.044). This age-related increase in infarct volume was predominantly a reflection of more extensive cortical infarction in the aged animal. There was no significant age-related increase in the volume of swelling following MCAo. The mean swelling volume in adult mice was 6.85 mm^3 ± 4.11 (n = 10), compared with 6.52 mm^3 ± 6.71 (n = 10) in aged mice (t = 1.73, df = 18, p = 0.900).

4.1.2 Histology 24 hours post MCAo

Histological examination of TTC stained coronal sections from animals that underwent MCAo revealed a consistent ischaemic zone (area of no staining) 24h after MCAo in the left cerebral hemisphere (see Figure 4.1). The infarct exhibited damage throughout the cortex from the mid dorsal neocortex to the lateral part of the piriform cortex; typically extending from the meningeal surface to the radiation of the corpus callosum, and occasionally the infarct included the outer margin of the caudate putamen. No such ischaemic zone was seen in sham-operated animals or in the contralateral cortex of experimental animals. The pattern of ischaemic damage in young adult and

aged animals was typical of the field of distribution of the left MCA, with aged animals having more extensive cortical damage (see Figure 4.2). On histological assessment using toluidine blue stained resin sections, there was a clear demarcation between the lesioned and non-lesioned cortex in both age groups at 24 hours, and the histological profiles of adult and aged animals were similar (see Figure 4.3).

On examination of toluidine blue stained resin sections, the infarcted area contained very few neurones, and surviving neurones were found mainly on the edges of the infarct. These remaining neurones were shrunken, with perineuronal vacuoles and condensed chromatin, often surrounded by a vacuolated neuropil. The infarct mostly consisted of small cell profiles with a small, dark, pyknotic nucleus surrounded by a vacuolated neuropil and no cytoplasm. These profiles (pyknotic profiles) are typical of cells having undergone ischaemic cell death (see Figure 4.4). Other cell types in the infarct had the morphological characteristics of *red neurones* and some cells contained fragments of condensed chromatin, similar to those observed in apoptotic cells (see Figure 4.4). These other cell types were present in very small numbers (see section 4.1.3.3). Occasionally the outer margin of the ipsilateral caudoputamen was slightly vacuolated and contained a few shrunken neurones, whereas the contralateral caudoputamen showed normal morphology. In the non-lesioned area of the ipsilateral cortex and in the contralateral cortex of experimental animals, large healthy neurones and glial cells were present (see Figure 4.4). The only exception to this was in one animal aged 30 months, which showed abnormal microvacuolations in the parenchyma around vessels in the contralateral cortex (see Figure 4.5). In this region there was also an increased distribution of glial cells, due to the extensive nature of this pathology it was excluded from the study.

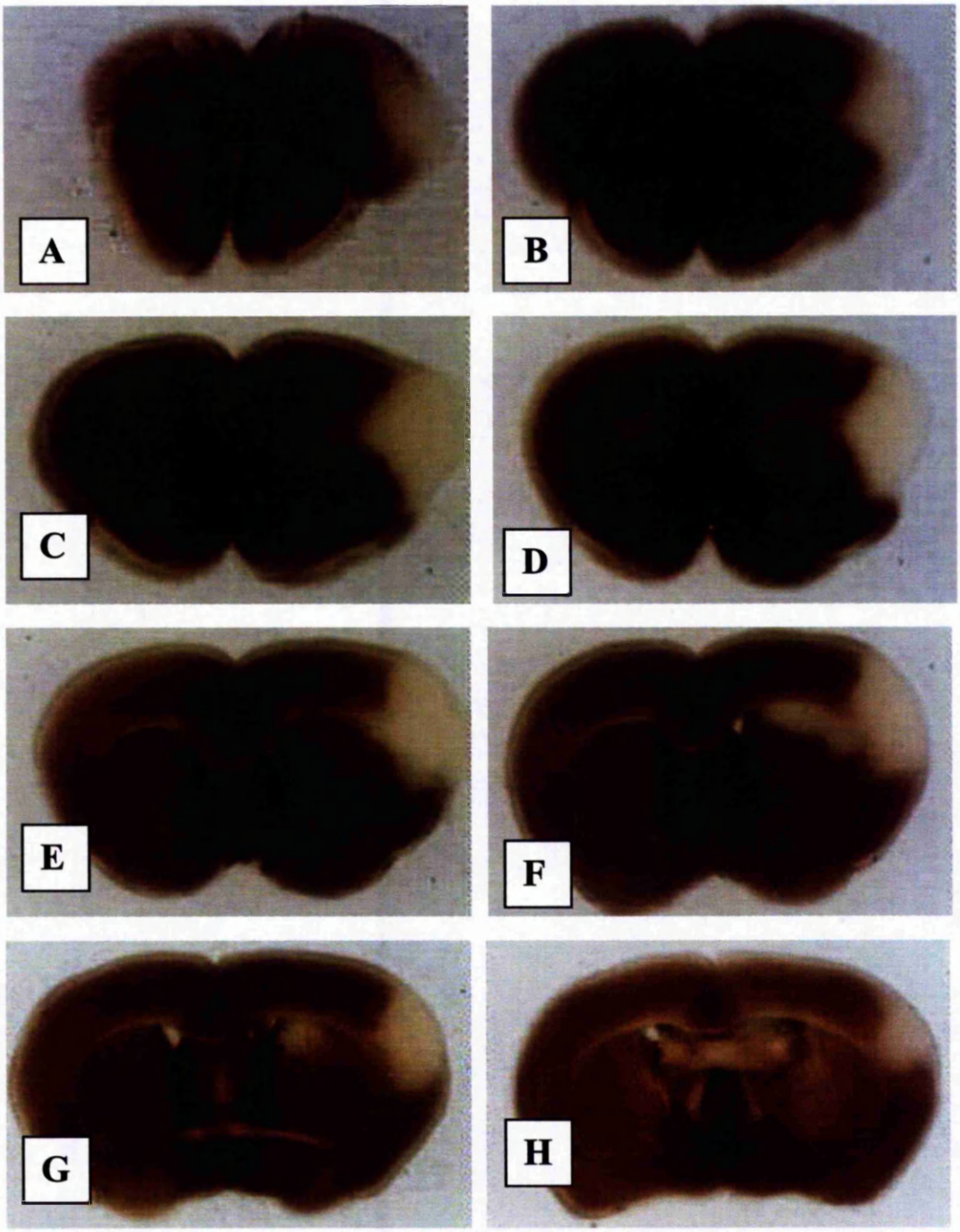

Figure 4.1: Photographs illustrating the distribution of a cerebral infarct in a 6 month animal 24 hours after MCAo on 500μm brain slices stained with TTC.

TTC stains viable cells red/purple, the infarcted area remains unstained. Rostro-caudal sequence (A-H), dorsal surface uppermost. Magnification x 6 Left hemisphere is shown on right.

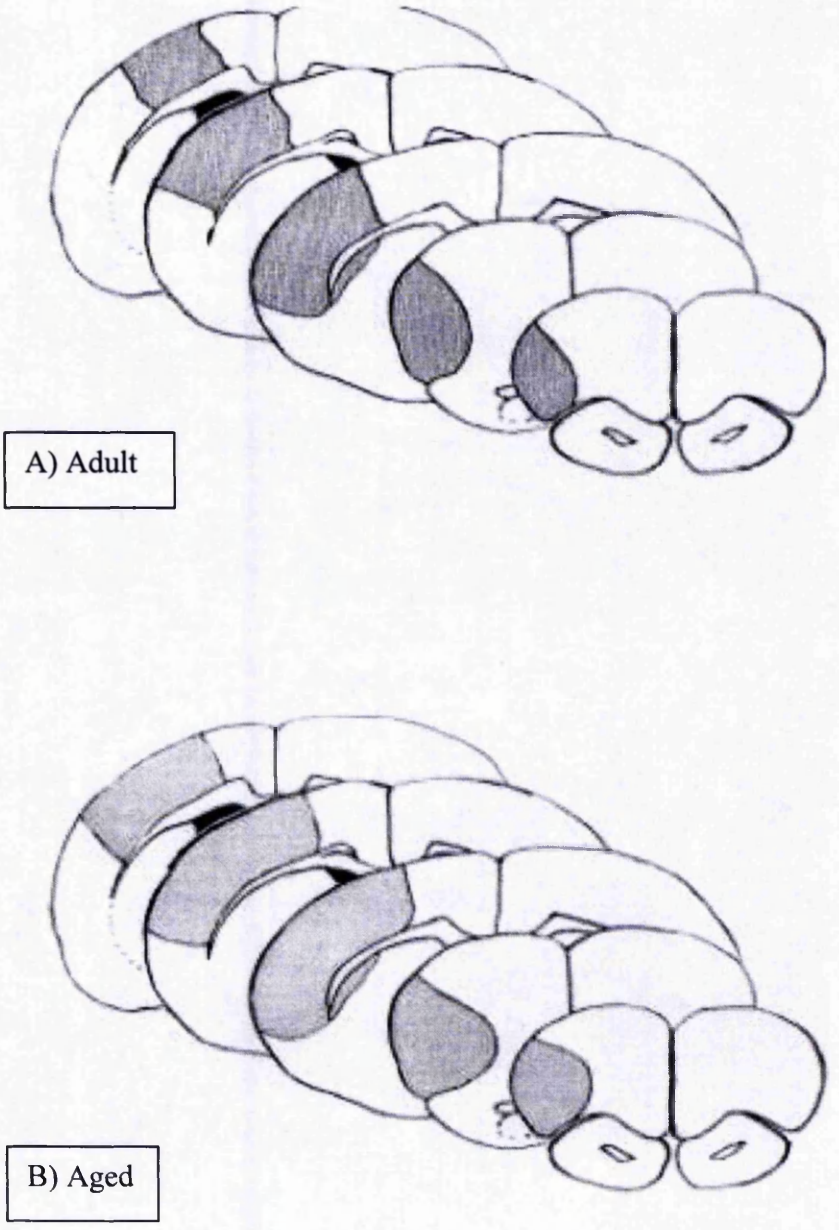

Figure 4.2: Illustration of the typical distribution of areas of damage 24 hours after MCAo in young adult (4-6 month) and aged (26-30 month) animals

On 500μm brain slices as translated onto stereotaxic brain maps (not all maps are shown) in A) adult and B) aged animals. Shaded regions indicate areas of infarcted tissue.

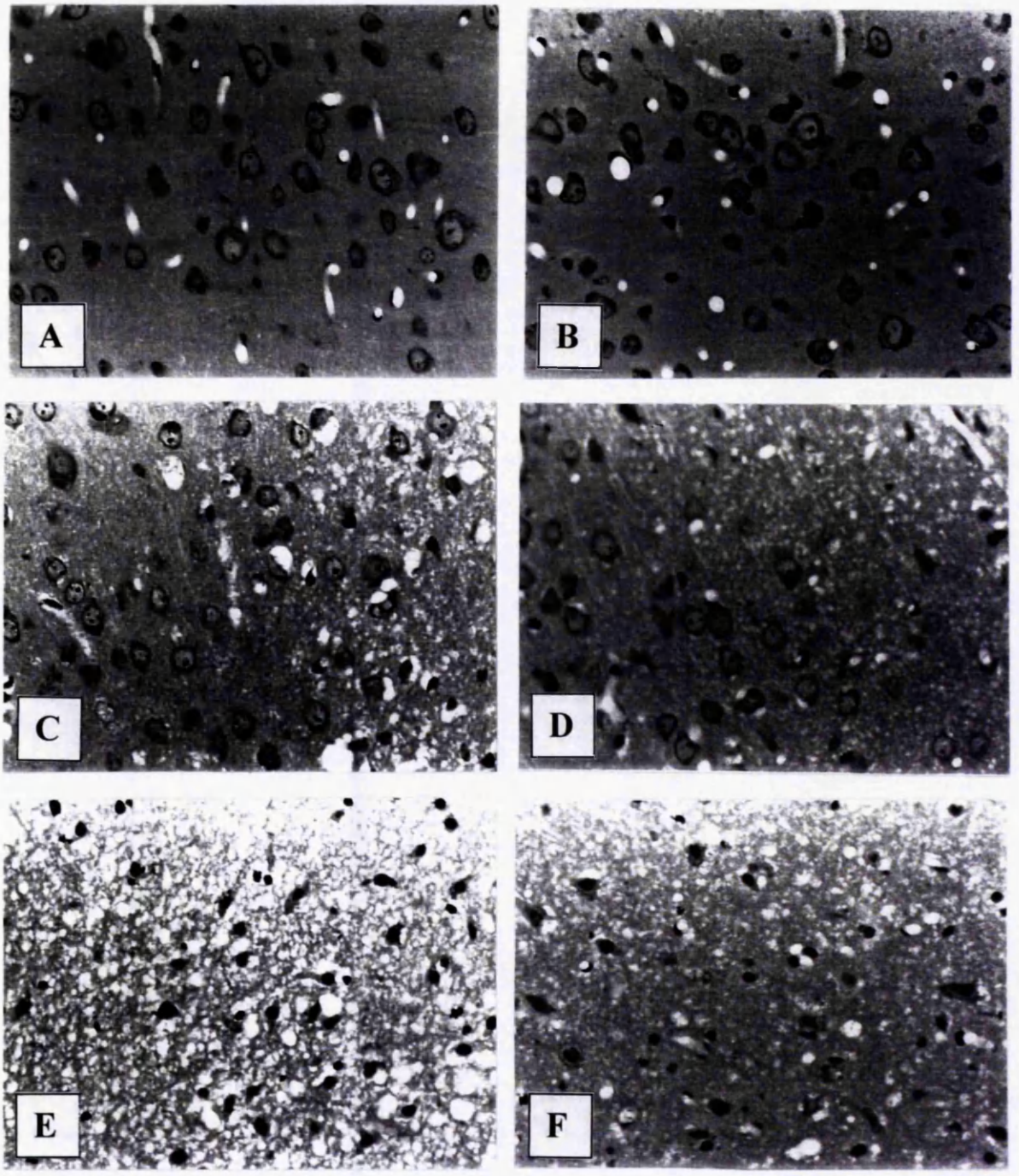

Figure 4.3: Photomicrographs of layer V of the frontal cortex in an adult (6 month) and aged (28 month) animal 24 hours after MCAo on 3μm resin sections stained with toluidine blue.

A-B) Appearance of neurones and glial cells in the non-infarcted area of the ipsilateral frontal cortex in A) adult and B) aged. C-D) Peri-infarct zone of C) adult and B) aged, there is a clear demarcation of the infarct in both ages. E-F) Pyknotic profiles in the infarct of E) adult and F) aged. Note that the histological profiles of adult and aged animals are similar. (Scale bars = 40 μm).

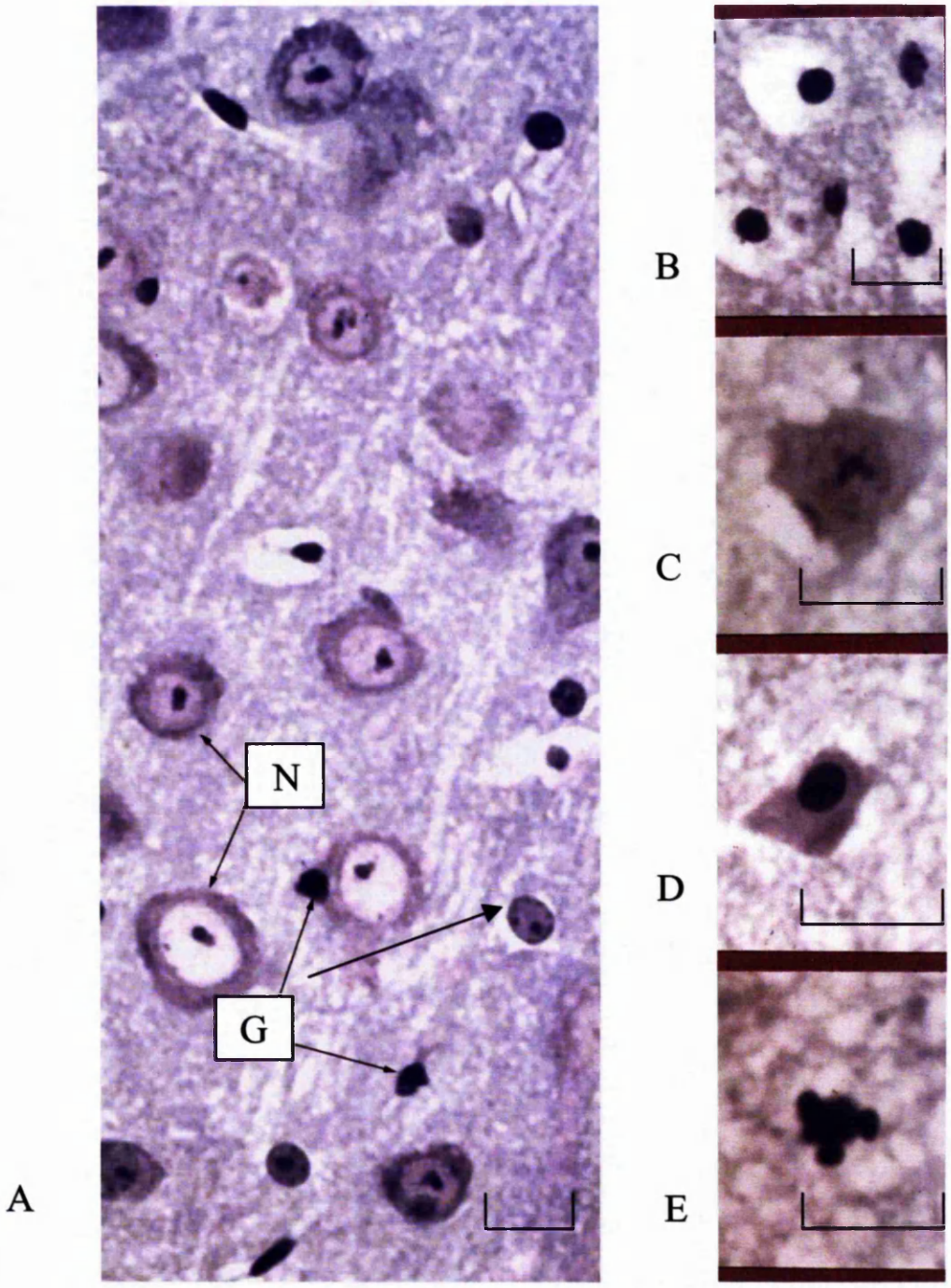

Figure 4.4: Photomicrographs of the various cell types found in layer V of the frontal cortex of a 6 month-old mouse 24 hours after MCAo on 3μm resin sections stained with toluidine blue.

Appearance of A) normal neurones (N) and glial cells (G) in the non-infarcted area of the ipsilateral cortex, B - E) cell profiles typical of having undergone ischaemic cell death in the infarct, B) pyknotic profiles C) non-dense profile, D) red-neurone-like profile E) apoptotic-like profile. Scale bar = 10 μm

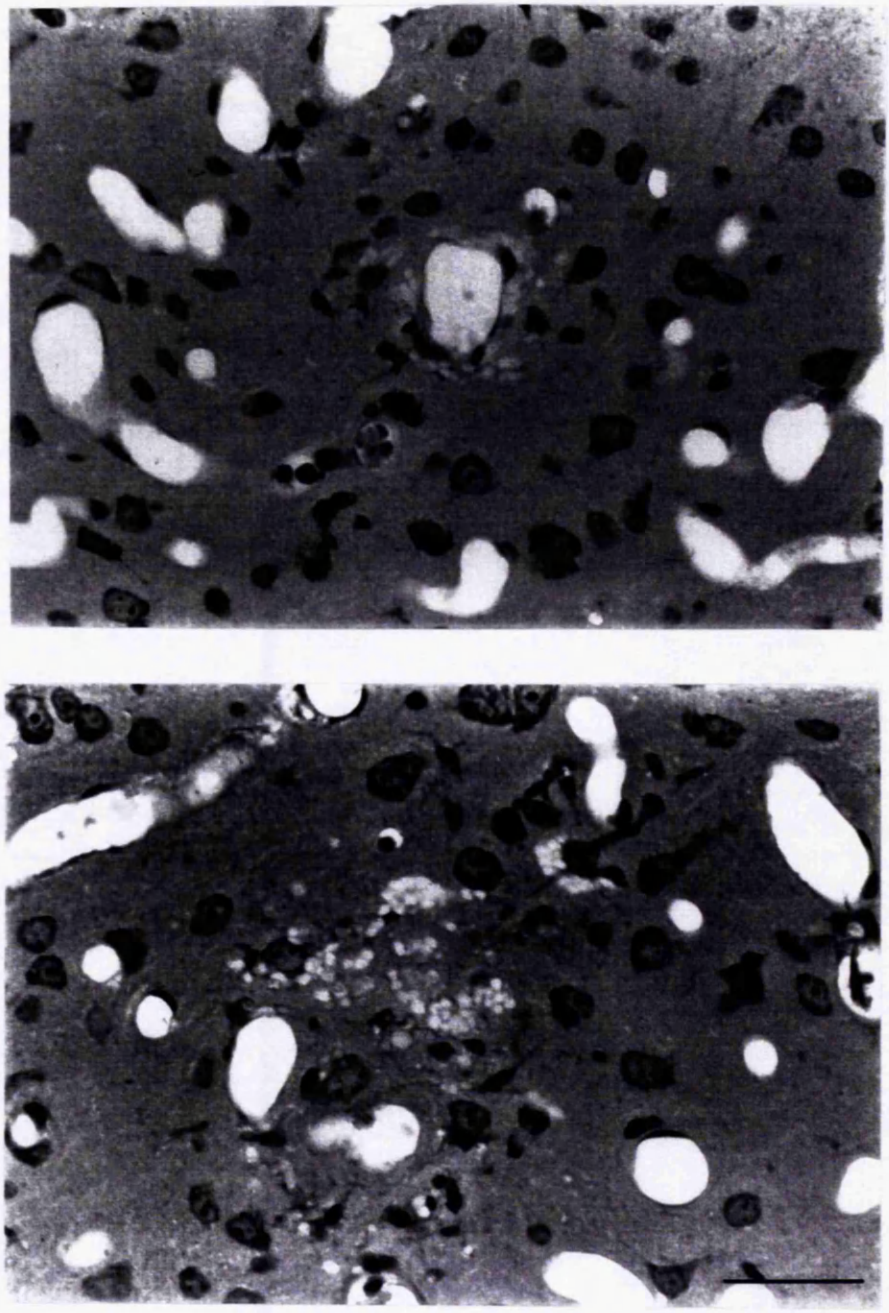

Figure 4.5: Photomicrographs of abnormal histology in layer V of the contralateral frontal cortex of an aged (30 month) mouse 24 hours after MCAo, on 3μm resin sections stained with toluidine blue.

The appearance of abnormal micro-vacuolations in the parenchyma around vessels, with an increase in the distribution of glial cells in this area. Due to the extensive nature of this pathology it was excluded from the study. (Scale bar = 40 μm).

4.1.3 Effects of age on cellular variables

To determine if age affected the number of different cell types found in both the cortex and the infarct, animals aged 6 months (adult, n = 7) and 28-30 months (aged, n = 7) were terminally anaesthetised 24 hours after MCAo and perfuse fixed transcardially. The brains were resin embedded and the disector method applied to 3μm resin sections stained with toluidine blue (see Chapter 3). Serial reconstruction of brain sections enabled parameters to be established for use in the disector method (see Chapter 3). Nv was calculated for neurones and glial cells in layer V of the frontal cortex adjacent to the infarct and pyknotic, apoptotic-like and non-dense/red neurone-like profiles in layer V of the lesioned cortex. Only neurones whose nucleoli were clearly visible, and glial cells with a well-outlined nucleus were included in the counts. Glial counts included astrocytes, oligodendrocytes and microglia. The data are presented as the mean cell count/mm^3 (Nv) ± S.D, and were analysed using the students *t*-test.

4.1.3.1 Neuronal and glial cells counts.

There was no significant difference in the number of neurones/mm^3 in layer V of the non-lesioned area of the ipsilateral cortex, between adult and aged animals (see Table 4.1). There was however a highly significant increase (35%) in the number of glial cells/mm^3 in layer V of the non-lesioned area of the ipsilateral cortex, between adult and aged animals (see Table 4.1). Since neuronal number remained constant, and glial cell numbers increased with age, the neurone:glia ratio was examined. There was a highly significant reduction (27%) in the neurone:glial cell ratio with age (see Table 4.1).

Cell Variable	Young adult animals	Aged animals	Students *t*-test
Nv neurones	46699 ± 5839	45846 ± 5766	t = 0.275, df = 12, p = 0.78
Nv glial cells	67374 ± 7583	91407 ± 10095	t = 5.036, df = 12, p <0.001
Neurone: glial cell ratio	0.696 ± 0.079	0.506 ± 0.078	t = 4.51, df = 12, p < 0.001

Table 4.1: Effect of age on mean neuronal and glial cell counts/mm^3 and neurone:glial cell ratio in layer V of the frontal cortex of young adult (4-6 month, n =7) and aged (26-30 month, n =7) mice.

4.1.3.2 Neuronal area and maximal neuronal nuclear diameter

To examine if there was any neuronal atrophy with age, the mean neuronal area (of neuronal soma and nucleus) and maximal neuronal nuclear diameter were measured on the same sections used to determine neuronal number. Neurones with a prominent nucleolus were selected and the area (μm^2) of the neuronal cytoplasm (and nucleus), and the maximal neuronal nuclear diameter (μm) were measured using Imagan 2 (Leitz, UK) image analysis software. The results are presented as the mean cell measurement ± S.D.

There was no significant difference in the mean neuronal area (μm^2) or the mean maximal neuronal nuclear diameter (μm) between adult and aged mice (see Table 4.2).

Cell Variable	Young adult animals	Aged animals	Students *t*-test
Mean neuronal area (μm^2)	137.6 ± 11.9	120.7 ± 18.3	t = 1.918, df = 12, p = 0.084
Maximal neuronal nuclear diameter (μm)	13.6 ± 0.32	12.6 ± 0.53	t = 1.618, df = 12, p = 0.137

Table 4.2: Effect of age on mean neuronal area (μm^2) and maximal neuronal nuclear diameter (μm) in layer V of the frontal cortex of young adult (4-6 month, n =7) and aged (26-30 month, n =7) mice.

4.1.3.3 Cell counts in the lesioned cortex of young adult and aged animals

There were no significant differences in the numbers of pyknotic, apoptotic-like or non-dense/ red neurone-like profiles per mm^3 in the lesioned cortex between adult and aged animals (see Table 4.3).

Cell Variable	Young adult animals	Aged animals	Students *t*-test
Nv pyknotic profiles	39358 ± 7968	39927 ± 5375	t = 0.145, df = 10, p = 0.888
Nv apoptotic-like profiles	569 ± 570	488 ± 436	t = 0.279, df = 10, p = 0.787
Nv for red neurone-like/ non-dense profiles	3496 ± 570	3171 ± 740	t = 0.852, df = 10, p = 0.414

Table 4.3: Effect of age on mean pyknotic, apoptotic-like and red neurone-like/ non-dense profile counts/mm^3 in the lesioned cortex of young adult (4-6 month, n =7) and aged (26-30 month, n =7) mice.

Since the neuronal population does not differ significantly between adult and aged mice, and there was an age-related increase in infarct volume, it would follow that there are more neurones lost with age following MCAo. By multiplying the mean neuronal number from each age group by the corresponding mean infarct volume, an estimate of the number of neurones lost in the infarct was found to be 898,120 in the adult and 1,126,345 in the aged mice.

4.2 Discussion

4.2.1 Effects of age on infarct and swelling volume following permanent MCAo

In this study C57/Icrfa^t mice were chosen due to their low incidence of spontaneous cancers and the similarity of their survival curve to that of humans

(Rowlatt, 1976). All animals used in this study were reared and maintained under specific pathogen free barrier husbandry conditions to ensure animals were free from infections or illness. The age at which an animal is considered to be aged varies according to the species and strain used, and the working definition of aged is above the 50% survival (Coleman and Flood, 1987; Miller and Nadon, 2000). Animals aged 26 months or over were used in this study, as this represents an aged population of mice obtained from survival curves for this species (maximal life expectancy = 38 months, mean life expectancy = 26 months; Davies and Schofield, 1980).

This study showed that there was a significant age-related increase in infarct volume following permanent occlusion of the left MCA. This supports an earlier study by Davis *et al.*, (1995) on the rat recording an increase in infarct volume in aged animals (28 month or over) after permanent MCAo (Davis *et al.*, 1995). However, permanent MCAo in Fischer-344 rats was not associated with an age-related increase in infarct volume (Duverger and Mackenzie, 1988). As pointed out by the authors the aged animals used in their study were only 20 months of age and this is below the 50% survival age for this strain. Other methods of inducing ischaemia have also produced variable results. Sutherland *et al.* (1996) showed there was an age-related increase in striatal and cortical infarct volume in rats (26-28 months) following forebrain ischaemia, induced by bilateral occlusion of the common carotid arteries. However, in transient focal ischaemia, induced by the intraluminal filament technique only striatal infarct volume increased with age (Sutherland *et al.*, 1996). A study in this laboratory comparing the effects of permanent ischaemia induced by two different methods (via craniotomy and electrocoagulation or intraluminal filament occlusion) in the mouse, found no significant difference in infarct volume with age when assessed using a more complex analytical approach combining the data from both methods of occlusion (Fotheringham *et al.*, 2000). Although no age-related difference was observed in the

volume of swelling after permanent MCAo in the present study, intraluminal filament MCAo in the mouse was associated with a significant age-related increase in the volume of swelling (Fotheringham *et al.*, 2000). The discrepancy in the effects of age on swelling volume may be related to the model used, and possibly by the high variation (higher than the mean) observed in swelling volume in aged animals in the present study which may have masked any possible difference. Assessment of oedema using the more sensitive wet/dry brain weights showed that the brains from aged animals take in more water irrespective of the method used to induce cerebral ischaemia (Fotheringham *et al.*, 2000). Comparisons on the effects of age on infarct volume are difficult as all the investigations differ in some fundamental way. With the exception of Fotheringham *et al.* (2000), the other mentioned studies did not correct infarct volume for the effects of oedema, or comment on the health status of the animals (Duverger and Mackenzie, 1988; Davis *et al.*, 1995; Sutherland *et al.*, 1996). Oedema has been reported to overestimate infarct volume by as much as 20% (Brint *et al.*, 1988; Lin *et al.*, 1993), therefore the age-related increase in oedema may cause more of an overestimate of infarct volume in aged animals compared to young animals. Other factors that may contribute to discrepancies between the studies include differences in the methods used to induce ischaemia, analysis of infarct volume, or the use of different strains of animal.

The mechanism(s) behind the age-associated increase in infarct volume found in this study are not known, but there are several documented changes that occur during ageing in rodent and human brains that could affect the ischaemic process and therefore, infarct volume (see Section 1.7). These include structural changes in the BBB and the accumulation of lipid peroxidation by-products that could effect the permeability of the BBB following injury (Mooradian and Smith, 1992; Mooradian, 1994; see Section 1.7.2). Other contributing factors may be related to functional deficiencies in the

handling of intracellular calcium (Verkhratsky and Toescu, 1998; see Section 1.7.1), and the diminished antioxidant defence mechanisms found in the aged brain (Bondy and LeBel, 1993). There are several morphological changes in neurones and glial cells with age, which may predispose them to increased damage following injury or affect their responses to injury (see Section 1.7 and below).

4.2.2 Effects of age on cellular variables

Neuronal loss in ageing humans has been an important and controversial subject of study for many years, and it was a long-standing belief that widespread cell death occurred in the human brain (see Johnson and Finch, 1996; Wickelgren, 1996). But better methods of identifying normal subjects from those with neurodegenerative diseases, and better quantitative methods (unbaised stereological techniques) have challenged this notion. It is now generally accepted that the loss of large numbers of neurones is doubtful with advancing age, however, there may be some attrition, but it is of a much smaller magnitude than originally thought (Johnson and Finch, 1996; Wickelgren, 1996; Peters *et al.*, 1997). If neuronal degeneration does occur with increasing age this may suggest that aged neurones are more susceptible to neurodegeneration following injury. Therefore this study examined the effects of age on the neuronal and glial cell populations of layer V of the frontal cortex, and the number of pyknotic profiles per mm^3 in the infarct in C57/Icrfa^t mice.

The present study found no significant differences in the numbers of neurones/mm^3 in layer V of the frontal cortex, or pyknotic profiles/mm^3 in the infarct with age. However, there was an age-related increase in the number of glial cells/mm^3 in layer V of the frontal cortex, and a significant reduction in the neurone:glial cell ratio with age. Assuming that ageing has a similar effect on the neuronal populations in other regions of the cerebral cortex ie. a stability in neuronal number, the age-related

increase in infarct volume suggests that more neurones were lost in aged animals after MCAo.

The data presented in this chapter are consistent with other reports finding no significant difference in the number of neurones/mm^3, and a significant increase in the number of glial cells/mm^3 with age in layer V of the frontal cortex between 3 and 24-30 month-old rats (Peinado *et al.*, 1993; 1997). These studies examined wax sections and used a different method of quantification (non-unbaised stereological) to this study. It should be noted however, that the health status of these rats was not defined. In contrast, Amenta *et al.* (1994) reported a decrease in the number of neurones/mm^2, but found a significant increase in glial cells/mm^2 in the frontal cortex of aged Sprague-Dawley rats maintained under barrier conditions. Cells were counted from resin sections using a semi-automated image analysis system, and random fields from layers II to V were counted. Therefore this study did not separate counts from the different cortical layers but grouped them (Amenta *et al.*, 1994). Terry *et al*, (1987) found no change in neuronal numbers but an increase in glial cells in layers I to VI of the frontal cortex in humans, using a semi-automated image analysis system where cells were detected by the density of their cytoplasm in wax sections. Neuronal numbers have been reported to remain constant with age in several other diverse cerebral cortical regions. C57Bl/6Nnia mice reared under barrier conditions showed no loss of neurones with age in the basal forebrain using a non-stereological method (Hornberger *et al.*, 1985). In their study, only cholinergic neurones were counted, and the aged animals were 53 months old. Vincent *et al.* (1989) found no loss of neurones (per nine cortical strips) from layers I to VI of the visual cortex with age in monkeys. However the variation in neuronal counts was high and they concluded that it would not be possible to detect a small loss of neurones. No loss of neurones was detected with age in the striate cortex of monkeys using the optical disector stereological technique (Kim *et al.*, 1997; Peters *et al.*, 1997).

Comparisons of cell counts between studies is difficult as they all differ in some way, such as the use of different methods of quantification, the use of different strains, age and health status of animal and the different areas analysed.

Although Terry *et al*, (1987) found no change in neuronal numbers with age, when the neurones were separated into large and small neurones, there was a significant decrease in the number of large neurones and a corresponding increase in the number of small neurones (though it was not significant). This and other studies have suggested that ageing causes neuronal atrophy, including the degeneration of dendrites and myelinated axons, rather than actual neuronal losses (Terry *et al.*, 1987; Vincent *et al.*, 1989; Finch, 1993; see Section 1.7). Quantification of neurone size is important for the evaluation of the integrity of remaining neurones in the aged brain, as the debate about whether atrophic neurones retain normal functioning still remains unanswered (Finch, 1993). In the present study although there was a trend towards smaller values for neuronal area (soma and nucleus) and maximal neuronal nuclear diameter in the aged animals, the difference did not reach significance. However, Terry *et al.* (1987) found that only large neurones atrophied with age, and the present study did not differentiate between large and small neurones, although there was an increase in the variance in these values with age which may have masked any possible differences. The data presented in this chapter agrees in principal with a previous study reporting a decrease in neuronal area in aged C57BL/6Nnia mice measured from vibratome sections (Hornberger *et al.*, 1985). Peinado *et al* (1993) using wax sections found no significant age-related change in neuronal area, but found a significant decrease in the nuclear area of neurones of aged rats in all cortical layers except layer I, suggesting structural atrophy. The way in which tissue is processed for examination can effect neuronal measurements, and different processing methods can lead to differential shrinkage of young and old brains (Coleman and Flood, 1987). Processing in resin rather than wax is

desirable as shrinkage in resin is minimal (Hughes and Lantos, 1987). Therefore discrepancies in measurements of neuronal atrophy may in part be related to different processing methods, regions of the brain analysed or species used.

Most studies of ageing suggest that there is an increase in glial cell numbers (Terry *et al.*, 1987; Peters *et al.*, 1991; Peinado *et al.*, 1993; 1997; Amenta *et al.*, 1994; see above). The present data, which document increased glial cell density with age, supports this hypothesis. However, ultrastructural studies that quantified astrocytes, oligodendrocytes and microglia separately found that only microglia increase with age (Peters *et al.*, 1991). In the present study, and in those reported above (Terry *et al.*, 1987; Peinado *et al.*, 1993; 1997; Amenta *et al.*, 1994), glial cell types were quantified together, consequently it is not known which cell type is responsible for the observed change. Further studies (using immunocytochemistry or ultrastructural assessment) are needed to differentiate between the glial cell populations, to determine which type(s) of glial cell increases with age in C57/Icrfa^{t} mice. As would be anticipated, increasing glial and unchanging neuronal populations resulted in a significant lowering of the neurone:glial cell ratio with age, which has also been reported by others (Miquel *et al.*, 1983; Terry *et al.*, 1987). The significance of these findings is not known. Glial cells are involved in many activities that are critical to brain function, such as maintenance of the BBB, uptake and inactivation of EAAs and regulation of extracellular water concentration. Following injury to the brain, glial cells are capable of both beneficial and damaging responses (see Sections 1.5.1.1 and 1.5.2.2), and changes in glial cell populations with age may affect their responses to injury.

There was no significant difference in the number of pyknotic profiles in the lesion with age. Other profiles in the infarct (red neuronal-like and apoptotic-like) were present in small numbers and did not change significantly with age. This may suggest that the balance between apoptosis (apoptotic-like profiles) and necrosis (pyknotic

profiles and red neuronal-like) is not affected with age. However, apoptosis is a very rapid process (1-2 hours), and the classical morphological criteria used in the histological identification of apoptosis may be recognised in only a small proportion of apoptotic cells at any given point in time. Therefore, any numerical estimate of apoptosis is subject to significant error (Webb *et al.*, 1997). Further studies using more sensitive biochemical techniques, such as DNA strand breaks demonstrated by *in situ* DNA nick-end labelling techniques or DNA "laddering" on electrophoretic gels (Webb *et al.*, 1997), would be required to determine whether apoptotic cell death following ischaemia is affected with age. Caution must also be exercised when interpreting findings obtained using these methods, as nicks can appear in cells that are not destined to die, in some necrotic cells and in poorly fixed tissue (Webb *et al.*, 1997; Dalkara and Moskowitz, 1999).

4.2.3 Conclusion

Ageing was associated with an increase in infarct volume following permanent MCAo. The mechanisms behind this are not known, but there are several age-related changes in neurones and glial cells that may influence their susceptibility to damage after injury (see Section 1.7). In this study there was no significant neuronal atrophy with age, as no significant difference was found with age in neuronal area, or maximal neuronal nuclear diameter. The preservation in the number of neurones/mm^3 in layer V of the frontal cortex in C57/Icrfa^t mice suggests that no significant neurodegenerative changes were taking place in aged animals in this region. Therefore, there was no real difference in the number of neurones that died per unit volume after injury in adult and aged animals. No significant differences were found in the number of different cell profiles in the infarct with age, suggesting there was no major difference with age in the way cells die after ischaemia. However, due to the increase in the size of the infarct

with age, more cells were lost in the aged brain after ischaemia. Ageing was associated with a significant increase in the number of glial cells/mm^3 in layer V of the frontal cortex, accompanied by a reduction in the neurone: glial cells ratio. Further investigations using more specific cell markers are required to determine which glial cell type(s) increase with age, and whether they react differently to injury.

Chapter 5

Glial activation, ICAM-1 and IL-1β expression and neutrophil invasion following MCAo in young adult and aged mice

5.0 Introduction

During the past decade, a considerable number of experimental studies have been devoted to elucidating the mechanisms of IBD mediated by EAAs and calcium (see Lee *et al.*, 1999). However, recent experimental studies have shed light on other aspects of the pathophysiology of IBD, one of which is the post-ischaemic inflammatory response, including glial cell activation and the invasion of peripheral immune cells. There are several changes in inflammatory responses with age including changes in the cytokine secretion profiles of peripheral immune cells and an increased activation state of glial cells (see section 1.7.3). However it is not known if these changes affect the post-ischaemic inflammatory responses in the aged brain.

Neurone-glial and glial-glial interactions are thought to play a critical role in neuronal survival and death following various kinds of CNS insults, and glial cell numbers have been reported to increase from 24 hours onwards after MCAo (Clark *et al.*, 1993; Garcia *et al.*, 1993b, Morioka *et al.*, 1993). In Chapter 4 it was shown that glial cells increased in numbers with age, but that immunocytochemistry was needed to determine whether this represented an increase in astrocytes, microglia or both. Since astrocytes and microglial cells are capable of both protective and neurotoxic responses (see section 1.5.1.1. and 1.5.1.2), the amount of glial cell activation may be important to the outcome of ischaemia. It is not known whether glial cell activation following cerebral ischaemia occurs in a similar manner in aged animals or if activation is affected with age. If there are any alterations in glial cell activation with age following CNS injury then it may affect the pathophysiology of IBD.

Another part of the post-ischaemic inflammatory response is the adhesion and migration of neutrophils, which occurs via highly specific receptor-ligand interactions. Adhesion to endothelial cells and migration by chemotactic factors are critical stages in the infiltration of neutrophils into the sites of tissue damage (see Section 1.5.2.1). This

adhesion is regulated in part by the interaction of ICAM-1 expressed on endothelial cells and integrin receptors on leukocytes (see Table 1.1). It is not known if the expression of ICAM-1 by endothelial cells that follows cerebral ischaemia is affected with age. If there are alterations in the expression of ICAM-1 with age this may in turn effect the infiltration of neutrophils into the injured brain. The accumulation of neutrophils is not only associated with the tissue-repair process, but may also result in further tissue damage (see Section 1.5.2.2).

The exact nature of the signalling mechanisms in brain inflammation following cerebral ischaemia remains to be determined but there is growing evidence that the cytokine IL-1 plays an important role (see Section 1.6.2). The exact cellular source of IL-1β protein following cerebral ischaemia is unclear and varies between studies. Some authors consider endothelial cells, microglia and invading immune cells to be the major source of IL-1β following cerebral ischaemia, while others have shown neurones, astrocytes and oligodendrocytes to be an important source (Touzani *et al.*, 1999; see Section 1.6.2.2). All these studies have been done using young adult animals. Ageing affects the cytokine secretion profile of isolated peripheral immune cells (see Section 1.7.3), but it is not known how ageing affects cytokine production in the brain. Ageing may influence the cellular source and levels of IL-1 following MCAo.

The aims of the experiments described in this chapter were to determine: 1) the number of GFAP positive astrocytes, GSA positive microglia/macrophages, ICAM-1 positive blood vessels and neutrophils, per unit area in sham-operated animals, or 12 and 24 hours after MCAo; 2) the cellular source(s) of IL-1β after MCAo, and determine the numbers of IL-1β positive cells/unit area in sham-operated animals, or 12 and 24 hours after MCAo. These parameters were examined in young adult (4-6 month) and aged (26-28 month) animals, using specific immunocytochemical and lectin histochemical markers, to assess if there are any associated changes with age.

5.1 GFAP positive astrocyte counts after MCAo.

The astrocytic response to experimental cerebral ischaemia induced by MCAo (see Section 2.3.2) was examined using the immunodetection of GFAP (see Section 2.9). GFAP positive astrocyte counts were performed in the peri-infarct zone of the frontal cortex, the corresponding area in the contralateral hemisphere and in the corpus callosum of both hemispheres (see Section 2.9.5). The data are presented as the mean cortical GFAP positive astrocyte number per unit area ($1.59mm^2$; 30 fields of view at x40) ± SD, or the mean white matter GFAP positive astrocyte number ($0.32mm^2$; 6 fields of view at x 40) ± SD. The data were analysed using 2-way ANOVA.

5.1.1 Results

GFAP immunostaining revealed sparse, weakly stained immunoreactive astrocytes (see Figure 5.1 a + b) within the contralateral hemisphere of experimental animals, and in both hemispheres of sham operated animals, especially in the radiation of the corpus callosum and in layer 1 of the cerebral cortex. GFAP positive cortical astrocytes from aged shams appeared to be more intensely stained than young adult cortical structures (see Figure 5.1 a + b). Many GFAP positive astrocytes in the parenchyma of both cerebral hemispheres were associated with blood vessels. 12 hours after MCAo, GFAP positive cortical astrocytes in the peri-infarct zone of both young adult and aged animals were more intensely stained (see Figure 5.1 c + d) than those in sham-operated animals. 24 hours after MCAo GFAP positive cortical astrocytes in the peri-infarct zone were more numerous and very intensely immunoreactive (see Figure 5.1 e + f). Additionally, these GFAP positive astrocytes had also increased in size, with larger cell bodies and thicker processes. There was an increase in the staining intensity of peri-infarct white matter GFAP positive astrocytes from sham-operated animals to those seen at 24 hours, in both young adult and aged animals (see Figure 5.2 a - d).

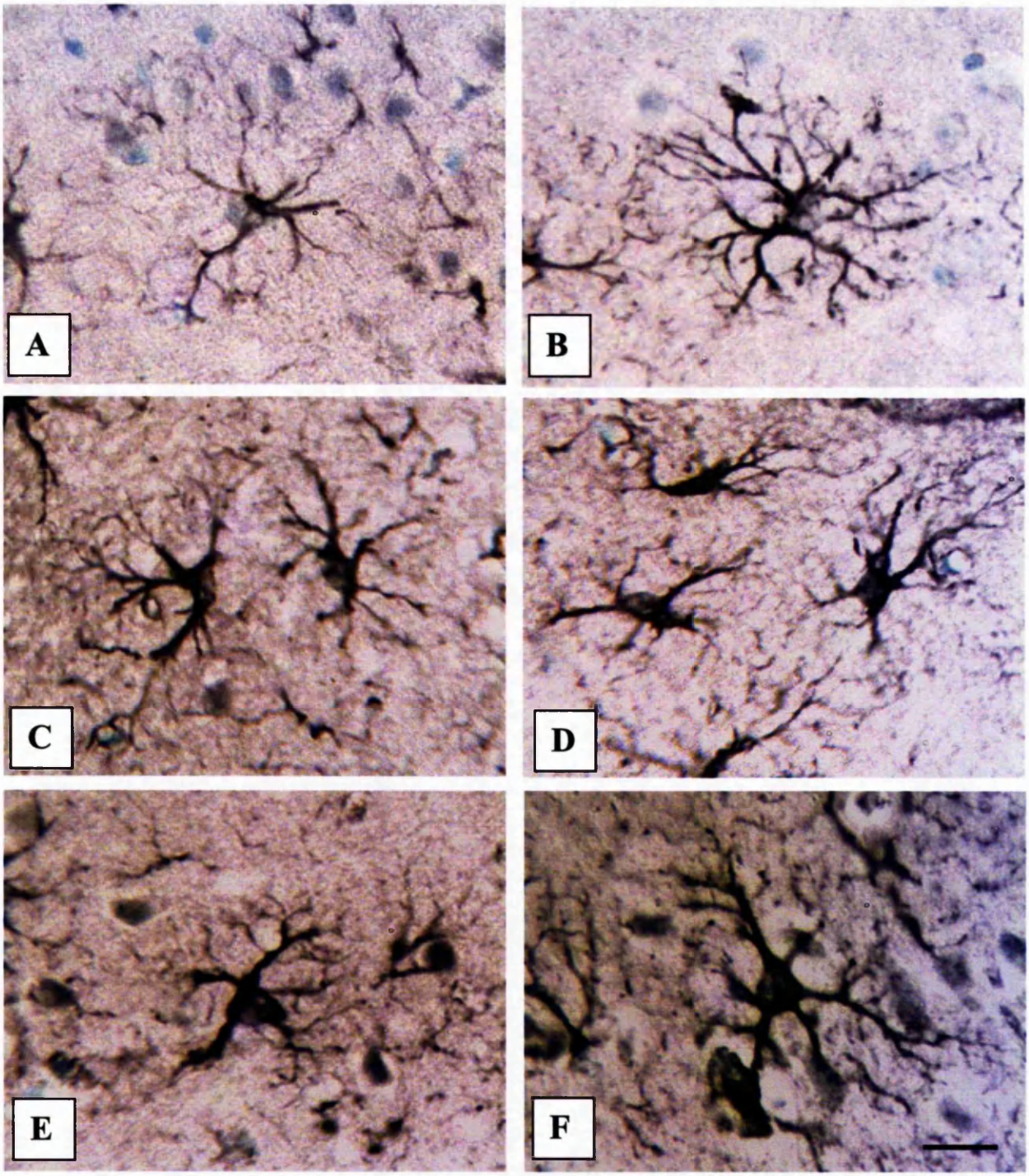

Figure 5.1: Ischaemic changes in astrocytes in the peri-infarct zone of the frontal cortex at different time points after MCAo in young adult (4 - 6 month) and aged (26 - 27 month) animals revealed by GFAP antibody.

Cryostat sections (10μm) are counterstained with 1% methyl green. Scale bars = 10μm. Appearance of astrocytes in sham-operated animals in a) adult sham; b) aged sham, note astrocyte from aged animal is more intensely stained. 12 hours post-MCAo astrocytes are more intensely stained in the peri-infarct zone of c) an adult and d) an aged animal. 24 hours post MCAo astrocytes are very intensely stained with enlarged cell bodies and thicker processes in the peri-infarct of e) an adult and f) an aged animal.

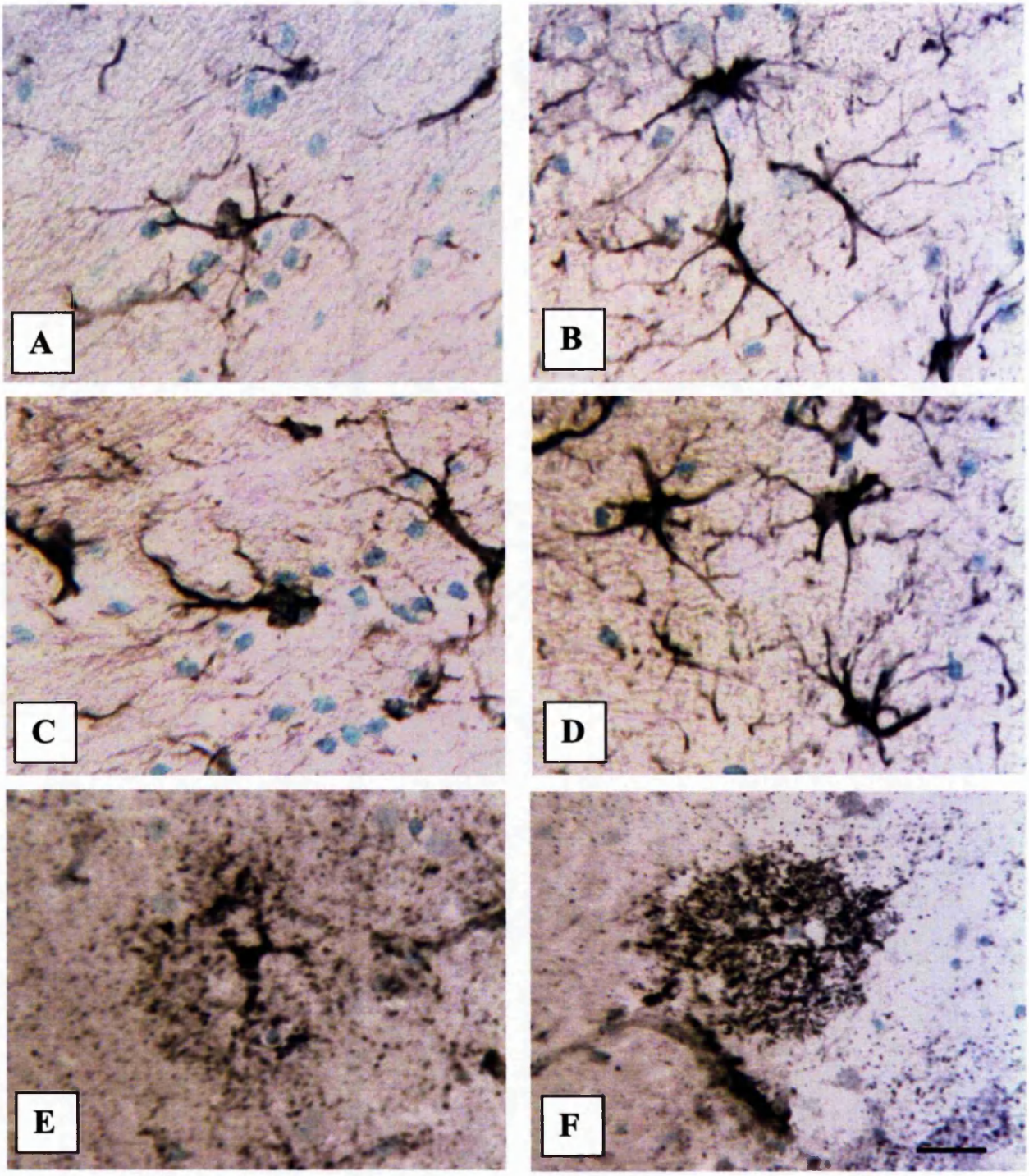

Figure 5.2: Appearance of GFAP immunoreactive astrocytes in various regions of the ipsilateral cortex of young adult (4 -6 month) and aged (26 -27 month) animals

Cryostat sections (10μm) are counterstained with 1% methyl green. Scale bars = 10 μm. A-D) Appearance of astrocytes in the white matter in A) an adult sham and C) an aged sham, and an increased staining intensity of astrocytes 24 hours post MCAo in B) an adult and D) an aged animal. E-F) Astrocytes in various stages of degeneration in the infarct 12 hours post MCAo in E) an adult and F) an aged animal.

Although not counted in this study, GFAP positive astrocytes were also observed in various stages of degeneration in the developing infarct 12 hours after MCAo (see Figure 5.2 e + f), but by 24 hours all astrocytes in the infarct had completely degenerated.

5.1.1.1 GFAP positive astrocytes in the peri-infarct zone of the ipsilateral hemisphere

The numbers of GFAP positive cortical astrocytes/unit area in the peri-infarct zone of the frontal cortex of sham-operated animals (denoted as time 0 hours), and 12 and 24 hours after MCAo in young adult and aged animals are presented in Table 5.1.

Time-point	**Number of cortical astrocytes/unit area in peri-infarct zone of ipsilateral hemisphere**	
	Adult (4-6 months)	**Aged (26-28 month)**
0 hours (Sham-operated)	44.67 ± 1.88	72.56 ± 2.04
12 hours	56 ± 4.1	80.56 ± 7.89
24 hours	81.44 ± 10.36	97.55 ± 4.19

Table 5.1: Number of GFAP positive cortical astrocytes/unit area in the peri-infarct zone of the ipsilateral frontal cortex in young adult and aged animals.

When the number of GFAP positive cortical astrocytes/unit area in the peri-infarct zone of the frontal cortex were analysed using 2-way ANOVA, there was a highly significant overall difference between the age groups ($F = 67.52$; $df = 1, 17$; $p < 0.001$), more astrocytes present in aged animals (see Figure 5.3). There was a highly significant difference over time ($F = 43.02$; $df = 2, 17$; $p < 0.001$), astrocyte numbers increasing with time particularly at 24 hours (82% overall increase in young adult

animals and a 34% increase in aged animals). There was no interaction between time and age ($F = 1.59$; $df = 2, 17$; $p = 0.244$) indicating that the number of cortical astrocytes in the peri-infarct zone increase in a similar manner in young adult and aged animals after MCAo.

The numbers of GFAP positive white matter astrocytes/unit area in the peri-infarct zone of the ipsilateral hemisphere of sham-operated animals (denoted as time 0 hours) and 12 and 24 hours after MCAo in young adult and aged animals are presented in Table 5.2.

Time-point	**Number of white matter astrocytes/unit area in peri-infarct zone of ipsilateral hemisphere**	
	Adult (4-6 months)	**Aged (26-28 month)**
0 hours (Sham-operated)	14.23 ± 2.84	15.56 ± 4.48
12 hours	13.55 ± 1.38	13.11 ± 1.35
24 hours	19.55 ± 0.77	22.78 ± 3.56

Table 5.2: Number of GFAP positive white matter astrocytes/unit area in the peri-infarct zone of the ipsilateral hemisphere in young adult and aged animals.

When the number of GFAP positive white matter astrocytes/unit area in the peri-infarct zone of the frontal cortex were analysed using 2-way ANOVA, there was no overall difference in number with age ($F = 1.13$; $df = 1, 17$; $p = 0.309$; see Figure 5.3). There was a significant difference over time ($F = 13.73$; $df = 2, 17$; $p = 0.01$), the graph indicates that numbers increase at 24 hours (37% increase in young adult, and 46% in aged animals), but there was no interaction between time and age ($F = 0.672$; $df = 2, 17$; $p = 0.529$). This suggests that the changes in the number of white matter astrocytes over time in the peri-infarct zone occur in a similar manner in young adult and aged animals after MCAo.

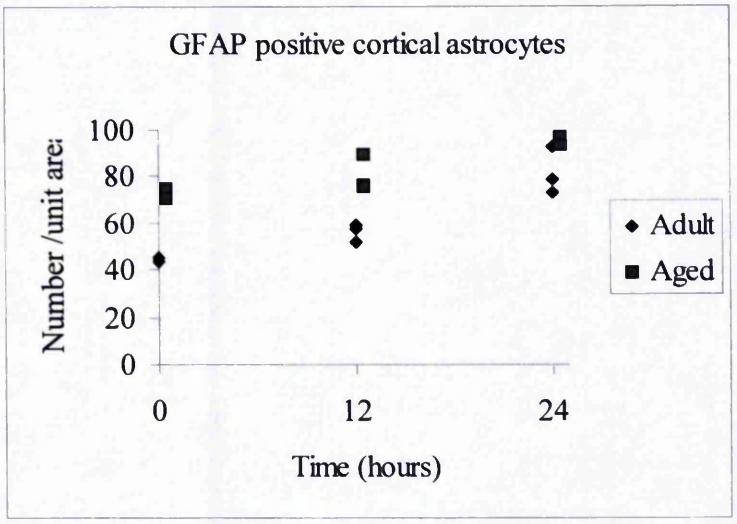

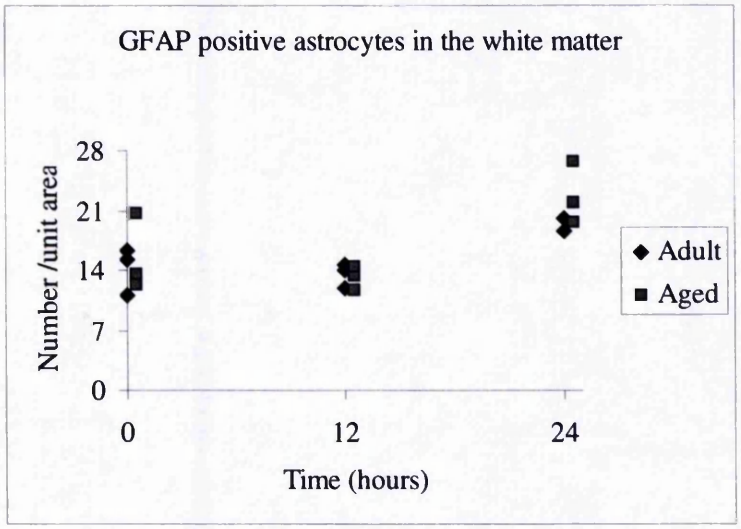

Figure 5.3: GFAP positive astrocyte numbers/unit area in the peri-infarct zone of the ipsilateral frontal cortex in young adult (4-6 month) and aged (26-28 month) animals (n = 3 per time point).

The number of astrocytes were counted on 10μm cryostat sections immunostained with GFAP in sham-operated animals (time = 0), and 12 and 24 hours after MCAo. Cortical astrocytes were counted from 10 non-overlapping fields of view of an eyepiece graticule (at x 40) on three sections from three regions 500μm apart. This was repeated for white matter astrocytes using 2 non-overlapping fields of view fields. The average values from each of the three regions were summed to give the number of GFAP positive astrocytes per unit area from each animal.

5.1.1.2 GFAP positive astrocytes in the contralateral hemisphere.

The numbers of GFAP positive cortical astrocytes/unit area in the frontal cortex of the contralateral hemisphere of sham-operated animals (denoted as time 0 hours) and 12 and 24 hours after MCAo in young adult and aged animals are presented in Table 5.3.

Time-point	Number of cortical astrocytes/unit area in peri-infarct zone of contralateral hemisphere	
	Adult (4-6 months)	**Aged (26-28 month)**
0 hours (Sham-operated)	45 ± 0.58	70.88 ± 2.36
12 hours	51 ± 6.84	72.67 ± 3.33
24 hours	54.11 ± 7.95	73.56 ± 6.06

Table 5.3: Number of GFAP positive cortical astrocytes/unit area in the contralateral frontal cortex in young adult and aged animals.

When the number of GFAP positive cortical astrocytes/unit area in the contralateral hemisphere were analysed using 2-way ANOVA (see Figure 5.4) there was a highly significantly overall difference with age ($F = 87.2$; $df = 1, 17$; $p < 0.001$), more present in aged animals. There was no overall difference in number of cortical astrocytes in the contralateral hemisphere with time ($F = 2.09$; $df = 2, 17$; $p = 0.166$) and no interaction between age and time ($F = 0.624$; $df = 2, 17$; $p = 0.552$).

The numbers of GFAP positive white matter astrocytes/unit area in the contralateral hemisphere of sham-operated animals (denoted as time 0 hours) and 12 and 24 hours after MCAo in young adult and aged animals are presented in Table 5.4.

Time-point	Number of white matter astrocytes/unit area in peri-infarct zone of contralateral hemisphere	
	Adult (4-6 months)	Aged (26-28 month)
0 hours (Sham-operated)	13.33 ± 1.73	12.56 ± 0.19
12 hours	13 ± 2.40	12.33 ± 1.67
24 hours	17.67 ± 0.88	19.22 ± 3.66

Table 5.4: Number of GFAP positive white matter astrocytes/unit area in the contralateral hemisphere in young adult and aged animals.

When the number of GFAP positive white matter astrocytes/unit area in the contralateral hemisphere was analysed there was no overall difference between the age groups ($F = 0.002$; $df = 1,17$; $p = 0.968$). There was a highly significant overall difference with time ($F = 16.33$; $df = 2, 17$; $p < 0.001$), astrocytes numbers increasing with time (33% increase in young adults, and 53% in aged animals), but no interaction between time and age ($F = 0.663$; $df = 2, 17$; $p = 0.533$). This indicates that the increase in astrocyte numbers with time in the contralateral white matter was similar in young adult and aged animals (see Figure 5.4).

To see if the increase in white matter astrocytes/unit area was different between the two hemispheres, the numbers were compared using 2-way ANOVA. There was no difference in astroglial numbers/unit area with time between the ipsilateral and contralateral white matter of young adult ($F = 0.22$; $df = 2, 17$; $p = 0.809$) or aged animals ($F = 1.29$; $df = 2, 17$; $p = 0.311$).

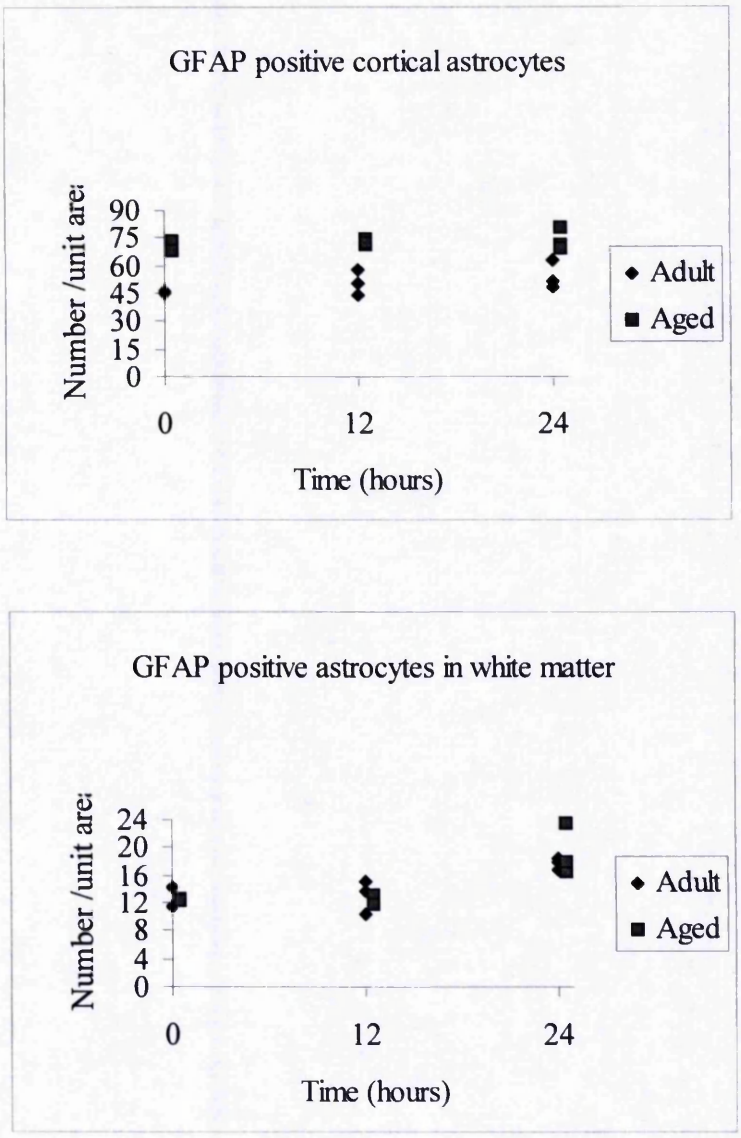

Figure 5.4: GFAP positive astrocyte numbers in the frontal cortex of the contralateral hemisphere of young adult (4-6 month) and aged (26-28 month) animals (n = 3 per time point).

The number of astrocytes were counted on 10μm cryostat sections immunostained with GFAP in sham-operated animals (time = 0), and at 12 and 24 hours after MCAo. Cortical astrocytes were counted from 10 non-overlapping fields of view of an eyepiece graticule (at x 40) on three sections from three regions 500μm apart. This was repeated for white matter astrocytes using 2 non-overlapping fields of view fields. The average values from each of the three regions were summed to give the number of GFAP positive astrocytes per unit area from each animal.

5.2 GSA positive microglia/macrophage counts after MCAo.

The microglial/macrophage response to experimental cerebral ischaemia induced by MCAo (see Section 2.3.2) was examined using lectin histochemistry (see Section 2.9). Microglia (and macrophages) can be stained specifically with the lectin binding method using isolectin B4 from *Griffonia simplicifolia* (GSA) seeds (Streit, 1990), which also stains blood vessels. The lectin histochemistry only weakly stains resting microglia/macrophages, as most of the molecules are not constitutively expressed, or are downregulated by resting microglia/macrophages (Kato *et al.*, 1998). Since microglia and macrophages share the same heritage, and once activated share the same cell surface markers they become virtually indistinguishable under pathological conditions (Stoll *et al.*, 1998). Therefore, because ischaemia is associated with the activation of microglia and the invasion of peripheral monocytes (macrophages), GSA positive cells in the present study are referred to as microglia/macrophages.

Microglial/macrophage cell counts were performed in the peri-infarct zone of the frontal cortex and the corresponding area in the contralateral hemisphere (see Section 2.9.5). Microglia/macrophages were separated into parenchymal microglia/macrophages and vascular associated microglia/ macrophages (those having a cell body or any cell process in association with a blood vessel). The data are presented as the mean GSA positive microglial/macrophage number per unit area ($1.59mm^2$; 30 fields of view at x40) ± SD. The data were analysed using 2-way ANOVA.

5.2.1 Results

GSA lectin staining revealed widespread, weakly stained microglia/macrophage cells (compared to those in the ipsilateral hemisphere) within the contralateral hemispheres of experimental animals, and in both hemispheres of sham operated mice, in all layers of the cerebral cortex (see Figure 5.5 a + b).

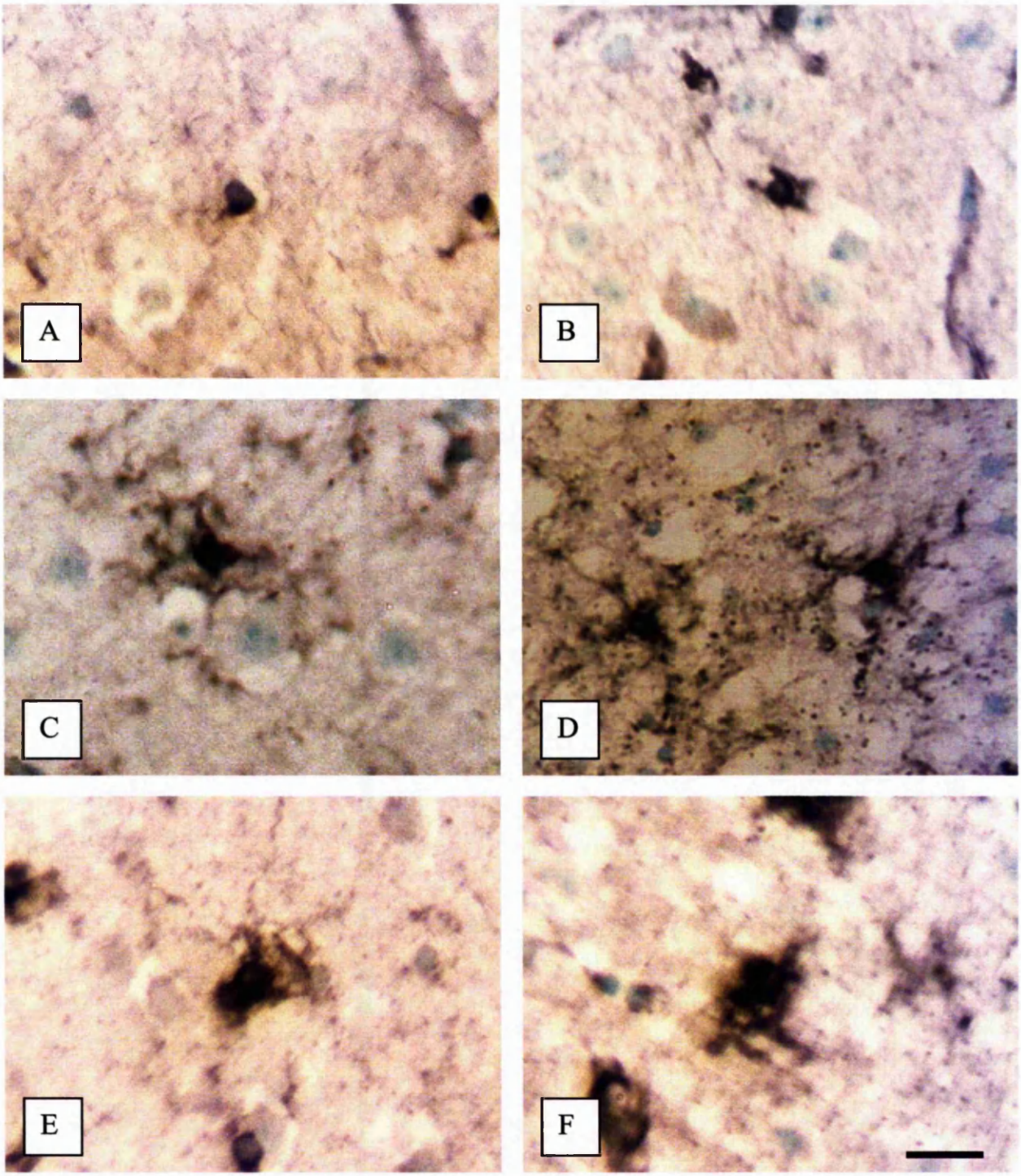

Figure 5.5: Ischaemic changes in microglia at different time points after MCAo in young adult (4-6 month) and aged (26/27 month) animals revealed by GSA lectin cytochemistry.

Cryostat sections (10 μm) are counterstained with 1% methyl green. Scale bars = 10 μm. Weakly stained microglia in A) Adult sham; B) aged sham. By 12 hours the staining intensity of microglia had increased in the peri-infarct zone in C) adult and D) aged animals. 24 hours post MCAo microglia are very intensely stained (compared to 12 hours) in the peri-infarct zone in E) adult and F) aged.

The microglia/macrophages from aged animals appeared to stain more intensely than microglia/macrophages from young adult animals (see Figure 5.5 a +b). Twelve hours after MCAo, GSA positive microglia/macrophages in the peri-infarct region of the ipsilateral hemisphere were more intensely stained compared to those in sham operated animals, in both young adult and aged mice (see Figure 5.5 c + d).By twenty-four hours the staining intensity of GSA positive microglia/macrophages in the peri-infarct region of the ipsilateral hemisphere had further increased in both young adult and aged animals (see Figure 5.5 e + f) and their cell processes had thickened.

5.2.1.1 GSA positive microglia/macrophages in the peri-infarct zone of the ipsilateral hemisphere

The number of GSA positive parenchymal microglia/macrophages per unit area in the peri-infarct zone of the frontal cortex of sham-operated animals (denoted as time 0 hours) and 12 and 24 hours after MCAo in young adult and aged animals are presented in Table 5.5.

Time-point	**Number of parenchymal microglia/ macrophages per unit area in peri-infarct zone of ipsilateral hemisphere**	
	Adult (4-6 months)	**Aged (26-28 month)**
0 hours (Sham-operated)	22.67 ± 2.60	26.22 ± 1.51
12 hours	19.89 ± 0.69	28.11 ± 0.77
24 hours	27.11 ± 2.22	34.78 ± 4.62

Table 5.5: Number of GSA positive parenchymal microglia/macrophages per unit area in the peri-infarct zone of the ipsilateral hemisphere in young adult and aged animals.

When the number of parenchymal microglia/macrophages per unit area in the peri-infarct zone of the frontal cortex were analysed using 2-way ANOVA, there was a highly significant overall difference between the age groups ($F = 32.99$; $df = 1,17$, $p < 0.001$), with more present in aged animals. There was a highly significant overall difference with time ($F = 15.83$; $df = 2,17$, $p < 0.001$), numbers increasing with time after MCAo (20% overall increase in young adult animals and a 33% overall increase in aged animals). However, there was no interaction between time and age ($F = 1.7$; $df = 2,17$, $p = 0.224$) indicating that parenchymal microglia/macrophages increase in a similar manner in young adult and aged animals (see Figure 5.6).

The number of GSA positive vascular associated microglia/macrophages per unit area in the peri-infarct zone of the frontal cortex of sham-operated animals, and 12 and 24h after MCAo in young adult and aged animals are presented in Table 5.6.

Time-point	**Number of vascular associated microglia/ macrophages per unit area in peri-infarct zone of ipsilateral hemisphere**	
	Adult (4-6 months)	**Aged (26-28 month)**
0 hours (Sham-operated)	18.89 ± 3.1	35.22 ± 5.01
12 hours	20.56 ± 1.5	39.67 ± 1.76
24 hours	33.78 ± 3.08	64.33 ± 5.78

Table 5.6: Number of GSA positive vascular associated microglia/macrophages per unit area in the peri-infarct zone of the ipsilateral hemisphere in young adult and aged animals.

When the number of vascular microglia/macrophages per unit area in the peri-infarct region were analysed, there was a significant interaction between time and age ($F = 6.16$; $df = 2,17$; $p = 0.014$), indicating there is an overall difference in the number of vascular associated microglia/macrophages between the two age groups over time.

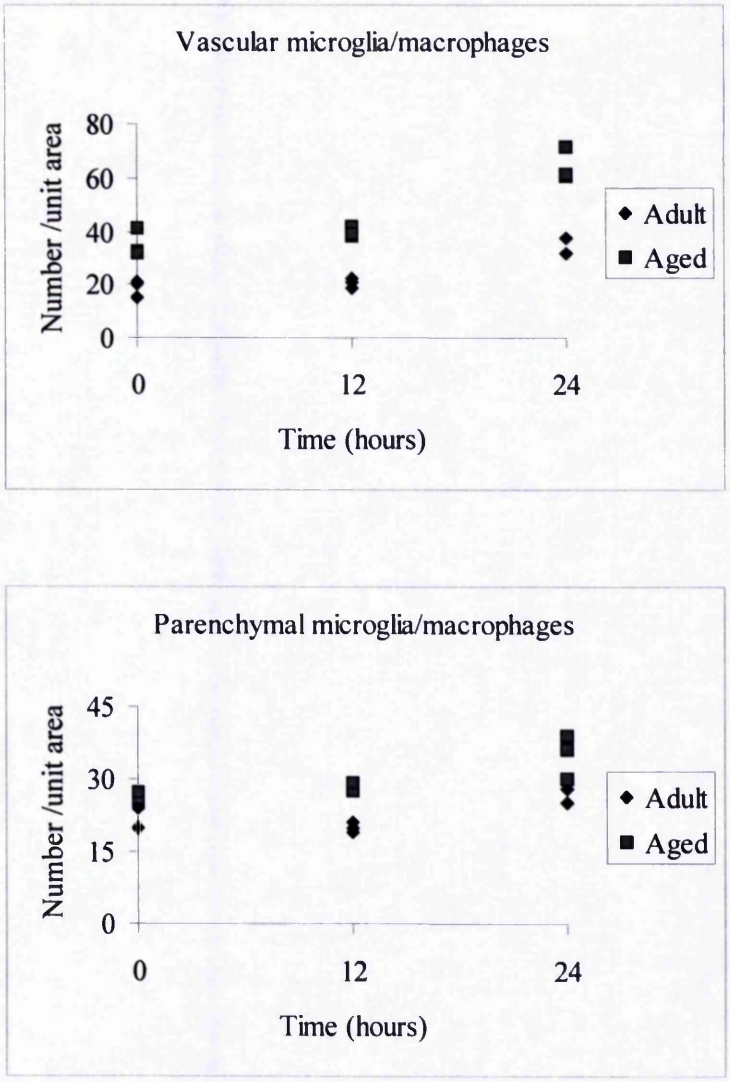

Figure 5.6: Microglia/macrophage numbers per unit area in the peri-infarct zone of the frontal cortex of young adult (4-6 month) and aged (26-28 month) animals (n = 3 per time point).

The number of microglia/macrophages were counted on 10μm cryostat sections stained with GSA in sham-operated animals (time = 0), and 12 and 24 hours after MCAo. Microglia/macrophages were counted from 10 non-overlapping fields of view of an eyepiece graticule (at x 40) on three sections from three regions 500μm apart. The average values from each of the three regions were summed to give the number of microglia/macrophages per unit area from each animal.

5.2.1.2 GSA positive microglia/macrophages in the contralateral hemisphere

The number of GSA positive parenchymal microglia/macrophages per unit area in the contralateral frontal cortex of sham-operated animals, and 12 and 24 hours after MCAo in young adult and aged animals are presented in Table 5.7.

Time-point	Number of parenchymal microglia/ macrophages per unit area in the contralateral hemisphere	
	Adult (4-6 months)	Aged (26-28 month)
0 hours (Sham-operated)	23.22 ± 2.22	25.89 ± 1.5
12 hours	21.22 ± 2.17	26.67 ± 1.86
24 hours	22.45 ± 1.9	30.67 ± 1

Table 5.7: Number of GSA positive parenchymal microglia/macrophages per unit area in contralateral hemisphere in young adult and aged animals.

When the number of parenchymal microglia/macrophages per unit area in the frontal cortex of the contralateral hemisphere were analysed using 2-way ANOVA there was a highly significant overall difference between the age groups ($F = 35.41$; $df = 1,17$, $p < 0.001$), with more present in aged animals. There was no overall difference with time ($F = 2.55$; $df = 2,17$, $p = 0.119$) and no interaction between age and time ($F = 3.65$; $df = 2,17$, $p = 0.058$; see Figure 5.7).

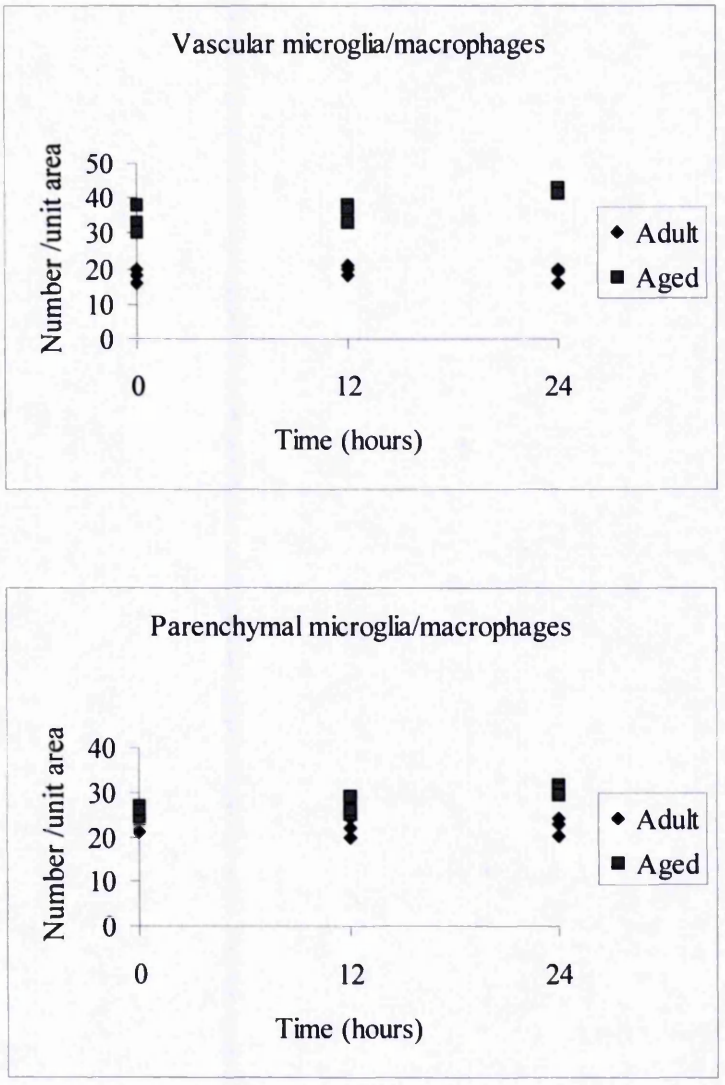

Figure 5.7: Microglia/macrophage numbers in the frontal cortex of the contralateral hemisphere of young adult (4 month) and aged (30 month) animals (n = 3 per time point).

The number of microglia/macrophages were counted on 10μm cryostat sections stained with GSA in sham-operated animals (time = 0), and 12 and 24 hours after MCAo. Microglia/macrophages were counted from 10 non-overlapping fields of view of an eyepiece graticule (at x 40) on three sections from three regions 500μm apart. The average values from each of the three regions were summed to give the number of microglia/macrophages per unit area from each animal.

The number of GSA positive vascular associated microglia/macrophages per unit area in the contralateral frontal cortex of sham-operated animals, and 12 and 24 hours after MCAo in young adult and aged animals are presented in Table 5.8.

Time-point	Number of vascular associated microglia/ macrophages per unit area in the contralateral hemisphere	
	Adult (4-6 months)	Aged (26-28 month)
0 hours (Sham-operated)	17.89 ± 1.84	33.67 ± 4.04
12 hours	19.56 ± 1.64	35.78 ± 2.71
24 hours	18.11 ± 1.9	41.89 ± 1.02

Table 5.8: Number of GSA positive vascular associated microglia/macrophages per unit area in the contralateral hemisphere in young adult and aged animals.

When vascular associated microglia/macrophages per unit area in the frontal cortex of the contralateral hemisphere were analysed using 2-way ANOVA, there was a significant interaction between age and time ($F = 5.29$; $df = 2,17$, $p = 0.023$). This indicates there is a significant difference in the number of vascular associated microglia/macrophages per unit area between the two age groups over time. It appears there is an increase in vascular associated microglia/macrophages in the contralateral hemisphere of aged animals 24 hours post MCAo, which does not appear to occur in young adult animals (see Figure 5.7).

To see if the increase in vascular associated microglia/macrophages per unit area with time is comparable in the ipsilateral and contralateral hemispheres of aged animals, the numbers were analysed using ANOVA. In aged animals there was a significant difference in the number of vascular associated microglia/macrophages between the contralateral and ipsilateral cortex ($F = 26.99$; $df = 1, 17$, $p < 0.001$). This represents a

83% increase over time in the ipsilateral hemisphere of aged animals, compared to a 24% increase over time in the contralateral hemisphere.

5.3 ICAM-1 expression after MCAo.

ICAM-1 positive vessels were identified using immunocytochemistry (see Section 2.9). Vessels were counted in four regions, the central zone of the infarct, the surrounding outer zone of the infarct, the peri-infarct zone of the frontal cortex and the corresponding area of the contralateral cortex (see Section 2.9.5). The data are presented as the mean number of ICAM-1 positive vessels per unit area ($1.59mm^2$; 30 fields of view at x40) ± SD. The data were analysed using 2-way ANOVA. In addition to vessels staining positive for ICAM-1, some glial cells were also immunoreactive and double immunostaining was used to identify which glial cell type was ICAM-1 positive (see Section 2.9.4).

5.3.1 Results

Moderate ICAM-1 positive labelling of the choroid plexus was present in sham and experimental animals. Blood vessels in both hemispheres of sham-operated animals and in the contralateral hemisphere of experimental animals showed faint widespread ICAM-1 positive staining throughout the brain (see Figure 5.8 a + b). There did not appear to be any difference in the staining intensity of ICAM-1 positive vessels in young adult and aged shams. Twelve hours after MCAo, ICAM-1 positive vessels within the infarct and peri-infarct zone of the frontal cortex were much more intensely stained compared to sham animals and those in the contralateral cortex in both young adult and aged animals (see Figure 5.8 c + d). Twenty-four hours after MCAo ICAM-1 positive vessels in the outer zone of the infarct and peri-infarct region were very intensely stained in both young adult and aged animals (see Figure 5.8 e).

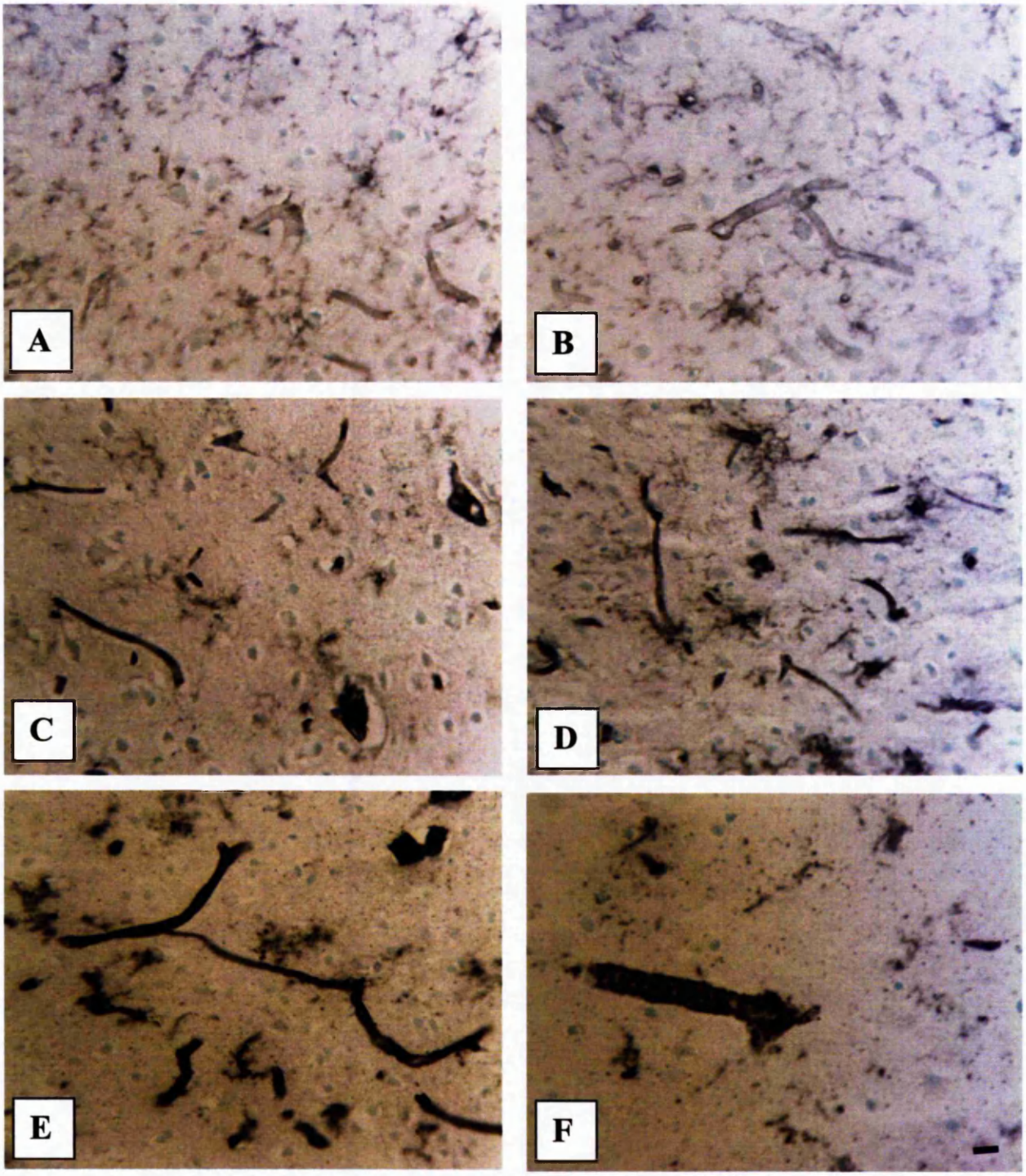

Figure 5.8: Ischaemic changes in ICAM-1 immunoreactivity on microvessels at different time points after MCAo in young adult (4 -6 month) and aged (26/27 month) animals.

Cryostat sections (10µm) counterstained with 1% methyl green. Scale bar = 10µm
Weak constitutive expression of ICAM-1 on microvessels in the frontal cortex of A) adult sham, and B) aged sham. At 12 hours microvessels are more intensely stained for ICAM-1 in the peri-infarct zone of the frontal cortex in C) an adult and D) an aged animal. E) very intensely stained vessels in the outer zone of the lesion at 24 hours, and F) larger vessel in central zone of lesion at 24 hours has a granular appearance compared to E. (E + F = aged)

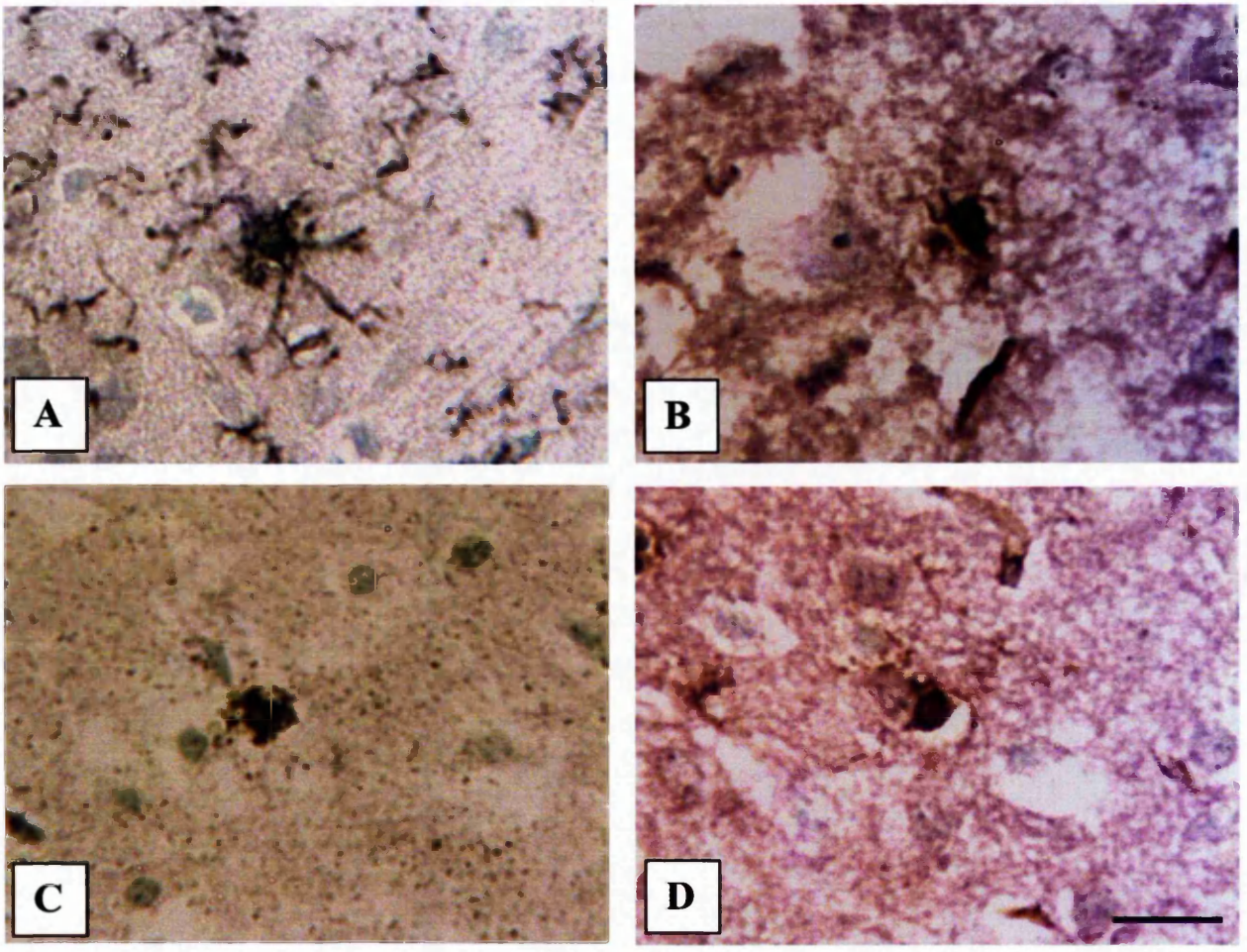

Figure 5.9: Identification of ICAM-1 immunoreactive microglial cells using double immunostaining

Cryostat sections (10μm) are counterstained with 1% methyl green. Scale bars = 10 μm.
A) ICAM-1 staining of glial cell using nickel DAB. B) appearance of double labeled microglial cell, the colour is different to the two single labeled control sections. C) single control section showing ICAM-1 labelling (brown) using DAB. D) single control section showing GSA labelling (purple) using VIP Vector kit.

ICAM-1 positive vessels in the central zone of the infarct had a more granular appearance compared to those at earlier time-points and are possibly disintegrating vessels (see Figure 5.8 f).

In addition to blood vessels staining positive for ICAM-1, microglial-like cells in sham operated animals and in the contralateral hemispheres of experimental animals were weakly stained for ICAM-1 (see Figure 5.9 a). The staining intensity of these cells was similar in young adult and aged animals and increased with time after MCAo. Double labelling of sections with ICAM-1 and GSA revealed that these cells were in fact microglia (see Figure 5.9 b -d).

5.3.1.1 Expression of ICAM-1 in blood vessels in the peri-infarct zone and corresponding region of the contralateral hemisphere

The number of ICAM-1 positive vessels/unit area in the peri-infarct zone of the frontal cortex of sham-operated animals, and 12 and 24 hours after MCAo in young adult and aged animals are presented in Table 5.9.

Time-point	No. ICAM-1 positive vessels/ unit area < 10μm diameter		No. ICAM-1 positive vessels/ unit area > 10μm diameter	
	Adult (4-6 months)	Aged (26-28 month)	Adult (4-6 months)	Aged (26-28 month)
0 h (Sham-operated)	137.3 ± 22.8	130.2 ± 10.7	7.2 ± 2.8	6.6 ± 1.2
12 hours	271.7 ± 32.7	246.7 ± 45.6	6 ± 1.2	9.4 ± 6
24 hours	310.6 ± 17.1	251.4 ± 11.4	6.9 ± 1.3	7.9 ± 2

Table 5.9: Number of ICAM-1 positive vessels/unit area in the peri-infarct zone of the ipsilateral frontal cortex in young adult and aged animals.

When the number of ICAM-1 positive vessels under 10μm in diameter in the peri-infarct zone was analysed using 2-way ANOVA, there was an overall difference

between the age groups ($F = 6.09$; $df = 1,17$, $p = 0.030$), with more present in young adult animals. There was a highly significant difference over time ($F = 55.57$; $df = 2,17$, $p < 0.001$), numbers increasing with time, but no interaction between time and age ($F = 1.54$; $df = 2,17$, $p = 0.254$). This indicates that the increase in ICAM-1 positive microvessels with time is similar in both age groups (see Figure 5.10). There were no significant differences in the number of ICAM-1 positive vessels over 10μm in diameter in the peri-infarct zone between the age groups or with time. Therefore, following MCAo the number of ICAM-1 positive vessels over 10 μm in diameter remains constant in both young adult and aged animals.

The number of ICAM-1 positive vessels/unit area in the contralateral frontal cortex hemisphere (corresponding to the region of the peri-infarct zone) of sham-operated animals, and 12 and 24 hours after MCAo in young adult and aged animals is presented in Table 5.10.

Time-point	No. ICAM-positive vessels/unit area < 10μm diameter		No. ICAM-positive vessels/unit area > 10μm diameter	
	Adult (4-6 months)	Aged (26-28 month)	Adult (4-6 months)	Aged (26-28 month)
0 h (Sham-operated)	136.6 ± 8.2	131.1 ± 6.6	6.3 ± 1	5.9 ± 1.4
12 hours	169.9 ± 15.2	136.6 ± 23.8	6.1 ± 2.5	8.1 ± 3.1
24 hours	147 ± 17.2	149.2 ± 8.8	9.2 ± 1.6	4.44 ± 2.7

Table 5.10: Number of ICAM-1 positive vessels/unit area in the contralateral frontal cortex of young adult and aged animals.

When the number of ICAM-1 positive vessels/unit area (both > and < 10μm in diameter) in the contralateral frontal cortex were analysed, there was no significant differences between the age groups or with time.

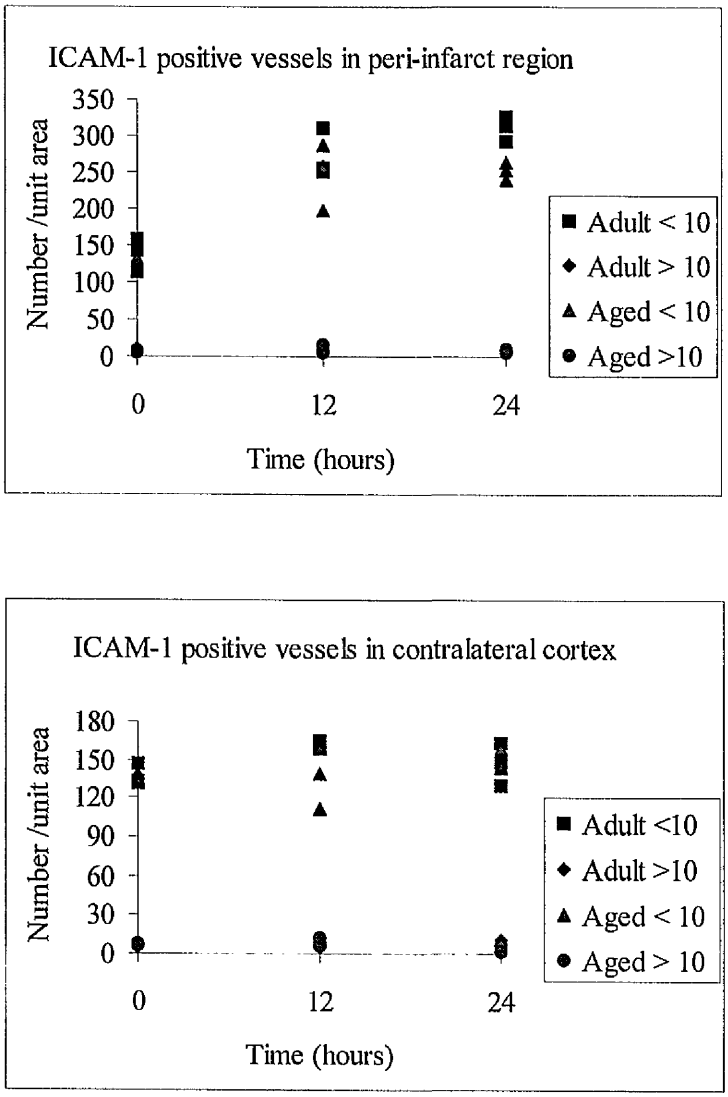

Figure 5.10: Numbers of ICAM-1 positive vessels/unit area in the peri-infarct zone of the frontal cortex and corresponding region in the contralateral frontal cortex of young adult (4 month) and aged (26/27 month) animals (n = 3 per time point).

The number of ICAM-1 positive vessels were counted on 10μm cryostat sections stained with rat anti mouse ICAM-1 in sham-operated animals (time = 0), and at 12 and 24 hours after MCAo. Vessels were counted from 10 non-overlapping fields of view of an eyepiece graticule (at x 40) on three sections from three regions 500μm apart. The average values from each of the three regions were summed to give the number of vessels per unit area from each animal.

Following MCAo there is no upregulation of ICAM-1 on vessels, under or over 10μm in diameter, in the contralateral hemisphere.

5.3.1.2 Expression of ICAM-1 in blood vessels in the central and outer zones of the infarct.

The number of ICAM-1 positive vessels/unit area in the outer zone of the infarct 12 and 24 hours after MCAo in young adult and aged animals are presented in Table 5.11.

Time-point	No. ICAM-positive vessels/unit area < 10μm diameter		No. ICAM-positive vessels/unit area > 10μm diameter	
	Adult (4-6 months)	Aged (26-28 month)	Adult (4-6 months)	Aged (26-28 month)
12 hours	318.2 ± 82.7	314.6 ± 19.2	6.9 ± 1.0	12 ± 3.6
24 hours	414.3 ± 36.3	340.2 ± 45	8.78 ± 1.1	10.3 ± 3.2

Table 5.11: Number of ICAM-1 positive vessels/unit area in the outer zone of the infarct in young adult and aged animals.

When the number of ICAM-1 positive vessels/unit area under 10μm in diameter in the outer zone of the infarct was analysed, there was no overall difference between the age groups ($F = 1.86$, $df = 1,17$, $p = 0.198$). There was a highly significant difference over time ($F = 53.85$; $df = 2,17$, $p < 0.001$), the numbers increasing with time but no interaction between time and age ($F = 1.38$; $df = 2,17$, $p = 0.288$). This indicates that the numbers of ICAM-1 positive vessels under 10μm in diameter increase in a similar manner in young adult and aged animals (see Figure 5.11). There were no significant differences in the number of ICAM-1 positive vessels over 10μm in diameter in the outer zone of the infarct between the age groups or with time. The number of ICAM-1 positive vessels/unit area in the central zone of the infarct 12 and 24 hours after MCAo in young adult and aged animals are presented in Table 5.12.

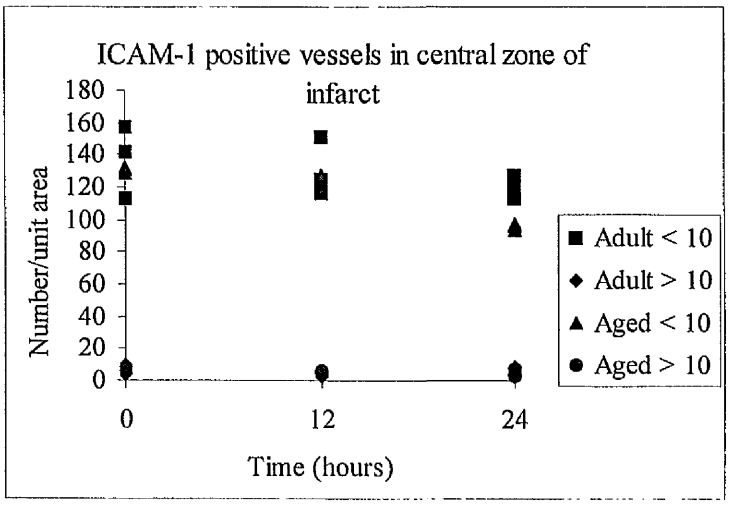

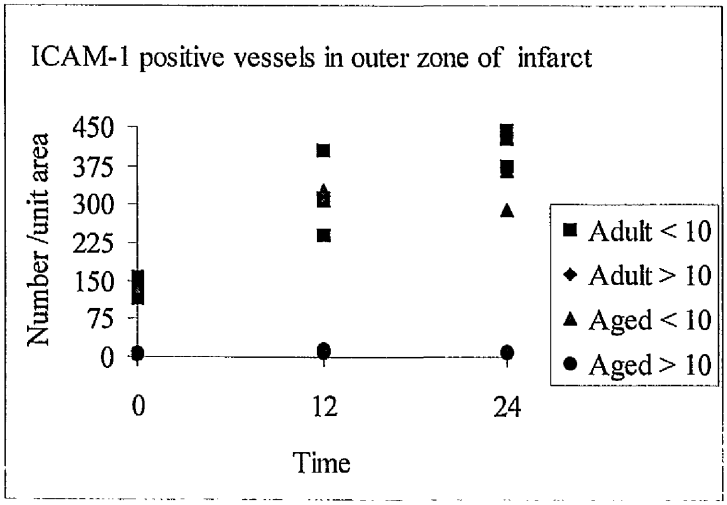

Figure 5.11: Numbers of ICAM-1 positive vessels/unit area in the central and outer zones of the infarct of young adult (4 month) and aged (26-28 month) animals (n = 3 per time point).

The number of ICAM-1 positive vessels were counted on 10μm cryostat sections stained with rat anti mouse ICAM-1 in sham-operated animals (time = 0), and 12 and 24 hours after MCAo. Vessels were counted from 10 non-overlapping fields of view of an eyepiece graticule (at x 40) on three sections from three regions 500μm apart. The average values from each of the three regions were summed to give the number of vessels per unit area from each animal.

Time-point	No. ICAM-positive vessels/unit area < 10μm diameter		No. ICAM-positive vessels/unit area > 10μm diameter	
	Adult (4-6 months)	Aged (26-28 month)	Adult (4-6 months)	Aged (26-28 month)
12 hours	131.6 ± 17.7	120.6 ± 15.6	3.9 ± 1.9	5 ± 1.2
24 hours	120.2 ± 6.8	95.7 ± 2.2	5 ± 2.7	5.1 ± 2.3

Table 5.12: Number of ICAM-1 positive vessels/unit area in the central zone of the infarct in young adult and aged animals.

When the number of ICAM-1 positive vessels under 10μm in diameter in the central zone of the infarct was analysed, there was a significant difference between the age groups ($F = 5.92$; $df = 1,17$, $p = 0.032$), with more present in young adult animals. There was a significant difference over time ($F = 6.87$; $df = 2,17$, $p = 0.01$), with numbers decreasing with time, but no interaction between time and age ($F = 0.83$; $df = 2,17$, $p = 0.46$; see Figure 5.11). Again there were no significant differences in the number of ICAM-1 positive vessels/unit area in the central zone of the lesion.

5.4 Neutrophil invasion after MCAo in young adult and aged animals.

Neutrophils were identified by staining frozen brain sections with a rat anti-mouse neutrophil (7/4 clone; see Section 2.9) antibody that recognises a polymorphic 40kD antigen expressed by mouse PMNLs, which is absent on resident tissue macrophages (data sheet; Serotec, UK). Neutrophil counts were performed in both the ipsilateral and contralateral cortex (see Section 2.9.5). Where many neutrophils appeared clumped together in a vessel and the individual neutrophils could not be separated from each other, the stained structure was counted as one, and therefore the counts probably represent an under-estimate of neutrophil number. Neutrophils were separated into parenchymal neutrophils, spherical with no histological evidence of a vessel being present, or intravascular, those found in association with a vessel (identified by focussing the section up and down) or having a tubular or elongated

shape. The data are presented as the mean neutrophil count /unit area ($9.79mm^2$) ± SD, and were analysed using 2-way ANOVA.

5.4.1 Results

In sham operated animals (see Figure 5.12 a) and in the contralateral cortex of experimental animals very few neutrophils were present, and these were mainly present within the vasculature. Twelve hours after MCAo the number of neutrophils in the ipsilateral cortex had increased (see Figure 5.12 b). These neutrophils were observed mainly in vessels throughout the developing infarct and the meningeal vasculature surrounding the infarct. Scattered neutrophils were also detected within vessels adjacent to the ischaemic infarct, and occasionally in the lateral part of the caudoputamen. Some neutrophils were also present in the brain parenchyma of the developing infarct. Twenty-four hours after MCAo more neutrophils were observed in both the parenchyma and the vasculature of the ipsilateral cortex than at 12 hours (see Figure 5.12 c + d). Neutrophils were seen in vessels throughout the ischaemic infarct, in the meningeal vasculature surrounding the infarct, and within vessels adjacent to the infarct, and occasionally in the lateral part of the caudoputamen. Fewer neutrophils were observed within the central zone of the infarct. Parenchymal neutrophils were present throughout the ischaemic infarct, and in brain tissue adjacent to the infarct.

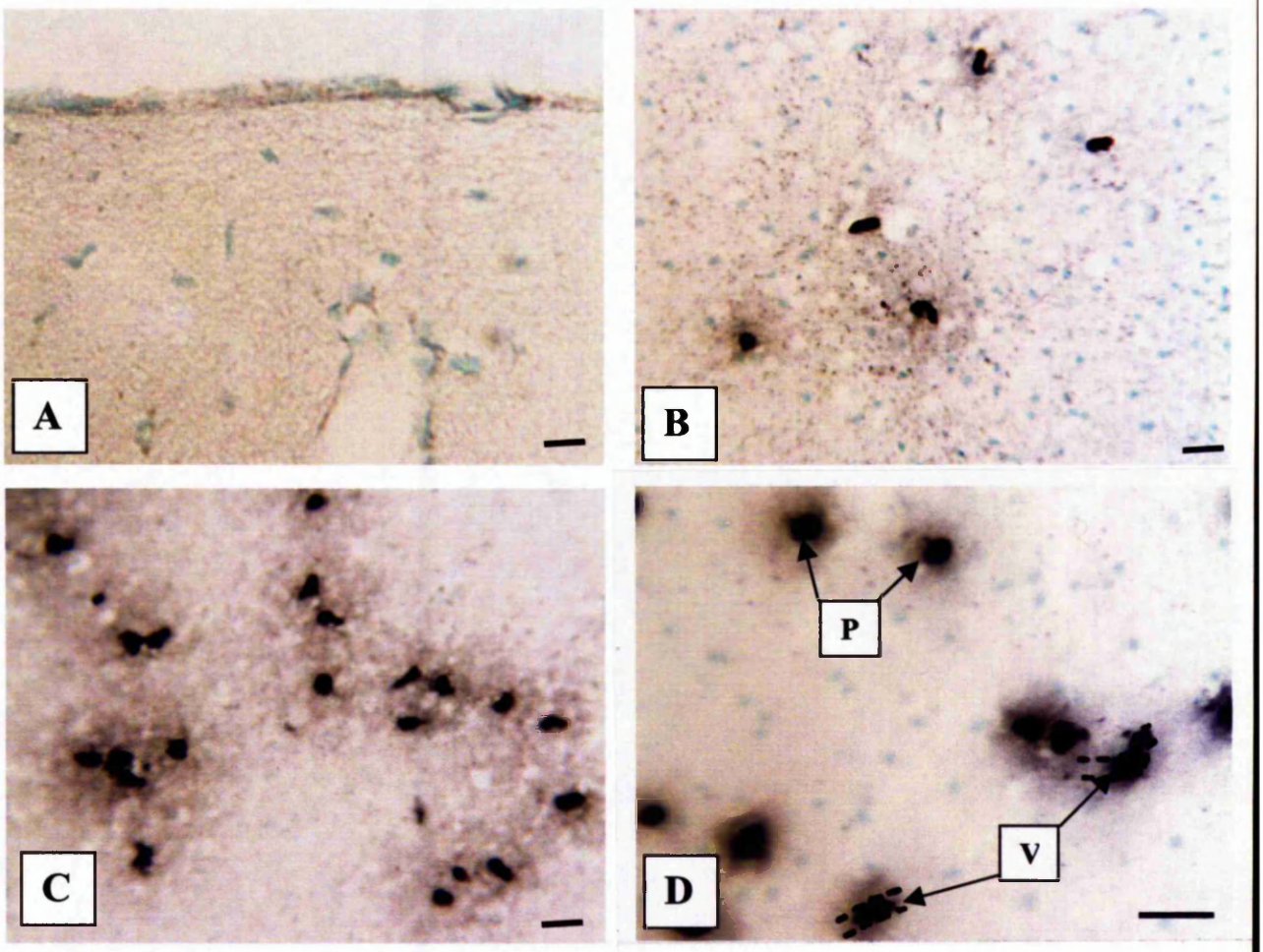

Figure 5.12: Invasion of neutrophils following MCAo revealed by anti-neutrophil antibody in young adult (4 -6 months) animals.

Cryostat sections (10μm) are counterstained with 1% methyl green. Scale bars = 20 μm.
A) Appearance of ipsilateral hemisphere of sham-operated animal, B) 12 hours post MCAo neutrophils are mainly intravascular. C) 24 hours post MCAo more neutrophils are present than at 12 hours, with more parenchymal neutrophils present. D) higher power to show vascular (V) and parenchymal (P) neutrophils.
The acetate overlay shows the position of the vessels observed by focussing up and down through the section.

5.4.1.1 Vascular neutrophils

The number of vascular neutrophils/unit area in the ipsilateral cortical hemisphere of sham-operated animals (denoted as time 0 hours), and at 12 and 24 hours after MCAo in young adult (4-6 month) and aged animals (26-28 month) are presented in Table 5.13. The numbers of vascular neutrophils/unit area in the contralateral hemispheres of sham-operated animals and experimental animals were similar to those of the ipsilateral sham values.

Time-point	**Number of vascular neutrophils /unit area in the lesioned cortex**	
	Adult (4-6 months)	**Aged (26-28 month)**
0 hours (Sham-operated)	16.3 ± 3.0	19.1 ± 13.7
12 hours	422.1 ± 86.5	324.5 ± 29.8
24 hours	856.6 ± 77.4	753.8 ± 129.4

Table 5.13: Number of vascular neutrophils /unit area in the lesioned cortex of young adult and aged animals.

When the number of vascular neutrophils/unit area were analysed using 2-way ANOVA, there was no overall difference between the age groups ($F = 0.56$; $df = 1,17$, $p = 0.467$). There was a highly significant difference over time ($F = 69.47$; $df = 2,17$, $p < 0.001$), numbers increasing with time, but no interaction between time and age ($F = 0.404$; $df = 2,17$, $p = 0.676$). This indicates that the increases in vascular neutrophils with time, occurs in a similar manner in young adult and aged animals after MCAo (see Figure 5.13).

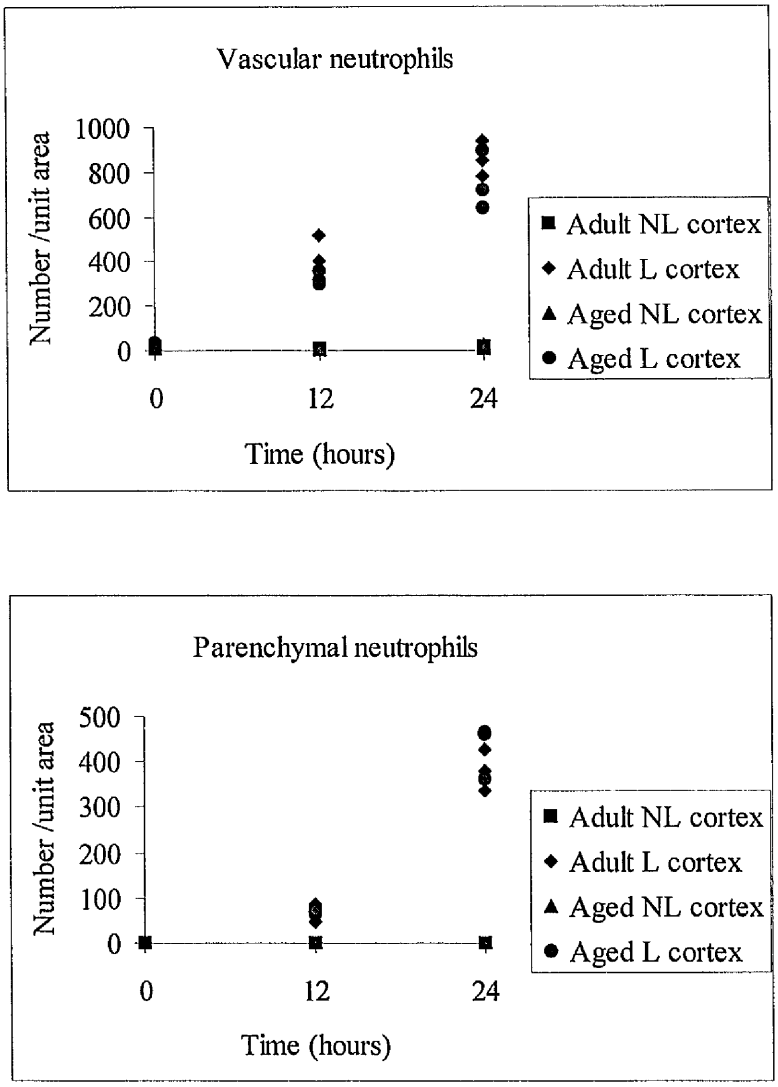

Figure 5.13: Neutrophil numbers/unit area in the lesioned (L) and non-lesioned cortex (NL) of young adult (4-6 months) and aged (26 - 28 months) animals (n = 3 per time point).

Neutrophils were counted on 10μm cryostat sections stained with an anti-mouse neutrophil antibody in sham-operated animals (time = 0), and at 12 and 24 hours after MCAo. The number of vascular and parenchymal neutrophils were counted in the ipsilateral and contralateral cortical hemispheres of three 10μm sections from each region. The average values from each of the three regions were summed to give the number of neutrophils /unit area for each animal.

5.4.1.2 Parenchymal neutrophils

The number of parenchymal neutrophils/unit area in the ipsilateral cortical hemisphere of sham-operated animals, and at 12 and 24 hours after MCAo in young adult (4-6 month) and aged animals (26-28 month) are presented in Table 5.14. The numbers of parenchymal neutrophils/unit area in the contralateral hemispheres of sham-operated animals and experimental animals were similar to those of the ipsilateral sham values.

Time-point	**Number of parenchymal neutrophils /unit area in the lesioned cortex**	
	Adult (4-6 months)	**Aged (26-28 month)**
0 hours (Sham-operated)	1.3 ± 0.4	0.89 ± 0.8
12 hours	71 ± 21.5	68.33 ± 4.16
24 hours	379.7 ± 44.7	429.22 ± 56.8

Table 5.14: Number of parenchymal neutrophils /unit area in the lesioned cortex of young adult and aged animals.

When the number of parenchymal neutrophils/unit area were analysed using 2-way ANOVA, there was no overall difference between the age groups ($F = 3.28$; $df = 1,17$, $p = 0.095$). There was a highly significant difference over time ($F = 83.59$; $df = 2,17$, $p < 0.001$), with numbers increasing over time, but no interaction between time and age ($F = 2.61$; $df = 2,17$, $p = 0.114$). This indicates that the increases in parenchymal neutrophils with time, occurs in a similar manner in young adult and aged animals after MCAo (see Figure 5.13). The proportion of parenchymal neutrophils 12 hours after MCAo, was 13% in young adult and 17% in aged animals. 24 hours after MCAo the proportion of parenchymal neutrophils was 31% in young adults and 36% in aged animals.

5.5 IL-1β expression after MCAo in young adult and aged animals.

The cellular source(s) of IL-1β were identified using double immunostaining of frozen brain sections with anti-IL-1β and either GSA, or GFAP (see Section 2.9.4). The numbers of IL-1β positive astrocytes and microglia/macrophages were counted at each time point (see Section 2.9.5). Counts were performed in the peri-infarct zone of the frontal cortex and the corresponding area in the contralateral hemisphere. In addition, IL-1β positive astrocytes were counted in the corpus callosum of both hemispheres. The data are presented as the mean number of IL-1β positive cells /unit area ($1.59mm^2$; 30 fields of view at x40) ± SD. The only exception to this was for IL-1β positive astrocytes in the white matter, which are presented as the mean cell number/unit area ($0.317mm^2$; 6 fields of view at x 40) ± SD. The data were analysed using 2-way ANOVA.

5.5.1 Results

IL-1β immunostaining revealed very sparse, weakly stained immunopositive cells (see Figure 5.14) within both hemispheres of sham operated animals, especially in the radiation of the corpus callosum. These IL-1β immunopositive cells were present in both young adult and aged animals. Double labelling of sections with GFAP revealed that astrocytes were labelled with IL-1β (see Figure 5.14). No other cell types were positive for IL-1β in sham-operated animals. 12 hours after MCAo, scattered, moderately stained IL-1β immunopositive cells were present in the outer border of the infarct and the peri-infarct zone of the ipsilateral cortex and within the corpus callosum of both hemispheres. Double labelling of sections with IL-1β and either GFAP (for astrocytes), or GSA (for microglia/macrophages) revealed that both cell types were labelled with IL-1β (see Figures 5.14 and 5.15 respectively).

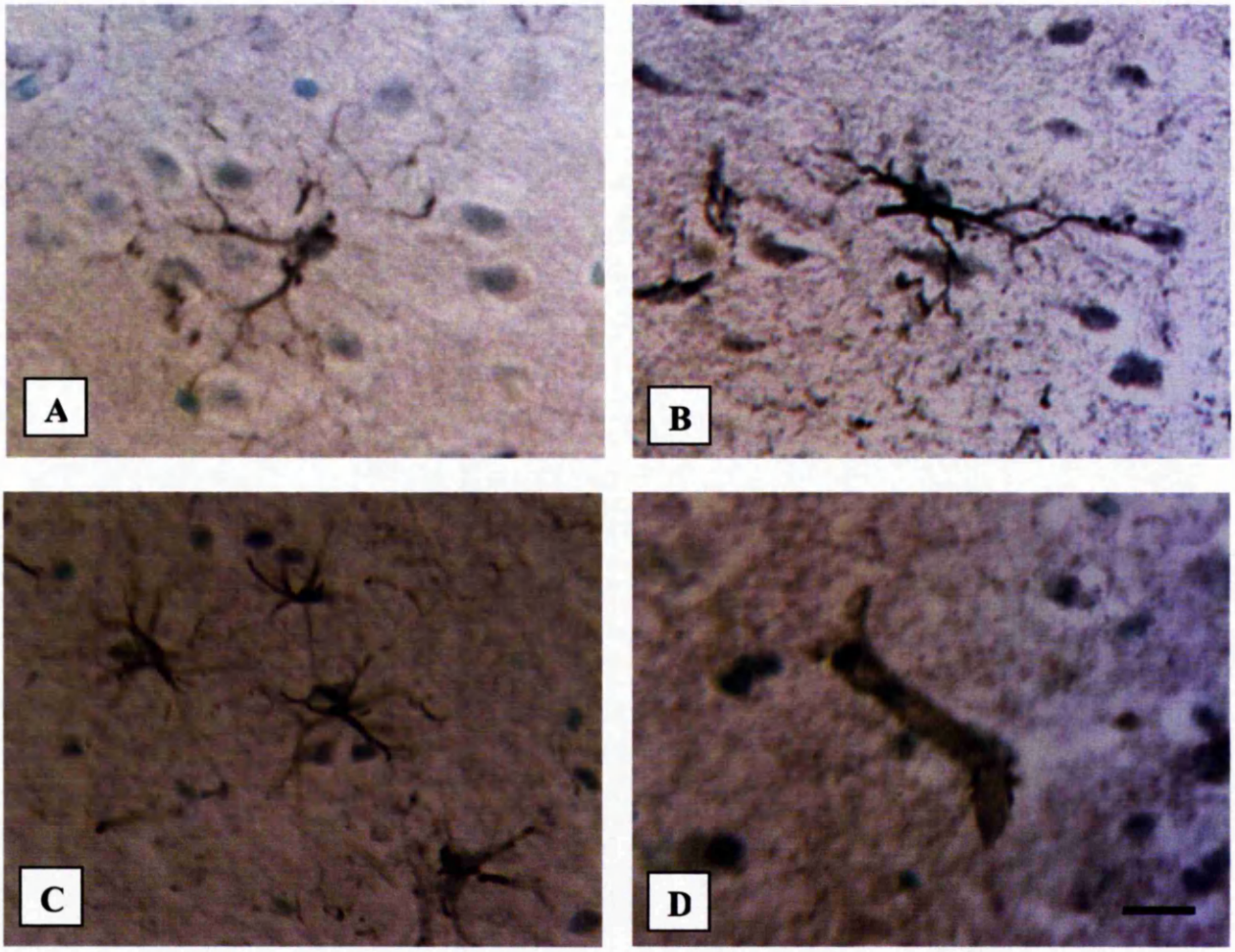

Figure 5.14: IL-1β positive cells in the ipsilateral frontal cortex of young adult (4 -6 month) and aged (27/27 months) animals.

10μm cryostat sections immunostained with anti IL-1β and counterstained with 1% methyl green. Scale bars = 10μm
IL-1β positive astrocyte-like cell in A) aged sham-operated animal and B) aged animal 12 hours post MCAo. Note the increase in staining intensity at 12 hours. C) double immunostaining on sections from young adult animals, 12 hours post MCAo confirmed the identity of the cells in A and B as astrocytes. IL-1β labelling appears brown with DAB and GFAP appears purple with VIP Vector kit. D) IL-1β also labelled the occasional vessel segment in the outer border of the infarct at 12 hours post MCAo.

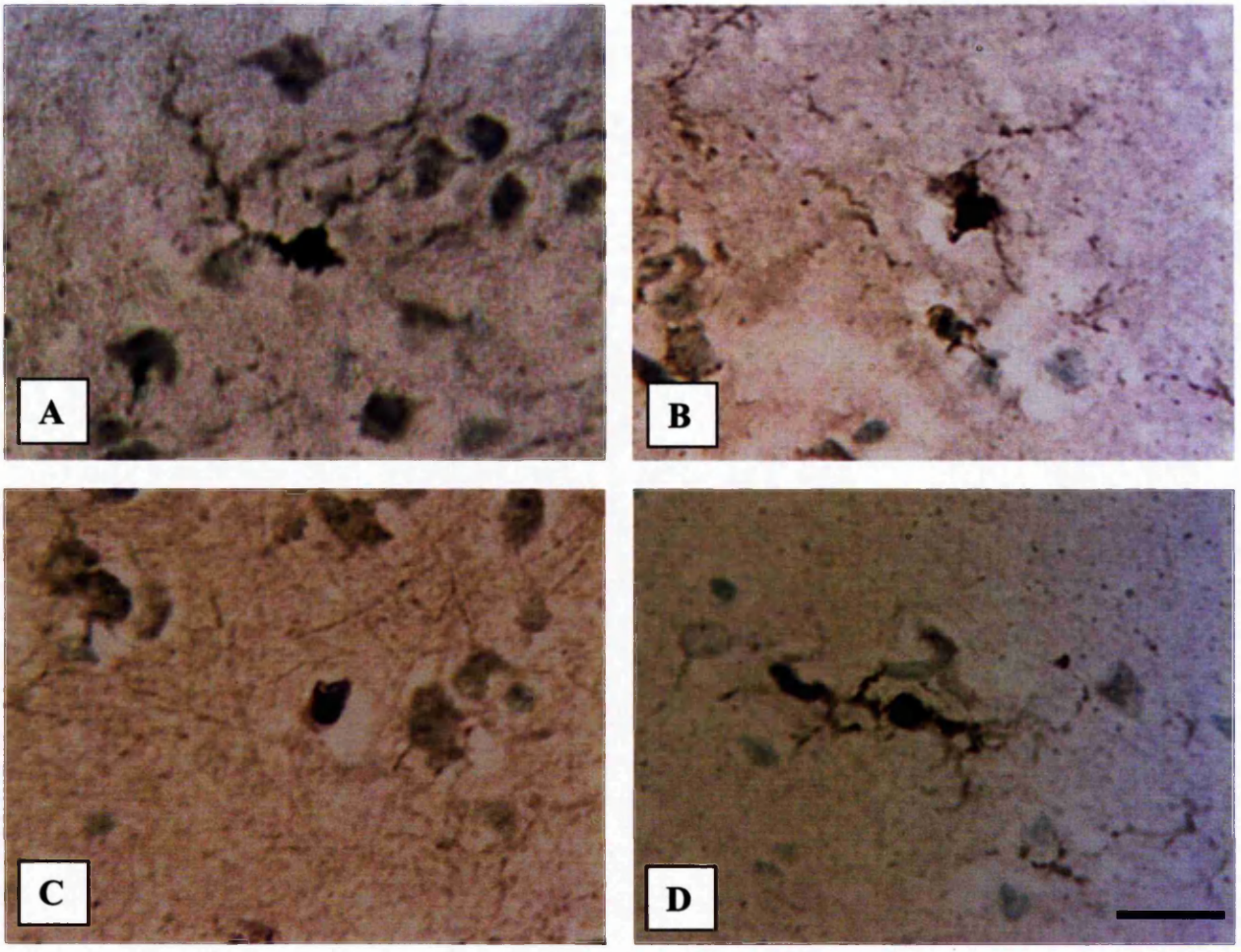

Figure 5.15: Identification of IL-1β immunoreactive microglial cells using double immunostaining on 10μm cryostat sections from a young adult (4 month) animal 12 hours post MCAo.

Sections are counterstained with 1% methyl green. Scale bars = 10 μm.
A) IL-1β staining of glial cell using nickel DAB. B-D) double immunostaining to identify IL-1β positive glial cell. B) appearance of double labeled microglial cell, the colour is different to the two single labeled control sections. C) single control section showing GSA labelling (purple) using VIP Vector kit. D) single control section showing IL-1β labelling (brown) using DAB.

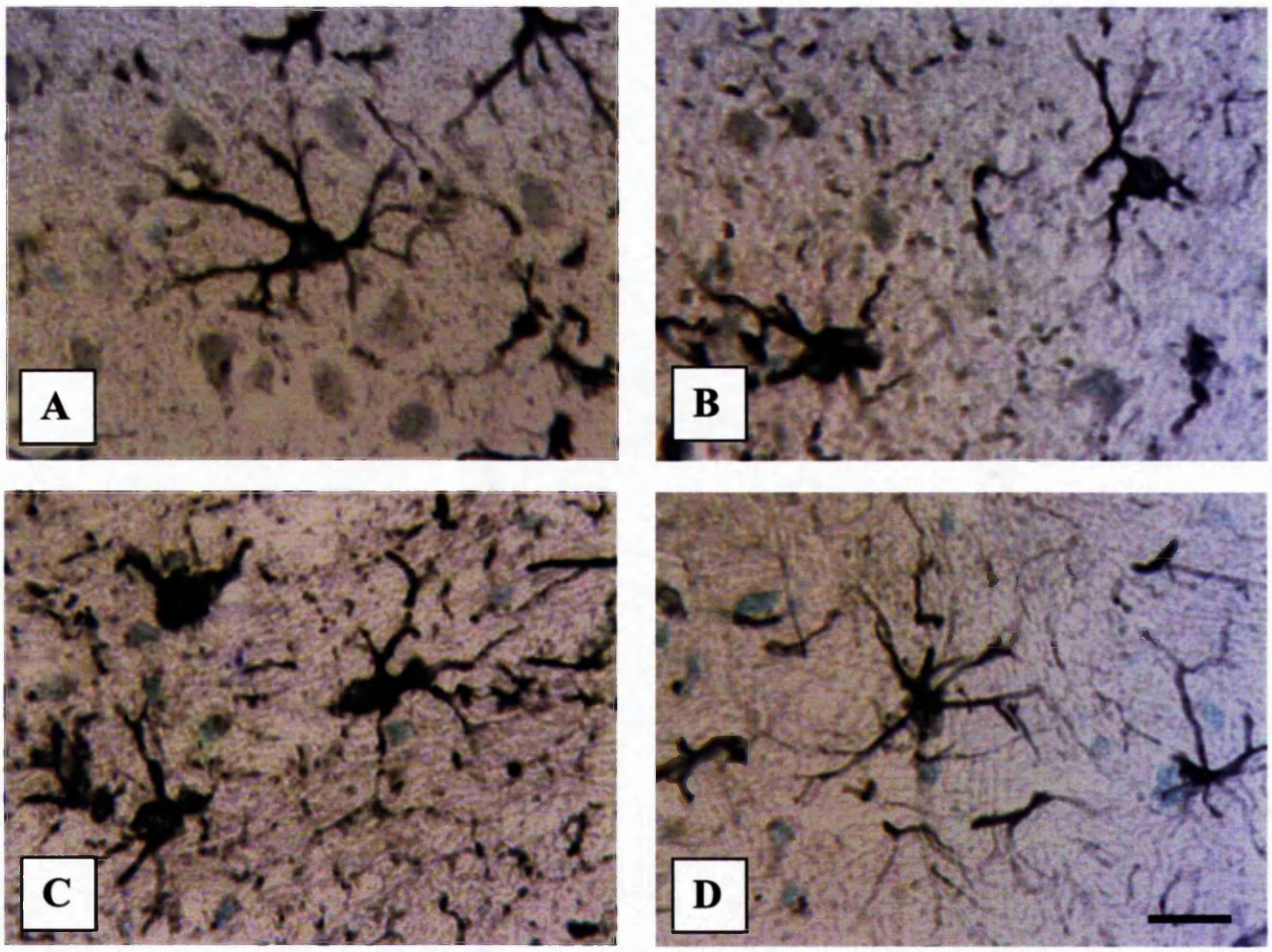

Figure 5.16: IL-1β positive astrocytes in young adult (4 -6 month) and aged (26/27 month) animals 24h after MCAo

10μm cryostat sections immunostained with anti-IL-1β and counterstained with 1% methyl green. Scale bars = 10μm.
A - B) Appearance of astrocytes in the peri-infarct zone of the frontal cortex in A) an adult and B) an aged animal. Astrocytes are very intensely stained for IL-1β. C) IL-1β positive astrocyte in the ipsilateral white matter of an aged animal at 24 hours and D) IL-1β positive astrocyte in the contralateral white matter from the same animal as C. Note that contralateral astrocytes are not as intensely stained as those in the ipsilateral hemisphere.

IL-1β immunopositive microglia/macrophages were only present in the peri-infarct zone and were not detected in the contralateral hemisphere. The occasional cerebral vessel in the outer border of the infarct was also immunopositive for IL-1β (see Figure 5.14). 24 hours after MCAo the density of IL-1β positive astrocytes had further increased and had a similar distribution to those observed at 12 hours. IL-1β positive astrocytes in the peri-infarct zone had become more intensely stained in the area medially adjacent to the infarct in both the cortex and white matter (see Figure 5.16). Very few IL-1β positive microglia/macrophages were detected at 24 hours.

5.5.1.1 IL-1β positive astrocyte in the peri-infarct zone of the ipsilateral hemisphere

The numbers of IL-1β positive cortical astrocytes/unit area in the peri-infarct zone of the frontal cortex of sham-operated animals (denoted as time 0 hours), and 12 and 24 hours after MCAo in young adult and aged animals are presented in Table 5.15.

Time-point	**Number of IL-1β positive cortical astrocytes/unit area in the peri-infarct zone**	
	Adult (4-6 months)	**Aged (26-28 month)**
0 hours (Sham-operated)	2.56 ± 1.38	5 ± 0.33
12 hours	10.22 ± 0.69	20.57 ± 5.85
24 hours	21.67 ± 4.18	34.11 ± 4.85

Table 5.15: Number of IL-1β positive cortical astrocytes/unit area in the peri-infarct zone of the ipsilateral frontal cortex in young adult and aged animals.

When the number of cortical IL-1β positive astrocytes/unit area in the ipsilateral hemisphere was analysed using 2-way ANOVA, there was a highly significant overall difference between the age groups ($F = 24.53$; $df = 1,17$, $p < 0.001$), more IL-1 β positive astrocytes were present in aged animals. There was a highly significant difference over time ($F = 67.27$; $df = 2,17$, $p < 0.001$), with numbers increasing with time after MCAo. However, there was no significant interaction between time and age ($F = 3.21$; $df = 2,17$, $p = 0.076$), indicating that the number of cortical IL-1β positive astrocytes/unit area in the ipsilateral hemisphere increase in a similar manner in young adult and aged animals (see Figure 5.17).

The numbers of IL-1β positive white matter astrocytes/unit area in the peri-infarct zone of sham-operated animals (denoted as time 0 hours), and 12 and 24 hours after MCAo in young adult and aged animals are presented in Table 5.16.

Time-point	**Number of IL-1β positive white matter astrocytes/unit area in the peri-infarct zone**	
	Adult (4-6 months)	**Aged (26-28 month)**
0 hours (Sham-operated)	4.33 ± 0.88	5.22 ± 0.77
12 hours	7 ± 0.58	9.22 ± 0.96
24 hours	9.33 ± 1	13.22 ± 1.26

Table 5.16: Number of IL-1β positive cortical astrocytes/unit area in the peri-infarct zone of the ipsilateral frontal cortex in young adult and aged animals.

When the number of IL-1β positive white matter astrocytes /unit area in the peri-infarct zone were analysed using 2-way ANOVA, there was a significant interaction between time and age ($F = 3.89$; $df = 2,17$, $p = 0.05$). Examination of the data indicates

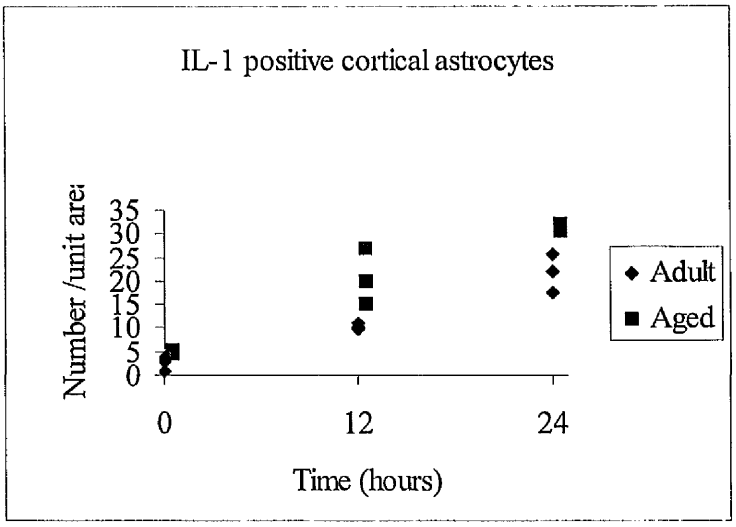

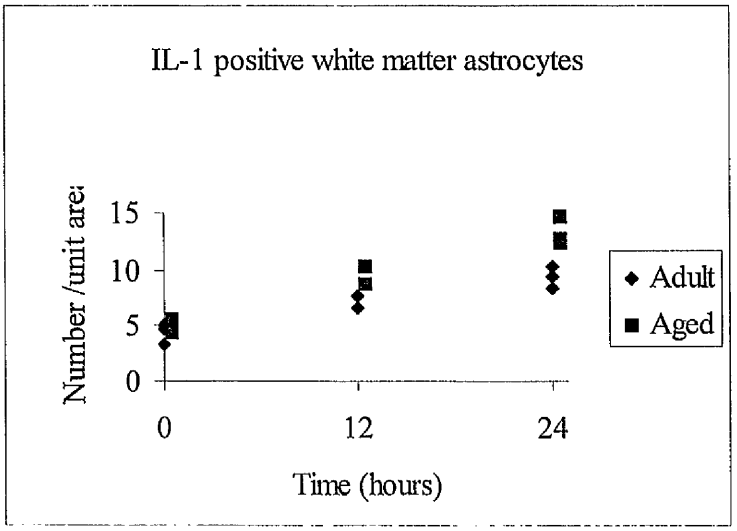

Figure 5.17: IL-1β positive astrocyte numbers/unit area in the peri-infarct zone of young adult (4-6 month) and aged (26-28 month) animals (n = 3 per time point).

The number of IL-1β positive astrocytes were counted on 10μm cryostat sections immunostained with anti-IL-1β antibody in sham-operated animals (time = 0), and at 12 and 24 hours after MCAo. Cortical astrocytes were counted from 10 non-overlapping fields of view of an eyepiece graticule (at x 40) on three sections from three regions 500μm apart. This was repeated for white matter astrocytes using 2 non-overlapping fields of view fields. The average values from each of the three regions were summed to give the number of astrocytes /unit area from each animal.

that higher numbers of IL-1β positive white matter astrocytes/unit area are seen over time after MCAo in aged animals (see Figure 5.17).

5.5.1.2 IL-1β positive astrocyte in the contralateral hemisphere

The number of IL-1β positive cortical astrocytes/unit area in contralateral frontal cortex of sham-operated animals (denoted as time 0 hours), and 12 and 24 hours after MCAo in young adult and aged animals are presented in Table 5.17.

Time-point	Number of IL-1β positive cortical astrocytes/unit area in the contralateral cortex	
	Adult (4-6 months)	Aged (26-28 month)
0 hours (Sham-operated)	1.9 ± 1.4	4.2 ± 0.8
12 hours	2.9 ± 0.8	4.9 ± 1.3
24 hours	3.3 ± 2.0	5.2 ± 0.5

Table 5.17: Number of IL-1β positive cortical astrocytes/unit area in the contralateral frontal cortex in young adult and aged animals.

When the number of cortical IL-1β positive astrocytes/unit area in the contralateral hemisphere were analysed using 2-way ANOVA, there was a highly significant overall difference between the age groups ($F = 24.05$; $df = 1,17$, $p < 0.001$), with more present in aged animals. There was a significant overall difference with time ($F = 5.93$; $df = 2,17$, $p = 0.017$), IL-1β positive astrocytes/unit area increasing with time after MCAo, but no interaction between time and age ($F = 1.53$; $df = 2,17$, $p = 0.256$). This indicates that the number of cortical IL-1β positive astrocytes/unit area in the contralateral hemisphere increase in a similar manner in young adult and aged animals after MCAo (see Figure 5.18). To see if the increase in cortical IL-1β positive

astrocytes/unit area with time is comparable between the two hemispheres, the numbers were analysed using 2-way ANOVA. There was a significant difference between the ipsilateral and contralateral cortex of young adult ($F = 78.23$; $df = 1, 17$, $p < 0.001$) and aged animals ($F = 91.06$; $df = 1,17$, $p < 0.001$). There were much larger increases (8-10 fold) in the numbers of cortical IL-1β positive astrocytes/unit area in the ipsilateral cortex compared to the contralateral cortex.

The number of IL-1β positive white matter astrocytes/unit area in the contralateral hemisphere of sham-operated animals (denoted as time 0 hours), and 12 and 24 hours after MCAo in young adult and aged animals are presented in Table 5.18.

Time-point	**Number of IL-1β positive white matter astrocytes/unit area in the contralateral cortex**	
	Adult (4-6 months)	**Aged (26-28 month)**
0 hours (Sham-operated)	4.3 ± 1.2	5.0 ± 0.3
12 hours	5.2 ± 0.5	5.2 ± 0.4
24 hours	5.8 ± 1.6	8.7 ± 0.6

Table 5.18: Number of IL-1β positive white matter astrocytes/unit area in the contralateral hemisphere of young adult and aged animals.

When the number of white matter IL-1β positive astrocytes/unit area in the contralateral hemisphere were analysed using 2-way ANOVA, there was a significant overall difference between the age groups ($F = 6.96$; $df = 1,17$, $p = 0.022$), again more present in aged animals. There was a significant overall difference with time ($F = 13.33$; $df = 2,17$, $p = 0.001$), numbers increasing with time after MCAo, but no significant interaction between time and age ($F = 3.70$; $df = 2,17$, $p = 0.056$).

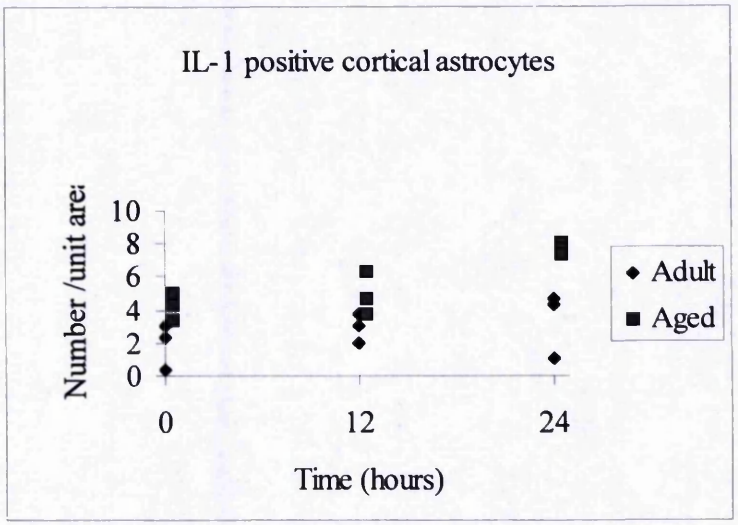

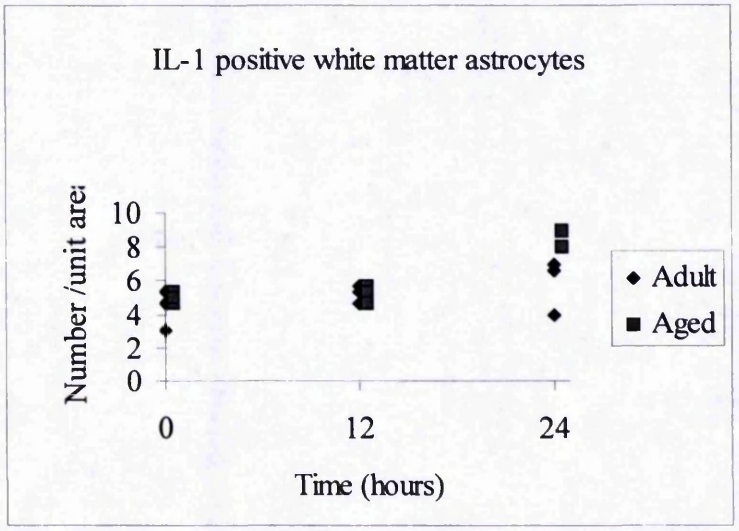

Figure 5.18: IL-1β positive astrocyte /unit area in the contralateral hemisphere of young adult (4-6 month) and aged (26-28 month) animals (n = 3 per time point).

The number of IL-1β positive astrocytes were counted on 10μm cryostat sections immunostained with anti-IL-1β antibody in sham-operated animals (time = 0), and at 12 and 24 hours after MCAo. Cortical astrocytes were counted from 10 non-overlapping fields of view of an eyepiece graticule (at x 40) on three sections from three regions 500μm apart. This was repeated for white matter astrocytes using 2 non-overlapping fields of view fields. The average values from each of the three regions were summed to give the number of astrocytes /unit area from each animal.

Therefore the number of white matter IL-1β positive astrocytes/unit area in the contralateral hemisphere increase in a similar manner in young adult and aged animals (see Figure 5.18).

To see if the increases in white matter IL-1β positive astrocytes/unit area with time are similar in the ipsilateral and contralateral hemispheres, the numbers were analysed using 2-way ANOVA. There was a significant difference between the hemispheres in both young adult ($F = 12.53$; $df = 1, 17$, $p = 0.004$) and aged animals ($F = 60.59$; $df = 1, 17$, $p < 0.001$). There were much larger increases (2-3 fold) in the numbers of white matter IL-1β positive astrocytes/unit area in the ipsilateral hemisphere compared to the contralateral hemisphere.

5.5.1.3 IL-1β positive microglial/macrophage counts

No IL-1β positive microglia/macrophages were detected in sham-operated animals of either age group or in the contralateral hemisphere of experimental animals following MCAo. The number of IL-1β positive microglia/macrophages per unit area in the peri-infarct zone of the frontal cortex at 12 and 24 hours after MCAo in young adult and aged animals are presented in Table 5.19.

Time-point	**Number of IL-1β microglia/ macrophages per unit area in peri-infarct zone of ipsilateral hemisphere**	
	Adult (4-6 months)	**Aged (26-28 month)**
12 hours	9 ± 1.3	10 ± 6.5
24 hours	2.3 ± 2.5	4.1 ± 3.7

Table 5.19: Number of IL-1β microglia/macrophages per unit area in the peri-infarct zone of the frontal cortex in young adult and aged animals.

When the number of IL-1β positive microglia/macrophages per unit area in the ipsilateral cortex was analysed using 2-way ANOVA, there was no significant difference in numbers between the age groups ($F = 0.34$; $df = 1,17$, $p = 0.573$). There was a highly significant difference over time ($F = 12.98$; $df = 2,17$, $p < 0.001$), but no significant interaction between time and age ($F = 0.11$; $df = 2,17$, $p = 0.896$). This indicates that the changes in the number of IL-1β positive microglia/macrophages with time, after MCAo are similar in young adult and aged animals (see Figure 5.19).

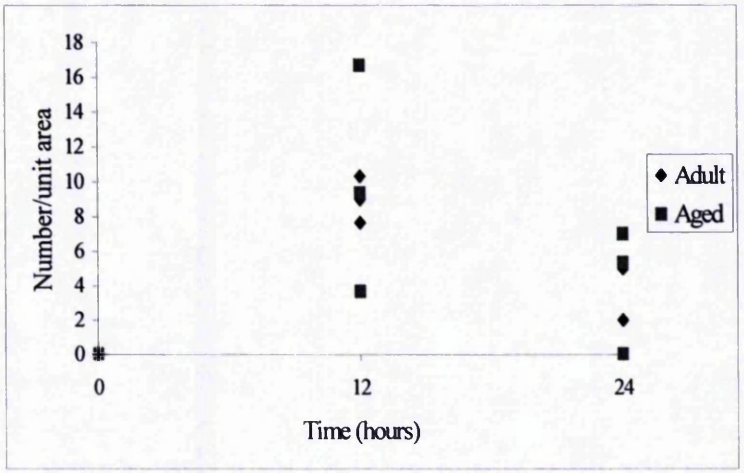

Figure 5.19: IL-1β positive microglia/macrophages per unit area in the peri-infarct zone of the frontal cortex of young adult (4-6 month) and aged (26-28 month) animals (n = 3 per time point).

The number of IL-1β positive microglia/macrophages were counted on 10μm cryostat sections immunostained with anti-IL-1β antibody in sham-operated animals (time = 0), and 12 and 24 hours after MCAo. Microglia/macrophages were counted from 10 non-overlapping fields of view of an eyepiece graticule (at x 40) on three sections from three regions 500μm apart. The average values from each of the three regions were summed to give the number of microglia/macrophages per unit area for each animal.

5.6 Discussion

5.6.1 GFAP positive astrocytes in young adult and aged animals.

Ageing is associated with the hypertrophy of astrocytes (astrogliosis), representing an increase in the size and fibrous appearance of astrocytes, accompanied by the accumulation of GFAP (see Johnson and Finch, 1996; Nichols, 1999; see Section 1.7.3.1). The present study found a significant increase in the number of GFAP immunoreactive astrocytes/unit area in the "normal" ageing brain. This reflected an increase in GFAP positive astrocytes in the cortex, but not in the white matter. Goss *et al.* (1991) using RNA gel-blot hybridisation found a substantial increase in GFAP mRNA in the cortex (3 fold increase) and hippocampus (2.5 fold increase) of aged mice. Since GFAP is the intermediate filament associated with astrocytes, this may represent an increase in astrocyte number, or an increase in the fibrous character of astrocytes, or both. Data presented in this chapter support the view that GFAP positive astrocytes actually increase in number with age, and is consistent with observations made by others (Hansen *et al.*, 1987; Topp *et al.*, 1989; Pilegaard and Ladefoged, 1996; Fotheringham *et al.*, 2000). GFAP is a reliable marker for the transformation of normal astrocytes into reactive astrocytes (Eddlestone and Mucke, 1993). Although the functional significance of astrogliosis with age is not fully understood, the presence of reactive astrocytes could influence intercellular communication and the regulation of the brain's microenvironment (Berciano, 1995; Vernadakis, 1996). If reactive astrocytes are compromised in their ability to carry out normal functions, additional physiological burdens may occur in the aged brain following injury (eg. cytotoxic oedema after ischaemia).

5.6.1.1 Effects of MCAo on GFAP positive astrocyte numbers

The increases in the number of GFAP positive astrocytes in aged mice did not represent a ceiling response, since following MCAo the number and staining intensity of GFAP positive astrocytes further increased over time in both young adult and aged animals. GFAP positive astrocyte numbers increased in the peri-infarct zone of the ipsilateral hemisphere, and in the white matter of both hemispheres. In agreement with the present study others have shown an increase in GFAP positive astrocyte numbers in the periphery of the infarct 24 hours after MCAo in young adult rats (Clark *et al.*, 1993; Garcia *et al.*, 1993; Davies *et al.*, 1998). GFAP mRNA has also been shown to increase as early as 6 hours after MCAo, and gradually increase from 12 hours to 3 days, with widespread induction also seen in non-infarcted areas (Yamashita *et al.*, 1996).

The increase in the number of GFAP positive astrocytes in the periphery of the infarct may be accounted for in several ways. Firstly it may represent an actual increase in astrocyte number through proliferation of the local astrocytes population, as proposed by Latov *et al.*, (1979). Although astrocyte mitotic figures are rare, evidence that astrocyte proliferation does occur, especially in situations associated with a breakdown of the BBB has been shown using double immunostaining for GFAP and 3H-thymidine, or receptor tyrosine kinase (see Norenberg, 1994). The signal for astrocytic division and the nature of the dividing cell after injury is unknown (Landis, 1994). Secondly, it may represent the migration of astrocytes from unaffected areas surrounding the infarct. Cultured astrocytes can be injected into the brains of normal experimental recipients and migrate throughout the brain preferentially in parallel with the course of axons in white matter tracts (Goldberg and Bernstein, 1988). Whether astrocyte migration occurs in the injured brain is still unknown, however, this idea is not supported by the available data of Hatton and Finkelstein (1993), who observed little evidence of astrocyte migration following local brain trauma (stab wound). The third explanation is

that it represents hypertrophy/differentiation of existing astrocytes, resulting in an increased expression of GFAP in cells that previously expressed either no GFAP or too little GFAP for our technique to detect. This explanation is consistent with the observation of an increase in the size and immunofluorescence of GFAP-positive cells in the infarcted hemisphere following permanent MCAo in the spontaneously hypertensive young adult rat (Clark *et al.*, 1993).

In the present study contralateral GFAP immunoreactive astrocytes were also found to increase in the white matter of both young adult and aged animals after MCAo, and were surprisingly of the same magnitude as the increases in the ipsilateral white matter. The significance of the observed increase in astrocyte activation in the corpus callosum of the contralateral hemisphere is not known. Increases in GFAP immunoreactivity have also been detected by others following MCAo in the contralateral corpus callosum (Clark *et al.*, 1993; Petito and Halaby, 1993; Yamashita *et al.*, 1996), but is apparently a transient effect. Following injury to the brain proximal reactive astrocytes develop in the immediate vicinity of the infarct and ultimately produce the glial scar. However distal reactive astrocytes occur at sites some distance from the injury, in a much less disturbed environment without the formation of a glial scar (Ridet *et al.*, 1997). Increases in GFAP may also occur in states of neuronal activation (Steward *et al.*, 1991) and increase in areas that show no obvious signs of tissue injury (see Norenberg, 1994). Therefore the activation of astrocytes at distal sites, such as in the contralateral corpus callosum does not imply brain injury is occurring at this site, but that these astrocytes may be responding to the brain injury and perhaps serve a protective role. It should be noted that astrocytes are not structurally independent cells and are connected to each other via gap junctions, thus creating a network that allows for ionic and metabolic coupling (Norenberg, 1997). This provides a means for long-distance communication and allows for functional responses extending

into areas that are considerably distant from the primary site of action (Norenberg, 1997).

The increases in the numbers of GFAP positive astrocytes with time after MCAo, were similar in young adult and aged animals, indicating that the astroglial response to cerebral ischaemia is not significantly altered with age. These results support qualitative observations made in this laboratory (Fotheringham *et al.*, 2000). In a forebrain ischaemia model, induced by bilateral occlusion of the common carotid arteries in the rat, the number of GFAP positive astrocytes in the hippocampus did not differ significantly between young adult and aged animals seven days after ischaemia (Sutherland *et al.*, 1996). However data from other brain regions was not presented and the number of astrocytes present in "normal" brains was not determined making comparisons with this study difficult. In contrast to these studies, an embolic stroke model in rats, reported that there was a decreased astroglial hypertrophy surrounding the infarct in aged rats examined 4 days after stroke (Futrell *et al.*, 1991). However this was a qualitative assessment and no measurements or counts were made. In the present study the astroglial response to injury was not assessed after 24 hours, so it is not known whether later responses are affected with age.

5.6.2 GSA positive microglia/macrophages in young adult and aged animals

The present study showed there was a significant increase in the number of GSA positive microglia/macrophages in the "normal" brains of ageing mice. These observations confirm qualitative studies made in this laboratory (Fotheringham *et al.*, 2000). GSA positive cells in the brains of uninjured animals are assumed to be activated microglia, as monocyte infiltration does not usually occur unless there is injury/illness, and have been reported to increase in number in the brains of aged

rodents (Ogura *et al.*, 1994; Nichols, 1999). Age-related increases in microglial cell number (identified by morphological examination of EM sections) have also been reported in the brains of aged monkeys (Peters *et al.*, 1991). However, the health status of the animals used in these studies is not reported, so it is not known if these animals had infections/illness that may have caused the increase in number (Peters *et al.*, 1991; Ogura *et al.*, 1994; Nichols, 1999). Microglia in the brains of aged rats have also been shown to express pro-inflammatory antigens, such as MHC class II, CR3 and the lysosomal membrane marker ED1 (Perry *et al.*, 1993; Ogura *et al.*, 1994; Nichols, 1999). These are downregulated or absent from microglia of young rats, suggesting microglia from aged animals are in an activated state. The proliferation and survival of cultured microglia from the dissociated cerebral cortex of rats, is increased as a function of donor age and by middle age (12 months), microglia are more resistant to inhibition of proliferation by treatment with TGF-β1 (Rozovsky *et al.*, 1998). Taken together, these data support a change in microglial cells during normal ageing that involves an increase in the number of activated microglial cells. The altered phenotype of aged microglia along with increased numbers may affect immune/inflammatory responses in the CNS that occur under pathological conditions such as cerebral ischaemia.

5.6.2.1 Effects of MCAo on GSA positive microglia/macrophage numbers

The number of GSA immunoreactive microglia/macrophages, in the peri-infarct zone of the ipsilateral frontal cortex, increased with time in both young adult and aged animals following MCAo. Both parenchymal and vascular associated GSA positive microglia/macrophages increased in number after ischaemia and these increases were most notable 24 hours after ischaemia. Morioka *et al.* (1993), studying MCAo in young adult rats, first observed GSA immunoreactive microglia/macrophages 18 hours after occlusion in the ipsilateral cortex. Davies *et al.* (1998), using the antibody OX-42

(CD11b) to stain for CR3 on microglia/macrophages, observed an increase in the number and staining intensity of ramified microglia/macrophages in the developing ischaemic area as early as 2 hours after MCAo in young adult rats. Possible reasons for the differences could be that OX-42 is a more sensitive marker for microglia/macrophages than GSA, and is found on resting microglia/macrophages (Kato, 1998), or it may be related to the use of different species of animals.

The increase in the number of GSA positive microglia/macrophages in the peri-infarct zone after MCAo was significantly larger in aged (61%) animals compared to young adult (47%) animals. The age-related increase was related to vascular associated GSA positive microglia/macrophages, and not to parenchymal GSA positive microglia/macrophages. This suggests that there is an increase in vascular associated microglia/macrophage activation with age. Interestingly in aged rats the majority of MHC class II immunoreactive microglial cells were associated with blood vessels, meninges and the choroid plexus (Perry *et al.*, 1993). Vascular associated microglia/macrophages are ideally situated to respond to the primary signals of IBD and due to the increased pro-inflammatory antigens on microglia of aged animals, they may be able to respond more rapidly than those from young adult animals. However, since GSA stains macrophages as well as microglia, the presence of peripheral macrophages (monocytes) cannot be excluded, and this increase may reflect an earlier accumulation of monocytes in the blood vessels of aged animals after MCAo. The recruitment of blood borne macrophages (monocytes) into an ischaemic infarct is reported to occur 2-3 days after ischaemia in young adult rodents (Kochaneck and Hallenbeck, 1992; Chiamulera *et al.*, 1993; Garcia *et al.*, 1994; Schroeter *et al.*, 1994; Kato *et al.*, 1996). However, the infiltration of macrophages into the infarcts of aged animals has not been examined in the first 3 days after ischaemia. One study has reported an age-related reduction in macrophage (monocyte) infiltration into the infarct 4 days after focal

ischaemia (Futrell *et al.*, 1991). Their study grouped infarcts (from one field of view at x40) into hypercellular infarct (those having greater than 30 monocytes) and hypocellular infarct (having less than 10 monocytes), but the number of macrophages/unit area was not determined. The present study is the first quantitative report on microglia/macrophage activation following MCAo in aged animals, and extends qualitative observations made previously in this laboratory (Fotheringham *et al.*, 2000).

There was also a significant age-related difference in the number of GSA positive microglia/macrophages in the contralateral hemisphere with time. Contralateral GSA positive microglia/macrophages increased in number with time after MCAo in the aged animals, but not in young adult animals. Again this increase was related only to an increase in vascular associated GSA positive microglia/macrophages. The contralateral increase in GSA immunoreactive microglia/macrophages in aged animals (22% increase over time) was of a smaller magnitude than the increase occurring in the ipsilateral hemisphere (61% over time). Increases in GSA immunoreactive microglia/macrophages have been observed 7 days after ischaemia in the contralateral cortex and hippocampus of young adult rats (Morioka *et al.*, 1993). Others have reported increases in OX-42 immunoreactive microglia/macrophages in the contralateral cortex and corpus callosum of young adult rats 24 hours after MCAo, but OX-42 immunoreactive microglia/macrophages were more numerous ipsilaterally (Kato *et al.*, 1996; Davies *et al.*, 1998). The reason for the observed differences in contralateral microglial/macrophage activation in the young adult rat and mouse are not known, but may be related to species differences. In the aged mouse the ischaemic infarct is more extensive than in the young adult mice (see Chapter 4), and this may be of sufficient magnitude to induce the acute contralateral response not seen in the young adult animal. This increased microglial/macrophage activity in the contralateral

hemisphere of aged animals following MCAo was not associated with any visible signs of cell damage. Although it is possible that ultrastructural investigation might have revealed subcellular changes that could eventually lead to cell death. Activation of microglia/macrophages at the local primary site of tissue damage (i.e. the peri-infarct zone) and at distal locations (both ipsilateral and contralateral to the primary site of damage) may occur due to retrograde and anterograde neuronal degeneration (Morioka *et al.*, 1993; Gehrmann *et al.*, 1995).

The increase in the number of GSA positive microglia/macrophages in the peri-infarct zone of both young adult and aged animals, and in the contralateral hemisphere of aged animals following MCAo may be due to either migration, or proliferation of microglial cells, or both. A unique feature of microglia is the apparent permanency of ramified microglia in adult tissue, with little or no turn over of these cells, which may be attributed to the presence of the BBB restricting the entry of blood borne monocytes (Davis *et al.*, 1994). However, a final differentiation property of microglia compared to macrophages is that they are capable of significant proliferation, replacing spent cells or increasing macrophage activity in the absence of monocyte infiltration in response to various brain injuries (Glenn *et al.*, 1992; Davis *et al.*, 1994). Neuronal degeneration induces the deposition of activated complement factors that act via the integrin Mac-1-receptor and are powerful chemoattractants for microglia cells (Nolte *et al.*, 1996). This can induce the accumulation of microglial cells at sites of neuronal injury and may also contribute to the increased numbers of microglia/macrophage cells observed in the peri-infarct zone. The mechanisms causing the initial activation of microglia/macrophages following injury are not known, it is likely that it is mediated by phagocytic signals arising from necrotic tissue such as that found in regions of infarcted tissue (Giulian *et al.*, 1989; Giulian and Robertson, 1990; Giulian and Vaca, 1993). Cytokines such as IL-1β, IL-4, IL-6 and particularly colony stimulating factors (CSFs) have also been

shown to increase microglial proliferation *in vitro* and induce the upregulation of surface molecules (Gehrmann *et al.*, 1995; Wood, 1998).

The increased activation level of microglia/macrophages during ageing may be due to periodic challenges to the immune system or may be an indication of subclinical pathology. This increase in the level of microglial/macrophage activation and the number of microglia/macrophages per unit area with age, could account for the increase in the magnitude of the microglial/macrophage response to injury as seen in this study. Potential mechanisms responsible for the exaggerated responsiveness of aged microglia/macrophages to ischaemic injury may include the following. Firstly injury may produce larger amounts of damage in the aged brain (as shown in Chapter 4), resulting in a larger microglial/macrophage 'activation signal' and therefore larger GSA induction. Secondly, microglia from the brains of aged animals may be more sensitive to activation, possibly due to the increase in pro-inflammatory surface antigens (Perry *et al.*, 1993), and thirdly the activation agent(s) may persist longer in the aged brain. What leads to the increased activation of microglia/macrophages with age is not known but a recent report has suggested a role of age-related accumulation of advanced glycation endproducts (AGE). AGE immunoreactivity was found to colocalise with MHC class II receptors on microglia in postmortem brain samples from patients with AD (Dickson *et al.*, 1996). The significance of the increased microglial/macrophage response with age to MCAo is not known. However increases in microglial/macrophage numbers and activation are associated with numerous pathological conditions, such as AD and MS (see Norenberg, 1994; Zielasek and Hartung, 1996; Wood, 1998) and may render the aged brain more susceptible to IBD.

5.6.3 ICAM-1 expression in young adult and aged animals after MCAo

There was no difference in the number of ICAM-1 positive vessels with age in sham-operated animals, and their numbers did not change in the contralateral cortex after ischaemia. Following cerebral ischaemia the numbers of ICAM-1 positive vessels, in the peri-infarct zone and central zone of the infarct increased significantly in both age groups over time. Significantly more were present in young adult animals but the increase over time was comparable in both young adult and aged animals. The number of ICAM-1 positive vessels in the outer zone of the infarct increased over time after ischaemia, with similar numbers in both age groups, and the increase was alike in young adult and aged animals. In all cases the increase in ICAM-1 positive vessels was related to an increase only in microvessels 10μm or under in diameter. Overall these results suggest that there was no difference in ICAM-1 upregulation following MCAo in young adult and aged animals.

Focal cerebral ischaemia induces the sequential upregulation of leukocyte-endothelial adhesion molecules (see Section 1.5.2.1). The present study has shown that there is weak constitutive expression of ICAM-1 in vessels and microglia/macrophages, in sham-operated animals and in the contralateral hemisphere of experimental/ischaemic mice. In the uninjured brain, others have observed constitutive expression of ICAM-1 immunoreactivity on vascular endothelial cells and some glial cells (Rössler *et al.*, 1992; Beehuizen and Furth, 1993; Wang *et al.*, 1994a). The present study observed increases in the staining intensity and number of ICAM-1 positive vessels within the central and outer zone of the infarct, and peri-infarct zone of the ipsilateral hemisphere 12 and 24 hours after the induction of MCAo, although earlier time-points were not examined. ICAM-1 mRNA has been shown to significantly increase at 3 hours, with peak expression 6-12 hours following permanent MCAo in the young adult rat (Wang *et al.*, 1994a), and remain elevated up to 5 days. The induction profile of ICAM-1

following transient MCAo was similar except increased levels of ICAM-1 mRNA were detected at 1 hour and gradually reached a peak at 10 - 12 hours (Wang *et al.*, 1994a; Zhang *et al.*, 1995). Double immuno-staining with von Willebrand factor or factor VIII, revealed that these upregulated adhesion molecules were localised to endothelial cells of intraparenchymal blood vessels in the ischaemic cortex (Wang *et al.*, 1994a; Zhang *et al.*, 1996; Zhang *et al.*, 1998a). Although there was no significant ipsilateral age/time effect in this study, indicating that the upregulation of ICAM-1 following cerebral ischaemia is not affected with age, higher numbers of ICAM-1 positive vessels were found in the peri-infarct zone and central zone of the infarct in young adult animals. It may be that with age cerebral vessels become slightly less sensitive to the signals involved in ICAM-1 upregulation. There are no other reports examining ICAM-1 expression in aged animals following ischaemia.

ICAM-1 positive vessels were detected throughout the infarct and peri-infarct zone. It was surprising to see ICAM-1 positive vessels in the infarct at 24 hours as all other cells were pyknotic, although some of these vessels appeared to be granular in structure and were perhaps disintegrating vessels (see Figure 5.8). No further material was available for a full morphological examination of material to confirm this. Although the vessels in the infarct stain for ICAM-1, it may not necessarily follow that these vessels are structurally and functionally intact, but it may account for the appearance of neutrophils throughout the infarct at both 12 and 24 hours. In this study double staining of ICAM-1 with GSA, revealed that microglia/macrophages also constitutively expressed ICAM-1. There was an increased ICAM-1 staining intensity of microglia/macrophages in the peri-infarct zone following MCAo in both young adult and aged animals. This is in agreement with observations following acute experimental CNS inflammation in adult rodents, where ICAM-1 upregulation was found not only on vascular endothelial cells but also on perivascular infiltrating cells and glial cells

(Cannella *et al.*, 1991; Wilcox *et al.*, 1990). Activated microglial cells in the process of axon phagocytosis express both the integrin adhesion molecules LFA-1 and VLA-4, as well as ICAM-1 (Cotman *et al.*, 1998), whereas reactive astrocytes, although phagocytically active, did not express detectable levels of these adhesion molecules (Hailer *et al.*, 1997). ICAM-1 has also been localised to activated microglial cells in brain tissue from patients with MS or AD (Boyle and McGeer, 1990; Hailer *et al.*, 1997; Cotman *et al.*, 1998). The pattern of adhesion molecule expression on activated microglial/macrophage cells could serve as a means to retain activated microglial/macrophage cells at sites of neuronal degeneration, because ICAM-1 and LFA-1 serving as a corresponding pair of ligands (see Table 1.1), would enable homotypic interactions of adjacent microglial/macrophage cells. Additionally, adhesion molecule expression on microglia/macrophages may help guide inflammatory cells (such as neutrophils and monocytes) to their sites of action.

The signal that induces the expression of ICAM-1 after ischaemia is not fully understood. It is of interest that following cerebral ischaemia the temporal induction profile of ICAM-1 mRNA is similar to that of IL-1β and TNF-α mRNA expression (Liu *et al.*, 1993; Liu *et al.*, 1994), and that these cytokines can induce the expression of ICAM-1 on endothelial cells and microglia/macrophages (Feuerstein *et al.*, 1994, Kim, 1996). Reductions in the number of ICAM-1 positive vessels in the lesioned hemisphere following cerebral ischaemia have been demonstrated by blocking the actions of endogenous TNF-α (Barone *et al.*, 1997; Yang *et al.*, 1998) and by adenoviral induced overexpression of IL-1ra (Yang *et al.*, 1999). Therefore it is possible that the increased expression of the proinflammatory cytokines, such as IL1-β and TNF-α following MCAo may lead to the elevated expression of ICAM-1 on glial cells and the vascular endothelium after focal ischaemia.

5.6.4 Neutrophil invasion in young adult and aged animals after MCAo

In this study there were negligible numbers of neutrophils in sham operated animals of both age groups. Twelve hours after MCAo, neutrophil numbers had increased and could be seen in all stages of infiltration, i.e. from within the vascular lumen of vessels in the ischaemic cortex, to within the brain parenchyma of the developing ischaemic region. The numbers of vascular and parenchymal neutrophils further increased up to 24 hours after cerebral ischaemia, with a higher percentage in the brain parenchyma than at 12 hours. Overall there was no difference in the invasion of neutrophils into the ischaemic hemisphere with age over time.

From this study it was shown that large numbers of neutrophils are present 12 hours after MCAo, and that although the majority of these were intravascular some neutrophils were present within the brain tissue (14% of total in young adult and 17% in aged), and are therefore present at a time when they may be involved in delayed neuronal damage. A study examining H&E sections from young adult animals subjected to permanent MCAo (via the suture method), first detected neutrophils 30 minutes post occlusion with intravascular neutrophils peaking at 12 hours, and parenchymal neutrophils increasing 12 to 72 hours after occlusion (Garcia *et al.*, 1994). Neutrophils may have been present earlier than 12 hours in the present study, but this was the earliest time point examined after MCAo. Although at 12 hours the developing infarct covers most of the area to that found at 24 hours, examination of Cresyl Violet sections revealed that not all cells within this region were affected. There were regions of apparently normal neurones and glial cells found between other regions where cells were pyknotic. Although neutrophils may not be involved in the early stages of IBD (taking place in the first few hours after stroke) they may be involved in the delayed progression of neurodegeneration. The present study also found that the accumulation of neutrophils in cerebral vessels and their migration into the brain parenchyma is not

effected with age. There are no other studies examining neutrophil invasion following ischaemia in aged animals.

Neutrophils were observed in both the ischaemic infarct and in the peri-infarct zone and although the presence of neutrophils adjacent to the infarct was expected, their ability to reach vessels supplied by the occluded MCA may be surprising. One explanation for the presence of neutrophils in vessels within the infarct may be their arrival through retrograde flow (Hallenbeck *et al.*, 1986). Such flow was demonstrated by Kamijyo and Garcia (1975) in cats, using carbon black injected *in vivo*. In their study, filling of the MCA distal to the occlusion was attributed to retrograde flow through the subarachnoid arterial-arterial anastomosis between the anterior and middle cerebral arteries. This is likely to have been the route of neutrophils that were identified within the vascular lumen in the ischaemic zone. Once inside the brain, adhesion molecules expressed by glial cells and chemokines may mediate their migration to target areas (Feuerstein *et al.*, 1994; Kim, 1996; Ransohoff and Tani, 1998).

The signal for the migration of neutrophils into ischaemic tissue has not been fully determined. ICAM-1 is necessary for neutrophil adhesion and is upregulated following cerebral ischaemia (see above, and Section 1.5.2.1). It has been demonstrated that injection of IL-1β into the striatum of juvenile rats results in an increased adhesion of neutrophils to the endothelium (Bolton *et al.*, 1998). These neutrophils also stain positive for phosphotyrosine, indicating that engagement of integrin receptors on the neutrophil surface and adhesion to the endothelial receptor (i.e. ICAM-1) triggers a signalling cascade (Bolton *et al.*, 1998). Various chemokines are also upregulated following IBD including IL-8 (significantly increased at 6 hours; Matsumoto *et al.*, 1997; Ransohoff and Tani, 1998), CINC (observed 6-24 hours, with peak expression at 12 hours; Liu *et al.*, 1993) and MCP-1 (peaks at 24-48 hours; Kim *et al.*, 1995; Gourmala *et al.*, 1997). The earlier increases in the expression of IL-1β (see Section

1.6.2.2) and TNF-α (see Section 1.6.3) after MCAo may be involved in the co-ordinated expression of the chemokines following cerebral ischaemia (Ransohoff and Tani, 1998). The time course of activation of the chemokines is consistent with the appearance of the different leukocytes, neutrophils infiltrating 12-24 hours after MCAo, and monocytes and macrophages at later stages (see above).

There is much controversy as to the role of neutrophils following ischaemic brain injury. It was initially thought they were simply involved in the clean up process that prepares the wound for healing. However, evidence is accumulating that suggests that neutrophils are actually involved in the pathological mechanisms leading to IBD (see Section 1.5.2.2). After leaving the circulation and migrating by chemotaxis to the site of inflammation/infarct, neutrophils must recognise and bind to the offending pathogen/tissue before activation of the respiratory burst (NADPH oxidase activation) takes place. This leads to the generation of reactive oxygen intermediates (free radicals) and the release of arachidonic acid from membrane phospholipids, and the neutrophils undergo degranulation releasing cytotoxic enzymes into the surrounding parenchyma (Edwards, 1995). There are no reports in the literature on the effects of adhesion molecule blockade or neutrophil depletion on IBD in aged animals. Since neutrophil accumulation and migration were not affected with age it is unlikely that damage caused by neutrophils contributes to the age-related increase in IBD. However, age-related increases in oxidative damage to DNA and diminished antioxidant defence mechanisms have been reported in the ageing rodent brain (Bondy and LeBel, 1993; Venugopal and Rao, 1993; Johnson and Finch, 1996). If the ageing rodent brain is less able to cope with the free radicals produced by neutrophils, this could predispose the aged brain to increased cellular damage after ischaemia.

5.6.5 Expression of IL-1β after MCAo in young adult and aged animals

This study showed that constitutive IL-1β immunostaining was very low in the 'normal' brain and restricted to a few astrocytes that were weakly stained. 12 and 24 hours after MCAo the number of IL-1β positive astrocytes in young adult and aged animals significantly increased in both cerebral hemispheres. There was also a significant increase in the number of IL-1β positive microglia/macrophages in young adult and aged animals after MCAo, with higher numbers present at 12 hours than at 24 hours. The identity of IL-1β immunopositive cells was confirmed by double labelling of sections with IL-1β and GFAP (to identify reactive astrocytes), or IL-1β and GSA (to identify microglia/macrophages). Some cerebral vessels in the outer zone of the infarct and peri-infarct zone were immunopositive for IL-1β after MCAo, but were present too infrequently to be counted.

A study examining IL-1β immunoreactivity after permanent MCAo in young adult rats, found that early expression occurred almost exclusively on microglial cells (at 6 hours) and meningeal macrophages (at 2 hours), with delayed expression in astrocytes (at 48 hours) and invading immune cells (Davies *et al.*, 1999). The highest numbers of IL-1β positive microglia/macrophages in the present study were observed 12 hours after MCAo with a decrease in numbers by 24 hours. This is consistent with Pearson *et al.* (1999), examining IL-1β immunoreactivity in the brains of young adult rats after excitotoxic damage. Their study found maximal IL-1β expression by microglia/macrophages 8 hours after onset, and then the number of IL-1β positive microglia/macrophages markedly declined by 24 hours. Others have reported that the main cellular source of IL-1β following permanent occlusion (via intraluminal filament occlusion) in young adult mice was on vessels in the ischaemic infarct, with the occasional IL-1β positive microglia/macrophage (Zhang *et al.*, 1998a). IL-1β positive

vessels were detected as early as 15 minutes after occlusion with numbers peaking at 1-2 hours, then slowly declining from 2 to 24 hours. The earliest time point examined after MCAo was 12 hours in the present study, therefore it is possible that IL-1β immunopositive cells were present earlier. The differences in the reported cellular sources and timings of IL-1β expression following MCAo may be related to several factors. These include differences in the species and strain of animal used, the different methods of inducing MCAo, or differences in the specificity of the respective antibodies.

Increases in IL-1β positive astrocytes were also observed in the contralateral hemisphere of both young adult and aged animals. However, this increase was of a much smaller magnitude than in the ipsilateral hemisphere. The increased immunolabeling of IL-1β in areas distant from the main site of injury, such as in the contralateral cortex and corpus callosum has been reported by others after MCAo (Zhang *et al.*, 1998a; Davies *et al.*, 1999). The causes and significance of this are unknown. It may be related to disturbances of anatomical pathways or spreading depression but it is not associated with any recognisable cell death. This suggests that the presence of IL-1β alone is not sufficient to cause neuronal death, and may only be neurotoxic when cells have been previously exposed to an ischaemic or excitotoxic insult.

The expression of IL-1β protein following MCAo coincided with the temporal profiles of IL-1β mRNA expression and IL-1β protein levels in the brain after focal ischaemia (Ianotti *et al.*, 1993; Loddick *et al.*, 1996; Hill *et al.*, 1999; see Section 1.6.2.2). The functional significance of the increased expression of IL-1β by these cells after MCAo is unknown at present. There are several potential actions of IL-1 that may lead to or inhibit neuronal damage (see Section 1.6.2.3). It is probable that low levels of

IL-1 may be neurotrophic/neuroprotective, whilst higher levels of IL-1 may have a neurotoxic effect.

The IL-1β antibody used in the present study, like those used by others (Scriptor *et al.*, 1997, Davies *et al.*, 1999; Pearson *et al.*, 1999), identifies both the precursor and mature forms of IL-1β. Therefore it is not possible at this stage to distinguish whether both forms are present in astrocytes and microglia/macrophages, or if pro-IL-1β accumulates in these cells. Expression of ICE has only been described so far in microglia and has been shown to be upregulated in these cells after ischaemic brain injury (Bhat *et al.*, 1996). However it may be possible that another, as yet uncharacterised, protease may be present in astrocytes to convert pro-IL-1β to its mature form (Pearson *et al.*, 1999). Discrepancy between IL-1β mRNA and protein expression may occur in a compromised energy state such as after ischaemia. Indeed, it has been shown that although large quantities of IL-1β mRNA can be induced, much of it is not translated and undergoes degradation (Roux-Lombard, 1998). Although there are no reports on the immunolocalisation of mature IL-1β, increases in bioactive IL-1β (identified by bioassay) has been reported within 30 minutes after permanent MCAo in the brains of young adult rats (Davies *et al.*, 1999), suggesting at least some mature IL-1β is produced.

In the present study there were no age-related differences in the numbers of IL-1β positive microglia/macrophages per unit area present in the brain following MCAo. There was a significant overall increase in the number of IL-1β positive astrocytes in aged animals. However, the increases in the number of IL-1β positive astrocytes after MCAo occurred in a similar manner in young adult and aged animals. The only exception to this was in the ipsilateral corpus callosum where higher numbers of IL-1β positive astrocytes were seen with time after MCAo in aged animals. The reasons for

this are not known. Astrocytes from the brains of aged animals in this region may be more sensitive to the signal to induce IL-1β production or have an enhanced ability to produce IL-1β. The age-related increase in IL-1β positive astrocytes may be related to the increased numbers of GFAP positive astrocytes found in aged animals. This is the first report of IL-1β protein expression following MCAo in aged animals. Increases in the expression of IL-1β have been reported in the hippocampus of 'normal' aged rats (22 month) compared to young adults rats (4 months; Murray *et al.*, 1997). Immunoblotting for IL-1β was only done in hippocampal homogenates and so the cellular source of IL-1β was not identified and other brain regions were not examined. The significance of the increase in the number of IL-1 positive astrocytes in the aged brain is not known. Since there are more IL-1 positive astrocytes in aged animals, more IL-1β may be produced by aged animals following injury to the brain. However, the present study did not measure bioactive IL-1β levels so it is not known whether there was a corresponding increase in IL-1β levels after MCAo in aged animals. Further studies would be needed to determine whether bioactive IL-1β levels are altered with age following MCAo.

5.6.6 Conclusion

Increases in the number of GSA positive microglia/macrophages and GFAP positive astrocytes were found in the brains of aged mice. This is consistent with the findings reported by others using different methods (Johnson and Finch, 1996; see Section 1.7.3.1). Following cerebral ischaemia the activation of astrocytes was similar in young adult and aged animals, however there was an age-related increase in the activation of GSA positive microglia/macrophages with time in both the ipsilateral and contralateral hemispheres. Therefore the microglial/macrophage response to IBD is

affected with age, though the functional significance of this has yet to be determined. No significant differences in the upregulation of ICAM-1 on blood vessels or the invasion of neutrophils after MCAo were found between young adult and aged animals. Therefore there appear to be no functional deficiencies with age in these mechanisms. The main cellular sources of IL-1β following MCAo in both young adult and aged animals were astrocytes and microglia/macrophages. There was an overall age-related increase in the number of IL-1β positive astrocytes in aged animals. However, the increases in the number of IL-1β positive astrocytes and microglia/macrophages with time after MCAo were similar in young adult and aged animals. The only exception to this was in the corpus callosum of aged animals where there was an increased expression of IL-1β with time by astrocytes. It is not known if this translates to differences in the levels of bioactive IL-1β in the brains of aged animals after injury. The observed age-related changes in glial cells may influence the pathophysiology of IBD and further studies are required to determine the functional significance of these changes. Changes in glial cells with age may affect the restoration of homeostasis or permeability of the BBB after injury.

Chapter 6

Effects of age on BBB permeability to the macromolecular tracer horseradish peroxidase (HRP) following MCAo

6.0 Introduction

Cerebral ischaemia is associated with two types of brain oedema, cytotoxic/cellular and vasogenic (Klatzo, 1994; Kimelberg, 1995; see Section 1.4.1). Cytotoxic oedema occurs very early after ischaemia where there is an abnormal uptake of water by injured brain cells. This leads to swelling of cellular elements, particularly astrocytes (Kimelberg, 1995). The initial cytotoxic oedema progresses further leading to severe tissue changes at which time there is usually disruption to the BBB. This allows the abnormal passage of serum proteins and water into the extracellular compartment. The extravasation of serum proteins contributes to the retention of water that is essential for the formation and persistence of vasogenic oedema.

Water content in the brain has been shown to significantly increase as early as 1 hour after permanent MCAo in adult rats (Hatashita and Hoff., 1990). There is a progressive increase in water content from 1 to 24 hours when brain water content reaches a plateau. Brains of aged mice have been shown to take in more water following MCAo than adult animals measured 24 hours after MCAo (Fotheringham *et al.*, 2000). The reasons for the age-related increase in brain water content after ischaemia are not known. However, there are several age-related changes in the BBB that could further compromise its integrity following cerebral ischaemia and perhaps lead to an increase in vasogenic oedema (see Section 1.7.2). Measurement of HRP extravasation, a protein tracer (molecular weight ~40,000 daltons) has been used extensively as an indicator of changes in BBB permeability (Broadwell, 1989; Sampaolo *et al.*, 1991; Pluta *et al.*, 1994). Most ageing studies have failed to show a significant age-related alteration in BBB permeability to HRP in the 'normal' brain (Mooradian, 1988, 1994; Wadhwani *et al.*, 1991), but there are no reports on the effect of age on BBB permeability following cerebral ischaemia.

The aim of the experiments described in this chapter is to assess whether ageing is associated with any changes in the permeability of the BBB to HRP following MCAo.

6.1 Measurement of BBB permeability to HRP

To determine if there are any age-related changes in BBB permeability to the tracer HRP animals 4-6 months (adult), or 28-30 months (aged) underwent MCAo or sham operation. The animals were injected (iv) via the tail vein, with 100mg/kg of type VI HRP (50μl; Sigma, UK) in PBS 30 minutes prior to death. Animals were sacrificed at various times following MCAo (30 minutes, 1, 2, 4 and 24 hours, $n \geq 3$ / age group at each time point). In addition some animals underwent sham-operation but the MCA was not occluded ($n \geq 3$ / age group). Animals were fixed by vascular perfusion (see Section 2.3.3) using Karnovsky's fixative, and 50μm coronal sections were cut on a vibratome. HRP extravasation was visualised by incubating the sections with Fahimi medium (see Section 2.8). The area of HRP extravasation from each slice region was measured using the semi-automated image analysis system Imagan 2 (Leitz, UK). The data are presented as the mean percentage of infarcted hemisphere where HRP staining was present ± SD. Photomicrographs of brain slices were taken using Tungsten Ektachrome colour film (100 ASA).

6.2 Results of BBB permeability to HRP in adult (4-6 month) and aged (28-30 month) animals

In sham-operated animals there was no HRP extravasation into the brain parenchyma, and vessel walls remained clear (see Figure 6.1). A few remaining red blood cells contained within cerebral blood vessels stained dark-brown. Positive dark brown peroxidase reaction product was identified in cells lining the third and fourth

ventricles. The distribution of endogenous peroxidase did not differ between adult and aged animals.

Thirty minutes after MCAo, a small area of HRP staining was present in the ipsilateral hemisphere of adult and aged brains, confined to the region of the developing lesion (see Figure 6.1). This region was variable amongst animals but usually included part of the insular or parietal cortex. The percentage of hemisphere where HRP staining was present was 3.65 % ± 2.19 in adult and 4.83 % ± 2.4 in aged animals. Faint HRP staining was also detected in vessel walls in the areas surrounding the developing infarct (see Figure 6.1) in both adult and aged animals. There was no positive staining of vessel walls or brain parenchyma in the contralateral cortex.

One hour after MCAo the percentage of hemisphere where HRP extravasation was present was 6.43 % ± 1.86 in adult and 9.49 % ± 3.15 in aged animals. The region of HRP staining again included variable regions of the insular and parietal cortex and was similar in adult and aged animals. Vessels in the regions surrounding the developing infarct were stained brown (see Figure 6.1), and several positive dark HRP granules were found in cells that were associated with vessels within the cortex and meninges (see Figure 6.1). There was no staining of vessels or brain parenchyma in the contralateral cortex.

Two and four hours (see Figure 6.1) after MCAo HRP extravasation was present within the brain parenchyma mainly in the region of the developing infarct which included parts of the insular and parietal cortex. Patches of HRP extravasation were also observed in the motor cortex in some animals of both ages. The staining was more extensive than at earlier time-points and was similar in both adult and aged animals. The amount of HRP staining was 10.46 % ± 3.68 in adult and 10.94 % ± 4.3 in aged

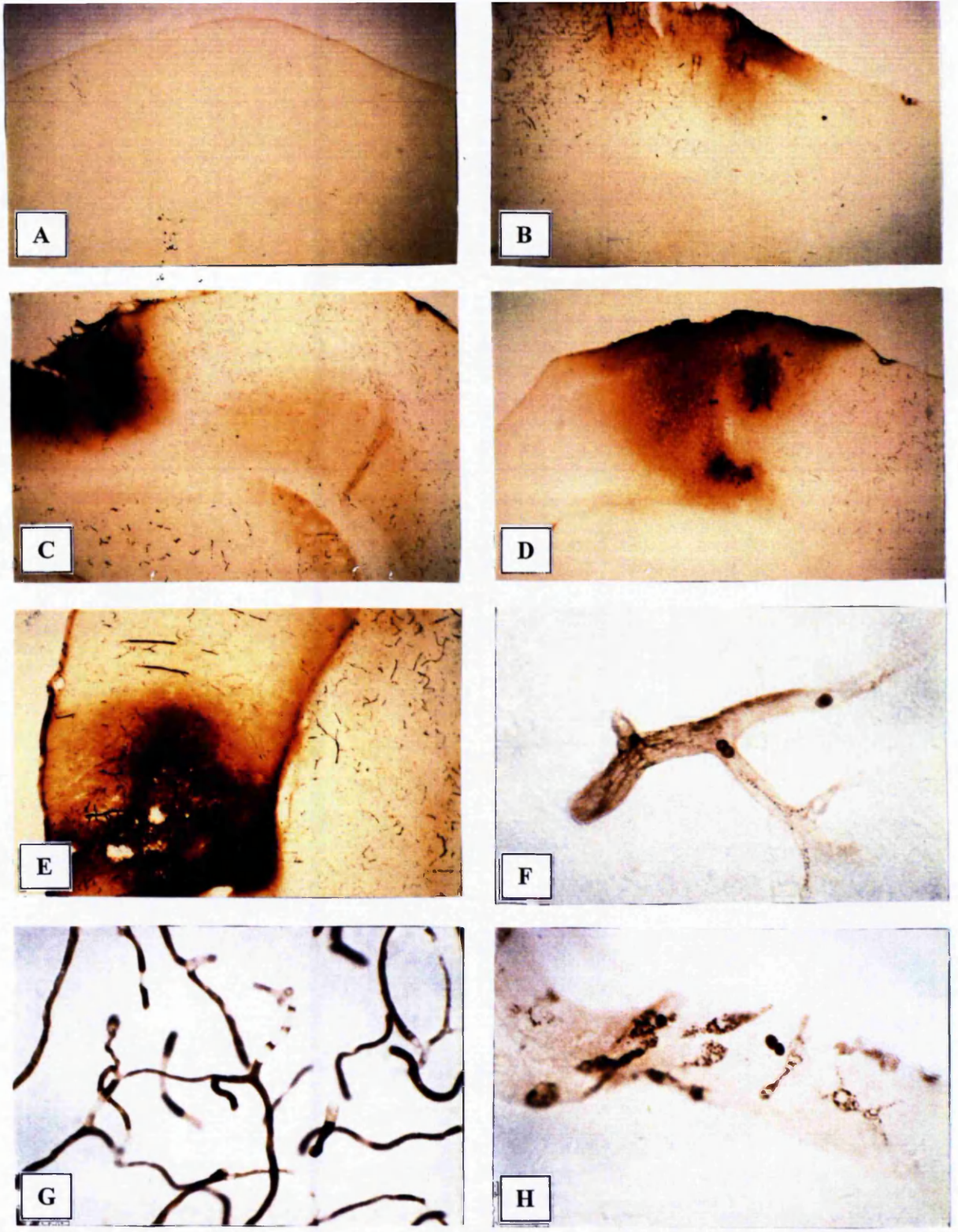

Figure 6.1: Typical appearance of HRP staining in the ipsilateral cortex at various time-points following MCAo or sham operation.

Animals were injected with 100mg/kg of type VI HRP 30 min prior to death. HRP extravasation was visualised by incubating 50μm coronal brain sections with Fahimi medium. A) In sham-operated animals there was no HRP staining. Appearance of HRP staining at B) 1/2 hour, C) 2 hours, D) 4 hours and E) 24 hours post MCAo, note there is an increase in the area of parenchyma with HRP staining from 1/2 hour to 24 hours. (A - E, magnification = x4).
HRP staining was also detected in vessel walls in the areas surrounding the developing infarct at F) 1/2 h and this staining intensity increased by G) 1hour. H) HRP granules were found in red blood cells and other cells that were associated with vessels within the cortex and meninges, possibly pericytes or macrophages. (F - H, magnification = x40).

animals at 2 hours, and 10.03% ± 2.31 in adult and 11.74% ± 1.74 in aged animals at 4 hours. The vessels outside this region had lost their brown staining and were now clear. Some cells associated with blood vessels were positive for HRP. There was no staining of vessels or brain parenchyma in the contralateral cortex.

Twenty-four hours after MCAo (see Figure 6.1), HRP staining was more extensive compared to earlier time-points and was similar in adult and aged animals. HRP staining was more dense in the peri-infarct zone and outer zone of the infarct (usually both the insular and part of the motor cortex) than in the central zone of infarct. Vessels found in and around the infarct were stained brown. The amount of HRP staining of the ipsilateral cortex was 17.48% ± 2.65 in adult and 17.30% ± 2.39 in aged animals. No HRP extravasation was observed in the contralateral hemisphere.

When the values for the percentage of hemisphere where HRP extravasation was present were analysed using 2-way ANOVA (see Figure 6.2) there was no overall difference between the age groups ($F = 1.98$; $df = 1, 31$; $p = 0.173$). There was a highly significant difference over time ($F = 19.56$; $df = 4, 31$; $p < 0.001$), HRP extravasation increasing over time, but no interaction between age and time ($F = 3.46$; $df = 4, 31$; $p = 0.762$). This suggests that the changes in HRP extravasation with time occur similarly in adult and aged animals.

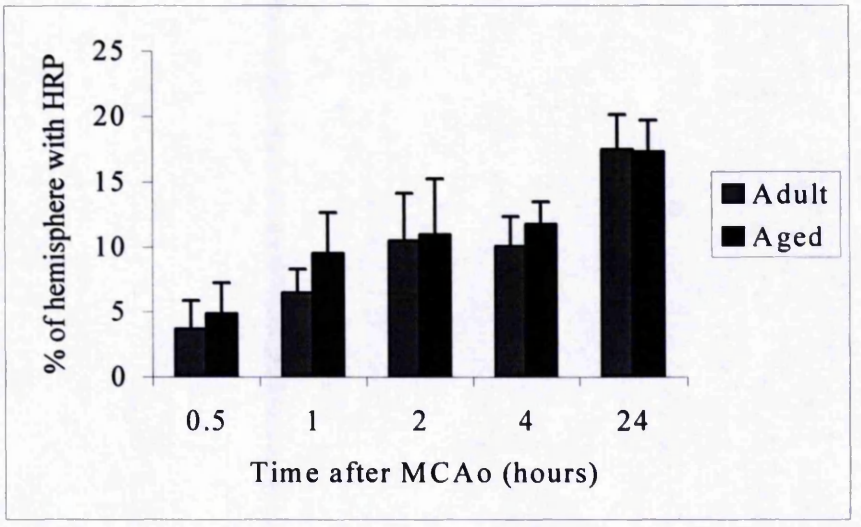

Figure 6.2: Graph showing the amount of HRP extravasation at various time-points following MCAo in adult (4 - 6 months) and aged (28 - 30 months) animals ($n \geq 3$ at each time-point).

The area of HRP extravasation was measured from 50μm coronal brain sections using the semi-automated image analysis system Imagan 2 (Leitz, UK). The data are presented as the mean percentage of infarcted hemisphere where HRP staining was present ± SD.

6.3 Discussion

The data presented above show there is an increase in BBB permeability to HRP over time in both adult and aged animals. There was no significant difference in the permeability of the BBB to HRP between adult and aged animals following MCAo.

In sham-operated animals there was no HRP extravasation into the brain parenchyma in adult or aged animals. Therefore in the 'normal' aged brain there was no alteration of BBB permeability to this tracer. This is in agreement with other studies that have found no age-related alteration of BBB permeability to HRP in the absence of other insults (Rudick and Buell, 1983; Mooradian, 1988, 1994). Following MCAo there was an increase in HRP extravasation in the brain parenchyma of the ipsilateral cortex from 30 minutes to 24 hours after MCAo. In addition to HRP extravasation into the

brain parenchyma, cells associated with vessels in the cortex and meninges also appeared to take up HRP. These cells could possibly be pericytes or astrocytes, both of which have been identified using electron microscopy to take up HRP following ischaemia (Westergaard *et al.*, 1976; Garcia *et al.*, 1994b). There was no significant difference in the permeability of the BBB to HRP following MCAo with age, despite the fact that the infarct volume was larger in aged animals. Initially the core of the lesion is small but there is a heterogenous penumbral region that eventually becomes incorporated into the core as the damage progresses. It appears that during the early period (1/2 hour to 4 hours) leakage may be through vessels in both the developing lesion and the penumbral region. The arrival of HRP in the developing lesion may be due to small amounts of backflow from collateral vessels into the occluded vessels as demonstrated by Kamijyo and Garcia using carbon black injected *in vivo* (1975). By 24 hours the leakage of HRP is restricted to penumbral regions. The observation that the area of HRP leakage was no higher in the aged animal despite the increase in infarct size (measured at 24 hours) suggests that the size of the penumbral region was similar in adult and aged. However, BBB permeability to smaller molecules, such as water soluble substances was not investigated in this study. Indeed the water content of the brains of aged mice is significantly higher than adult brains after ischaemia (Fotheringham *et al.*, 2000). Further studies using small molecular weight tracers (such as sodium fluorescein) would be required to address this. This is the first report on BBB permeability following ischaemia in aged animals.

Some reports of cerebral ischaemia have indicated that the BBB is initially intact in adult animals and that leakage of protein tracers, such as HRP and Evans Blue occurs relatively late (from 3 to 6 hours onwards) following the production of the infarct (Hossmann and Olsson, 1971; Gotoh *et al.*, 1985; Hatashita and Hoff., 1990). These are in contrast to the early (30 minute) observation of HRP extravasation seen in the present

work. However, other studies have observed a much earlier leakage of HRP into the brain parenchyma after ischaemia (Petito, 1979; Westergaard *et al.* 1976; Pluta *et al.*, 1994). In the study by Petito (1979) there was an almost immediate permeability to HRP (after 1 minute) although breakdown of the BBB to Evans Blue was a later event. The reasons for the discrepancies between reports are not known though it may be due to several factors. These include the use of different species of animal, the different methods of assessment or the numerous methods used to induce cerebral ischaemia.

Electron microscopic examination of brain regions with HRP extravasation has shown two routes of barrier permeability to HRP following cerebral ischaemia (Petito, 1979; Garcia *et al.*, 1994b; Pluta *et al.*, 1994). In the early post-ischaemic period (1 minute to 1 hour) HRP is transported via pinocytotic vesicles (an active energy-requiring process) through endothelial cells in areas of brain containing ischaemic neurones. Swelling of endothelial cells and perivascular astroglial processes was also observed within 30 minutes of the arterial occlusion. In the later post-ischaemic period (1.5 hours onwards), HRP was found in the parajunctional region, the basement membrane and adjacent extracellular space reflecting a breakdown of the BBB. Therefore HRP can passively leak into the brain tissue through the walls of necrotic vessels in the infarcted area. The present study did not investigate the route through which HRP entered the brain parenchyma.

The triggers for the increase in BBB permeability or its breakdown following cerebral ischaemia are not known. Several mechanisms have been proposed including the accumulation of erythrocytes, leukocytes and platelets that can damage vascular endothelial cells by releasing proteases or free radicals (Shiga *et al.*, 1991; Pluta *et al.*, 1994; see Section 1.5.2.2). Inflammatory mediators that have been shown to increase the permeability of the BBB include the cytokine IL-1, arachidonic acid and its metabolites (such as the eicosanoids and leukotrienes) and bradykinin (Abbott and

Revest, 1991; Quagliarello *et al.*, 1991; De Vries *et al.*, 1994). Glial swelling, particularly of astrocytes is an early event following cerebral ischaemia (Garcia *et al.*, 1994; Davies *et al.*, 1998). The factors responsible for astrocytic swelling following ischaemia include the accumulation of lactic acid and glutamate, and the uptake of K^+ (Kempski *et al.*, 1990; Kimelberg, 1995). In the region of the developing infarct these swollen astrocytes disintegrate and may contribute to the breakdown of the BBB following ischaemia (Garcia *et al.*, 1994b; Davies *et al.*, 1998).

6.3.1 Conclusion

There was an increase in the permeability of the BBB to HRP, in the ipsilateral hemisphere in adult and aged animals following MCAo. This indicates that there is a breakdown in the BBB after ischaemia. However, there were no significant differences in the permeability of the BBB to HRP between adult and aged animals after ischaemia. This suggests that the permeability of the BBB to large molecules is not significantly altered with age following cerebral ischaemia. This does not exclude the possibility that the permeability of the BBB to small molecular weight molecules is affected with age and this requires further investigation.

Chapter 7

The effects of rIL-1ra on IBD following MCAo

7.0 Introduction

The exact nature of the signalling mechanisms in brain inflammation following cerebral ischaemia remains to be fully elucidated, but there is growing evidence that the cytokine IL-1 (amongst others) has an important role. Injection of recombinant IL-1β (icv) has been shown to disrupt the BBB (Quagliarello *et al.*, 1991) and enhance oedema formation following focal ischaemia (Yamasaki *et al.*, 1995). IL-1 also induces the expression of adhesion molecules on the vascular endothelium, and the proliferation and differentiation of glial cells (Merrill, 1991). Some of the actions of IL-1 following injury are beneficial and promote the repair process, however several reports implicate IL-1 in neuronal death following cerebral ischaemia (see Section 1.6.2.2).

Inhibition of the actions of endogenous IL-1 using rIL-1ra (central or peripheral administration) has been shown to reduce infarct volume in rats (see Section 1.6.2.2). However, with the exception of adenoviral induced overexpression of IL-1ra (Yang *et al.*, 1998), the effects of administration of rIL-1ra have not been reported in mice. In this study the effects of central administration of rIL-1ra on IBD were assessed in adult mice subjected to MCAo. Aged animals are not as robust as adult animals and central administration of rIL-1ra would probably be too traumatic for them, due to the prior surgery required for implantation of the guide cannula. Therefore the effects of peripheral administration of rIL-1ra on IBD were also assessed in adult mice, as this would be the route of administration if tested in aged animals.

All methods of inducing cerebral ischaemia are associated with variation in the size of the infarct (Duverger and Mackenzie, 1988; Ginsberg and Busto, 1989; Barone *et al.*, 1993). This variation may arise from several sources such as: the use of different strains of mice (Barone *et al.*, 1993; Yang *et al.*, 1997), choice of anaesthetic agent (Bederson *et*

al., 1986), variability in the site of occlusion of the artery (Niiro *et al.*, 1996), and the age of the animal (see Chapter 4). From the above it is evident that a new operator must establish the consistency of the technique in the chosen animal before undertaking novel investigations.

The aims of the present chapter are to establish the reproducibility of MCAo on infarct size performed under the conditions in this laboratory, and assess the effects of central and peripheral administration of rIL-1ra on IBD in adult mice.

7.1 Reproducibility of infarct size 24 hours after MCAo

Animals aged 4-6 months (n = 20) were subjected to MCAo (see Section 2.3.2). Infarct volume was measured 24 hours after MCAo, on brain sections stained with TTC (see Section 2.5.2), using a Seescan image analysis system (Seescan, UK; see Appendix 5). The data were analysed using the Students *t*-test for unpaired data (two-tailed) and are presented as the mean infarct volume (mm^3) ± S.D, or mean swelling volume (mm^3) ± S.D.

The mean infarct volume was 16.54 ± 5.22 mm^3, and the volume of swelling was 3.64 ± 2.58 mm^3 (this represents a 4.2 % increase in hemisphere volume; see Figure 7.1). A cumulative means plot, of the mean infarct volumes obtained using 1 - 20 animals, showed that 6 animals are needed per experimental group to obtain an infarct volume ± 5% of the total group infarct volume (see Figure 7.2).

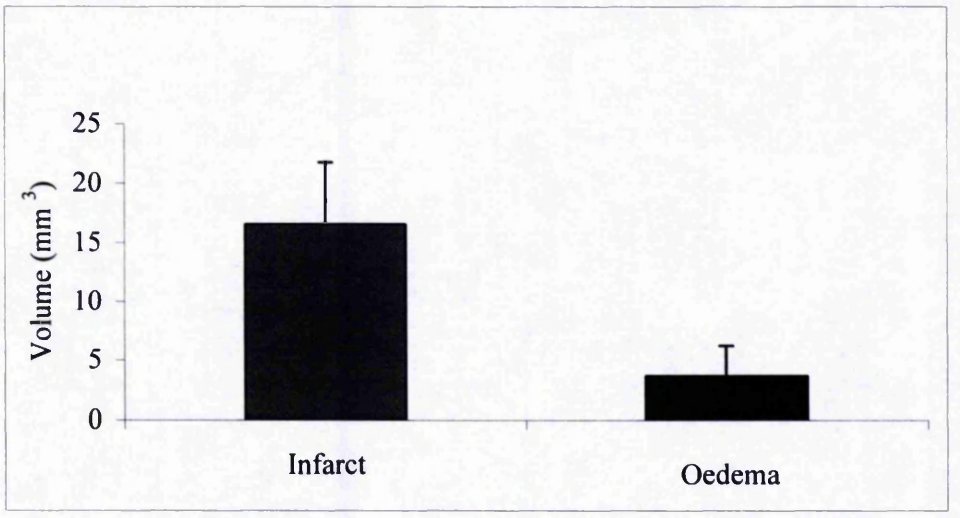

Figure 7.1: Infarct and swelling volume (mm^3) measured 24 hours after MCAo in 4-6 month-old mice (n = 20)

Infarct volume was measured on 500μm coronal brain sections stained with TTC. Bars indicate standard deviation.

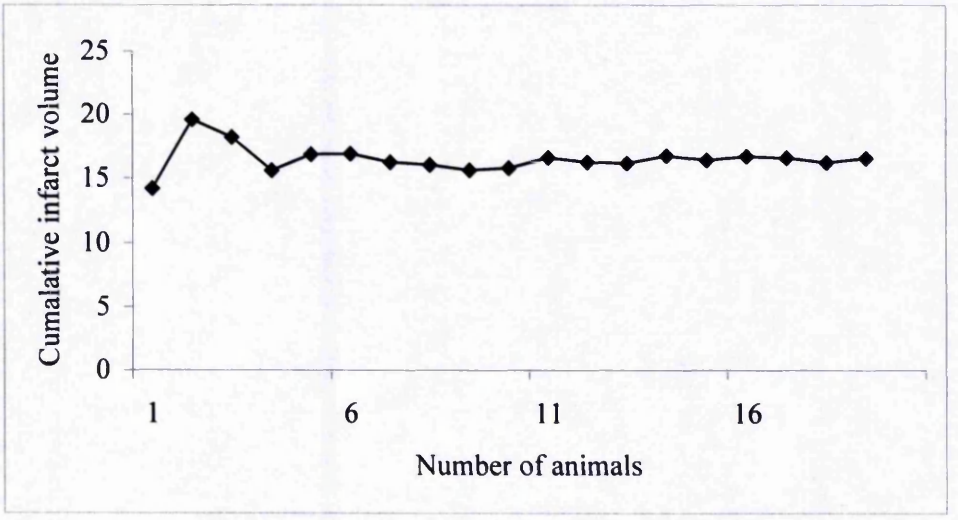

Figure 7.2: Cumulative means plot of infarct volume (mm^3) measured 24 hours after MCAo in 4-6 month mice (n = 20).

Infarct volume was measured on 500μm coronal brain sections stained with TTC. The cumulative means plot, of the mean infarct volume obtained using 1 - 20 animals, showed that 6 animals are needed per experimental group to give a value ± 5% of the mean infarct volume obtained using a larger group (n = 20).

7.2 Effect of central administration of rIL-1ra on infarct volume

Animals aged 6 months were injected icv (via pre-implanted guide cannulae into the lateral ventricle, see Section 2.3.1) with rIL-1ra (2.5μg in 1μl), or an equivalent volume of vehicle (0.9% non-pyrogenic sterile saline), both 30 minutes before and 10 minutes after MCAo (see Sections 2.3.2 and 2.4.1). Damage was measured 24 hours later by Seescan image analysis of TTC stained brain slices (see Section 2.5.3; Appendix 5). The data were analysed using the Students *t*-test for unpaired data (two-tailed) and are presented as the mean infarct volume (mm^3) ± S.D, or mean swelling volume (mm^3) ± S.D.

7.2.1 Results

Animals subjected to MCAo in both experimental groups consistently exhibited damage throughout the cortex from the mid dorsal neocortex to the lateral part of the piriform cortex. The damage typically extended from the meningeal surface to the radiation of the corpus callosum, and occasionally the infarct included the outer margin of the caudate putamen. Central administration of rIL-1ra resulted in a highly significant reduction in infarct volume (46% reduction, $p < 0.001$) compared to vehicle treated animals. The mean infarct volume in vehicle treated animals was 18.98 mm^3 ± 3.33, compared with 10.31 mm^3 ± 4.49 in rIL-1ra ($t = 5.88$, $df = 26$, $p < 0.001$; see Figure 7.3) treated animals. rIL-1ra had no significant effect on swelling volume (vehicle = 3.33 ± 1.75; rIL-1ra volume = 1.81 ± 0.85; $t = 1.38$, $df = 26$, $p = 0.178$). Because these animals were cannulated, the effect of cannulation only on swelling volume was assessed in a separate experiment by comparing the left hemisphere to the right hemisphere in both the control animals (those undergoing sham cannulation only, n = 8) and the cannulated animals (n = 8). Cannulation does not significantly contribute to the volume of swelling in experimental

animals (t = 1.001, df = 14, p > 0.1).

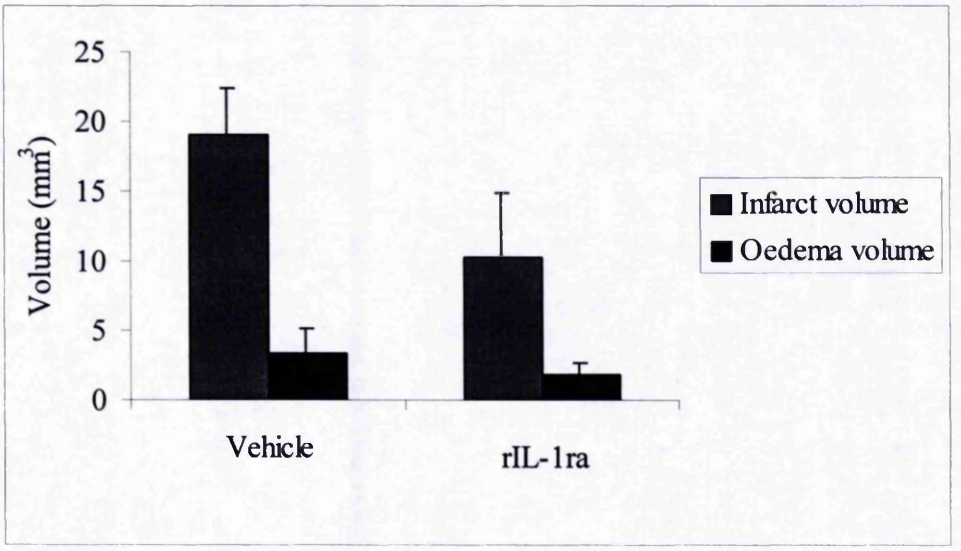

Figure 7.3: Effect of central administration of rIL-1ra on infarct and swelling volume (mm^3) measured 24 hours after MCAo.

Animals were injected (icv) with either rIL-1ra (2.5μg) or saline, 10 minutes before and 30 minutes after MCAo. Damage was assessed on 500μm brain slices stained with TTC using Seescan Image analysis. Treatment with rIL-1ra significantly reduced infarct volume (46%, $p < 0.001$), but had no effect on the volume of oedema ($p = 0.178$). All bars indicate standard deviation.

7.3 Effects of central administration of rIL-1ra on cell counts

To determine if central rIL-1ra treatment affected the number of different cell types found in both the cortex and the infarct, animals (6 month) were injected icv (via pre-implanted guide cannulae, see 2.3.1) with rIL-1ra (2.5μg in 1μl, n = 7), or an equivalent volume of vehicle (0.9% non-pyrogenic sterile saline; n = 7), both 30 minutes before and 10 minutes after MCAo (see Sections 2.3.2 and 2.4.1). 24 hours after MCAo animals were terminally anaesthetised and perfuse fixed transcardially (see Section 2.3.1). The brains were resin embedded and the disector method applied to 3μm resin sections stained with

Toluidine Blue (see Chapter 3). Serial reconstruction of brain sections enabled parameters to be established for use in the disector method (see Chapter 3). Nv (mean cell count/mm^3) was calculated for neurones and glial cells in layer V of the frontal cortex adjacent to the infarct, and pyknotic, apoptotic-like and non-dense/red neurone-like profiles in layer V of the lesioned cortex. Only neurones whose nucleoli were clearly visible, and glial cells with a well-outlined nucleus were included in the counts. Glial counts included astrocytes, oligodendrocytes and microglia. The data are presented as the mean cell count/mm^3 (Nv) ± S.D, and were analysed using the students *t*-test.

7.3.1 Results

There were no significant differences in the numbers of neurones or glial cells per mm^3 in layer V of the frontal cortex adjacent to the infarct between vehicle and rIL-1ra treated animals (see Table 7.1).

Cell Variable	Vehicle treated	rIL-1ra treated	Students *t*-test
Nv neurones	49339 ± 5847	45042 ± 5975	t = 1.34, df = 12, p = 0.204
Nv glial cells	81951 ± 11714	71974 ± 9934	t = 1.92, df = 12, p = 0.078

Table 7.1: Effects of rIL-1ra and vehicle treatment on mean neuronal and glial cell counts/mm^3 in layer V of the frontal cortex adjacent to the infarct in adult (6 month, n =7/group) mice.

There were also no significant differences in the numbers of pyknotic, apoptotic-like or non-dense/ red neurone-like profiles per mm^3 in the infarct between vehicle and IL-1ra treated animals (see Table 7.2).

Cell Variable	Vehicle treated	rIL-1ra treated	Students *t*-test
Nv pyknotic profiles	60806 ± 11300	61452 ± 9275	t = 0.12, df = 12, p = 0.908
Nv apoptotic-like profiles	1575 ± 1457	1124 ± 385	t = 0.85, df = 12, p = 0.413
Nv for red neurone-like/ non-dense profiles	1254 ± 1663	2064 ± 2193	t = 0.75, df = 12, p = 0.465

Table 7.2: Effects of rIL-1ra and vehicle treatment on mean pyknotic, apoptotic-like and red neurone-like/ non-dense profile counts per mm^3 in the infarct of adult (6 month, n =7/group) mice.

Since the mean neuronal density does not differ significantly between vehicle and rIL-1ra treated animals, and rIL-1ra results in a significant reduction in infarct volume, it would follow that less neurones are lost after MCAo in IL-1ra treated animals. By multiplying the mean neuronal density from each treatment group by the corresponding mean infarct volume, an estimate of the number of neurones lost in the infarct was found to be 9×10^5 in the vehicle group and 5×10^5 in the rIL-1ra treated group.

7.4 Effect of peripheral administration of rIL-1ra on infarct volume

Animals aged 6 months were injected subcutaneously with either 100mg/kg rIL-1ra (in 150µl), or an equivalent volume of 0.9% non-pyrogenic sterile saline, at time 0, and 4, 8, 12, and 18 hours after MCAo (see Sections 2.3.2 and 2.4.1). Damage was measured 24 hours after MCAo by Seescan image analysis of TTC stained brain slices (see Section 2.5.3). Data are presented as the mean infarct volume (mm^3) ± SD, or mean swelling volume (mm^3) ± SD, and were analysed using the Students *t*-test.

7.4.1 Results

Peripheral administration of rIL-1ra resulted in a significant reduction in infarct volume (40% reduction, p = 0.01) compared to vehicle treated animals (see Figure 7.5). The mean infarct volume in vehicle treated animals was 17.61mm^3 ± 6.62 (n = 13), compared with 10.55 mm^3 ± 5.39 (n = 13) in rIL-1ra treated animals (t =2.98, df = 24, p = 0.01). Peripheral rIL-1ra had no effect on the swelling volume (vehicle = 4.67 ± 3.49; rIL-1ra = 2.58 ± 2.23; t = 1.83, df = 24, p = 0.08; see Figure 7.5).

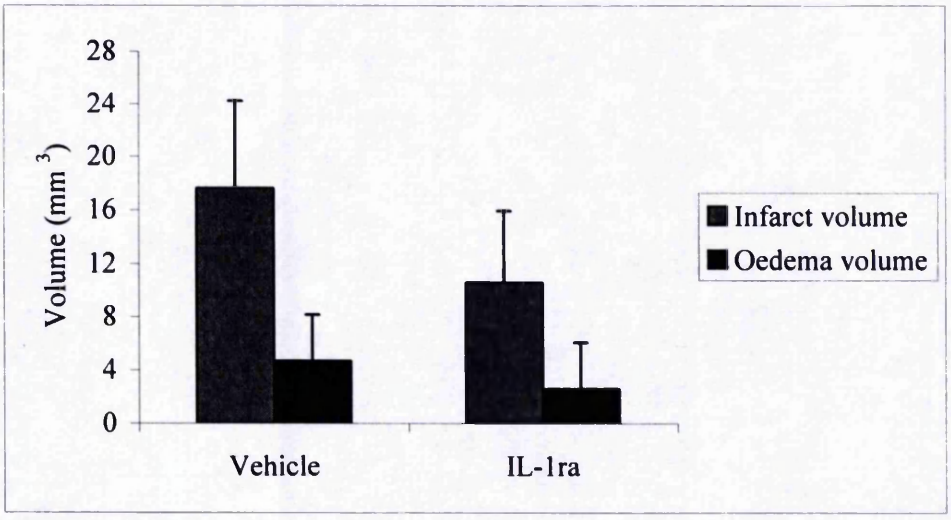

Figure 7.5: Effect of peripheral administration of rIL-1ra on infarct and swelling volume (mm^3) measured 24 hours after MCAo.

Animals were injected subcutaneously with either rIL-1ra (100mg/kg, n = 13) or saline (n = 13) at time 0, and 4, 8, 12, and 18 hours after MCAo. Damage was assessed on 500μm brain slices stained with TTC using Seescan Image analysis. Treatment with peripheral rIL-1ra significantly reduced infarct volume (40%; p = 0.01), but had no effect on the volume of swelling (p = 0.08). All bars indicate standard deviation.

7.5 Discussion

7.5.1 Variability in infarct volume

The purpose of the experiments described in this chapter was to assess the effects of central and peripheral administration of rIL-1ra on IBD. Firstly the reproducibility of MCAo as performed under the conditions in this laboratory needed to be established as it is essential to obtain consistent results that allow detection of small differences between experimental groups. The variation in infarct volume observed in this study (31.6 %) compares well with other published studies using the same method of inducing permanent MCAo in mice (36.9% by Benavides *et al.*, 1990; 32.6% by Lopez and Lanthorn, 1993). Factors that may contribute to inter-animal infarct variation include discrepancies in the collateral circulation in the region of the MCA, the precise site of occlusion of the artery and variations in physiological parameters such as blood pressure, blood gases, blood glucose and brain temperature (Bederson *et al.*, 1986; Busto *et al*, 1987; Brint *et al.*, 1988; Duverger and MacKenzie, 1988; Niiro *et al.*, 1996; Yang *et al.*, 1997). In order to limit variation in this study mice of similar body weights and age were used, surgery was performed on a heated pad (to maintain body temperature at approximately 37°C) and the artery was occluded in the same position. The identification and exclusion of animals with abnormal physiological responses to either stroke or treatment was not done in this experiment, as repeated blood samplings in mice is difficult due to their small blood volume (see Section 1.1.1).

7.5.2 Effect of rIL-1ra on IBD.

The data presented in the present study show that central and peripheral administration of rIL-1ra significantly reduced infarct volume 24 hours after MCAo in adult

mice. In addition administration of rIL-1ra in the mouse did not cause significant differences in the number of neurones or glial cells per mm^3 in the peri-infarct zone, or alter the number of different cell types/mm^3 in the lesion. Since the mean neuronal density does not differ significantly between vehicle and rIL-1ra treated animals, this implies that rIL-1ra does lead to a reduction in the number of neurones lost after ischaemia. The neuroprotective effects of rIL-1ra in the mouse agree with previous studies done in the rat. Injection of rIL-1ra in the rat results in a significant reduction in infarct volume when administered centrally (Relton and Rothwell, 1992; Loddick and Rothwell, 1996; Stroemer and Rothwell, 1997) and peripherally (Garcia *et al.*, 1995; Relton *et al.*, 1996) after permanent MCAo. It has been confirmed that the protection offered by rIL-1ra is permanent and does not merely delay neuronal death, as infarct volume was almost identical when assessed 24 hours or 7 days after permanent MCAo in the rat (Loddick and Rothwell, 1996). Overexpression of IL-1ra in the brain, through the use of an adenovirus significantly reduces ischaemic injury in rats and mice following permanent MCAo (Betz *et al.*, 1995; Yang *et al.*, 1998). Significant increases in infarct volume have been reported by blocking the action of endogenous IL-1ra (by passive immunoneutralization) in rats after permanent MCAo (Loddick *et al.*, 1997). These studies indicate that IL-1 has an important role in the pathways involved in the progression of IBD.

Recombinant IL-1ra is a large protein and therefore does not readily cross the BBB, but it still offered significant neuroprotection when administered peripherally in this study. Pharmacokinetic studies have shown that rhIL-1ra is cleared rapidly from the circulation and that subcutaneous injection is the most effective route of administration to maintain a constant plasma level of this compound (Kim *et al.*, 1995). The dosing regime used in this study was 100mg/kg every 4 hours and has been shown to maintain a plasma concentration

of 10μg/ml (Kim *et al.*, 1995). Gutierrez *et al.* (1994) reported that in the uninjured mouse 0.33 to 0.65% of circulating rIL-1ra entered the brain. Following cerebral ischaemia there is breakdown of the BBB (see Chapter 6) and this could have provided an additional route for the entry of peripherally administered rIL-1ra into the brain.

Although it is well established that IL-1β expression is induced rapidly after cerebral ischaemia (see Section 1.6.2.2), the expression of IL-1α has not been extensively studied. A recent investigation into the temporal profile of mRNA induction for IL-1α and IL-1β following permanent MCAo in the mouse found that IL-1α was induced much earlier than IL-1β (Hill *et al.*, 1999). IL-1α mRNA levels increased from 4 hours and IL-1β mRNA levels at 7.5 hour after MCAo, and both reached peak levels at 10 hours. It remains unclear if IL-1α expression contributes to neuronal damage. Since IL-1ra blocks all known actions of IL-1β and IL-1α, it does not distinguish the importance of either form of IL-1. Studies using anti-IL-1β criteria, by injection of IL-1β antibodies (Yamasaki *et al.*, 1995) or by using inhibitors of ICE (see Section 1.6.2.2), support the concept that IL-1β is the prevalent form involved in IBD. However in ICE knockout mice levels of IL-1α are also reduced but not to the same extent as the levels of IL-1β (Dinarello, 1997). The cellular sources of IL-1β following MCAo in this study were found to be mainly from astrocytes and microglia (see Chapter 5). There were no available IL-1α or IL-1γ/IL-18 antibodies to determine their presence following MCAo, so their contributions to IBD cannot be excluded.

7.5.2.1 Possible mechanisms of IL-1 in IBD: Effects on the cerebrovasculature and the post-ischaemic inflammatory response.

Although there is compelling evidence to implicate IL-1 in the pathogenesis of IBD, the mechanisms and mediators of IL-1 actions in neurodegeneration remain unclear. The observation that IL-1β is also induced to a lesser extent in the contralateral hemisphere indicates that the presence of IL-1β alone is not always detrimental (see Chapter 5). The present study did not investigate the mechanisms by which IL-1 mediates neuronal death in the ipsilateral hemisphere but several actions have been proposed (see Dinarello, 1996; Touzani *et al.*, 1999; Section 1.6.2.3). Of particular interest to this study are the effects of IL-1 on the cerebrovasculature and the post-ischaemic inflammatory response.

Using an *in vitro* model of the BBB, IL-1β was shown to decrease the transendothelial electrical resistance (reflecting a decrease in the integrity of the BBB) and this effect could be abolished by IL-1ra (de Vries *et al.*, 1995a). This indicates that IL-1β may have a direct effect on the integrity of the BBB. Interestingly IL-1β immunoreactivity in the present study was found mainly in astrocytes and their processes (see Chapter 5), which induce the formation of the BBB. Injection of recombinant IL-1β (rIL-1β) has been shown to increase brain water content following transient MCAo in rats (Yamasaki *et al.*, 1995). High concentrations of rIL-1β have even been reported to induce brain oedema in normal rats (Gordon *et al.*, 1990). Studies on transgenic mice deficient in the ICE gene have also demonstrated they have less brain oedema following permanent MCAo (Schielke *et al.*, 1998). Furthermore, injection of anti-IL-1β antibody or zinc protoporphyrin (an IL-1 blocker), decreases brain water content after transient MCAo in the rat (Yamasaki *et al.*, 1993; Yamasaki *et al.*, 1995). In this study although administration of rIL-1ra caused a

trend towards a reduction in swelling volume (an indicator of oedema) it was not significant. In the study by Relton *et al.* (1996), peripheral administration of rIL-1ra caused a significant, albeit small reduction (0.5%) in the percentage of water content in the infarcted hemisphere. Further studies using the more sensitive wet/dry brain weight measurement of oedema are needed in the mouse to address this discrepancy. Overall these studies indicate that IL-1 may contribute to the development of post-ischaemic oedema formation by decreasing the integrity of the BBB. The mechanisms behind this are not fully understood, but it has been shown that IL-1 stimulates rat cerebral endothelial cells to produce eicosanoids that can increase BBB permeability (De Vries *et al.*, 1995b).

One of the known actions of IL-1 is the induction of adhesion molecules on the vascular endothelium (Kim, 1996; Meager, 1999; see Section 1.5.2.1). Adhesion molecules facilitate the migration of neutrophils from the periphery into the brain after ischaemia (see Section 1.5.2.1). Mice deficient in the ICE gene have significantly reduced ICAM-1 protein levels and reduced numbers of ICAM-1 vessels in the ischaemic lesion (Yang *et al.*, 1999). Interestingly IL-1β protein expression has been localised to vascular endothelial cells as early as 15 minutes to 2 hours after MCAo (Zhang *et al.*, 1998b). This precedes the expression of ICAM-1 and E-selectin which begins 2 to 4 hours after MCAo (Wang *et al.*, 1994a; Wang and Feuerstein, 1995; Wang *et al.*, 1995; Zhang *et al.*, 1998a). Histological examination of animals treated with anti-IL-1β antibody, rIL-1ra or zinc protoporphyrin reveal that the number of neutrophils present in the brain is decreased (Yamasaki *et al.*, 1993; Yamasaki *et al.*, 1995). Depletion of circulating neutrophils, blocking adhesion molecules or their receptors have all been shown to reduce infarct volume following cerebral ischaemia (see Sections 1.5.2.1 and 1.5.2.2). Taken together these results suggest that induction of adhesion molecules with subsequent infiltration of

neutrophils may also be responsible for the damaging effects of IL-1 following ischaemia.

In addition to its effects on the endothelium, IL-1 induces the proliferation and differentiation of astrocytes and microglia (Merrill, 1991). IL-1 induces a number of factors in glial cells that can exacerbate BBB disruption, such as chemokine expression in both microglia and astrocytes, and the production of NO (a potent vasodilator) in astrocytes (McManus *et al.*, 1998; Liu *et al.*, 1996). IL-1 can also induce the production of other pro-inflammatory cytokines such as TNF-α and IL-6 in astrocytes, and induce its own gene expression in microglia (DeGraba, 1998; Touzani *et al.*, 1999). Conversely IL-1 can stimulate the synthesis of anti-inflammatory cytokines such as IL-1ra, IL-4 and TGF-β, which may serve to dampen down the inflammatory response. Therefore the level of IL-1β following injury to the brain may be important in determining whether pro- or anti-inflammatory mechanisms are activated.

7.5.3 Conclusion

Administration of rIL-1ra (both centrally and peripherally) resulted in significant reduction in infarct volume following permanent MCAo in adult mice. These findings are consistent with the effects of rIL-1ra in the rat. The mechanisms behind this are not known, but IL-1 has been implicated in several of the post-ischaemic inflammatory responses (see above and Section 1.6.2.3). The effects of rIL-1ra have not yet been investigated in aged animals. Increases in the levels of IL-1β expression have been reported in aged animals (Murray *et al.*, 1997) and increased numbers of IL-1β positive astrocytes were observed after MCAo in aged mice (see Section 5.6.5). Therefore further investigations are required to determine if IL-1ra is neuroprotective in aged animals, and if the higher expression of

IL-1 in the aged brain contributes to the age-related increase in infarct volume.

Chapter 8

General discussion

8.0 General discussion

Focal cerebral ischaemia, or stroke, is most commonly caused by the obstruction of blood flow in a major cerebral vessel that results in a complex series of pathological events ultimately leading to cell death. There is immediate neuronal and glial cell death in the region of the brain where there is a total cessation of blood flow (the *core*). Surrounding the ischaemic core is a *penumbral* region of reduced blood supply where tissue remains viable for some time before progressing to infarcted tissue. Several mechanisms have been attributed to the progression of the infarct and recent observations suggest that the inflammatory response in the brain has an important role. The invasion of leukocytes into the ischaemic region and the development of brain oedema characterise the ischaemia-induced inflammation. In addition resident brain cells, such as astrocytes, microglia and endothelial cells become activated in response to the ischaemic injury. The mechanisms responsible for the initiation and propagation of the post-ischaemic inflammatory reaction are poorly understood, though much of it appears to be mediated by cytokines.

Despite the importance of age in the prevalence of stroke the vast majority of *in vivo* studies have used young adult animals, and there are several reported changes in the aged brain that may influence its response to injury (see Section 1.7). These include alterations in the cerebrovasculature, the BBB, and neuronal and glial cells. The objective of the present study was to investigate whether age-related changes in the brains of C57/Icrfa^t mice lead to altered cellular responses to cerebral ischaemia.

Ageing was associated with an increase in cortical damage after permanent MCAo in C57/Icrfa^t mice. As there was no significant difference in neuronal density between adult and aged mice, this represented an increase in the number of neurones lost after IBD. Therefore it appears that the neurones from aged animals are more vulnerable to neurodegeneration, and are less likely to survive a traumatic insult such as

ischaemia. Other studies have reported an increase in the extent of damage in the brains of aged animals after ischaemia (Davis *et al.*, 1995; Sutherland *et al.*, 1996) and after administration of neurotoxins (Ricaurte *et al.*, 1987; Wozniak *et al.*, 1991), though these animals were not maintained under SPF conditions. The mechanisms behind the age-associated vulnerability to neurodegeneration are not understood and require extensive investigation. The present study investigated whether cellular responses to ischaemia were affected with age.

The main cellular change in the uninjured ageing brain (in the region examined) was found to be a significant increase in the number of glial cells. Increases were found in both the number of reactive astrocytes (GFAP positive) and activated microglia/macrophages (GSA positive). These findings are consistent with those reported by others, in both human and rodent brains (see Johnson and Finch, 1996; Nichols, 1999). The remaining glial cells in the brains of aged animals were still capable of becoming reactive in response to IBD, as their numbers increased in both adult and aged animals. This confirms qualitative studies made in this laboratory (Fotheringham *et al.*, 2000), suggesting that if glial cells from aged animals can respond to a physiological insult that their functions may be maintained. However, much additional work is required to unravel this.

A significant age-related increase was found in the number of vascular associated microglia/macrophages with time after MCAo. However, because GSA labels both activated microglia and peripheral macrophages (Streit, 1990), it is not known if this reflects an increase in the transformation of resident microglia into *amoeboid* macrophages, or whether this reflects an increase in the accumulation of peripheral macrophages (monocytes). It may be that the accumulation of peripheral macrophages in the cerebral circulation, and their migration into the brain occurs much earlier after ischaemia in the aged animal. Alternatively vascular associated microglia

from the brains of aged rats have been shown to express pro-inflammatory antigens, that are not detectable in young animals, and may therefore be able to respond more quickly to inflammatory stimuli (Perry *et al.*, 1993). *In vitro* studies have shown that the proliferation of microglia increases as a function of donor age (Rozovsky *et al.*, 1998). Therefore further investigations are needed to determine whether the observed findings represent an increase in microglia, or an accumulation of monocytes.

The ability of astrocytes to respond to injury, as measured by an increase in the number of reactive astrocytes, appeared to be maintained in aged animals and although the response seemed to be lower in aged animals it was not significant. Due to the small number of animals in each age group it may not have be possible to detect small changes in the astrocytic response. In support of these findings, Gordon *et al.* (1997) found that the astrocytic response to another form of brain injury (a stab wound) was not affected in aged rats. However, in mice receiving a fimbria/fornix lesion, aged mice showed a more exaggerated astrocytic response that developed more slowly (Goss and Morgan, 1995). In the present study only early responses (in the first 24 hours) were examined, therefore further studies extending the timepoints after MCAo are required to determine if later astrocytic responses are affected with age.

There was an increase in the permeability of the BBB to the macromolecular tracer HRP in adult and aged animals with time after MCAo. These findings are consistent with other reports in adult animals (Petito, 1979; Westergaard *et al.* 1976; Pluta *et al.*, 1994). No significant differences in BBB permeability to HRP were observed in the aged brain. Therefore the function of the BBB to large molecules (such as proteins) appears to be maintained with age after injury, and suggests that aged animals are not more susceptible to vasogenic oedema (see Section 1.4.1). Previous reports have not examined the permeability of the BBB after ischaemia in aged animals. The permeability of the BBB to small molecular weight molecules and water may be

affected with age following injury, but was not examined in the present study. Although there was no significant difference with age in the volume of swelling after permanent MCAo in this study, the more severe intraluminal filament MCAo that causes damage in both the cortex and striatum, was associated with an age-related increase in swelling volume (Fotheringham *et al.*, 2000). In addition a significant decrease was found in the water content of the brains of aged mice, and after ischaemia the water content significantly increased in the brains of aged animals regardless of the method used to induce ischaemia (Fotheringham *et al.*, 2000). The age-related increase in oedema after ischaemia may be related to the amount of damage caused by the injury, and/or the ability of astrocytes to withstand cytotoxic oedematous changes, or to alterations in the permeability of the BBB to small molecules and water. Further studies are required to resolve this.

There was an increased expression of ICAM-1 on vessels in the lesion and peri-infarct zone in adult and aged animals after ischaemia. These findings are consistent with those reported by others in adult rats (Wang *et al.*, 1994a; Wang and Feuerstein, 1995; Zhang *et al.*, 1998). No significant differences were observed in the number of ICAM-1 immunoreactive vessels between adult and aged animals after MCAo. Therefore it appears that the mechanisms responsible for the upregulation of ICAM-1 on vessels are not altered significantly with age. Increases in the numbers of neutrophils were observed 12 and 24 hours after MCAo in adult and aged animals. These findings are consistent with other studies made in adult rats after permanent MCAo (Garcia *et al.*, 1994; Zhang *et al.*, 1994; Kato, 1998). No significant differences were detected in neutrophil numbers (both vascular and parenchymal) between adult and aged animals in the present study. Therefore, it appears that the mechanisms for the adhesion and migration of neutrophils into the brain in the early stages (first 24 hours) after ischaemia are not significantly affected with age. Previous reports have not

investigated these responses in aged animals. The only other report on leukocyte invasion in aged animals after ischaemia, examined monocyte invasion into the brain 4 days after ischaemia, which suggested there was a reduction in monocyte infiltration in aged animals (Futrell *et al.*, 1991), although it was only semi-quantitative. Further work is required to extend the time-points after MCAo to see if there are other changes in cellular dynamics (such as monocyte infiltration) with age.

The exact signalling mechanisms in the post-ischaemic inflammatory response remain to be determined, but there is growing evidence that the cytokine IL-1 has an important role (see Section 1.6.2). IL-1 has been shown to induce the expression of adhesion molecules on the vascular endothelium (Kim, 1996), and enhance the invasion of immune cells into the brain after injury (Yamasaki *et al.*, 1993; Yamasaki *et al.*, 1995). In addition IL-1 induces the proliferation and differentiation of glial cells (Merrill, 1991) and has been implicated in the development of cerebral oedema (Yamasaki *et al.*, 1995; Relton *et al.*, 1996). The present study identified astrocytes and microglia as the main cellular sources of IL-1β after MCAo in adult and aged animals. There was a significant overall increase in the numbers of IL-1β positive astrocytes in the brains of aged animals compared to young animals. Following MCAo there was an age-related increase in the number of IL-1β positive astrocytes present in the white matter, but the numbers of IL-1β positive microglia were not altered. These findings suggest that aged mice are not defective in their capacity to develop an IL-1 response to ischaemia, and that there is actually an increased IL-1 response by astrocytes from the brains of aged animals. It remains to be determined whether there is a corresponding increase in the level of bioactive IL-1β in the brains of aged mice after ischaemia. Increases in IL-1β (measured by immunoblotting) have been detected in the brains of normal aged rats, although these animals were not kept in SPF conditions (Murray *et al.*, 1997). Since there are several potential actions of IL-1 that may enhance neuronal

damage (such as increase BBB permeability and leukocyte invasion), changes with age in this cytokine could have significant effects on the pathophysiology of IBD (see Section 1.6.2.2).

In the present study the effects of rIL-1ra on IBD were examined in adult mice, and it was shown to cause a significant reduction in infarct volume when administered both centrally and peripherally. This agrees with previous reports on the effects of rIL-1ra after MCAo in adult rats (see Section 1.6.2.2; Touzani *et al.*, 1999). The neuroprotective effects of an NMDA receptor antagonist were reduced in aged animals after stroke (Davis *et al.*, 1995), therefore the pharmacological effects of a treatment in younger animals may not necessarily translate to older animals. This together with the reported altered cellular responses to ischaemia in the brains of aged animals highlights the need to assess potential neuroprotective agents in aged animals. The effect of peripheral rIL-1ra on IBD was intended to be investigated in this thesis but due to circumstances beyond my control there were not enough animals aged 26-30 months available for this experiment. Further studies are required to examine if peripheral administration of rIL-1ra is neuroprotective in aged mice, and whether it has differential effects on cellular responses in adult and aged animals.

An important issue that should be mentioned when using aged animals, and was recently raised by Miller and Nadon (2000), is the use of animals that are free from infections and illness. With a few exceptions, most of the published literature on the effects of age on various parameters has used animals of unknown health status. Therefore it is not known if an observed effect in aged animals is a *true* effect of ageing, or if it is a response to infection or illness (see Miller and Nadon, 2000). The animals used in the present study are *clean*, they are kept under strict SPF barrier conditions, the microbiological status of the animals is known and they conform to the current FELASA health guidelines (Rehbinder *et al.*, 1995). This may be of particular

importance when examining inflammatory responses in the brains of adult and aged animals.

The reasons for the age-associated increase in infarct size are yet to be determined. It does not appear to be due to differences in astrocyte activation, adhesion molecule upregulation, neutrophil invasion, or BBB permeability following MCAo. There are several structural alterations in neurones and glial cells with age including damage to DNA and lipid membranes, and this wear and tear with age may just render them more vulnerable to other insults. Alterations in the cerebrovasculature with age such as decreased capillary density and an increase in arteriovenous shunting may reduce collateral circulation to penumbral regions quickening the time before blood flow falls below the LCT. The increases in the upregulation of pro-inflammatory antigens on microglia from aged animals and their increased activation following injury may contribute to increased damage as suppression of microglial protein synthesis and secretion has been shown to be neuroprotective following brain injury. Changes in the cytokine secretion profiles of brain cells from aged animals could alter post-ischaemic inflammatory responses and perhaps lead to exaggerated responses. Conversely any defects in negative feedback regulatory mechanisms e.g. the decreased inhibitory effects of glucocorticoids on glial cell activation with age may prolong their activation with damaging consequences. Much additional research is required to unravel the mechanisms behind the increased vulnerability of the aged CNS to ischaemic injury.

The data presented in this thesis have shown that there are some differences in the cellular responses of adult and aged animals after the induction of ischaemia. These differences may be of fundamental importance to the progression of IBD and emphasise the importance of age in animal models of cerebral ischaemia. Aged animals are considerably more expensive and less accessible than young animals and therefore the use of young adult animals are necessary for stroke research. However, once a

mechanism of damage or a potential neuroprotective agent has been identified in young animals, its effects should also be examined in aged animals as their responses may well differ. Identifying differences in the responses of the brains of aged animals may lead to new therapeutic targets for stroke intervention.

8.1 Suggestions for further experiments

The data presented here has revealed new topics of study and a brief list of potential experiments are given below:

1) Extending the time-points (eg. to include 3 days and 7 days) to examine if later responses by astrocytes and microglia, and neutrophil infiltration are affected with age.

2) Examination of a variety of cell markers to monocytes and microglia using immunocytochemistry (eg. F4/80 or SC6 (mouse microglia/macrophage marker), ED1 (macrophage/ monocyte marker), and CD11a (marker for neutrophils/monocytes)) at different timepoints after MCAo (eg. 12h, 24h, 3 days and 7 days) in adult and aged animals. This will determine whether the age-related increase in the microglia/macrophage response is due to increased activation of microglia or the accumulation of monocytes, and determine if monocyte invasion into the brain is effected with age.

3) Examination of the permeability of the BBB to small molecular weight tracers (such as sodium fluorescein), to see if there are any alterations with age.

4) Measuring the levels of bioactive IL-1β (eg. by bioassay) in the brains of adult and aged animals subjected to MCAo, to see if the levels of this cytokine are altered with age.

5) Evaluation of the effects of peripheral rIL-1ra on infarct volume in aged animals, and its effects on ICAM-1 and IL-1β expression, glial cell activation and immune cell invasion in the brains of adult and aged animals.

References

ABBOTT, N. J and REVEST, A. R (1991). Control of brain endothelial permeability. *Cerebrovasc. Brain Metab. Rev.* **3**, 39-72

AKINS, P. T., LIU, P. K., and HSU, C. Y. (1996). Immediate early gene expression in response to cerebral ischaemia: Friend or foe? *Stroke* **27**, 1682-1687.

ALBERT, M.S, and MOSS, M.B. (1996). Neuropsychology of aging: Findings in humans and monkeys. In "Handbook of the biology of aging" (E. L. Schneider, and J. W. Rowe, Eds), Fourth edition, pp. 217- 233. Academic Press, London.

AMENTA, F., BORGRANI, S.,CADEL, S.,FERRANTE, F., VALSECCHI, B. VEGAS, J. A. (1994). Microanatomical changes in the frontal cortex of aged rats: Effects of L-Deprenyl treatment. *Brain research bulletin.* **34 (2)**. 125-131.

ANDREW, D. P., SPELLBERG, JP., TAKIMOTO, H., SCHMITS, R., MAK, T. W., and ZUKOWSKI, M. M. (1998). Transendothelial migration and trafficking of leukocytes in LFA-1-deficient mice. *Eur. J. Immunol.* **28**, 1959-1969.

ASTRUP, J., SIESJO, B. K., and SYMON, L. (1981). The thresholds in cerebral ischaemia - the ischaemic penumbra. *Stroke* **12**, 723-725.

BAN, E., HAOUR, F., and LEINSTRA, R. (1992). Brain interleukin-1 gene expression induced by peripheral lipopolysaccharide administration. *Cytokine* **4**, 48-54.

BAN, E., MILON, G., PRUDHOMME, N., FILLION, G., and HAOUR, F. (1991). Receptors for interleukin-1 (alpha and beta) in mouse brain mapping and neuronal localization in hippocampus. *Neuroscience* **43**, 21-30.

BARGER, S. W. et al. (1995). TNFα and TNFβ protect hippocampal neurones against amyloid á-peptide toxicity: Evidence for involvement of a kB-binding factor and attenuation of peroxide and Ca2+ accumulation. *Proc. Natl Acad. Sci. U.S.A.* **92**, 9328-9332.

BARONE, F. C., ARVIN, B., WHITE, R. F., MILLER, A., WEB, C. L., WILLETTE, R. N., LYSKO, P. G., and FEUERSTEIN, G. Z. (1997). Tumor-necrosis factor alpha. A mediator of focal ischaemic brain injury. *Stroke* **28**, 1233-1244.

BARONE, F. C., and FEUERSTEIN, G. Z. (1999). Inflammatory Mediators and Stroke: New Opportunities for Novel Therapeutics. *J. Cereb. Blood Flow Metab.* **19** (8), 819-834.

BARONE, F. C., HILLEGASS, L. M., PRICE, W. J., WHITE, R. F., LEE, E. V., FEUERSTEIN, G. Z., SARAU, H. M., CLARK, R. K., and GRISWOLD, D. E. (1991). Polymorphonuclear leukocyte infiltration into cerebral focal ischemic tissue: Myeloperoxidase activity assay and histological verification. *J. Neurosci. Res.* **29**, 336-345.

BARONE, F. C., KNUDSEN, D. J., NELSON, A. H., FEUERSTEIN, G. Z., and WILLETTE, R. N. (1993). Mouse strain differences in susceptibility to cerebral vascular anatomy. *J. Cereb. Blood Flow Metab.* **13**, 683-692.

BAZAN, N. G., ALLAN, G., and RODRIGUEZ DE TURCO, E. B. (1993). Role of phospholipase A_2 and membrane derived second messengers in membrane function and transcriptional activation of genes: implications in cerebral ischaemia and neuronal excitability. *Progress in Brain Research* **96**, 247-257.

BAZAN, J. F., TIMANS, J. C., and KASTELEIN, R. A. (1996). A newly defined interleukin-1. *Nature* **379**, 591.

BEDERSON, J., PITTS, L., TSUJI, M., NISHIMURA, M., DAVIS, R., and BARTKOWSKI, H. (1986). Rat middle cerebral artery occlusion: Evaluation of the model and development of a neurologic examination. *Stroke* **17**, 472-476.

BEEKHUIZEN, H., and VAN FURTH, R. (1993). Monocyte adherence to human vascular endothelium. *J.Leukocyte Biol.* **54**, 363-378.

BELL, M. D., and PERRY, V. H. (1995). Adhesion molecule expression on murine cerebral endothelium following the injection of a pro-inflammagen or during acute neuronal degeneration. *Journal of Neurocytology* **24**, 695-710.

BENAVIDES, J., CAPDEVILE, C., DAUPHIN, F., DUBOIS, A., DUVERGER, D., FAGE, D., GOTTI, B., MACKENZIE, E., and SCATTON, B. (1990). The quantification of brain lesions with an W3 site ligand: a critical analysis of animal models of cerebral ischemia and neurodegeneration. *Brain Res.* **522**, 275-289.

BERCIANO, M. T., ANDRES, M. A., CALLE, E., and LAFARGA, M. (1995). Age-induced hypertrophy of astrocytes in rat supraoptic nucleus: a cytological, morphometric, and immunological study. *Anat. Rec.* **243**, 129-144.

BETZ, A. L., YANG, G.-Y., and DAVIDSON, B. L. (1995). Attenuation of stroke size in rats using an adenoviral vector to induce overexpression of interleukin-1 receptor antagonist in brain. *J. Cereb. Blood Flow Metab.* **15**, 547-551.

BHASKAR, M. S., and RAO, K. S. (1994). Altered conformation and increased strand breaks in neuronal and astroglial DNA of ageing rat brain. *Biochem. Mol. Biol. Int.* **33**, 377-384.

BHAT, R., DIROCCO, R., MARCY, V. R., et al. (1996). Increased expression of IL-1 converting enzyme in hippocampus after ischemia: selective localization in microglia. *J. Neurosci.* **16**, 4146-4153.

BOLTON, S. J., ANTHONY, D. C., and PERRY, V. H. (1998). Loss of the tight junction proteins occludin and zonula occuludens-1 from cerebral vascular endothelium during neutrophil-induced blood-brain barrier breakdown in-vivo. *Neuroscience* **86(4)**, 1245-1257.

BOND, A., O'NEILL, M. J., HICKS, C. A., MONN, J. A., and LODGE, D. (1998). Neuroprotective effects of a systemically active group II metabotropic glutamate receptor agonist model of global ischemia. *Neuropharmacology and Neurotoxicology* **9(6)**, 1191-1193.

BONDY, S. C., and LEBEL, C. P. (1993). The relationship between excitotoxicity and oxidative stress in the central nervous system. *Free Rad. Biol, Med.* **14**, 633-642.

BOTCHKINA, G. I., MEISTRELL, M. E., BOTCHKINA, I. L., and TRACEY, K. J. (1997). Expression of TNF and TNF receptors (p55 and p75) in the rat brain after focal cerebral ischemia. *Mol. Med.* **3**, 765-781.

BOYLE,E.A., MCGEER,P.L. (1990). Cellular immune response in multiple sclerosis plaques. *Am. J. Pathol.* **137**, 575-584.

BRAQUET, P., TOUQUI, L., SHEN, T. S., and VARGAFTIG, B. B. (1987). Perspectives in platelet-activating factor research. *Pharmacol. Rev.* **39**, 97-145.

BRAUGHLER, J. M., and HALL, E. D. (1989). Central nervous system trauma and stroke: 1/ Biochemical considerations for oxygen free radical formation and lipid peroxidation. *Free Radical Biol. Med.* **6**, 289-301.

BREDER, C., DINARELLO, C. A., and SAPER, C. B. (1988). Interleukin-1 immunoreactive innervation of the human hypothalamus. *Science* **240**, 321-324.

BRINT, S., JACEWICZ, M., KIESSLING, M., TANABE, J., and PULSINELLI, W. (1988). Focal brain ischemia in the rat: Methods for reproducibility, neocortical infarction using tandem occlusion of the distal middle cerebral and ipsilateral common carotid arteries. *J. Cereb. Blood Flow Metab.* **8**, 474-485.

BRISCOE, D. M., COTRAN, R. S., and POBER, J. S. (1992). Effects of tumor necrosis factor, lipopolysaccharide, and IL-4 on the expression of vascular cell adhesion molecule-1 in vivo. *J.Immunol.* **149**, 2954-2960.

BROADWELL, R. D., and BRIGHTMAN, M. W. (1983). Horseradish Peroxidase: A tool for the study of the neuroendocrine cell and other peptide-secreting cells. *Endocrinology* **103**, 187-218.

BROADWELL, R. D. (1989). Movement of macromolecules across the blood brain barrier. Cerebrovascular Diseases. Eds Ginsberg, M. D., Dietrich, W., Dalton,. Raven Press. New York.

BRUCE, A. J., BOLING, W., KINDY, M. S., PESCHON, J., KRAEMER, P. J., CARPENTER, M. K., HOLTSBERG, F. W., and MATTSON, M. P. (1996). Altered neuronal and microglial responses to excitotoxic and ischemic brain injury in mice lacking TNF receptors. *Nature Medicine* **2(7)**, 788-794.

BUCHAN, A. M., LESIUK, H., BARNES, K. A., LI, H., HUANG, Z.-G., SMITH, K. E., and XUE, D. (1993). AMPA antagonists: Do they hold more promise for clinical stroke trials than NMDA antagonists. *Stroke* **24(Suppl. I)**, I-148,-I-152.

BURNS, E. M., BUSCHMANN, M. B. T., KRUCKEBERG, T. W., GAETANO, P. K., and MEYER, J. N. (1981). Blood-brain barrier, Aging, Brain blood flow and sleep. In "Advances in neurology" (A. L. Carney, and E. M. Anderson, Eds.), Vol. 30, pp. 301-306. Raven Press, New York.

BUSTO, R., DIETRICH, W. D., GLOBUS, M. Y.-T., VALDES, I., SCHEINBERG, P., and GINSBERG, M. D. (1987). Small differences in intraischaemic brain temperature critically determine the extent of ischaemic neuronal injury. *J. Cereb. Blood Flow Metab.* **7**, 729-738.

BUTTINI, M., APPEL, K., SAUTER, A., GEBICKE-HAERTER, P. J., CARPENTER, M. K., HOLTZBERG, F. W., and MATTISON, M. P. (1996). Expression of tumor necrosis factor alpha after focal cerebral ischemia in rat. *Neuroscience* **71**, 1-16.

BUTTINI, M., SAUTER, A., and BODDEKE, H. (1994). Induction of interleukin-1 beta mRNA after focal cerebral ischaemia in the rat. *Mol. Brain Res.* **23**, 126-134.

CAMPBELL, I. L., ABRAHAM, C. R., MASLIAH, E., KEMPER, P., INGLIS, J. D., OLDSTONE, M. B. A., and MUCKE, L. (1993). Neurological disease induced in transgenic mice by cerebral overexpression of interleukin-6. *Proc. Natl Acad. Sci. U.S.A.* **90**, 10061-10065.

CANNELLA, B., CROSS, A. H., and RAINE, C. S. (1991). Adhesion related molecules in the CNS. Upregulation correlates with inflammatory cell influx during relapsing experimental autoimmune encephalomyelitis. *Laboratory Investigation* **65**, 23-31.

CHALMERS-REDMAN, R. M. E., FRASER, A. D., JU, W. Y. H., WADIA, J., TATTON, N. A., and TATTON, W. G. (1997). Mechanisms of nerve cell death: Apoptosis or necrosis after cerebral ischaemia. In "Neuroprotective agents and cerebral ischaemia" (A. R. Green, and A. J. Cross, Eds.), pp. 1-25. Academic Press, London.

CHAN, P. H. (1996). Role of oxidants in ischemic brain damage. *Stroke* **27**, 1124-1129.

CHAN, P. H., EPSTAIN, C. J., LI, Y., HUANG, T. T., CARLSON, E., KINOUCHI, H., YANG, G., KAMII, H., MIKAWA, S., and KONDO, T. (1995). Transgenic mice and knockout mutants in the study of oxidative stress brain injury. *J. Neurotrauma* **12(5)**, 815-824.

CHAN, P. H., KERLAN, R., and FISHMAN, R. A. (1983). Reductions of γ-aminobutyric acid and glutamate uptake and (Na+ and K+)-ATPase activity in brain slices and synaptosomes by arachidonic acid. *J. Neurochem.* **40**, 309-316.

CHAO, C. C., HU, S., and PETERSON, P. K. (1996). Glia: the not so innocent bystanders. *Journal of NeuroVirology* **2**, 234-239.

CHEN, H., CHOPP, M., and ZHANG, R. L. (1994). Anti-CD11b monoclonal antibody reduces ischemic cell damage after transient focal cerebral ischemia in rats. *Ann. Neurol.* **35**, 447-452.

CHEN, Z. L., and STRICKLAND, S. (1997). Neuronal death in the hippocampus is promoted by plasmin-catalysed degradation of laminin. *Cell* **91**, 917-925.

CHENG, B., CHRISTAKOS, S., and MATTSON, M. P. (1994). Tumor necrosis factor protects neurons against metabolic-excitotoxic insults and promote maintenance of calcium homeostasis. *Neuron* **12**, 139-153.

CHIAMULERA, C., TERRON, A., REGGIANI, A., and CRISTOFORI, P. (1993). Qualitative and quantitative analysis of the progressive cerebral damage after middle cerebral artery occlusion in mice. *Brain Res.* **606**, 251-258.

CHIANG, C. S., STALDER, A., SAMIMI, A., and CAMPBELL, I. L. (1994). Reactive gliosis as a consequence of IL-6 expression in the brain: Studies in transgenic mice. *Dev. Neurosci.* **16**, 212-221.

CHOI, D. W. (1993). NMDA receptors and AMPA/kainate receptors mediate parallel injury in cerebral cortical cultures subjected to oxygen-glucose deprivation. *Progress in Brain Research* **96**, 137-143.

CHOI, D. W. (1994). Glutamate receptors and the induction of excitotoxic neuronal death. *Progress in Brain Research* **100**, 47-51.

CHOI, D. W., and KOH, J. Y. (1998a). Zinc and brain injury. *Ann. Rev. Neurosci.* **31**, 347-375.

CHOI, D. W., LOBNER, D., and DUGAN, L. L. (1998b). Glutamate receptor-mediated neuronal death in the ischemic brain. *Monogr. Clin. Neurosci. Basel, Karger* **16**, 2-13.

CHOPP, M., LI, Y., JIANG, R. L., and PROSTAK, J. (1996). Antibodies against adhesion molecules reduce apoptosis after transient middle cerebral artery occlusion in the rat brain. *J. Cereb. Blood Flow Metab.* **16**, 578-584.

CHOPP, M., ZHANG, R. L., CHEN, H., LI, Y., JIANG, N., and RUSCHE, J. R. (1994). Post-ischaemic administration of Anti-Mac-1 antibody reduces ischaemic cell damage after middle cerebral artery occlusion in rats. *Stroke* **25**, 869-876.

CLARK, R. K., LEE, E. V., FISH, C. J., WHITE, R. F., PRICE, W. J., JONAK, Z. L., FEUERSTEIN, G. Z., and BARONE, F. C. (1993). Development of tissue damage, inflammation and resolution following stroke: An immunohistochemical and quantitative planimetric study. *Brain Res.* **31**, 565-572.

COGGESHALL, R. E. (1992). A consideration of neural counting methods. *TINS* **15**, 9-13.

COLEMAN, P. D., and FLOOD, D. G. (1987). Neuron numbers and dendritic extent in normal aging and Alzheimer's disease. *Neurobiol. Aging* **8**, 521-545.

COLOTTA, F., RE, F., MUZIO, M., BERTINI, B., POLENTARUTTI, N., SIRONI, M., GIRI, J. G., DOWER, S. K., SIMS, J. E., and MANTOVANI, A. (1993). Interleukin-1 type II receptor: a decoy target for IL-1 that is regulated by IL-4. *Science* **261**, 472-475.

COTMAN, C. W., HAILER, N. P., PFISTER, K. K., SOLTESZ, I., and SCHACHNER, M. (1998). Cell adhesion molecules in neural plasticity and pathology: Similar mechanisms, distinct organisations? *Progress in neurobiology* **55**, 659-669.

COTMAN, C.W, and NEEPER,S. (1996). Activity-dependent plasticity and the ageing brain. In "Handbook of the biology of aging" (E. L. Schneider, and J. W. Rowe, Eds), Fourth edition, pp. 283-299. Academic Press, London.

COURAUD, P. O. (1994). Interactions between lymphocytes, macrophages and central nervous system cells. *J. Leucocyte Biology* **56**, 407-415.

DALKARA, T., and MOSKOWITZ, M. A. (1994). The complex role of nitric oxide in the pathophysiology of focal cerebral ischemia. *Brain Pathology* **4**, 49-57.

DALKARA, T., IRIKURA, K., HUANG, N., PANAHIAN, N., and MOSKOWITZ, M. A. (1995). Cerebrovascular responses under controlled and monitored physiological conditions in the anaesthetized mouse. *J. Cereb. Blood Flow Metab.* **15**, 631-638.

DALKARA, T., and MOSKOWITZ, M. A. (1999). Recent developments in experimental stroke. *Neuroscience News* **2**, 20-27.

DAVIES, C. A., LODDICK, S. A., TOULMOND, S., STROEMER, R. P., HUNT, J., and ROTHWELL, N. J. (1999). The progression and topographic distribution of interleukin-1á expression after permanent middle cerebral artery occlusion in the rat. *J. Cereb. Blood Flow Metab.* **19**, 87-98.

DAVIES, C. A., LODDICK, S.A, STROEMER, P., HUNT, J., and ROTHWELL, N. J. (1998). An integrated analysis of the progression of cell responses induced by permanent focal middle cerebral artery occlusion in the rat. *Exp. Neurol.* **154**, 199-212.

DAVIES, I., and SCHOFIELD, J. D. (1980). Connective tissue ageing: The influence of a lathyrogen (Beta-aminopropionitrile) on the life span of female C57BL/Icrfat mice. *Gerontology* **15**, 487-494.

DAVIS, E. J., FOSTER, T. D., and THOMAS, W. E. (1994). Cellular forms and functions of brain microglia. *Brain Res. Bull.* **34**, 73-78.

DAVIS, M., MENDELOW, A. D., PERRY, R., CHAMBERS, I. R., and JAMES, O. F. W. (1995). Experimental stroke and neuroprotection in the aging rat brain. *Stroke* **26**, 1072-1078.

DAWSON, D. A. (1994). Nitric oxide and focal cerebral ischaemia: Multiplicity of actions and diverse outcome. *Cerebrovasc. Brain Metab. Rev.* **6**, 299-324.

DAWSON, D. A., MARTIN, D., and HALLENBECK, J. M. (1996). Inhibition of tumour necrosis factor-alpha reduces focal cerebral ischemic injury in the spontaneously hypertensive rat. *Neurosci. Lett.* **218**, 41-44.

DAWSON, R. J., and WALLACE, D. R. (1992). Kainic acid-induced seizures in aged rats: neurochemical correlates. *Brain Res. Bull.* **29**, 459-468.

DEGRABBA, T. J. (1998). The role of inflammation after acute stroke. *Neurology* **51 (Suppl 3)**, s62-s67.

DE JONG, G. I., DE WEERD, H., SCHUURMAN, T., TRABER, J., and LUITEN, P. G. M. (1990). Microvascular changes in aged rat forebrain. Effects of chronic nimodipine treatment. *Neurobiol. Aging* **11**, 381-389.

DEL ZOPPO, G. J., SCHMID-SCHONBEIN, G. W., MORI, E., COPELAND, B. R., and CHANG, C. M. (1991). Polymorphonuclear leukocytes occlude capillaries following MCA occlusion and reperfusion in baboons. *Stroke* **22**, 1276-1283.

DEL ZOPPO, G. J., WAGNER, S., and TAGAYA, M. (1997). Trends and future developments in the pharmacological treatment of acute ischaemic stroke. *Drugs* **54 (1)**, 9-38.

DE VRIES, E., BLOM-ROOSEMALEN, M., OOSTEN, M., DE BOER, A. G., BREIMER, D. D., VAN BERKEL, T. J. C., and KUIPER, J. (1995a). The influence of cytokines on the blood brain barrier in vitro. In "Characteristics of blood-brain barrier endothelial cells in response to inflammatory stimuli" (E. de Vries, Ed.). pp. 147-157. Costar Europe Ltd, Badhoevedorp.

DE VRIES, H. E., HOOGENDOORN, K. H., VAN DIJK, J., ZIJLSTRA, F. J., BREIMER, D. D., VAN BERKEL, TJ. C., DE BOER, A. G., VAN DAM, A.-M., and KUIPER, J. (1995b). Eicosanoid production by rat cerebral endothelial cells; stimulation by LPS, IL-1 and IL-6. In "Characteristics of the blood-brain barrier endothelial cells in response to inflammatory stimuli" (E. de Vries, Ed.). pp. 111-122. Costar Europe Ltd, Badhoevedorp.

DICKSON, D. W., SINICROPI, S., YEN, S. H., KO, L. W., MATTIACE, L. A., BUCALA, R., and VLASSARA, H. (1996). Glycation and microglia reaction in lesion of alzheimer's disease. Neurobiol. *Aging* **17**, 733-743.

DINARELLO, C. A. (1991). Interleukin-1 and interleukin-1 antagonism. *Blood* **8**, 1627-1652.

DINARELLO, C. (1993). Modalities for reducing IL-1 activity in disease. *Trends Pharmacol. Sci.* **14**, 155-159.

DINARELLO, C. A. (1996). Biological basis for Interleukin-1 in disease. *Blood* **87**, 2095-2147.

DINARELLO, C. A. (1997). Induction of interleukin-1 and interleukin-1 receptor antagonist. *Semin Oncol* **24(Suppl. 9)**, s9,81-s9,93.

DINARELLO, C. A., and THOMPSON, R. C. (1991). Blocking IL-1: interleukin-1 receptor antagonist in vivo and in vitro. *Immunology* **12 (11)**, 404-410.

DIRNAGL, U., IADECOLA, C., and MOSKOWITZ, M. A. (1999). Pathobiology of ischaemic stroke: an integrated view. *Trends Neurosci.* **22**, 391-397.

DU, C., HU, R., CSERNANSKY, C. A., HSU, C. Y., and CHOI, D. W. (1996). Very delayed infarction after mild focal cerebral ischemia- a role for apoptosis. *J. Cereb. Blood Flow Metab.* **16**, 195-201.

DUVERGER, D., and MACKENZIE, E. T. (1988). The quantification of cerebral infarction following focal ischemia in the rat: Influence of strain, arterial pressure, blood glucose concentration and age. *J. Cereb. Blood Flow Metab.* **8**, 449-461.

EDDLESTON, M., and MUCKE, L. (1993). Molecular profile of reactive astrocytes-implications for their role in neurological disease. *Neuroscience* **54**, 15-36.

EDVINSSON, L., MACKENZIE, E. T., and MCCULLOCK, J. (1993). The aged brain. In "*Cerebral Blood Flow and Metabolism*". Academic Press. London. pp 647-660.

EDWARDS, S. W. (1995). Cell signaling by integrins and immunoglobulin receptors in primed neutrophils. *Trends Biochem. Sci.* **20**, 362-367.

EISENBERG, S. P., EVANS, R. J., AREND, W. P., VERDERBER, E., BREWER, M. T., HANNUM, C. H., and THOMPSON, R. C. (1990). Primary structure and functional expression from complementary DNA of a known interleukin-1 receptor antagonist. *Nature* **343**, 341-346.

FABRY, Z., RAINE, C., and HART, M. (1994). Nervous tissue as an immune compartment, the dialect of the immune response in the central nervous system. *Immunology* **15(5)**, 218-224.

FAGNI, L., OLIVIER, M., LAFON-CAZAL, M., and BOCKAERT, J. (1995). Involvement of the divalent ions in the nitric oxide induced blockade of NMDA receptors in cerebellar granule cells. *Mol.Pharmacol.* **47**, 1239-1247.

FAROOQUI, A. A., and HORROCKS, L. A. (1992). Excitatory amino acid receptors, neuronal membrane phospholipid metabolism and neurological disorders. *Brain Res.Rev.* **16**, 171-179.

FASSBENDER, K., ROSSOL, S., and KAMMER, T. (1994). Proinflammatory cytokines in serum of patients with acute cerebral ischaemia: kinetics to secretion and relation to the extent of brain damage and outcome of disease. *J. Neurol. Sci.* **122**, 135-139.

FEUERSTEIN, G. Z., LIU, T., and BARONE, F. C. (1994b). Cytokines, Inflammation, and brain injury, Role of TNF-alpha. *J. Cereb. Blood Flow Metab.* **6**, 341-360.

FINCH, C. (1993). Neuron atrophy during aging: Programmed or sporadic? *Trends Neurosci.* **16**, 104-110.

FINCH, C. E., and MORGAN, D. G. (1990). RNA and protein metabolism in the aging brain. *Ann. Rev. Neurosci.* **13**, 75-87.

FLANDERS, K. C., REN, R. F., and LIPPA, C.F. (1998). Transforming growth factor-βs in neurodegenerative disease. *Prog. Neurobiol.* **54**, 71-85.

FLOOD, D. G., and COLEMAN, P. D. (1988). Neuron numbers and sizes in aging brain: Comparisons of human, monkey and rodent data. *Neurobiol. Aging* **9**, 453-463.

FORSTER, C., CLARK, H. B., ROSS, M.E., and IADECOLA,C. (1999). Inducible nitric oxide synthase expression in human cerebral infarcts. *Acta Neuropathol.* **97**, 215-220.

FOTHERINGHAM, A. P., DAVIES, C. A., DAVIES, I.(2000). Oedema and glial cell involvement in the aged mouse brain after permanent focal ischaemia. *Neuropathol. Appl. Neurobiol.* **26**, 412-423.

FREEMAN, G. B., and GIBSON, G. E. (1987). Selective alteration of mouse brain neurotransmitter release with age. *Neurobiol. Aging* **8**, 147-152.

FRENCH, R. A., VANHOY, R. W., CHIZZONITE, R., ZACHARY, J. F., DANTZER, R., PARNET, P., BLUTHE, R. M., and KELLEY, K. W. (1999). Expression and localization of p80 and p68 interleukin-1 receptor proteins in the brains of adult mice. *J. Neuroimmunol.* **93**, 194-202.

FURLAN, M., GILLES, M., VIADER, F., DERLON, J. M., and BARON, J. C. (1996). Spontaneous neurological recovery after stroke and the fate of the ischemia penumbra. *American neurological association* **40**, 216-226.

FURUKAWA, K., FU, W., LI, Y., WITKE, W., KWIATKOWSKI, D. J., and MATTSON, M. P. (1997). The actin-severing protein gelsolin modulates calcium channel and NMDA receptor activities and vulnerability to excitotoxicity in hippocampal neurons. *J. Neurosci.* **21**, 8178-8186.

FUTRELL, N., GARCIA, J. H., PETERSON, E., and MILLIKAN, C. (1991). Embolic stroke in aged rats. *Stroke* **22**, 1582-1591.

GABELLEC, M.-M., GRIFFAIS, R., FILLION, G., and HAOUR, F. (1995). Expression of interleukin-1 alpha and interleukin-1 receptor antagonist mRNA in mouse brain: regulation by bacterial lipopolysaccharide (LPS) treatment. *Mol. Brain Res.* **31**, 122-130.

GARCIA, J. H. (1984). Experimental Ischemic Stroke: A review. *Stroke* **15**, 5-14.

GARCIA, J. H., LIU, K. F., YOSHIDA, Y., LIAN, J., CHEN, S., and DEL ZOPPO, G. J. (1994). Influx of leukocytes and platelets in an evolving brain infarct (Wistar rats). *Am.J.Pathol.* **144**, 188-199.

GARCIA, J.H., LIU, K. F., YOSHIDA, Y., CHEN, S., and LIAN, J. (1994b). Brain microvessels: factors altering their patency after the occlusion of the middle cerebral artery (Wistar rat). *Am.J.Pathol.* **145**, 728-740.

GARCIA, J. H., LIU, K.-F., and RELTON, J. K. (1995). Interleukin-1 receptor antagonist decreases the number of necrotic neurones in rats with middle cerebral artery occlusion. *Am.J.Pathol.* **147**, 1477-1486.

GARCIA, J., YOSHIDA, Y., CHEN, H., LI, Y., ZHANG, Z., LIAN, J., CHEN, S., and CHOPP, M. (1993). Progression from ischemic injury to infarct following middle cerebral artery occlusion in the rat. *Am.J.Pathol.* **142**, 623-635.

GEHRMANN, J., BANATI, R. B., WIESSNER, C., HOSSMANN, K. A., and KREUTZBERG, G. W. (1995). Reactive microglia in cerebral ischaemia: an early mediator of tissue damage. *Neuropathol. Appl. Neurobiol.* **21**, 277-289.

GEHRMANN, J., BONNEKOH, P., MIYAZAWA, T., OSCHLIES, U., DUX, E., HOSSMANN, K.-A., and KREUTZBERG, G. W. (1992). The microglial reaction in the rat hippocampus following global ischaemia: immuno-electron microscopy. *Acta Neuropathol.* **84**, 588-595.

GINSBERG, M. D. (1996). The validity of rodent brain ischemia models is self-evident. *Arch. Neurol.* **53**, 1065-1067.

GINSBERG, M. D., and BUSTO, R. (1989). Progress review : Rodent models of cerebral ischemia. *Stroke* **20**, 1627-1642.

GIULIAN, D., BAKER, T. J., SHISH, L. N., and LACHMAN, L. B. (1986). Interleukin-1 of the central nervous system is produced by ameboid microglia. *J. Exp. Med.* **164**, 594-604.

GIULIAN, D., CHEN, J., INGEMAN, J. E., GEORGE, J. K., and NOPONEN, M. (1989). The role of mononuclear phagocytes in wound healing after traumatic injury to adult mammalian brain. *J. Neurosci.* **9(12)**, 4416-4429.

GIULIAN, D., and ROBERTSON, C. (1990). Inhibition of mononuclear phagocytes reduces ischemic injury in the spinal cord. *Annls Neurol.* **27**, 33-42.

GIULIAN,, D, and VACA, K. (1993). Inflammatory glia mediate neuronal damage after ischemia in the central nervous system. *Stroke* **24(Suppl I)**, 184-190.

GLENN, J. A., BOOTH, P. L., and THOMAS, W. E. (1991). Pinocytotic activity in ramified microglia. *Neurosci. Lett.* **123**, 27-31.

GLENN, J. A., WARD, S. A., STONE, C. R., BOOTH, P. L., and THOMAS, W. E. (1992). Characterisation of ramified microglial cells - detailed morphology, morphological plasticity and proliferative capability. *The Anatomical Record* **180**, 109-118.

GOLDBERG, W. J., and BERNSTEIN, J. J. (1988). Fetal cortical astrocytes migrate from cortical homografts throughout the host brain and over the glia limitans. *J. Neurosci. Res.* **20**, 138-145.

GOLDMAN, J. E., CALINGASAN, N. Y., and GIBSON, G. E. (1994). Aging and the brain. *Curr.Opin.Neurol.* **7**, 287-293.

GONZALES, R. A., BROWN, L. M., JONES, T. W., TRENT, R. D., WESTBROOK, S. L., and LESLIE, S. W. (1992). NMDA mediated responses decrease with age in Fischer 344 rat brains. *Neurobiol. Aging* **12**, 219-225.

GORDON, C. R., MERCHANT, R. S., MARMAROU, A., RICE, C. D., and YOUNG, H. R. (1990). Effect of murine interleukin-1 on brain oedema in the rat. *Acta Neurochiurgica Suppl.* **1**, 268-270.

GORDON, M.N., and MORGAN, D.G. (1991). Increased GFAP expression in the aging brain does not result from increased astrocyte density. *Soc. for Neurosci. Abstracts* **17**, 53 (No. 26.4)

GORDON, M.N., SCHREIER, W. A., OU, X., HOLCOMB, L. A., and MORGAN, D. G. (1997). Exaggerated astrocyte reactivity after nigrostriatal deafferentation in the aged rat. *Journal of Comparative Neurology* **388**, 106-119.

GOSS, J. R., FINCH, C. E., and MORGAN, D. G. (1991). Age-related changes in glial fibrillary acidic protein mRNA in the mouse brain. *Neurobiol. Aging* **12**, 165-170.

GOSS, J. R., and MORGAN, D. J. (1995). Enhanced glial fibrillary acidic protein RNA response to fornix transection in aged mice. *J. of Neurochem.* **64**, 1351-1360.

GOTOH, O., ASANO, T., KOIDE, T., TAKAKURA, K. (1985). Ischemic brain edema following occlusion of the middle cerebral artery in the rat. *Stroke*. **16**. 101-109.

GOURMALA, N. G., BUTTINI, M., LIMONTA, S., SAUTER, A., and BODDEKE, H. W. (1997). Differential and time dependant expression of monocyte chemoattractant protein-1 mRNA by astrocytes and macrophages in rat brain: effects of ischemia and peripheral lipopolysaccharide administration. *J.Immunol.* **74**, 35-44.

GREEN, A. R., and CROSS, A. J. (1997). Techniques for examining neuroprotective drugs in vivo. In "Neuroprotective agents and cerebral ischaemia" (A. R. Green, and A. J. Cross, Eds.), pp. 47-68. Academic Press Limited, London.

GRIFFIN,W.S.T., SHENG, J.D., MRAK,R.E., (1998) Senescence-accelerated overexpression of S100B in brain of SAMP6 mice. *Neurbiol. Aging.* **19**, 71-76.

GUNDERSON, H. J. G., BAGGER, P., BENDTSEN, T. F., EVANS, S. M., KORBO, L., MARCUSSEN, N., MOLLER, A., NIELSEN, K., NYENGAARD, J. R., PAKKENBERG, B., SORENSEN, F. B., VESTERBY, A., and WEST, M. J. (1988). The new stereological tools: Disector, fractionator, nucleator and point sampled intercepts and their use in pathological research and diagnosis. *APMIS* **96**, 857-881.

GUTIERREZ, E. G., BANKS, W. A., and KASTIN, A. J. (1994). Blood-borne interleukin-1 receptor antagonist crosses the blood-brain barrier. *J.Immunol.* **55**, 153-160.

HAILER, N. P., BECHMANN, I., HEIZMAN, S., and NITSCH, R. (1997). Adhesion molecule expression on phagocytic microglial cells following anterograde degeneration of perfurant path axons. *Hippocampus* **7(3)**, 341-349.

HALL, E. D. (1993). Cerebral ischaemia, free radicals and antioxidant protection. *Biochemical Society Transactions* **21**, 334-339.

HALLENBECK, J. M., DUTKA, A. J., TANISHIMA, T., KOCHANEK, P. M., KUMAROO, K. K., THOMPSON, C. B., OBRENOVITCH, T. P., and CONTERAS, T. J. (1986). Polymorphonuclear leukocyte accumulation in brain regions with low blood flow during the early post-ischemic period. *Stroke* **17**, 246-253.

HAMA, T., KUSHIMA, Y., MIYAMOTO, M., KUBOTA, M., TAKEI, N., and HATANAKA, H. (1991). Interleukin-6 improves the survival of mesencephalic catecholaminergic and septal cholinergic neurons from postnatal two week old rats in cultures. *Neuroscience* **40**, 445-452.

HANSEN, L. A., ARMSTRONG, D. M., and TERRY, R. D. (1987). An immunohistochemical quantification of fibrous astrocytes in the aging human cerebral cortex. *Neurobiol. Aging* **8**, 1-6.

HAOUR, F., BAN, E., MARQUETTE, C., MILON, G., and FILLION, G. (1992). Brain interleukin-1 receptors: mapping, characterization and modulation. In "Interleukin-1 in the brain" (N. J. Rothwell, and R. Dantzer, Eds.), pp. 13-25. Pergamon press, Oxford.

HARA, H., FINK, K., ENDRES, M., FRIEDLANDER, R. M., GAGLIARDINI, V., YUAN, J., and MOSKOWITZ, M. A. (1997a). Attenuation of focal cerebral ischemic injury in transgenic mice expressing a mutant ICE inhibitory protein. *J. Cereb. Blood Flow Metab.* **17**, 370-375.

HARA, H., FRIEDLANDER, R. M., GAGLIARDINI, V., AYATA, C., AYATA, G., HUANG, Z., SHIMIZU-SASAMATA, M., YUAN, J., and MOSKOWITZ, M. (1997b).

Inhibition of ICE family proteases reduces ischemic and excitotoxic neuronal damage. *Proc. Natl Acad. Sci. U.S.A.* **94**, 2007-2012.

HARA, H., HUANG, PL., PANAHIAN, N., FISHMAN, M. C., and MOSKOWITZ, M. (1996). Reduced brain edema and infarction volume in mice lacking the neuronal isoform of nitric oxide synthase after transient MCA occlusion. *J. Cereb. Blood Flow Metab.* **16**, 605-611.

HARLAN, J. M., WINN, R. K., VEDDER, N. B., DOERSCHUK, C. M., and RICE, C. L. (1992). In vivo models of leukocyte adherence to endothelium. In "Adhesion" (J. M. Harlan, and D. Y. Liu, Eds.), pp. 117-150. W. H. Freeman and Company, New York.

HATASHITA, S., and HOFF, J. T. (1990). Role of blood-brain barrier permeability in focal ischemic brain edema. In "Advances in Neurology" (D. Long, Ed.), Vol. 52, pp. 327-333. Raven Press, New York.

HATTON, J. D., and FINKELSTEIN, J. P. (1993). Native astrocytes do not migrate *de novo* or after local trauma. *Glia* **9**, 18-24.

HAYWARD, N. J., ELLIOT, P. J., SAWYER, S. D., BRONSON, R. T., and BARTUS, R. T. (1996). Lack of evidence for neurtophil participation during infarct formation following focal cerebral ischemia in the rat. *Exp. Neurol.* **139**, 188-202.

HILL, J. K., GUNION-RINKER, L., KULHANEK, D., LESSOV, N., KIM, S., CLARK, W. M., DIXON, M. P., NISHI, R., STENZEL-POORE, M. P., and ECKENSTEIN, F. P. (1999). Temporal modulation of cytokine expression following focal cerebral ischemia in Mice. *Brain Res.* **820**, 45-54.

HOBBS, M. V., WEIGLE, W. O., NOONAN, D. J., TORBETT, B. E., MCEVILLY, R. J., KOCH, R. J., CARDENAS, G. J., and ERNST, D. N. (1993). Patterns of cytokine gene expression by CD4+ T cells from young and old mice. *J. Immunol.* **150**, 3602-3614.

HOPKINS, S. J., and ROTHWELL, N. J. (1995). Cytokines and the nervous system I: expression and recognition. *Trends Neurosci.* **18**, 83-88.

HORNBERGER, J. C., BUELL, S. J., FLOOD, D. G., MCNEILL, T. H. AND COLEMAN, P. D. (1985). *Neurobiol Aging.* **6**. 269-275.

HOSSMANN, K.-A. (1994). Viability thresholds and the penumbra of focal ischemia. *Ann. Neurol.* **36**, 557-565.

HUGHES, C. C. W., and LANTOS, P. L. (1987). A morphometric study of blood vessel, neuron and glial cell distribution in young and old rat brain. *J. Neurol. Sci.* **79**, 101-110.

HUNTER, A., GREEN, A. R., and CROSS, A. J. (1995). Animal models of stroke: can they predict clinically successful neuroprotective drugs? *Trends Pharmacol. Sci.* **16**, 123-128.

HUNTER, A. J., MACKAY, K. B., and ROGERS, D. C. (1998). To what extent have functional studies of ischemia in animals been useful in the assessment of potential neuroprotective agents? *Trends Pharmacol. Sci.* **19**, 59-66.

IADECOLA, C. (1997). Bright and dark sides of nitric oxide in ischemic brain injury. *Trends Neurosci.* **20**, 132-139.

IANOTTI, F., KIDA, S., WELLER, R., BUHAGIER, G., and HILLHOUSE, E. (1993). Interleukin-1β in focal cerebral ischemia in rats. *J. Cereb. Blood Flow Metab.* **13 (suppl 1)**, S125.

JIANG, N., MOYLE, M., SOULE, H. R., ROTE, W. E., and CHOPP, M. (1995). Neutrophil inhibitory factor is neuroprotective after focal ischemia in rats. *Ann. Neurol.* **38**, 935-942.

JOHNSON, S. A. and FINCH, C. A. (1996). Changes in gene expression during brain ageing: A survey. In "Handbook of the Biology of Aging" (E.L, Schneider, J.W, Rowe, Eds.), Fourth edition, pp. 300-327. Academic Press, London.

JONES, G. B., WAHLSTEN, D., and BLOM, G. (1977). Precision stereotaxic procedure for the mouse: Method and instrumentation. *Physiol. Behav.* **19**, 445-448.

KACZMAREK, L. K. (1987). The role of protein kinase C in the regulation of ion channels and neurotransmitter release. *Trends Neurosci.* **10**, 30-34.

KAMIJYO, Y., and GARCIA, J. H. (1975). Carotid arterial supply of the feline brain: Applications to the study of regional cerebral ischemia. *Stroke* **6**, 361-369.

KATO, H. (1998). Inflammatory markers in stroke. In "Neuroinflammation" (P. L. Wood, Ed.), pp. 91-107. Humana press, Totowa, New Jersey.

KATO, H., KOGURE, K., ARAKI, T., and ITOYAMA, Y. (1995). Graded expression of immunomoloecules on activated microglia in the hippocampus following ischemia in the rat model of ischemic tolerance. *Brain Res.* **694**, 85-93.

KATO, H., KOGURE, K., LIU, X.-H., ARAKI, T., and ITOYAMA, Y. (1996). Progressive expression of immunomolecules on activated microglia and invading leukocytes following focal cerebral ischemia in the rat. *Brain Res.* **734**, 203-212.

KATSURA, K., KRISTIAN, T., and SIESJO, B. K. (1994). Energy metabolism, ion homeostasis, and cell damage in the brain. *Biochemical Society Transactions* **22**, 991-996.

KAUFMANN, A. M., FIRLIK, A. D., FUKUI, M. B., WECHSLER, L. R., JUNGRIES, C. A., and YONAS, H. (1999). Ischemic core and penumbra in human stroke. *Stroke* **30**, 93-99.

KEANE, K. M., GIEGEL, D. A., LIPINSKI, W. J., CALAHAN, M. J., and SHIVERS, B. D. (1995). Cloning, tissue expression and regulation of rat interleukin-1β converting

enzyme. *Cytokine* **7**, 105-110.

KEMPSKI, O., STAUB, F., JANSEN, M., BAETHMANN. (1990). Molecular mechanisms of glial cell swelling in acidosis. *Adv. Neurol.*. **52**. 39-45.

KESSLAK, J. P., YUAN, D., NEEPER, S., and COTMAN, C. W. (1995). Vulnerability of the hippocampus to kainate excitotoxicity in the aged, mature and young adult rat. *Neurosci. Lett.* **188**, 117-120.

KIKKAWA, U., and NISHIZUKA, Y. (1986). The role of protein kinase C in transmembrane signaling. Annu. Rev. *Cell Biol.* **2**, 149-178.

KIM, J. S. (1996b). Cytokines and adhesion molecules in stroke and related diseases. *J. Neurol. Sci.* **137**, 69-78.

KIM, J. S., CHOPP, M., CHEN, H., LEVINE, S. R., CAREY, J. L., and WELCH, K. M. A. (1995). Adhesive glycoproteins CD11a and CD11b are upregulated in the leukocytes from patients with ischemic stroke and transient ischemic attacks. *J. Neurol. Sci.* **128**, 45-50.

KIM, C. B., PIER, L. P., and SPEAR, P. D. (1997). Effects of aging on numbers and sizes of neurons in histochemically defined sub-regions of monkey striate cortex. *The Anatomical Record* **247**, 119-128.

KIM, D. C., REITZ, D. F., CARMICHAEL, D. F., and BLOEDOW, D. (1995a). Kidney as a major clearance organ for recombinant human interleukin-1 receptor antagonist (IL-1ra). *J Pharm Sci* **84**, 575-580.

KIMELBERG, H. K. (1995). Current concepts of brain edema. *J. Neurosurg.* **83**, 1051-1059.

KLATZO, I. (1994). Evolution of brain edema concepts. *Acta Neurochirgica Suppl.* **60**, 3-6.

KOCHANEK, P. M., and HALLENBECK, J. M. (1992). Polymorphonuclear leukocytes and monocytes/macrophages in the pathogenesis of cerebral ischemia and stroke. *Stroke* **23**, 1367-1379.

KOEHLER, R. C. (1996). Editorial Comment. *Stroke* **27**, 1668.

KOHNO, K., and KURIMOTO, M. (1998). Interleukin-18, a cytokine which resembles IL-1 structurally and IL-12 functionally but exerts its effect independently of both. *Clinical Immunology and Immunopathology* **86**, 11-15.

KONDO, T., REAUME, A., HUANG, T. T., CARLSON, E., CHEN, S., SCOTT, R., EPSTEIN, C. J., and CHAN, P. H. (1995). Target disruption of CuZn-superoxide dismutase gene in mice causes exacerbation of cerebral infarction and neurological deficits in after focal cerebral ischemia and reperfusion. *Society of Neuroscience Abstracts* **21**, 1268.

KONIGSMARK, B. W. (1970). Methods for the counting of neurones. In "Contemporary Research Methods in Neuroanatomy" (W. J. H. Nauta, and S. O. E. Ebbesson, Eds.), pp. 315-340. Springer Verlag, Heidelberg, Berlin, New York.

KORTHUIS, R. J., and GRANGER, D. N. (1994). Pathogenesis of ischemia/reperfusion: Role of neutrophil-endothelial cell adhesion. In "Adhesion Molecules", pp. 163-190. Academic Press Limited.

KRAIG, R. P., LASCOLA, C. D., and CAGGIANO, A. (1995). Glial response to brain ischemia. In "Neuroglia" (H. Kettenmann, and B. R. Ransom, Eds.), pp. 964-976. Oxford University Press, Oxford.

KRISTIAN, T., and SIESJO, B. K. (1998). Calcium in ischemic cell death. *Stroke* **29(3)**, 705-718.

LANDIS, D.M.D.,(1994). The early reactions of non-neuronal cells to brain injury. *Ann. Rev. Neurosci.* **17**, 133-151.

LARGO, C., CUEVAS, P., and HERRERAS, O. (1996). Is glia dysfunction the initial cause of neuronal death in ischemic penumbra? *Neurological Research* **18**, 445-448.

LATOV, N., NILAVER, G., ZIMMERMAN, E. A., JOHNSON, W. G., SILVERMAN, A. J., DEFENDI, R., and COTE, L. (1979). Fibrillary astrocytes proliferate in response to brain injury: A study combining immunoperoxidase technique for GFAP and auto radiography of tritiated thimadine. *Dev. Biol.* **72**, 381-384.

LAWRENCE, M. S., HO, D. Y., SUN, G. H., STEINBERG, G. K., and SAPOLSKY, R. M. (1996). Overexpression of bcl-2 with herpes simplex virus vectors protects CNS neurons against neurological insults in vitro and in vivo. *J. Neurosci.* **16**, 486-496.

LECHAN, R. M., CLARK, T. B. D., CANNON, J. G., SHAW, A. R., DINARELLO, C. A., and REICHLIN, S. (1990). Immunoreactive IL-1 beta localization in rat forebrain. *Brain Res.* **514**, 135-140.

LEE, J. M., ZIPFEL, G. J., and CHOI, D. W. (1999). The changing landscape of ischaemic brain injury mechanisms. *Nature* **399**, A7-A14.

LEES, G. J. (1993). The possible contribution of microglia and macrophages to delayed neuronal death after ischemia. *J. Neurol. Suppl.***114**, 119-122.

LENNARD, A. C. (1995). Interleukin-1 receptor antagonist. *Critical Reviews in Immunology* **15**, 77-105.

LI, Y., VICTOR, G., SHAROV, P., JIANG, N., ZALOGA, C., SABBAH, H. N., and CHOPP, M. (1995). Ultrastructural and light microscope evidence of apoptosis after middle celebral artery occlusion in the rat. *Am.J.Pathol.* **146**, 1045-1051.

LICINIO, J., WONG, M.-L., and GOLD, P. W. (1991). Localization of interleukin-1

receptor antagonist mRNA in rat brain. *Endocrinology* **129**, 562-564.

LIN, T., HE, Y., WU, G., KHAN, M., and HSU, C. Y. (1993). Effect of brain edema on infarct volume in a focal cerebral ischemia model in rats. *Stroke* **24**, 117-121.

LINDSBERG, P. J., SIRIN, A., FEUERSTEIN, G. Z., and HALLENBECK, J. M. (1995). Antagonism of neutrophil adherence in the deteriorating stroke model in rabbits. *J. Neurosurg.* **82**, 269-277.

LINNIK, M. D., ZOBRIST, R. H., and HATFIELD, M. D. (1993). Evidence supporting a role of programmed cell death in focal cerebral ischemia. *Stroke* **24**, 2002-2009.

LINSBERG, P. J., CARPEN, O., PAETAU, A., KARJALAINEN-LINDSBERG, M. L., and KASTE, M. (1996). Endothelial ICAM-1 expression associated with inflammatory response in human ischemic stroke. *Circulation* **94**, 939-945.

LIPTON, S. A., CHOI, Y. B., PAN, Z. H., LEI, S. Z., CHEN, H. V., SUCHER, N. J., LOSCALZO, J., SINGEL, D. J., and STAMLER, J. (1993). A redox-based mechanism for the neuroprotective and neurodestructive effects of nitric oxide and related compounds. *Nature* **364**, 626-632.

LIU, C., CHALMERS, D., MAKI, R., and DE SOUZA, E. B. (1996). Rat homolog of mouse interleukin-1 receptor accessory protein: cloning, localization and modulation studies. *J. Neuroimmunol.* **66(1-2)**, 41-48.

LIU, T., CLARK, R. K., MCDONNELL, P. C., YOUNG, P. R., WHITE, R. F., BARONE, F. C., and FEUERSTEIN, G. Z. (1994). Tumor necrosis factor-α expression in ischemic neurones. *Stroke* **25**, 1481-1488.

LIU, T., MCDONNELL, P. C., YOUNG, P. R., WHITE, R. F., SIREN, A. L., HALLENBECK, J. M., BARONE, F. C., and FEUERSTEIN, G. Z. (1993). Interleukin-1 beta mRNA expression in ischemic rat cortex. *Stroke* **24**, 1746-1751.

LODDICK, S. A. (1996). "The role of interleukin-1 in cerebral ischaemia" [Ph.D. Dissertation]. (University of Manchester).

LODDICK, S. A., MACKENZIE, A., and ROTHWELL, N. J. (1996). An ICE inhibitor, z-VAD-DCB attenuates ischaemic brain damage in the rat. *NeuroReport* **7**, 1465-1468.

LODDICK, S. A., and ROTHWELL, N. J. (1996). Neuroprotective effects of human recombinant interleukin-1 receptor antagonist in focal cerebral ischaemia in the rat. *J. Cereb. Blood Flow Metab.* **16**, 932-940.

LODDICK, S. A., TURNBULL, A. V., and ROTHWELL, N. J. (1998). Cerebral interleukin-6 is neuroprotective during permanent focal cerebral ischemia in the rat. *J. Cereb. Blood Flow Metab.* **18**, 176-179.

LODDICK, S. A., WONG, M. L., BONGIORNO, B., GOLD, W., LICINIO, J., and ROTHWELL, N. J. (1997). Endogenous Interleukin-1 receptor antagonist is

neuroprotective. *Biochem. Biophys. Res. Commun.* **234**, 211-215.

LOJDA, Z., GOSSRAU, R., and SCHIEBLER, T. H. (1979). . In "Enzyme histochemistry: A laboratory manual" (Z. Lojda, R. Gossrau, and T. H. Schiebler, Eds.), pp. 274-290. Springer-Verlag, New York.

LOPEZ, O. T., and LANTHORN, T. H. (1993). Anti-neutrophil antiserum reduces infarct volume after mouse permanent middle cerebral artery occlusion without producing neutropenia. *Neurosci. Res. Comm.* **13**, 45-53.

LOTAN, M., and SCHWARTZ, M. (1994). Cross talk between the immune system and the nervous system in response to injury: implications for regeneration. *FASEB J.* **8**, 1026-1033.

MALE, D., PRYCE, G., HUGHES, C., and LANTOS, P. (1990). Lymphocyte migration into brain modelled in vitro: control by lymphocyte activation, cytokines and antigen. *Cell. Immunol.* **127**, 1-11.

MARIN, J. (1995). Age-related changes in vascular responses: a review. *Mech. Ageing Dev.* **79**, 71-114.

MARLETTA, M. A. (1994). Nitric oxide synthase aspects concerning structure and catalysis. *Cell* **78 (6)**, 927-930.

MARQUETTE, C., VAN DAM, M. A., BAN, E., LANIECE, P., CRUMEYROLLE-ARIAS, M., FILLION, G., BERKENBOSCH, F., and HAOUR, F. (1995). Rat interleukin-1β binding sites in rat hypothalamus and pituitary gland. *Neuroendocrinol.* **62**, 362-369.

MARTIN, M. U., and FALK, W. (1997). The Interleukin-1 Receptor Complex and Interleukin-1 Signal Transduction. *Eur. Cytokine Netw.* **8 (1)**, 5-17.

MARTIN, R. L., LLOYD, H. G. E., and COWAN, A. I. (1994). The early events of oxygen and glucose deprivation: Setting the scene for neuronal death? *TINS* **17**, 251-257.

MARTIN, D., MILLER, G., NEUBERGER, T., RELTON, J., and FISHER, N. (1997). Role of IL-1 in neurodegeneration: Preclinical findings with IL-1ra and ICE inhibitors. In "Neuroinflammation: Mechanisms and management" (P. L. Wood, Ed.), pp 197-219, Humana Press Inc., Totowa.

MARTIN, L. J., PARDO, C. A., CORK, L. C., and PRICE, D. L. (1994). Synaptic pathology and glial responses to neuronal injury precede the formation of senile plaques and amyloid deposits in the aging cerebral cortex. *Am. J. Pathol.* **145**, 1358-1381.

MARTIN, L. J., SISODIA, S. S., KOO, E. H., CORK, L. C., DELLOVADE, T. L., WEIDEMANN, A., BEYREUTHER, K., MASTERS, C., and PRICE, D. L. (1991). Amyloid precursor protein in aged non-human primates. *Proc. Natl Acad. Sci. U.S.A.* **88**, 1461-1465.

MATSUMOTO, T., IKEDA, K., MUKAIDA, N., HARADA, A., MATSUMOTO, Y.,

YAMASHITA, J., and MATSUSHIMA, K. (1997). Prevention of cerebral edema and infarct in cerebral reperfusion injury by antibody to interleukin-8. *Laboratory Investigation* **77**, 119-125.

MCCULLOCH, J. (1994). Glutamate receptor antagonists in cerebral ischaemia. *J. Neural Transm.* **43(Suppl)**, 71-79.

MCLEAN, I. W., and NAKANE, P. K. (1974). Periodate-lysine-paraformaldehyde fixative. A new fixative for immuno-electron microscopy. *Journal of Histochemistry and Cytochemistry* **22**, 1077-1083.

MCMANUS, C. M., BRONSON, C. F., and BERMAN, W. (1998). Cytokine induction of MIP-1 alpha and MIP-1 Beta in human fetal microglia. *Immunology* **160**, 1449.

MEAGER, A. (1999). Cytokine regulation of cellular adhesion molecule expression in inflammation. *Cytokine and Growth Factor Reviews* **10**, 27-39.

MECOCCI, P., MACGARVEY, U., KAUFMAN, A. E., KOONTZ, D., SHOFFNER, J. M., WALLACE, D. C., and BEAL, M. F. (1993). Oxidative damage to mitochondrial DNA shows marked age-dependent increase in human brain. *Ann. Neurol.* **34**, 609-616.

MEERSCHAERT, J., and FURIE, M. B. (1995). The adhesion molecules used by the monocytes for migration across the endothelium include CD11a/CD18, CD11b/CD18 and VLA-4 on monocytes and ICAM-1, VLAM-1, and other ligands on endothelium. *J.Immunol.* **154**, 4099-4112.

MERRILL, J. E. (1991). Effects of interleukin-1 and tumor necrosis factor-α on astrocytes, microglia, oligodendrocytes, and glial precursors in vitro. *Dev. Neurosci.* **13**, 130-137.

MICHAELIS, M. L., JOHE, K., and KITOS, T. E. (1984). Age-dependent alterations in synaptic membrane systems for calcium regulation. *Mech. Ageing Dev.* **25**, 215-225.

MIKAWA, S., LI, Y., HUANG, T. T., CARLSON, E., CHEN, S., KONDO, T., MURAKAMI, K., EPSTEIN, C. J., and CHAN, P. H. (1995). Cerebral infarction is exacerbated in mitochondrial manganese superoxide dismutase (Sod-2) knockout mice after focal cerebral ischemia and reperfusion. *Society of Neuroscience Abstracts* **21**, 1268.

MILLER, R. A. (1991). Aging and immune function. *Int. Rev. Cytol* **124**, 187-215.

MILLER, R.A. (1996). Aging and the immune response. In "Handbook of the Biology of Aging" (E.L, Schneider, J.W, Rowe, Eds.), Fourth edition, pp.355-392. Academic Press, London.

MILLER, R. A., and NADON, N. L. (2000). Principals of animals use for gerontological research. *J. of Gerontol: Biol. Sci.* **55**, B117-B123.

MILLIKAN, C. (1992). Editorial : Animal stroke models. *Stroke* **23**, 795-797.

MIQUEL, J., JOHNSON, J. E. J., and CERVOS-NAVARRO, J. (1983). Comparison of

central nervous system aging in human and experimental animals. In "Brain Aging, Neuropathology and Neuropharmacology" (J. Cervos-Navarro, and H. I. Sarkander, Eds.), Vol. 21, pp. 231-258. Raven Press, New York.

MOHR, J. P., GAUTIER, J. C., HIER, D., and STEIN, R. W. (1986). . In "Pathophysiology, Diagnosis and Management" (H. J. M. Barnett, B. M. Stein, J. P. Mohr, and fm Yatsu, Eds.), pp. 377-450. Churchill Livingstone, New York.

MONTAGUE, P. R., GANCAYLO, C. D., WINN, M. J., MARCHASE, R. B., and FRIEDLANDER, M. J. (1994). Role of nitric oxide in NMDA receptor mediated neurotransmitter release in cerebral cortex. *Science* **263**, 973-977.

MOORADIAN, A. D. (1988). Effect of aging on the blood brain barrier. *Neurobiol. Aging* **9**, 31-39.

MOORADIAN, A. D. (1994). Potential mechanisms of the age-related changes in the blood-brain barrier. *Neurobiol. Aging* **15**, 751-755.

MOORADIAN, A. D., and MCCUSKEY, R. S. (1992). In vivo microscopic studies of age-related changes in the structure and the reactivity of cerebral microvessels. *Mech. Ageing Dev.* **64**, 247-254.

MOORADIAN, A. D., and SMITH, T. L. (1992). The effect of age on lipid composition and order of rat cerebral microvessels. *Neurochem.Res.* **17**, 233-237.

MORI, E., DEL ZOPPO, G. J., CHAMBERS, J. D., COPELAND, B. R., and ARFORS, K. E. (1992). Inhibition of polymorphonuclear leukocyte adherence suppresses no-reflow after focal cerebral ischemia in baboons. *Stroke* **23**, 712-718.

MORIKAWA, E., ZHANG, S. M., SEKO, Y., TOYODA, T., and KIRINO, T. (1996). Treatment of focal cerebral ischemia with synthetic oligopeptide corresponding to lectin domain of selectin. *Stroke* **27(5)**, 951-955.

MORIOKA, T., KALEHUA, A. N., and STREIT, W. J. (1993). Characterization of microglial reaction after middle cerebral artery occlusion in rat brain. *Journal of Comparative Neurology* **327**, 123-132.

MORLEY, P., HOGAN, M. J., and HAKIM, A. M. (1994). Calcium-mediated mechanisms of ischemic injury and protection. *Brain Pathology* **4**, 37-47.

MULLEY, G. P. (1992). Stroke. In "Textbook of geriatric medicine and gerontology" (J. C. Brocklehurst, R. C. Tallis, and H. M. Fillit, Eds.), 4th Ed., pp. 365-388. Churchill Livingstone, London.

MURRAY, C. A., MCGAHON, B., MCBENNETT, S., and LYNCH, M. A. (1997). Interleukin-1beta inhibits glutamate release in hippocampus of young but not aged rats. Neurobiol. *Aging* **18(3)**, 343-348.

NAGATA, K., TAKIE, N., NAKAJIMA, K., SAITO, K., and KOHSAKA, S. (1993). Microglial conditioned medium promoted survival and development of cultured mesencephalic dopaminergic neurons from embryonic rat brain. *J. Neurosci. Res.* **34**, 357-363.

NEDERGAARD, M., and HANSEN, A. J. (1988). Spreading depression is not associated with neuronal injury in the normal brain. *Brain Res.* **449**, 395-398.

NEWMAN, P. J. (1997). The biology of PECAM-1. *J. Clin. Invest.* **100 (11 Suppl)**, S25-29.

NICHOLS, N. R. (1999). Glial responses to steroids as markers of brain aging. *Neurobiol. Aging* **40**, 585-601.

NICHOLSON, D. W., and THORNBERRY, N. A. (1997). Caspases: killer proteases. *Trends Biochem. Sci.* **22**, 299-306.

NIIRO, M., SIMON, R. P., KADOTA, K., and ASAKURA, T. (1996). Proximal branching patterns of MCA in rats and their influence on the infarct size produced by MCA occlusion. *J. Neurosci.* **64**, 19-23.

NOLTE, C., MULLER, T., WALTER, T., and KETTENMANN, H. (1996). Complement 5a controls motility of murine microglial cells in vivo via activation of an inhibitory G-protein and the arrangements of actin cytoskeleton. *Neuroscience* **73**, 1091-1107.

NORENBERG, M. D. (1994). Astrocyte responses to CNS injury. *J.Neuropath.Exp.Neurol.* **53**, 213-220.

NORENBERG, M. D. (1997). Astrocytes: Normal aspects and response to CNS injury. In "Immunologically active cells". (M. D. Wood, Ed.), 173-199. Academic Press, New York.

OBRENOVITCH, T. P. (1995). The ischemic penumbra: Twenty years on. *Cerebrovasc. Brain Metab.* **Rev. 7**, 297-323.

OBRENOVITCH, T. P., and RICHARDS, D. A. (1995). Extracellular neurotransmitter changes in cerebral ischaemia. Cerebrovasc. *Brain Metab.* **Rev. 7**, 1-54.

OGURA, K., OGAWA, M., and YOSHIDA, M. (1994). Effects of ageing on microglia in the normal rat brain: Immunohistochemical observations. *NeuroReport* **5**, 1224-1226.

OLNEY, J. W., HO, O. L., and RHEE, V. (1971). Cytotoxic effects of acidic and sulphur containing amino acids on the infant mouse central nervous system. *Exp.Brain Res.* **14**, 61-76.

O'NEILL, L. A. J. (1995). Towards an understanding of the signal transduction pathways for interleukin-1. *Biochemica et Biophysica Acta* **1266**, 31-44.

O'NEILL, L. A., and KALTSCHMIDT, C. (1997). NF- kappa B: a crucial transcription

factor for glial and neuronal cell function. *Trends Neurosci.* **20**, 252-258.

PEARSON, V. L., ROTHWELL, N. J., and TOULMOND,S. (1999). Excitotoxic brain damage in the rat induces interleukin-1 beta protein in microglia and astrocytes. *Glia* **25**, 311-323.

PEINADO, M. A., MARTINEZ, M., PEDROSA, J. A., QUESADA, A., and PEINADO, J. M. (1993). Quantitative morphological changes in neurones and glia in the frontal lobe of the aging rat. *The Anatomical Record* **237**, 104-108.

PEINADO, M. A., QUESADA, A., PEDROSA, J. A., MARTINEZ, M., ESTEBAN, F. J., MORAL, M. L., and PEINADO, J. M. (1997). Light microscopic quantification of morphological changes during aging in neurons and glia of the rat parietal cortex. *The Anatomical Record.* **247**, 420-425.

PERRY, V. H., MATYSAK, M. K., and FEARN, S. A. (1993). Altered antigen expression of microglia in the aged rodent CNS. *Glia* **7**, 60-67.

PETERS, A., JOSEPHSON, K., and VINCENT, S. L. (1991). Effects of ageing on the neuroglial cells and pericytes within area 17 of the rhesus monkey cerebral cortex. *The Anatomical Record* **229**, 384-398.

PETERS, A., NIGRO, N. J., and MCNALLY, K. J. A. (1997). A further evaluation of the effect of age on striate cortex of the rhesus monkey. *Neurobiol. Aging* **18**, 29-36.

PETITO, C. K. (1979). Early and late mechanisms of increased vascular permeability following experimental cerebral infarction. *J. Neuropathol. Exp. Neurol.* **38**. 222-244.

PETITO, C. K., and HALABY, I. A. (1993). Relationship between ischemia and ischemic neuronal necrosis to astrocyte expression of glial fibrillary acidic protein. *Int.J.Devl.Neurosci.* **11**, 239-247.

PIKE, C. J., WALENCEWICZ, A. J., GLABE, C. G., and COTMAN, C. W. (1991). In vitro aging of β-amyloid protein causes peptide aggregation neurotoxicity. *Brain Res.* **563**, 311-314.

PILEGAARD, K., and LADEFOGED, O. (1996). Total number of astrocytes in the molecular layer of the dendate gyrus of rats at different ages. *Anal. Quant. Cytol. Histol.* **18**, 279-285.

PLANAS, A. M., SORIANO, M. A., BERRUEZO, M., JUSTICIA, C., ESTRADA, A., PITARCH, S. and FERRER, I. (1996). Induction of STAT 3, a signal transducer and transcription factor, in reactive microglia following transient focal cerebral ischemia. *Eur.J.Neurosci.* **8**, 2612-2618.

PLUTA, R. LOSSINSKY, A.S., WISNIEWSKI, H. M., MOSSAKOWSKI, M. J. (1994). Early blood-brain barrier changes in the rat following transient complete cerebral ischemia by cardiac arrest. *Brain Research.* **633**. 41-52.

QUAGLIARELLO, V. J., WISPELWEY, B., LONG, W. J., and SCHELD, W. M. (1991). Recombinant human interleukin-1 induces meningitis and blood-brain barrier injury in the rat. *J. Clin. Invest.* **87**, 1360-1366.

RANSHOFF, R. M., and TANI, M. (1998). Reviews: Do chemokines mediate leukocyte recruitment in post-traumatic CNS inflammation? *Trends Neurosci.* **21**, 154-159.

READ, S. J., HIRANO, T., ABOTT, D. F., SACHINIDIS, J. I., TOCHAN-DANGUY, H. J., CHAN, J. G., EGAN, G. F., SCOTT, A., BLADIN, C. F., MCKAY, W. J., and DONNAN, G. A. (1998). Identifying hypoxic tissue after acute ischemic stroke using PET and 18F-fluoromisonidazole. *Neurology* **51**, 1617-1621.

REHBINDER, C., BANEUX, P., FORBES, D., VAN HERCK, H., NICKLAS, W., RUGAYA, Z., and WINKLER, TG. (1996). FELASA recommendations for the health monitoring of the mouse, rat, hamster, gerbil, guineapig, and rabbit experimental units. Report of the Federation of European Laboratory Animals Science Associations (FELASA) Working Group on Animal Health accepted by the FELASA Board of Management. *Lab. Anim.* **30**, 192-208.

RELTON, J. K., MARTIN, D., THOMPSON, R. C., and RUSSEL, D. A. (1996). Peripheral administration of interleukin-1 receptor antagonist inhibits brain damage after focal cerebral ischemia in the rat. *Exp. Neurol.* **138**, 206-213.

RELTON, J. K., and ROTHWELL, N. J. (1992). Interleukin-1 receptor antagonists inhibits ischemic and excitotoxic neuronal damage in the rat. *Brain Res. Bull.* **29**, 243-246.

RICAURTE, G. A., IRWIN, L. S., FORNO, L. S., DELANNEY, E., LANGSTON, E., and LANGSTON, J. W. (1987). Aging and 1-methyl-4-phenyl-1,2,3,6-tetrahydropyridine-induced degeneration of dopaminergic neurons in the substantia nigra. *Brain Res.* **403**, 43-51.

RIDET, J. L., MALHOTRA, S. K., PRIVAT, A., and GAGE, F. H. (1997). Reactive astrocytes: cellular and molecular clues to biological function. *Trends Neurosci.* **20**, 570-577.

RÖSSLER, K., NEUCHRIST, C., KITZ, K., SCHEINER, O., KRAFT, D., and LASSMANN, H. (1992). Expression of leukocyte adhesion molecules at the blood brain barrier (BBB). *J. Neurosci. Res.* **31(2)**, 365-374.

ROSENBLUM, W. I. (1995). Editorial Comment. *Stroke* **26**, 2090.

ROTHMAN, S. M., and OLNEY, J. W. (1986). Glutamate and the pathophysiology of hypoxic-ischemic brain damage. *Ann. Neurol.* **19**, 105-111.

ROTHWELL, N. J. (1996). The role of cytokines in neurodegeneration. In "Cytokines in the nervous system" (N. J. Rothwell, Ed.), pp. 145-162. Landes Company, London.

ROTHWELL, N. J. (1997). Sixteenth Gaddum memorial lecture December 1996: Neuroimmune interactions: The role of cytokines. *BR.J.Pharm.* **121**, 841-847.

ROTHWELL, N. J. (1998). Interleukin-1 and neurodegeneration. *Neuroscientist* **4(3)**, 195-201.

ROTHWELL, N. J., ALLAN, S., and TOULMOND, S. (1997a). The role of interleukin-1 in acute neurodegeneration and stroke: Pathophysiological and therapeutic implications. *J. Clin. Invest.* **100**, 2648-2652.

ROTHWELL, N. J. R., and HOPKINS, S. J. (1995). Interactions between cytokines and the nervous system. *TINS* **18**, 130-136.

ROTHWELL, N. J., LODDICK, S. A., and LAWRENCE, C. (1995). Cytokines and neurodegeneration. In "Immune responses in the nervous system" (N. J. Rothwell, Ed.), pp. 77-99. BIOS Scientific.

ROTHWELL, N. J., LODDICK, S. A., and STROEMER, P. (1997b). Interleukins and cerebral ischaemia. In "Neuroprotective agents and cerebral ischaemia", pp. 281-297. Academic Press Limited.

ROTHWELL, N. J., and LUHESHI, G. (1994). Pharmacology of interleukin-1 actions in the brain. In "Advances in pharmacology" (J. T. August, M. W. Anders, and F. Murad, Eds.), Vol. 25, pp. 1-20. Academic press, London.

ROTHWELL, N., and RELTON, J. (1993). Involvement of cytokines in acute neurodegeneration in the CNS. *Neurosci. Biobehav.* **Rev. 17**, 217-227.

ROTHWELL, N. J., and STRIJBOS, P. J. L. M. (1995). Cytokines in neurodegeneration and repair. *Int.J.Devl.Neurosci.* **13**, 179-185.

ROTHWELL, N. J., STROEMER, P., and DAVIES, C. (1996). Actions of IL-1 in neurodegeneration. In "Pharmacology of cerebral ischemia" (J. Krieglstein, Ed.), pp. 125-129.

ROUX-LOMBARD, P. (1998). The interleukin-1 family. *Eur. Cytokine Netw.* **9**, 565-576.

ROWLATT, C., CHESTERMAN, F. C., and SHERIFF, M. U. (1976). Lifespan, age changes and tumour incidence in an ageing C57BL mouse colony. *Lab. Animals*, **10**, 419-442

ROZOVSKY, I., FINCH, C. E., and MORGAN, T. E. (1998). Age related activation of microglia and astrocytes: in-vitro studies show persistent phenotypes of aging, increased proliferation and resistance to down regulation. *Neurobiol. Aging* **19**, 97-103.

RUDDICK, R. A., BUELL, S. J. (1983). Integrity of the BBB to peroxidase in senescent mice. *Neurobiol. Ageing.* **4**. 283-287.

SAIRANEN, T. R., LINDSBERG, P. J., BRENNER, M., and SIREN, A. L. (1997). Global

forebrain ischemia results in differential cellular expression of interleukin-1beta and its receptors at mRNA and protein level. *J. Cereb. Blood Flow Metab.* **17**, 1107-1120.

SAMDANI, A. F., DAWSON, T. M., and DAWSON, V. L. (1997). Nitric oxide synthase in models of focal ischemia. *Stroke* **28**, 1283-1288.

SAMPAOLO, S., NAKAGAWA, Y., IANOTTI, F., CERVOS-NAVARRO, J., BONAVITA, V., (1991). Blood brain barrier permeability to micromolecules and edema formation in the early phase of incomplete continuous ischemia. *Acta. Neuropathologica.*

SAUNDERS, D. E., HOWE, F. A., BOOGAART, A., MCLEAN, M. A., GRIFFITHS, J. R., and BROWN, M. M. (1995). Continuing ischemic brain damage after acute middle cerebral artery infarction in humans demonstrated by short-echo proton spectroscopy. *Stroke* **26**, 1007-1013.

SCHIELKE, G. P., YANG, G. Y., SHIVERS, B. D., and BETZ, A. L. (1998). Reduced ischemic brain injury in interleukin-1 beta converting enzyme-deficient mice. *J. Cereb. Blood Flow Metab.* **18**, 180-185.

SCHINDLER, R., MANCILLA, J., ENDRES, S., GHORBANI, R., CLARK, S. C., and DINARELLO, C. A. (1990). Correlations and interactions in the production of interleukin-6, IL-1, and tumor necrosis factor in human blood mononuclear cells:IL-6 suppresses IL-1 and TNF. *Blood* **75**, 40-47.

SCHMIDLEY, J. W. (1990). Free radicals in central nervous system ischemia. *Stroke* **21**, 1086-1090.

SCHOBITZ, B., HOLSBOER, F., and DE KLOET, E. R. (1994). Cytokines in the healthy and diseased brain. *NiPS* **9**, 138-142.

SCHROETER, M., JANDER, S., WITTE, O. W., and STOLL, G. (1994). Local immune responses in the rat cerebral cortex after middle cerebral artery occlusion. *J.Immunol.* **55**, 195-203.

SCRIPTER, J. L., KO, J., ARIMURA, A., and IDE, C. F. (1997). Regulation by interleukin-1β of formation of a line of delimiting astroctyes following prenatal trauma to the brain mouse. *Exp. Neurol.* **145**, 329-341.

SEGAL, R., DAYAN, M., GLOBERSON, A., HABUT, B., SHEARER, G. M., and MOZES, E. (1997). Effect of aging on cytokine production in normal and experimental systemic lupus erthythramatosus afflicted mice. *Mech. Ageing Dev.* **96**, 47-58.

SHEFFIELD, L. G., and BERMAN, N. E. J. (1998). Microglial expression of MHC class II increases in normal aging of nonhuman primates. *Neurobiol. Aging* **19(1)**, 47-55.

SHENG, J. G., MRAK, R. E., ROVNAGHI, C. R., KOSLOWSKA, E., VAN ELDIK, L. J., and GRIFFIN, W. S. T. (1996). Human brain S100B mRNA expression increases with age: Pathogenic implications for Alzheimers disease. *Neurobiol. Aging* **17**, 359-363.

SHIGA, Y., ONODERA, H., KOGURE, K., YAMASAKI, Y., YASHIMA, Y., SYOZUHARA, H., SENDO, F., (1991). Neutrophil as a mediator of ischemic edema formation in the brain. *Neuroscience letters*. **125**. 110-112.

SIDMAN, R.L., ANGEVINE, Jr. J. B., and TABER PIERCE, E. (1971). Atlas of the mouse brain and spinal cord. Harvard University Press, Massachusetts.

SIESJO, M. D. (1992). Pathophysiology and treatment of focal cerebral ischemia part 2/: Mechanisms of damage and treatment. *J. Neurosurg*. **77**, 337-354.

SILVER, B., WEBER, J., and FISCHER, M. (1996). Medical therapy for ischemic stroke. *Clin. Neuropharmacol.* **19**, 101-128.

SIMS, J., GAYLE, M. A., SLACK, J. L., ALDERSON, M. R., BIRD, T. A., GIRI, J. G., COLOTTA, F., RE, F., MANTOVANI, A., SHANEBECK, K., GRABSTEIN, K. H., and DOWER, S. K. (1993). Interleukin-1 signaling occurs exclusively via the type I receptor. *Proc. Natl Acad. Sci. U.S.A.* **90**, 6155-6159.

SIREN, A. L., LIU, Y., FEUERSTEIN, G., and HALLENBECK, J. M. (1993). Increased release of TNF-α into the cerebrospinal fluid and peripheral circulation of aged rats. **Stroke** *24*, 880-886.

SOBIN, S.S., BERNICK, S., and BALLARD, K.W. (1992). Histochemical characterization of the aging microvasculature in the human and other mammalian and non-mammalian vertebrates by periodic acid-Schiff reaction. *Mech. Age. and Dev.* **63**, 183-192.

SORIANO, S. G., LIPTON, S. A., WANG, Y. F., XIAO, M., SPRINGER, T. A., GUTIERREZ-RAMOS, J. C., and HICKEY, P. R. (1996). Intercellular adhesion molecule-1-deficient mice are less susceptible to cerebral ischemia-reperfusion injury. *Ann. Neurol.* **39(5)**, 618-624.

STERIO, D. C. (1984). The unbaised estimation of number and sizes of arbitrary particles using the disector. *J.Microsc.* **134**, 127-136.

STEWARD, O., TORRE, E. R., TORNASULO, R., and LOTHMAN, E. (1991). Neural activity up-regulates astroglial gene expression. *Proc. Natl Acad. Sci. U.S.A.* **88(15)**, 6819-6823.

STOLL, G., JANDER, S., and SCHROETER, M. (1998). Inflammation and glial responses in ischemic brain lesions. *Progress in neurobiology* **56**, 149-171.

STREIT, W. J. (1990). An improved staining method for rat microglial cells using the lectin from Griffonia simlicifolia (GSA I-B4). *Journal of Histochemistry and Cytochemistry* **38**, 1683-1686.

STREIT, W. J., SEMPLE-ROWLAND, S.L., HURLELY, S. D., MILLER, R. C., POPOVICH, P. G., and STOKES, B. T. (1998). Cytokine mRNA profiles in contused spinal cord and axotomized facial nucleus suggest a beneficial role in inflammation and

gliosis. *Exp. Neurol.* **152**, 74-87.

STRIJBOS, P. J. L. M. (1998). Nitric oxide in cerebral ischemic neurodegeneration and excitotoxicity. *Crit. Rev. Neurobiol.* **12(3)**, 223-243.

STROEMER, R. P., and ROTHWELL, N. J. (1988). Exacerbation of ischemic brain damage by localised striatal injection of interleukin-1 beta in the rat. *J. Cereb. Blood Flow Metab.* **18,** 833-839.

SUTHERLAND, G. R., DIX, G. A., and AUER, R. N. (1996). Effect of age in rodent models of focal and forebrain ischemia. *Stroke* **27**, 1663-1668.

SWANSON, R., MORTON, M., TSAO-WU, G., SAVALOS, R., DAVIDSON, C., and SHARP, F. (1990). Short communication: A semi-automated method for measuring brain infarct volume. *J. Cereb. Blood Flow Metab.* **10**, 290-293.

SYMON, L., BRANSTON, N. M., STRONG, A. J., et al. (1977). The concepts of thresholds of ischemia in relation to brain structure and function. *J. Clin. Pathol.* **30(Suppl. 11),** 149-154.

TAMURA, A., GRAHAM, D. I., MCCULLOCH, J., and TEASDALE, G. M. (1981). Focal cerebral ischemia in the rat:. *J. Cereb. Blood Flow Metab.* **1**, 53-60.

TARKOWSKI, E., ROSENGREN, L., BLOMSTRAND, C., WIKKELS™, C., JENSEN, C., EKHOLM, S., and TARKOWSKI, A. (1995). Early intrathecal production of interleukin-6 predicts the size of brain lesion in stroke. *Stroke* **26**, 1393-1398.

TERRY, R. D., DETERESA, R., and HANSEN, L. A. (1987). Neocortical cell counts in normal human adult aging. *Ann. Neurol.* **21**, 530-539.

THOMAS, W. E. (1992). Brain macrophages: evaluation of microglia and their functions. *Brain Res. Rev.* **17**, 61-74.

THORNBERRY, N. A., BULL, H. G., CALAYCAY, J. R., CHAPMAN, K. T., HOWARD, A. D., KOSTURA, M. J., MILLER, D. K., MOLINEAUX, S., WEIDNER, J. R., AUNINS, J., SCHMIDT, J. A., and TOCCI, M. (1992). A novel heterodimeric cysteine protease is required for interleukin-1á processing in monocytes. *Nature* **356**, 768

TOPP, K. S., FADDIS, B. T., and VIJAYAN, V. K. (1989). Trauma-induced proliferation of astrocytes in the brains of young and aged rats. *Glia* **2**, 201-211.

TOUZANI, O., BOUTIN, H., CHUQUET, J., and ROTHWELL, N. (1999). Potential mechanisms of interleukin-1 involvement in cerebral ischaemia. *J. Neuroimmunol.* **100**, 203-215.

UENO, M., AKIGUCHI, I., YAGI, H., NAIKI, H., FUJIBAYASHI, Y., KIMURA, J., and TAKEDA, T. (1993). Age-related changes in barrier function in mouse brain. I. Accelerated age-related increase of brain transfer of serum albumin in accelerated

senescence prone SAM-P/8 mice with deficits in learning and memory. *Arch. Gerontol. Geriatr.* **16**, 233-248.

VENUGOPAL, J., and RAO, K. S. (1991).Oxidative damage in the aging rat brain. J. Neurochem. 56, 812-817.

VERKHRATSKY, A., and TOESCU, E. C. (1998). Calcium and neuronal ageing. *Trends Neurosci.* **21**, 2-7.

VERNADAKIS, A. (1996). Glia-neuron intercommunications and synaptic plasticity. *Prog. Neurobiol.* **49**, 185-214.

VINCENT, S. L., PETERS, A., and TIGGES, J. (1989). Effects of ageing on the neurones within area 17 of rhesus monkey cerebral cortex. *The Anatomical Record* **223**, 329-341.

VORBRODT, A. W., and DOBROGOWKA, D. H. (1994). Immunocytochemical evaluation of blood-brain barrier to endogenous albumin in adult, newborn and aged mice. *Folia Histochemica et Cytobiologica* **32**, 63-70.

WADHWANI, K. C., KOISTINAHO, J., BALTO, A., and RAPOPORT, S. I. (1991). Blood nerve and blood-brain barrier permeabilities and nerve vascular space in Fischer-344 rats of different ages. *Mech. Ageing Dev.* **58**, 177-190.

WAKIKAWA, A., UTSUYAMA, M., WAKABAYASHI, A., KITAGAWA, M., and HIROKAWA, K. (1999). Age related alteration of cytokine production profile by T cell subsets in mice: a flow cytometric study. *Exp. Gerontol.* **34(2)**, 231-242.

WALZ, W. (1997). Role of astrocytes in the spreading depression signal between ischemic core and penumbra. *Neurosci. Biobehav. Rev.* **21**, 135-142.

WANG, X., and FEUERSTEIN, G. Z. (1995). Induced expression of adhesion molecules following focal brain ischemia. *J. Neurotrauma* **12**, 825-832.

WANG, X., SIREN, A., LIU, Y., YUE, T., BARON, F. C., and FEUERSTEIN, G. Z. (1994a). Upregulation of intercellular adhesion molecule 1 (ICAM-1) on brain microvascular endothelial cells in rat ischaemic cortex. *Mol. Brain Res.* **26**, 61-68.

WANG, X., YUE, Y. L., BARONE, F. C., WHITE, R. F., GAGNON, R. C., and FEURESTEIN, G. Z. (1994b). Concomitant cortical expression of TNF-α and IL-1β mRNAs follows early response gene expression in transient focal ischaemia. *Mol. Chem. Neuropathol.* **23**, 103-114.

WANG, X., BARONE, F. C., AIYAR, N. V., and FEUERSTEIN, G. Z. (1997). Interleukin-1 receptor and receptor antagonist gene expression after focal stroke in rats. *Stroke* **28**, 155-162.

WEBB, S. J., HARRISON, D. J., and WYLLIE, A. H. (1997). Apoptosis: An overview of the process and its relevance in disease. In "Apoptosis: Pharmacological implications and

therapeutic opportunities" (S. H. Kaufmann, Ed.), Vol. 41, pp. 1-34. Academic Press, London.

WEIGLE, W. (1993). The effects of aging on cytokine release and associated immunologic functions. *Immunological Problems in the Aged* **13**, 551-569.

WELSH, F. A., SAKAMOTO, T., MCKEE, A. E., and SIMS, R. E. (1987). Effect of lactacidosis on pyridine nucleotide stability during ischemia in mouse brain. *J. Neurochem.* **49**, 846-851.

WENK, G. L., WALKER, L. C., PRICE, D. L., and CORK, L. C. (1991). Loss of NMDA but not GABA-A binding in the brains of aged rats and monkeys. *Neurobiol. Aging* **12**, 93-98.

WESTERGAARD, E., GO,. G., KLATZO, I., SPATZ, M. (1976). Increased permeability of cerebral vessels to horseradish peroxidase induced by ischemia in mongolian gerbils. *Acta. Neuropath.* **35**. 307-325.

WICKELGREN, I. (1996). The aging brain: For the cortex, neuron loss may be less than thought. *Science* **273**, 48-50.

WILCOX, C. E., WARD, A. M. V., EVANS, A., BAKER, D., ROTHLEIN, R., and TURK, J. L. (1990). Endothelial expression of the intercellular adhesion molecule-1 in the CNS of guinea pigs during acute and chronic relapsing experimental allergic encephalomyelitis. *J. Neuroimmunol.* **30**, 43-51.

WINK, D. A., HANBAUER, I., KRISHNA, M. C., DEGRAFF, W., GAMSON, J., and MITCHELL, J. B. (1993). Nitric oxide protects against cellular damage and cytotoxicity from reactive oxygen species. *Proc. Natl Acad. Sci. U.S.A.* **90**, 9813-9817.

WOLF, P. A., D'AGOSTINO, R. B., O'NEAL, M. A., SYTKOWSKI, P., KASE, C. S., BELANGER, A. J., and KANNEL, W. B. (1992). Secular trends in stroke incidence and mortality. *Stroke* **23**, 1551-1555.

WONG, G. H. (1995). Protective roles of cytokines against radiation: Induction of mitochondrial MnSOD. *Biochem. Biophys. Acta.* **1271**, 205-209.

WOOD, P. L. (1998). Role of CNS macrophages in neurodegeneration. In "Neuroinflammation: mechanisms and management" (P. L. Wood, Ed.), pp. 1-59. Humana Press, Totowa, New Jersey.

WOZNIAK, D. F., STEWART, G. R., MILLER, J. P., and OLNEY, J. W. (1991). Age-related sensitivity to kainate neurotoxicity. *Exp. Neurol.* **114**, 250-253.

XING, Z., GAULDIE, J., and COX, G. (1998). IL-6 is an anti-inflammatory cytokine required for controlling local or systemic acute inflammatory responses. *J. Clin. Invest.* **101**, 311-320.

YAMADA, M., and HATANAKA, H. (1994). IL-6 protects rat hippocampal neurons against glutamate induced cell death. *Brain Res.* **643**, 227-236.

YAMASAKI, Y., YAMAYA, H., MATSUURA, N., ONODERA, H., and KOGURE, K. (1993). Interleukin-1 as a pathogenic mediator on ischemic brain edema formation. *J. Cereb. Blood Flow Metab.* **13 Suppl.1**, s25.

YAMASAKI, Y., MATSUURA, N., SHOZUHARA, H., ONODERA, H., ITOYAMA, Y., and KOGURE, K. (1995). Interleukin-1 as a pathogenic mediator of ischemic brain damage in rats. *Stroke* **26**, 676-681.

YAMASHITA, K., VOGEL, P., FRITZE, K., BACK, T., HOSSMANN, K. A., and WIESSNER, C. (1996). Monitoring the temporal and spatial activation pattern of astrocytes in focal cerebral ischemia using in situ hybridization to GFAP mRNA: comparison with sgp-2 and hsp 70 mRNA and the effect of glutamate receptor antagonists. *Brain Res.* **735**, 285-297.

YANG, G. Y., and BETZ, A. L. (1994). Reperfusion induced injury to the blood-brain barrier after MCAO in rats. *Stroke* **25**, 1658-1664.

YANG, G. Y., GONG, C., QIN, Z., YE, W., MAO, Y., and BERTZ, L. A. (1998). Inhibition of TNF-α attenuates infarct volume and ICAM-1 expression in ischemic mouse Brain. *NeuroReport* **9**, 2131-2134.

YANG, G., KITAGAWA, K., MATSUSHITA, K., MABUCHI, T., YAGITA, Y., YANAGIHARA, T., and MATSUMOTO, M. (1997). C57BL/6 strain is most susceptible to cerebral ischemia following bilateral common carotid occlusion among seven mouse strains: selective neuronal death in the murine transient forebrain ischemia. *Brain Res.* **752**, 209-218.

YANG, G. Y., MAO, Y., ZHOU, L. F., GUNG, C., GE, H. L., and BETZ, A. (1998). Expression of intercellular adhesion molecule-1 (ICAM-1) is reduced in permanent cerebral focal ischemic mouse brain using an adenoviral vector to induce over expression of interleukin-1 receptor antagonist. *Mol. Brain Res.* **65(2)**, 143-150.

YANG, G. Y., SCHIELKE, G. P., GONG, C., MAO, Y., GE, H. L., LIU, X. H., and BETZ, A. L. (1999). Expression of TNF-α and ICAM-1 after focal ischemia in IL-1β converting enzyme deficient mice. *J. Cereb. Blood Flow Metab.* **19**, 1109-1117.

YANKNER, B. A., DAWES, L. R., FISHER, S., VILLA-KOMAROFF, L., OSTER-GRANITE, M. L., and NEVE, R. L. (1989). Neurotoxicity of a fragment of the amyloid precursor associated with Alzheimer's disease. *Science* **245**, 417-420.

YAO, H., OOBOSHI, H., IBAYASHI, S., UCHIMURA, H., and FUJISHIMA, M. (1993). Cerebral blood flow and ischemia induced neurotransmitter release in the striatum of aged spontaneously hypertensive rats. *Stroke* **24**, 577-580.

YU, A. C. H., CHAN, P. H., and FISHMAN, R. A. (1986). Effects of arachidonic acid on

glutamate and ç-aminobutyric acid uptake in primary cultures of rat cerebral cortical astrocytes and neurones. *J. Neurochem.* **47**, 1181-1189.

YU, B. P. (1993). Oxidative damage by free radicals and lipid peroxidation in aging. In "Free radicals in aging" (B. P. Yu, Ed.), pp. 57-88. CRC Press, Boca Raton, FL.

ZHANG, R. L., CHOPP, M., YI, L., ZALOGA, C., and WARD, P. A. (1994). Anti-ICAM-1 antibody reduces ischemic cell damage after transient MCAO in the rat. *Neurology* **44**, 1747-1751.

ZHANG, R. L., CHOPP, M., JIANG, N., TANG, W. X., PROSTAK, J., MANNING, A. M., and ANDERSON, D. C. (1995). Anti-intercellular adhesion molecule-1 antibody reduces ischemic cell damage after transient but not permanent middle cerebral artery occlusion in the Wistar rat. *Stroke* **26**, 1438-1443.

ZHANG, R-L., CHOPP, M., ZALOGA, C., ZHANG, Z. G., JIANG, N., GAUTAM, S. C., TANG, W. X., TSANG, W., ANDERSON, D.C., and MANNING, A. M. (1995). The temporal profiles of ICAM-1 protein and mRNA expression after transient MCA occlusion in the rat. *Brain Res.* **682**, 182-188.

ZHANG, Z., CHOPP, M., GOUSSEV, A., and POWERS, C. (1998a). Cerebral vessels express interleukin-1β after focal cerebral ischemia. *Brain Res.* **784**, 210-217.

ZHANG, R., CHOPP, M., ZHANG, Z., JIANG, N., and POWERS, C. (1998b). The expression of P- and E-selectins in three models of middle cerebral artery occlusion. *Brain Res.* **785**, 207-214.

ZHANG, R. L., ZHANG, Z. G., and CHOPP, M. (1999). Increased therapeutic efficacy with rt-PA and anti-CD18 antibody treatment of stroke in the rat. *Neurology* **52**, 273-279.

ZHAO, Q., PAHLMARK, K., SMITH, M.L., and SIESJO, B.K. (1994). Delayed treatment with the spin trap alpha-phenyl-N-tert-butyl nitrone (PBN) reduces infarct size following transient middle cerebral artery occlusion in rats. *Acta Physiol. Scand* **152**, 349-350.

ZIELASEK, J., and HARTUNG, H. P. (1996). Molecular mechanisms of microglia activation. *Advances in Neuroimmunology* **6**, 191-222.

APPENDICES

Appendix 1: Tissue fixative solutions

1) 4% phosphate buffered formaldehyde

a) 10% Formaldehyde (Stock solution)

50g of paraformaldehyde (BDH Chemicals, UK) was weighed in a fume cupboard and dissolved in approximately 300 ml of distilled water on a magnetic stirrer/hot plate and heated to 60°C. When this temperature was reached 1-2ml of 1 M NaOH was added until the solution cleared. The solution was allowed to cool in the fume cupboard and made up to 500ml with distilled water, bottled and labelled biohazard. The solution can be stored at room temperature.

b) Sodium phosphate solutions (0.2M)

The following 0.2M stock solutions were made by weighing:

31.201g of $NaH_2PO_4.2H_2O$ (BDH Chemicals, UK)

35.598g of $Na_2HPO_4.2H_2O$ (BDH Chemicals, UK)

These were weighed into separate beakers and made up to 1L using distilled water.

c) For 4% Phosphate buffered formaldehyde solution

To make 500ml of 4% phosphate buffered formaldehyde the following solutions were mixed in a fume cupboard:

47.5ml of 0.2M $NaH_2PO_4.2H_2O$

202.5ml of 0.2M $Na_2HPO_4.2H_2O$

200ml of 10% Formaldehyde solution

The pH of this solution is adjusted to pH7.4 using drops of concentrated sodium hydroxide (NaOH). The solution is made up to a final volume of 500ml with distilled water, bottled and labelled biohazard.

2) Karnovsky fixative (for fixing brains that are to be used in HRP staining)

To make 500ml of Karnovsky fixative the following solutions were mixed in a fume cupboard:

47.5ml of 0.2M $NaH_2PO_4.2H_2O$

202.5ml of 0.2M $Na_2HPO_4.2H_2O$

0.2g of $MgCl_2.6H_2O$ (BDH Chemicals, UK)

100ml of 10% Formaldehyde solution

50ml of 25% Glutaraldehyde solution (BDH Chemicals, UK)

The pH of this solution is adjusted to pH 7.4 using drops of concentrated NaOH. The solution is made up to a final volume of 500ml with distilled water, bottled and labelled biohazard. The solution is stored at 4°C for no longer than 6 months.

3) Periodate-lysine-paraformaldehyde (PLP) fixative (for fixing brains that are to be used for immunostaining)

a) D-L lysine and phosphate buffer

i) For the phosphate buffer (pH7.4) add 9.5ml of sodium dihydrogen orthophosphate (NaH_2PO_4, 0.1M, stock stored at room temperature) to 40.5ml of disodium hydrogen orthophosphate (Na_2HPO_4, 0.1M, stock stored at room temperature).

ii) Dissolve 1.37g of DL-lysine monohydrochloride (Sigma, UK) in 37.5ml of distilled water and pH to 7.4 with dihydrogen orthophosphate (0.1M). Make up to 75ml with 0.1M phosphate buffer. Make fresh on day.

b) 8% paraformaldehyde

80g of paraformaldehyde (BDH Chemicals, UK) was weighed in a fume cupboard and dissolved in approximately 800 ml of distilled water on a magnetic stirrer/hot plate and heated to 60°C. When this temperature was reached 1-2ml of 1 M NaOH was added until the solution cleared (depolymerised). The solution was allowed to cool in the fume cupboard and made up to 1L with distilled water, bottled and labelled biohazard.

c) For 100ml PLP fixative

25ml of 8% paraformaldehyde (20ml of 10% paraformaldehyde + 5ml of distilled water) was added to 75ml of D-L lysine and phosphate buffer.

0.214g of sodium m-periodate (Sigma, UK) was added just before use and the solution placed on ice.

Appendix 2: Staining solutions

Tetrazolium staining solution

To make 10ml of 0.4% tetrazolium blue chloride solution, 40mg of 3,3'-[3,3'-Dimethoxy (1,1'-biphenyl)-4,4'-diyl]-bis[2,5-diphenyl-2H-tetrazolium] dichloride (Sigma, UK) was dissolved in 0.5ml dimethyl sulfoxide (DMSO; Sigma, UK) and made up to a 10ml volume with distilled water. The powder was dissolved by sonication, for one hour, and 10 ml aliquots of stock solution stored at -20°C until required.

On the day of use the following solutions were mixed together to make 40 ml of 0.1% phosphate buffered tetrazolium (pH 7.4) solution:

10ml of 0.4% tetrazolium chloride solution

16ml of 0.2M $Na_2HPO_4.2H_2O$

4ml of 0.2M $NaH_2PO_4.2H_2O$

10ml of 8mM $MgCl_2$

Toluidine Blue staining

Resin sections were stained in 0.1% toluidine blue (BDH Chemicals, UK) for 30 seconds. The sections were rinsed in distilled water and left to air dry before being coverslipped in DPX.

Haematoxylin and Eosin

Frozen sections were stained in haematoxylin for 2 minutes, blued in running tap water for about 1 minutes and stained in eosin for 1 minutes. The sections were rinsed in water, dehydrated through the alcohols and coverslipped in DPX.

Cresyl violet staining

Frozen brain sections were defrosted for a minimum of 1 hour before being stained in 0.1% cresyl violet (Sigma, UK) for 45 seconds. The sections were rinsed in water and dehydrated through alcohols for 30 seconds in each (95% and 2 x absolute) and coverslipped in DPX.

Appendix 3 Subbed slides

Gelatin coated slides

A 1% gelatin solution (1L) was prepared by adding 10g gelatin (BDH Chemicals,UK) to 0.5g of chrome alum (Chromium (III) potassium sulphate, BDH chemicals, UK). The gelatin was dissolved on a magnetic stirrer/hot plate at 40°C, allowed to cool and filtered through Whatman no.1 filter paper. Microscope slides were placed in staining racks, washed in IMS (99%) for 2 minutes and dipped in the gelatin solution for 5 minutes, removed and dried in the oven at 37°C overnight.

APES coated slides

Microscope slides were placed in staining racks, washed in 95% IMS and left to air-dry. The slides were then dipped in 4% 3-aminopropyltriethoxysilane (APES; Sigma, UK) in acetone for 5 minutes, removed and rinsed in fresh acetone, before being washed in distilled water and dried in the oven at 37°C overnight.

Appendix 4: Tissue processing

JB-4 resin processing

The following solutions were made:

a) Infiltration solution was prepared by adding 0.9g of catalyst (benzoyl peroxide; Polysciences, Inc., USA) to 100ml of JB-4 solution A (Polysciences, Inc., USA) and stirred for approximately 15 minutes until dissolved.

b) Embedding solution was prepared by adding 0.2ml of JB-4 Solution B (Polysciences, Inc., USA) to 5ml of infiltration solution and mixed thoroughly. This is done immediately prior to use on ice to give a longer working time with the resin.

1mm slices from brains that had been perfuse fixed, in 4% phosphate buffered formaldehyde were cut on a vibratome and placed into clean multiwell plates and underwent the following processing schedule:

70% alcohol	30 minutes*
95% alcohol	30 minutes*
100% alcohol	2 x 30 minutes*
Infiltration solution	3 x 60 minutes*

* Continuous agitation on an orbital mixer

The specimens were then positioned in polyethylene moulds and covered with embedding solution. Nylon stubbs (25 mm) were then placed over the specimens and placed in the Taab embedding oven at room temperature in the fume cupboard through which nitrogen is circulated for 2 minutes since oxygen inhibits the polymerisation. Embedding is complete in about 5 minutes. 3μm resin sections were cut on a LKB historange using an 8mm glass knife, and mounted on gelatin subbed slides.

Appendix 5: Seescan image analysis

Infarct volumes were determined for each brain as follows. An image analysis system (Seescan, Cambridge.) was used to create a digitised pseudocolour image of each section, with pixel colours corresponding to the optical densities of the section. The lowest optical densities of gray matter present in the non-lesioned cortex were then used as the threshold value for recognition of normal gray matter versus infarcted tissue by the image analysis system. All non-infarcted gray matter areas have optical densities equal to or greater than this threshold value. The thresholds were established for each section to control for any variability of staining intensity or section thickness. However, in practice, there was almost no variation in the threshold values amongst sections from a given brain.

Before analysing, the non-lesioned (right) and lesioned (left) sides are separated by drawing an exclusion line between the two. The image analyser counts the number of pixels (calibrated to area) in the non-lesioned cortex equal to or greater than the threshold value. This gives a value for the area of the non-lesioned cortex. If the threshold level is changed to include the optical density of the infarcted tissue, then the area of the lesioned cortex (including both non-infarcted and infarcted areas) can be measured. The image analyser was then used to measure only the number of pixels with an optical density less than the threshold and this gives a value for the area of the infarct.

Appendix 6: Immunocytochemistry on vibratome sections

General protocol for immunostaining

1) Defrost the slides at room temperature for two hours, initially in the cling film covered rack (to prevent formation of ice crystals) and then section side up on slide trays

2) Ring the section with a Dako pen to produce a closed environment

3) Block endogenous peroxidase activity for 15 minutes in 0.3% hydrogen peroxide in 0.05M TBS. (45µl of 30% H_2O_2 + 5ml TBS- make fresh).

4) Rinse in distilled water for 5 sec.

5) 3 x 5 minutes wash in 0.05M TBS in a coplin jar.

6) Place slides in humidity chamber. Incubate with 10% animal in 0.1%BSA/0.05M TBS for 45 minutes.

7) Tip off the serum.

8) Incubate with primary antibody in 0.1% BSA/TBS at appropriate concentration at room temperature for 2 hours in a humid chamber.

9) Rinse gently with 0.05M TBS from a wash bottle, then a further 2 x 5 minutes washes with 0.05M TBS in a coplin jar.

10) Incubate with secondary biotinylated at 1:200 for 45 minutes at room temperature in a humid chamber.

11) Rinse gently with 0.05M TBS from a wash bottle, then a further 2 x 5 minutes washes with 0.05MTBS.

12) Visualisation with diaminobenzidine (DAB), using a Vectastain ABC kit (Elite)

(a) Apply the complex (prepared 30 minutes previously, 2 drops each of solution A and B in 5mls of Tris buffer) for 30 minutes in humid chamber

(b) Wash 3 x 5 minutes with 0.05M TBS

(c) Apply the DAB substrate (see below).

(d) Leave for (3-10 minutes) minutes in a dark fume cupboard

(e) Rinse in tap water in a coplin jar to stop reaction, then in running water for 1minutes (disposing of DAB into bleach).

(f) Counterstain in 1% methyl green for 30 seconds, rinse in tap water.

13) Dehydrate sections through ascending alcohols, clear in xylene (fume cupboard) and mount coverslips with DPX or Practamount.

GSA staining

1) to 5) as above

6) Incubate sections with 0.25mg/ml of trypsin in 0.05M TBS/1mM$CaCl_2$ at 37°C for 4 minutes.

7) 3 x 5 minute wash in 0.05M TBS/1mM$CaCl_2$

8) Incubate sections in 20μg/ml GSA-B4 in 0.05MTBS/1mM$CaCl_2$for 120 minutes.

9) Steps 11 to 13 as above.

Solutions used in immunostaining

1) 0.5M stock Tris buffered saline (TBS)

81g of NaCl and 60.57g of Tris (hydroxymethyl) methylamine (BDH, UK) was dissolved in approximately 800ml of distilled water, and the pH adjusted to 7.6 using drops of hydrochloric acid. The final volume was made up to 1L with distilled water. The solution is stored at 4°C.

2) 0.05M Tris buffered saline (TBS)

100ml of 0.5M stock Tris buffered saline is added to 900ml of distilled water. The solution is stored at 4°C.

3) 0.05M TBS + 1mM Calcium Chloride

0.111g of anhydrous calcium chloride (Sigma, UK) was added to 100ml of 0.05M TBS, and stored at 4°C. (This is used for trypsin and some wash phases in GSA staining.).

4) DAB solution

a) 0.2M sodium acetate buffer pH6

8.203g of anhydrous sodium acetate (Sigma, UK) is added to 500 ml of distilled water and the pH adjusted to 6 with HCl. The solution is stored at 4°C.

b) Solution A of DAB substrate

The following components were mixed together in a fume cupboard and stored at 4°C:

7.25g Ammonium Nickel (II) Sulphate (Sigma, UK)

150ml of 0.2M sodium acetate buffer pH6

600mg Glucose (Sigma, UK)

120mg Ammonium Chloride (Sigma, UK)

c) Solution B of DAB substrate

150mg of 3,3'-diaminobenzidine tetrahydrochloride dihydrate (DAB; Aldrich Chemical Company, UK) was dissolved in 150ml of distilled water in a fume cupboard and frozen in 10ml vials.

d) Final DAB substrate

The DAB substate is made fresh on the day of staining by mixing together 10 ml of Solution A to 10ml of Solution B. This mixture is filtered and just prior to use 0.5mg of glucose oxidase Type VII (Sigma, UK) added.

e) 0.2M glycine-HCL buffer (pH 2.2)

The following stock solutions were made:

0.2M glycine (mwt = 75.07); 8g in $100cm^3$ of distilled water = solution A

0.2M HCL (mwt = 36.46); $1.7cm^3$ of HCL in $100cm^3$ of distilled water = solution B

For 0.2M glycine-HCL (ph 2.2) add 50ml of solution A to 50.44ml of solution B

Appendix 7: Miscellaneous

1) PBS

1 phosphate buffered saline tablet (Sigma, UK) was added to 200ml of distilled water to obtain a 0.01M phosphate buffered solution.